THE JOURNAL
OF
CHEMICAL PHYSICS

VOLUME 15

THE JOURNAL
OF
CHEMICAL PHYSICS

VOLUME 15, NUMBER 7 JULY, 1947

The Size and Vibration Frequency of the Excited Benzene Molecule*

VIRGINIA GRIFFING
The Catholic University of America, Washington, D. C.
(Received April 15, 1947)

It is shown that the change in size and vibration frequency of a polyatomic molecule upon electronic excitation can be calculated if the excitation energy is known as function of the distance. This is applied to benzene, for which this function is calculated both with the Heitler-London-Slater-Pauling method and the molecular orbital method. Upon comparison with experiment, it is found that both methods give the right sign and order of magnitude for the change in size, but the wrong sign for the change in frequency.

I. INTRODUCTION

THIS paper is an attempt to connect the resonance energy—considered as a function of the distance between atoms—in a polyatomic molecule with the change of its size and vibration frequency caused by electronic excitation.

Consider first a diatomic molecule. If one plots the binding energy as function of the distance, the minimum of the curve gives the size of the molecule, the curvature gives the restoring force, and, therefore, the frequency of the vibration.

If one can calculate the electronic excitation energy as a function of the nuclear distance, and can add this to the energy of the ground state taken from experiment, one gets, as a function of the distance, the energy of the excited state, and from it the size of the excited molecule and its vibrational frequency.

The same argument can be applied to a polyatomic molecule of sufficient symmetry that it has a "breathing" vibration, in which it can be characterized by a single distance.

This idea will be applied here to molecules having resonance, in particular to benzene—in which excitation consists in a transition to a state differing from the ground state only by resonance splitting.

It is then generally assumed that the in-plane bonds are not affected by excitation, i.e., the energy curve of the ground state is the sum of two energy curves, that of the in-plane bonds and that of the ground state of the π-bonds. Similarly, the energy curve of the excited state is given by the sum of the energy curves of the unmodified in-plane bonds and of the excited π-bonds.

The difference between the energy curves of the excited state and of the ground state as function of the distance—from which the change in the size of the molecule and the change in frequency of the breathing vibration can be calculated—is therefore equal to the excitation energy of the resonance π-bonds as function of the distance.

* A dissertation submitted to the Faculty of the Graduate School of Arts and Sciences of the Catholic University of America in partial fulfillment of the requirements for the degree of Doctor of Philosophy.

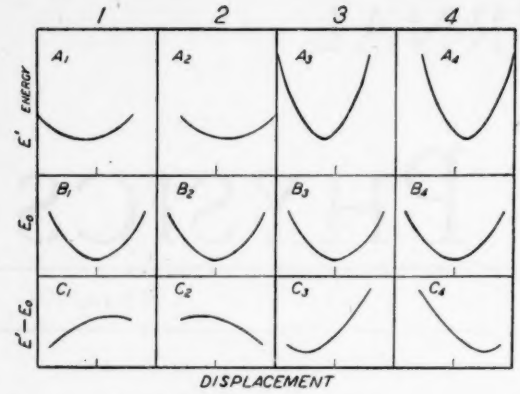

FIG. 1. The four possible excitation energy curves (C) as function of the distance; the energy of the ground state, (B); the energy of the excited state (C). Case I, the excited molecule is smaller and has lower frequency. Case II, the excited molecule is larger and has lower frequency (e.g., benzene). Case III, the excited molecule is smaller and has higher frequency. Case IV, the excited molecule is larger and has higher frequency.

II. DISCUSSION OF THE FORM OF POSSIBLE FUNCTIONS

Consider a polyatomic molecule in its vibrationless ground state. Assume that this state is perturbed by a symmetrical breathing vibration that is characterized by a displacement $(R-R_0)$, of the atoms from an equilibrium position R_0. Call n the number of significant bonds which partake in resonance excitation and are stretched in the breathing vibration ($n=6$ for benzene, $n=N-1$ for a polyene with N carbon atoms). If the breathing vibration is of small amplitude then the energy of this state can be written

$$E(R)=E_0(R_0)+\tfrac{1}{2}nK(R-R_0)^2, \qquad (1)$$

where E_0 is the energy of the vibrationless ground state, and K is the force constant whose magnitude is determined from the frequency of vibration. The validity of this approximation can be checked experimentally by the constancy of the frequency differences between the members of a sequence of vibration bands. In the excited state both the size of the molecule and the force constant may have changed so that the energy is written

$$E'(R)=E_1(R_1)+\tfrac{1}{2}nK'(R-R_1)^2. \qquad (2)$$

R_1 is the equilibrium position and K' the force constant in the excited state.

In polyatomic molecules it is often impossible to calculate $E_0(R_0)$ and $E_1(R_1)$ separately, but if one calls $E_1(R_1)-E_0(R_0)=U_0$, U_0 is independent of R and is the energy of an electronic transition from the vibrationless ground to the vibrationless excited state. Then the excitation energy $\Delta E(R)$ as function of R can be written

$$\Delta E(R)=E'(R)-E(R)$$
$$=U_0+\tfrac{1}{2}nK'(R-R_1)^2-\tfrac{1}{2}nK(R-R_0)^2.$$

Now if $R_0=R_1-\delta$ then

$$\Delta E(R)=U_0-nK'\delta[R-(R_0+R_1)/2]$$
$$+\tfrac{1}{2}n(K'-K)(R-R_0)^2. \qquad (3)$$

Furthermore,

$$(d\Delta E(R)/dR)=n(K'-K)(R-R_0)-nK'\delta,$$

that is, in the region of vibration of very small amplitude when $(R-R_0)$ is small, the slope of the curve representing the excitation energy is determined by the change in the equilibrium distance. Therefore, the change in the size of the molecule upon excitation is given by

$$\delta=-\frac{n}{K'}\left[\frac{d\Delta E}{dR}\right]_{R_0}=-\frac{n}{K}\left[\frac{d\Delta E}{dR}\right]_{R_1}. \qquad (4)$$

According to the definition of curvature

$$L=\frac{d^2\Delta E/dR^2}{[1+(d\Delta E/dR)^2]^{\frac{3}{2}}}. \qquad (5)$$

Since the denominator is always positive, the sign of the curvature is the same as the sign of $d^2\Delta E/dR^2$. Specifically, the curvature is positive (concave upward) if $(K'-K)$ is positive as is the case when the force constant is larger in the excited than in the ground state. The curvature is negative (concave downward) if $(K'-K)$ is negative, i.e., the frequency of the vibration is smaller in the excited than in the ground state.

The four possible cases are shown in Fig. 1. Curves A_n (Eq. 2) are the potential energy curves for the excited state. Assume the same curve B (Eq. 1) in the four cases for the ground state. C_n (Eq. 3) shows the difference $(B-A)$, namely, the excitation energy.

Case I—$K>K'$, $R_0>R_1$. This is the case of a molecule that is smaller in the excited than in the ground state and the restoring force, thus the frequency of vibration is smaller in the excited state. Therefore, for vibrations of small amplitude the excitation energy can be represented by

a quadratic curve with a positive slope and negative curvature as shown in C_1, Fig. 1.

Case II—$K>K'$, $R_0<R_1$. This represents a molecule that is larger in the excited state while the force constant is smaller in the excited state. For this case the excitation energy gives a quadratic curve with negative slope and negative curvature (C_2, Fig. 1).

Case III—$K<K'$, $R_0>R_1$. In this case the molecule is smaller and the frequency of vibration larger in the excited state. The excitation energy is represented by a quadratic curve with positive curvature and positive slope (C_3, Fig. 1).

Case IV—$K<K'$, $R_0<R_1$. This is a molecule that is larger and has a larger frequency of vibration in the excited than in the ground state. The excitation energy (C_4, Fig. 1) is represented by a quadratic curve with negative slope and positive curvature.

For cases where $K=K'$, the excitation energy is represented by a straight line; if $R=R_0$ it is horizontal. Therefore, given a method of accurately determining the excitation energy of symmetrical polyatomic molecules as a function of a characteristic coordinate, it is possible to determine the change in size of the molecule from the slope of the curve and the change in the frequency of the symmetrical vibration from the curvature.

In general the excitation energy of a polyatomic molecule might be represented by a curve such as shown in Fig. 2. This curve approaches a constant value as the distance between the atoms becomes very large. The numbers in Fig. 2 show in what part of the general excitation energy curve one finds sections having one of the four different shapes just discussed. In what part of the excitation energy curve the ground state equilibrium dimension R_0 will fall is, of course, determined by the energy curve of the ground state as function of the distance and therefore strongly influenced by the in-plane bonds.

III. EXPERIMENTAL DATA FOR BENZENE

Benzene is a polyatomic molecule with a high degree of symmetry in both the ground (E_0) and the first excited (E_{2s}) state. A detailed analysis of the absorption spectra of benzene in the region of 2600A has been made by Sponer, Nordheim, Sklar, and Teller.[1] In this analysis the totally symmetrical breathing vibrations of both the C−C and C−H bonds have been identified in both the ground and excited state, and the change in the size of the molecule is estimated. These quantities taken from reference 1 are tabulated in Table I along with the force constants that will be discussed below:

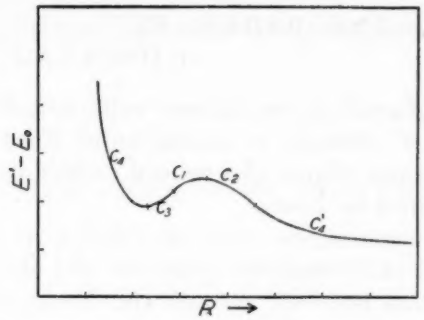

FIG. 2. The general form of excitation energy as function of a characteristic distance.

TABLE I.

	C−C frequency cm^{-1}	C−H frequency cm^{-1}	C−C force constant dynes 10^5/cm	C−C force constant ev/(R units)^2	C−C equilibrium distance A	C−C equilibrium distance R units
Ground state	992	3062	7.603	1.3138	1.400	8.37
Excited state	923	2565	6.602	1.1408	1.418	8.49

Wilson[2] has discussed the possible vibrations of a mechanical system of mass points such as benzene and has calculated the frequencies of the totally symmetrical breathing vibration in terms of simple potential functions involving only the force constants of the C−C and C−H bonds. Following Wilson[2] and making use of the frequencies given in Table I, the C−C force constants as given in Table I were calculated. These force constants are for vibrations of small amplitude about the equilibrium positions.

The values of the force constants and equilibrium positions from Table I are substituted in Eq. (3) and the value of $U_0=5$ ev taken from Sklar,[3] so that the excitation energy of the first electronic shift found by experiment can be written**

[1] H. Sponer, G. Nordheim, A. L. Sklar, E. Teller, J. Chem. Phys. **7**, 207 (1939).
[2] E. B. Wilson, Jr., Phys. Rev. **45**, 706 (1934).
[3] A. L. Sklar, J. Chem. Phys. **5**, 669 (1937).
** $0.5190=6\times\frac{1}{2}(1.3138-1.1408)$.

$$E_{2s}-E_0=5.000-0.8214(R-R_0)-0.5190(R-R_0)^2, \quad (6)$$

where $E_{2s}-E_0$ is in electron volts and R/Z is the C−C distance in atomic units. $Z=3.18$ is the effective charge of a neutral carbon atom as determined by Zener.[4]

The experimental value of 38089 wave numbers (or 4.71 electron volts) for the zero-zero band does not only contain the energy of the electronic jump, but also the differences of the zero-point energies of all vibrations in the excited state and the ground state. However, this difference in zero-point energies will surely not exceed 10 percent of the corresponding electronic energies, and since in our comparison we are not concerned with a high accuracy, that will be neglected. The use of 5 ev in the place of 4.71 enters the calculation of the dependence on R only in one place (Section IV c), where a factor 0.4636 is used to fit the theoretical and experimental values together at the equilibrium position.

Thus according to experiments as interpreted in reference 1, benzene is an example of Case II, Section II. In other words, the molecule is larger and the vibration frequency is lower in the excited than in the ground state; the C−C distance increases about 1.5 percent, and the vibration frequency decreases about 7 percent.

According to Sklar[5] the frequency of the breathing vibration in the E_{1s} level (in the region of 2000A) is still about 920 cm^{-1}. The spectroscopic data in this region have not been sufficiently analyzed to estimate the shift in the C−C distance.

IV. THEORETICAL TREATMENT OF BENZENE

(a) General Considerations

Sklar[3] has calculated the electronic states of benzene according to the Heitler-London-Slater-Pauling (HLSP) method. The same problem has been considered according to the method of antisymmetrized molecular orbitals by Goeppert-Mayer and Sklar[6] (hereafter referred to as GMS paper). There is good agreement between the two methods in predicting the experimentally observed electronic absorption spectra of benzene in the region of 2600A. The excitation energy used in these discussions is a function of the C−C distance. The numerical evaluations were made only for the experimentally determined C−C equilibrium distance. However, this assumption does not enter in principle into the calculations. Therefore, it is the purpose of this section to extend both of these theoretical treatments to the calculation of the excitation energy for a small range of R in the region of the equilibrium position. This corresponds to two independent theoretical determinations of the excitation energy as a function of R. From these it should be possible to predict the change in frequency of the totally symmetric C−C vibration and the change in the size of the benzene molecule in the excited state.

Both methods have the following assumptions in common. According to Hückel[7] the charge distribution associated with each carbon atom in the benzene ring can be considered thus: Two inner electrons are considered to be on the nucleus and the remaining four electrons are valence electrons; three of the valence electrons are represented by sp^2 hybridized wave functions in the plane of the ring; the fourth, a $2p\pi$ electron, is described by a $2p\pi$ wave function with its node in the plane of the ring and the charge distribution perpendicular to the ring so that there is little overlap with the electrons forming the in-plane bonds. Thus the two sets of electrons can be considered independently, and only the six $2p\pi$ electrons concern us. It is assumed that excitation to the excited states considered here does not affect the in-plane bonds at all, except insofar as the distance between atoms is changed. Consequently this is a six electron problem with the hexagonal symmetry of the benzene ring. All interactions, except coulomb, of electrons between particles farther apart than neighbors are neglected.

(b) Notations

The following notations used in this paper are slightly different from those of the GMS paper.

H the Hamiltonian operator of the benzene molecule, including the repulsion between electrons.

[4] C. Zener, Phys. Rev. **36**, 51 (1930).
[5] A. L. Sklar, Rev. Mod. Phys. **14**, 232 (1942).
[6] M. Goeppert-Mayer and A. L. Sklar, J. Chem. Phys. **6**, 645 (1938).
[7] E. Hückel, Zeits. f. Physik **70**, 204 (1931).

$K(\nu)$ the $2p\pi$ wave function of the Kth carbon atom.

i.e., $I(\nu)$, $II(\nu)$, $\cdots VI(\nu)$.

$\nu, \mu = 1 \cdots 6$ denote the six $2p\pi$ electrons.

S_{V+1} the overlap integrals

$$\int K(\nu)[K+V](\nu)d\tau_\nu.$$

α single exchange integral between neighbors for the benzene molecule.

E_0 energy of the ground state.

E_{ns} energy of the nth singlet electronic state.

R/Z the C−C distance in atomic units.***

Z = the effective nuclear charge for a neutral carbon atom.

$R_0 = 8.37$, i.e., the equilibrium distance of t C−C nuclei in benzene in the ground state.he

I ionization energy of a carbon atom in the valence state (taken as negative).

τ_ν volume of space in terms of the coordinates of electron ν.

The atomic coulomb integrals

$$A_N = \int\int \frac{e^2}{r_{\nu\mu}} K^2(\nu)[K+N]^2(\mu)d\tau_\nu d\tau_\mu.$$

The atomic mixed exchange and coulomb integral

$$B_{12} = \int\int \frac{e^2}{r_{12}} I^2(1)I(2)II(2)d\tau_1 d\tau_2.$$

The atomic exchange integral

$$C_{12} = \int\int \frac{e^2}{r_{12}} I(1)II(1)I(2)II(2)d\tau_1 d\tau_2.$$

The atomic penetration integrals

$$Q = -\int H_I(\nu)K^2(\nu)d\tau_\nu,$$

$$T = -\int H_I(\nu)K(\nu)[K+I](\nu)d\tau_\nu (R \text{ in GMS}),$$

where H_I is the attraction of a neutral carbon atom in the valence state for the electron ν.

ϵ_l energy of the lth molecular orbital caused by the potential of the benzene ring.

The coulomb integrals between molecular orbitals

$$\gamma_{ll'} = \int\int \frac{e^2}{r_{\nu\mu}} |\phi_l(\nu)|^2 |\phi_{l'}(\mu)|^2 d\tau_\nu d\tau_\mu.$$

The exchange integrals between molecular orbitals

$$\delta_{ll'} = \int\int \frac{e^2}{r_{\nu\mu}} [\phi_l(\nu)\phi_{l'}(\mu)][\phi_l(\mu)\phi_{l'}(\nu)]^* d\tau_\nu d\tau_\mu,$$

where

$$\phi_l(\nu) = (6\sigma_l)^{-\frac{1}{2}} \sum_{k=1}^{6} \exp\frac{2\pi ilk}{6} K(\nu),$$

the lth molecular orbital and σ_l = normalization coefficients.

(c) The Heitler-London-Slater-Pauling Method

Using the simplified HLSP method Sklar[3] showed that the energies of the five different electronic states were due to resonance splitting of the five homopolar structures without including any polar structures. Thus he was able to express the energy difference between the ground and the excited states in terms of the single exchange integral, α, which is defined by the following equation

$$\alpha = \int\int\int\int\int\int I(1)II(2)III(3)IV(4) \times V(5)VI(6)HI(2)II(1)III(3) \times IV(4)V(5)VI(6)d\tau_1 d\tau_2 d\tau_3 d\tau_4 d\tau_5 d\tau_6. \quad (7)$$

For the energy difference between the ground and the lowest electronic state Sklar obtained the following:

$$E_{2s} - E_0 = -2.6\alpha. \quad (8a)$$

Sklar did not calculate the value of α but used an experimental thermochemical value of the resonance energy (1.11α) to obtain the energy difference given in his paper. Since H is a function of R, α was calculated as a function of R from (7)

$$\alpha = C_{12} - S_1\left\{4T + 2B_{12} + S_1\left[6Q + 6A_1 + 5A_2 + 3A_3 - 6I - \frac{6Z}{R}(1+\tfrac{1}{3}+\tfrac{1}{4})\right]\right\}. \quad (9a)$$

The numerical values of the integrals occurring in

*** R is called ρ by Sklar and Lyddane in reference 8.

TABLE II. The HLSP method.

C–C distance A	C–C distance R units	a $\alpha-6S_1^2I$	b α (Eq. 9a)	c $E_{2s}-E_0$	d $E_{2s}-E_0$ (Eq. 8c)
1.484	8.87	−1.7599 ev	−2.9916 ev	3.6061 ev	3.7150 ev
1.450	8.67	−2.0448	−3.4219	4.1248	4.1294
1.433	8.57	−2.2033	−3.6579	4.4092	4.3868
1.417	8.47	−2.3748	−3.9110	4.7143	4.6765
1.400	8.37	−2.5571	−4.1788	5.0371	5.0001
1.383	8.27	−2.7589	−4.4706	5.3889	5.3667
1.367	8.17	−2.9624	−4.7677	5.7470	5.7471
1.333	7.97	−3.4938	−5.5014	6.6314	6.6275
1.300	7.77	−4.1057	−6.3343	7.6354	7.6413

Eq. (9) as a function of R are given in the appendix of this paper. Although it was known that this approximate calculation would not give the correct absolute value of $E_{2s}-E_0$ it was hoped that the relative variation with R would be reliable. $(\alpha-6S_1^2I)$ was first calculated because the estimated value of I was not very reliable. These values are listed in Table II*a*. α as a function of R calculated by this equation for an estimated value of I is given in Table II*b*.

In order to discuss the results conveniently the best quadratic equation to fit the numbers in Tables II*a* and II*b* was obtained by the method of least squares

$$(\alpha-6S_1^2I)=-2.5218+1.941(R-R_0)-1.162(R-R_0)^2,$$

$$-2.6(\alpha-6S_1^2I)=6.5567-5.046(R-R_0)+3.021(R-R_0)^2,$$

$$S_1^2=0.06754-0.03678(R-R_0)+0.0089(R-R_0)^2.$$

We set I 4 ev as the ionization energy[8] for the carbon atom in the valence state, then

$$\alpha=-4.1491+2.823(R-R_0)-1.383(R-R_0)^2 \quad (9b)$$

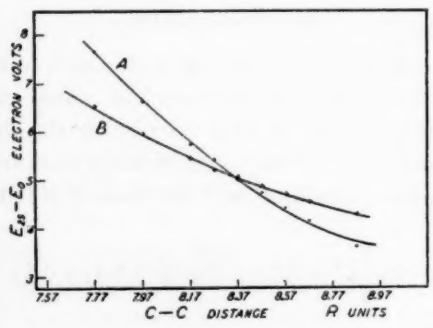

FIG. 3. The excitation energy of benzene $(E_{2s}-E_0)$ as a function of the C–C distance.

[8] J. Duschesne, P. Goldfinger, B. Rosen, Nature **159**, 131 (1947).

or

$$E_{2s}-E_0=-2.6\alpha=10.7877-7.340(R-R_0)+3.596(R-R_0)^2. \quad (9c)$$

Adjusting Eq. (9c) to give the correct value for α at $R=R_0$ by multiplying the entire equation by the proper numerical constant, 0.4636, we get

$$E_{2s}-E_0=5.000-3.402(R-R_0)+1.667(R-R_0)^2. \quad (8b)$$

In Fig. 3, the curve A was obtained from the quadratic form 8b (see Table II*c*). The points are the values obtained by calculation according to Eq. (9a) and multiplication of all values by 0.4636 for the purpose of adjusting these values to fit at $R=R_0$ (Table II*c*).

According to Eq. (4) it is possible to calculate the change in the size of the molecule if one knows the experimental value for the force constant in the ground state. A better comparison is with the experimental Eq. (6) which is of the same form as Eq. (8b). From this comparison it can be seen that the calculated change in size has the right sign and is of the right order of magnitude, especially since the experimental value is a rough approximation. However, the frequency shift predicted by this calculation has the wrong sign; i.e., this calculation gives an increase in the force constant and consequently a higher frequency for the totally symmetrical breathing vibration in the excited state. Experiment gives a decrease in frequency of this vibration in the excited state.

(d) Antisymmetrized molecular orbitals

The second method used is an extension to different values of R of the GMS paper, which applies the method of antisymmetrized products of molecular orbitals. The GMS paper expresses the energy as the sum of certain integrals but gives the values of these integrals and of their coefficients only for R_0. The values of these quantities for a range of R are given in the appendix of this paper. Detailed discussion is confined to the first excited level (E_{2s}), which is interpreted as the upper state of the observed band at 2600A. This is the only electronic level for which there is detailed experimental analysis of the structure caused by vibrations. The excitation energy is made up of three parts.

The first part, $(\epsilon_2-\epsilon_1)$, is that part of the energy difference common to all excited states due to the interaction of the electrons with the $2p\pi$-less carbon skeleton and is given by Eq. (31) of the GMS paper

$$\epsilon_2-\epsilon_1=\frac{\sigma_1-\sigma_2}{\sigma_1\sigma_2}\{-2Q-2A_1-2A_2-A_3\}+\frac{\sigma_1+\sigma_2}{\sigma_1\sigma_2}\{T+B_{12}\}. \quad (10)$$

The second, $E^1-E_0-(\epsilon_2-\epsilon_1)$ is the interaction caused by the mutual repulsion of the six $2p\pi$ electrons common to all excited states; it is given by Eq. (25) of the GMS paper.

$$E^1-E_0-(\epsilon_2-\epsilon_1)=-2\gamma_{01}+2\gamma_{02}-3\gamma_{11}+3\gamma_{12}+\delta_{01}-\delta_{02}+\delta_{1-1}. \quad (11)$$

Now expressing the molecular integrals in terms of atomic integrals according to Eq. (19) of the appendix, Eq. (11) becomes

$$\begin{aligned}E^1-E_0-(\epsilon_2-\epsilon_1)&=\left[\frac{1}{6\sigma_0\sigma_1}+\frac{1}{6\sigma_0\sigma_2}-\frac{1}{3\sigma_1\sigma_1}+\frac{1}{2\sigma_1\sigma_2}\right]A_0\\&+\left[-\frac{1}{2\sigma_0\sigma_1}+\frac{5}{6\sigma_0\sigma_2}-\frac{7}{6\sigma_1\sigma_1}+\frac{1}{\sigma_1\sigma_2}\right]A_1\\&+\left[-\frac{5}{6\sigma_0\sigma_1}+\frac{5}{6\sigma_0\sigma_2}-\frac{7}{6\sigma_1\sigma_1}-\frac{1}{\sigma_1\sigma_2}\right]A_2\\&+\left[-\frac{1}{2\sigma_0\sigma_1}+\frac{1}{6\sigma_0\sigma_2}-\frac{1}{3\sigma_1\sigma_1}+\frac{1}{2\sigma_1\sigma_2}\right]A_3\\&+\left[-\frac{1}{\sigma_0\sigma_1}+\frac{1}{3\sigma_0\sigma_2}-\frac{5}{3\sigma_1\sigma_1}\right]B_{12}\\&+\left[-\frac{1}{6\sigma_0\sigma_1}-\frac{5}{6\sigma_0\sigma_2}+\frac{1}{6\sigma_1\sigma_1}-\frac{1}{2\sigma_1\sigma_2}\right]C_{12}. \quad (11a)\end{aligned}$$

The third part is that part of the interaction caused by electron repulsion responsible for the splitting between the various excited states so that the excitation energies are given by Eq. (23) of the GMS paper. Below are given the equations only for the first and second singlet states which are of primary interest in this paper

$$E_{2s}-E_0=(E^1-E_0)+\frac{1}{6\sigma_1\sigma_2}\times\{-A_0-2A_2+3A_3+5C_{12}\}\quad {}^1\Gamma_{10}(B_{2u}), \quad (12)$$

$$E_{1s}-E_0=(E^1-E_0)+\frac{1}{6\sigma_1\sigma_2}\times\{A_0-6A_1+8A_2-3A_3+C_{12}\}\quad {}^1\Gamma_9(B_{1u}). \quad (13)$$

TABLE III. The molecular orbital method.

C–C distance A	C–C distance R units	a $E_{2s}-E_0$ (Eq. 12)	b $E_{2s}-E_0$ (Eq. 14)	c $E_{1s}-E_0$ (Eq. 13)	d $\Sigma_2-\Sigma_1$ (Eq. 10)
1.484	8.87	4.3014 ev	4.3001 ev	5.1220 ev	−4.9302 ev
1.450	8.67	4.5556	4.5439	5.2450	−5.3420
1.433	8.57	4.6898	4.6904	5.3100	−5.5420
1.417	8.47	4.8520	4.8533	5.3940	−5.7347
1.400	8.37	5.0215	5.0326	5.4810	−5.9248
1.383	8.27	5.2073	5.2283	5.5810	−6.1145
1.367	8.17	5.4299	5.4404	5.7130	−6.2791
1.333	7.97	5.9430	5.9138	6.0234	−6.5883
1.300	7.77	6.5350	6.4528	6.3950	−6.8502

Equations (12) and (13) are evaluated for a range of R, and the numerical values for these energy differences are given in electron volts in Table III*a* and *c*. The best quadratic equation (Eq. 14) to represent the numbers in III*a* (Eq. 12) was obtained

$$E_{2s}-E_0=5.0326-1.875(R-R_0)+0.8174(R-R_0)^2. \quad (14)$$

The values calculated according to Eq. (14) are given in Table III*b* and are shown in the smooth curve *B*, Fig. 3, while the points are the calculated points according to Eq. (13), (Table III*a*). No correction factor was used in this case.

Comparing the quadratic Eq. (14) with the experimental Eq. (6), one predicts a change in the size of the molecule that is about twice that estimated from experiment (Eqs. 4, 6, and 14—since the factor of $R-R_0$ is 1.875 against 0.8214—). The change in frequency is of the right order of magnitude but has the wrong sign.

In the following an attempt is made to trace the origin of the difficulty with the curvature. In Fig. 4, curve *A* is $(\epsilon_2-\epsilon_1)$ (Eq. 10), curve *B* is $E^1-E_0-(\epsilon_2-\epsilon_1)$ (Eq. 11), and curve *C* is $E_{2s}-E^1$. The sum of these three curves is the excitation energy $E_{2s}-E_0$, curve *D*, (Eq. 13) which has already been shown as curve *B*, Fig. 3. All of these curves are approximately straight

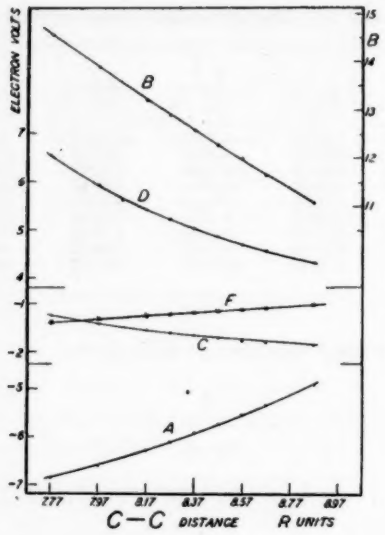

FIG. 4. Curves calculated according to the method of antisymmetrical molecular orbitals.

Curve A: $\epsilon_2-\epsilon_1$ (Eq. 10)
Curve B: $E^1-E_0-(\epsilon_2-\epsilon_1)$ (Eq. 11)
Curve C: $E_{2s}-E^1$
Curve D: $E_{2s}-E_0(A+B+C)$ (Eq. 12)
Curve F: $E_{1s}-E^1$.

lines except curve A, $(\epsilon_2-\epsilon_1)$: curve A, therefore, has about the same curvature as the final excitation energy curve. Therefore, any difficulty with the curvature seems to lie with $(\epsilon_2-\epsilon_1)$; if one inserts numerical values in Eq. (10) (Table III*d*) it is found to be negative, although general arguments would point to a higher value of ϵ_2 (energy of the excited orbital) than ϵ_1 (energy of the ground orbital). (This difficulty was pointed out orally to us by A. London.) This makes it appear plausible that the present calculation of $\epsilon_2-\epsilon_1$ is not accurate enough, both as to absolute value and sign of curvature as function of R.

Curve F shows $E_{1s}-E^1$ and is a straight line just as $E_{2s}-E^1$ (curve C), indicating that the change in frequency of the totally symmetrical vibration in the 2000A band is about the same as in the 2600A band (since $E_{2s}-E_{1s}$ is a straight line). This seems in agreement with the statement (see Section III) that a sequence with wave number difference 920 appears in the 2000A band; this shows that the frequency of the breathing vibration is the same in the E_{2s} and E_{1s} levels. No analysis giving the experimental approximation of the size of the molecule in the E_{1s} level has been made. The theory (slope of $E_{2s}-E_{1s}$) predicts a change in size of 0.017A in the E_{1s} excited state, if one assumes the experimental value of the force constant $K'=6.602\times10^5$ dynes/cm. Therefore, the molecule is smaller in the E_{1s} than in the E_{2s} level. The theory predicts a change in the C—C distance 53 percent as great as it predicts in the E_{2s} level.

V. DISCUSSION

Experimental data show that the benzene molecule increases in size while the frequency of the breathing vibration decreases by excitation to the lowest electronic excited state. According to the arguments of Section II, the excitation energy as a function of R must have a negative slope and a negative curvature corresponding to Fig. 1c. The calculated curves for the excitation energy both have a negative slope of the right order of magnitude, possibly slightly too large; however, both the HLSP and the MO method give positive curvature (which would mean an increase in the frequency of the breathing vibration in the excited state).

To explain the experimental facts one needs an excitation energy curve of the somewhat peculiar shape shown in Fig. 2.

There are two assumptions which might explain the wrong curvature given by the two theoretical methods. It could be that the force constant of the in-plane bonds is changed in going from the ground to the excited state contrary to the assumption made in both the HLSP and the antisymmetrized molecular orbital methods. Or the assumption that the wave function associated with the $2p$ electrons can be represented by a simple $2p$ wave function with the nuclear charge chosen to give minimum energy for the free carbon atom may be too simple. This assumption is probably sufficiently good in evaluating the coulomb integrals but the overlaps, and consequently the normalization factors and the exchange integrals, are particularly sensitive to the wave function used. A smaller value of the overlap might change the curvature predicted by both methods. A smaller value of the overlap would also give better agreement for the absolute value of the energy difference between theory and experiment in the HLSP method.

It seems worth while to rewrite the calculated

expressions for the excitation energy of the E_{2s} level according to the two methods here for a comparison. The first is according to the HLSP method (Eq. 9 multiplied by -2.6)

$$E_{2s}-E_0=2.6C_{12}-2.6S_1(4T+2B_{12})$$
$$-2.6S_1^2\left(6Q+6A_1+5A_2+3A_3-6I-\frac{6Z}{R}\left(1+\frac{1}{\sqrt{3}}+\frac{1}{4}\right)\right) \quad (15)$$

and the second by the antisymmetrized molecular orbitals (Eq. 12).

$$E_{2s}-E_0=\frac{\sigma_1-\sigma_2}{\sigma_1\sigma_2}\{-2Q-2A_1-2A_2-A_3\}$$
$$+\frac{\sigma_1+\sigma_2}{\sigma_1\sigma_2}\{T+B_{12}\}$$
$$+\left\{-\frac{1}{6\sigma_0\sigma_1}+\frac{1}{6\sigma_0\sigma_2}-\frac{1}{3\sigma_1\sigma_1}+\frac{2}{3\sigma_1\sigma_2}\right\}A_0$$
$$+\left\{-\frac{1}{2\sigma_0\sigma_1}+\frac{5}{6\sigma_0\sigma_2}-\frac{7}{6\sigma_1\sigma_1}\right\}A_1$$
$$+\left\{-\frac{5}{6\sigma_0\sigma_1}+\frac{5}{6\sigma_0\sigma_2}-\frac{7}{6\sigma_1\sigma_1}+\frac{14}{6\sigma_1\sigma_2}\right\}A_2$$
$$+\left\{-\frac{1}{2\sigma_0\sigma_1}+\frac{1}{6\sigma_0\sigma_2}-\frac{1}{3\sigma_1\sigma_1}\right\}A_3$$
$$+\left\{-\frac{1}{\sigma_0\sigma_1}+\frac{1}{3\sigma_0\sigma_2}-\frac{5}{3\sigma_1\sigma_1}\right\}B_{12}$$
$$+\left\{-\frac{1}{6\sigma_0\sigma_1}-\frac{5}{6\sigma_0\sigma_2}+\frac{1}{6\sigma_1\sigma_1}-\frac{1}{3\sigma_1\sigma_2}\right\}C_{12}. \quad (16)$$

If one neglects S_2 and S_3 which is consistently assumed in the HLSP method

$$\sigma_0\sigma_1=1+3S_1+2S_1^2,\quad \sigma_0\sigma_2=1+S_1-2S_1^2,$$
$$\sigma_1\sigma_2=1-S_1^2,\quad \sigma_1-\sigma_2=2S_1,\quad \sigma_1+\sigma_2=2.$$

Both of these equations are sums of the same atomic integrals multiplied by functions of the overlap integral. In Eq. (15) (HLSP) the ionization energy I of the carbon atom occurs which includes the contribution of the A_0 integral which occurs in Eq. (16) (MO). The kinetic energy included in I and the term

$$\frac{6Z}{R}\left(1+\frac{1}{\sqrt{3}}+\frac{1}{4}\right)S_1^2,$$

the contribution of the coulomb interaction between the nuclei does not occur in (16). All of the atomic integrals except A_0 occur explicitly in both Eqs. (15) and (16); however, the coefficients are very different. In Eq. (15) the overlap S_1 occurs as a linear and quadratic coefficient while in Eq. (16) the coefficients are of the form

$$\frac{a+bS_1+cS_1^2}{a'+b'S_1+c'S_1^2+d'S_1^3+e'S_1^4}.$$

The following Table IV shows the numerical value of the coefficients of the atomic integrals in the two expressions for the excitation energy for R equal to R_0, the equilibrium position in the ground state.

TABLE IV.

Atomic integral	Coefficients HLSP	AMO
A_0		0.5982
A_1	1.05408	−1.4653
A_2	0.8784	1.06039
A_3	0.52704	−0.90387
C_{12}	−2.6	−1.07355
B_{12}	1.35174	0.84365
T	2.70348	2.22198
Q	1.05408	−1.11998
I	−1.05408	

ACKNOWLEDGMENTS

The author wishes to thank Professors Karl F. Herzfeld, who suggested the problem, and Francis E. Fox for many helpful discussions and advice concerning this paper. The author also wishes to thank Dr. Maria Goeppert-Mayer for reading the manuscript.

TABLE V.

C−C distance A	R units	A_0	A_1	A_2	A_3
1.484	8.87	16.8063 ev	8.643 ev	5.370 ev	4.698 ev
1.450	8.67	16.8063	8.804	5.482	4.798
1.433	8.57	16.8063	8.882	5.543	4.850
1.417	8.47	16.8063	8.964	5.604	4.906
1.400	8.37	16.8063	9.046	5.664	4.958
1.383	8.27	16.8063	9.133	5.725	5.015
1.367	8.17	16.8063	9.215	5.790	5.071
1.333	7.97	16.8063	9.388	5.920	5.188
1.300	7.77	16.8063	9.570	6.054	5.309
notation of reference 9		*aa; aa*	*aa; bb*	*aa; cc*	*aa; dd*
		B_{12}	C_{12}	Q	T
1.484	8.87	3.651 ev	0.7063 ev	0.5365 ev	1.5204 ev
1.450	8.67	3.950	0.7902	0.6076	1.658
1.433	8.57	4.112	0.8384	0.6461	1.732
1.417	8.47	4.288	0.8925	0.6872	1.810
1.400	8.37	4.478	0.9527	0.7305	1.890
1.383	8.27	4.677	1.0133	0.7786	1.972
1.367	8.17	4.889	1.0800	0.8271	2.069
1.333	7.97	5.365	1.2330	0.9310	2.275
1.300	7.77	5.902	1.4000	1.1272	2.502
notation of reference 9		*ab; bb*	*ab; ab*	Q_{22}	Q_{12}

TABLE VI.

C−C distance A	C−C distance R units	σ_0	σ_1	σ_2	S_1
1.484	8.87	1.5232	1.1852	0.7572	0.2265
1.450	8.67	1.5584	1.1928	0.7422	0.2395
1.433	8.57	1.5767	1.1964	0.7347	0.2462
1.417	8.47	1.5958	1.1999	0.7269	0.2530
1.400	8.37	1.6153	1.2034	0.7189	0.2599
1.383	8.27	1.6356	1.2068	0.7108	0.2671
1.367	8.17	1.6564	1.2101	0.7025	0.2743
1.333	7.97	1.7003	1.2165	0.6852	0.2892
1.300	7.77	1.7469	1.2225	0.6672	0.3047

APPENDIX

The evaluation of the integrals that occur in this paper have been made by Sklar and Lyddane[9] for several values of R. The notation of Sklar and Lyddane is given in parenthesis following the notation used in this paper as defined in Section III(b). It was possible to obtain an interpolation for the atomic coulomb integrals which was good to four significant figures over the range given in Table I of Sklar and Lyddane.

$$A_1(aa;bb)=\frac{2}{R}-\frac{7.528}{R^{2.6}},$$

$$A_2(aa;cc)=A_1(\sqrt{3}R): \quad A_3(aa;dd)=A_1(2R).$$

The exchange integral, C_{12}, $(ab;ab)$, the hybrid coulomb-exchange integral, $B_{12}(ab;bb)$, and the exchange penetration integral, T, (Q_{12}) for atomic orbitals were obtained by extrapolation of curves drawn from the tables of Sklar and Lyddane. The coulomb penetration integral, $Q(Q_{22})$ was calculated in closed form as given by Sklar and Lyddane, Eq. (18). A consistent numerical error was noted in the values given in Table VI of reference 9. The numbers given in their Table VI are larger by a factor 2.34 than those given by their Eq. (18).

The resultant numerical values of the energy integrals occuring in this paper as function of R are given in Table V. The units are electron volts.

The normalization coefficients are defined as in the GMS paper thus:

$$\sigma_l=1+2S_1\cos\frac{2\pi l}{6}+2S_2\cos\frac{4\pi l}{6}+(-1)^l S_3, \quad (17)$$

where S_V are overlaps and were calculated from the closed form[10]

$$S_1=\int I(1)II(1)d\tau_1=\frac{6}{120}\left\{\exp\left(\frac{-R}{2}\right)\right\}\times\{(R^3+12R^2+60R+120)\}, \quad (18)$$

$$S_2=S_1(\sqrt{3}R), \quad S_3=S_1(2R).$$

The values of the normalization coefficients σ_0, σ_1, σ_2 and the overlap S_1 are given in Table VI.

The general expression for the coulomb and interaction integrals (see GMS) between molecular orbitals is given below. All interactions of electrons, except coulomb, on atoms farther apart than neighbors are neglected.

$$\gamma_{ll'}=\frac{1}{6\sigma_l\sigma_{l'}}\left\{A_0+2A_1+2A_2+A_3+4B_{12}\left(\cos\frac{2\pi l}{6}+\cos\frac{2\pi l'}{6}\right)+4C_{12}\left(\cos\frac{2\pi l}{6}\cos\frac{2\pi l'}{6}\right)\right\},$$

$$\delta_{ll'}=\frac{1}{36\sigma_l\sigma_{l'}}\left\{6A_0+12C_{12}+A_1\left(10\cos\frac{2\pi(l-l')}{6}+2\cos\frac{10\pi(l-l')}{6}\right)+B_{12}\left(20\cos\frac{2\pi l'}{6}+20\cos\frac{2\pi l}{6}+4\cos\frac{10\pi l'}{6}+4\cos\frac{10\pi l}{6}\right)+C_{12}\left(2\cos\frac{10\pi(l+l')}{6}+10\cos\frac{2\pi(l+l')}{6}\right)+A_3(6\cos\pi(l-l'))+A_2\left(4\cos\frac{8\pi(l-l')}{6}+8\cos\frac{4\pi(l-l')}{6}\right)\right\}. \quad (19)$$

[9] A. L. Sklar and R. H. Lyddane, J. Chem. Phys. **7**, 374 (1939).

[10] *Handbuch der Physik* (Verlagsbuchhandlung, Julius Springer, Berlin, 1933), Vol. XXIV, p. 643.

Equilibrium Atom and Free Radical Concentrations in Carbon Monoxide Flames and Correlation with Burning Velocities

CHARLES TANFORD[1] AND ROBERT N. PEASE
Department of Chemistry, Princeton University, Princeton, New Jersey

(Received March 5, 1947)

Calculations have been made of equilibrium concentrations of hydroxyl radicals and of hydrogen and oxygen atoms in moist carbon monoxide flames. Comparison with burning velocities, measured by Jahn by the Bunsen burner method, reveals a close correlation between observed burning velocities and such calculated hydrogen atom concentrations. Only a slight correlation exists with hydroxyl radical concentrations and none at all with calculated oxygen atom concentrations. A theoretical basis for these observations will be presented in a subsequent paper.

INTRODUCTION

WHILE early theories of burning velocity[2] were based entirely on heat conduction, recent studies[3,4] have emphasized the importance of diffusion as well. A difficulty in treating the latter has been the evaluation of concentrations of active particles (chain carriers) in the reaction mixture, for kinetic steady state calculations are limited by uncertainty as to the velocities of the elementary reactions which are occurring. There is, however, one set of concentrations which statistical methods allow us to compute with some certainty—namely, the equilibrium concentrations corresponding to the equilibrium flame temperature and over-all composition. It may perhaps be questioned whether such calculations correspond to reality, since combustion may not always proceed to thermodynamic equilibrium; nevertheless, it has seemed worth while to make such calculations and to explore in some well investigated case the possibility that a correlation might exist between these equilibrium concentrations and observed burning velocities.

A particularly suitable example is the combustion of moist carbon monoxide, on which an extensive series of measurements have been performed by Jahn,[5] using the Bunsen burner method first developed by Gouy.[6] Such measurements are open to some question;[7] however, the method and underlying assumptions are simple and certainly permit an estimate of relative velocities at the very least. Accordingly, we have computed for a number of the mixtures used by Jahn, the equilibrium flame temperatures and the corresponding concentrations of hydroxyl radicals and of hydrogen and oxygen atoms. These have been compared with Jahn's observed burning velocities.

METHOD OF CALCULATION

Equilibrium partial pressures of free radicals in flames can be calculated by use of appropriate equilibrium constants, provided that the flame temperature is known. (The concentrations of oxygen, carbon monoxide, and carbon dioxide, of course, are also assumed to be at equilibrium.) To evaluate this flame temperature a modification of the method of Lewis and von Elbe[8] has been used, involving a balancing of the heat of reaction to the final products (which will be partly dissociated into atoms and radicals) against the heat required to raise these products to the flame temperature. The flame temperature and the degrees of dissociation of the various product molecules are thus clearly interdependent, and a procedure involving trial and error must be adopted for the calculation.

The equilibrium constants used in the calculations reported in this paper have been taken from

[1] National Research Council Predoctoral Fellow in Chemistry, 1946–1947.
[2] E. Mallard and H. L. Le Chatelier, Ann. des Mines (8) **4**, 274 (1883).
[3] B. Lewis and G. von Elbe, J. Chem. Phys. **2**, 283 (1934).
[4] Y. Zeldovich and N. Semenov, J. Exp. Theoret. Phys. U.S.S.R. **10**, 1116 (1940). Translation in N.A.C.A. Tech. Memo. No. 1084 (1946).
[5] G. Jahn, *Der Zündvorgang in Gasgemischen* (Oldenbourg, Berlin, 1942).
[6] M. Gouy, Ann. Chim. Phys. (5) **18**, 1 (1879).
[7] B. Lewis and G. von Elbe, J. Chem. Phys. **11**, 75 (1943).
[8] B. Lewis and G. von Elbe, Phil. Mag. **20**, 44 (1935).

TABLE I. Free radical concentrations and burning velocities in carbon monoxide flames.

Composition	Flame temperature (calc.) °K	Equilibrium partial pressures of radicals (calc.) P_O atm. $\times 10^3$	P_{OH} atm. $\times 10^4$	P_H atm. $\times 10^4$	Burning velocity (Jahn) cm/sec.
35% CO,* 8.5% O_2, 56.5% N_2	1730	—	0.016	0.11	25.5
26.5% CO,* 44.1% O_2, 29.4% N_2	2320	1.14	20.6	0.68	29.5
40% CO,** 12.6% O_2, 47.4% N_2	2320	0.12	3.4	2.5	30
40% CO,* 12.6% O_2, 47.4% N_2	2320	0.11	4.9	3.8	40
40% CO,** 59.1% O_2, 0.9% N_2	2720	28	56	5.6	48
40% CO,* 24% O_2, 36% N_2	2660	10.5	56	11.6	50.5
45% CO,* 22% O_2, 33% N_2	2710	10.0	58	16.0	57
40% CO,* 59.1% O_2, 0.9% N_2	2720	28	88	9.2	60
60% CO,** 39.4% O_2, 0.6% N_2	2930	42	86	24	68
50% CO,* 30% O_2, 20% N_2	2810	22	91	24	72
80% CO,** 19.7% O_2, 0.3% N_2	2860	7.6	39	29	72
60% CO,* 24% O_2, 16% N_2	2850	17.6	90	38	83
60% CO,* 39.4% O_2, 0.6% N_2	2930	42	134	39	93
70% CO,* 24% O_2, 6% N_2	2900	20.3	102	52	98
80% CO,* 19.7% O_2, 0.3% N_2	2860	10.0	78	59	106

* CO contains 1.35% H_2O and 1.5% H_2.
** CO contains 1.35% H_2O.

the convenient compilation of Lewis and von Elbe,[9] except those involving hydroxyl radical. The latter have been recalculated by the authors on the basis of Dwyer and Oldenberg's new value for the heat of dissociation of water into hydroxyl and hydrogen.[10] Heat content functions required in the calculations have been taken from tables prepared at the Bureau of Standards.[11]

CALCULATIONS FOR CARBON MONOXIDE FLAMES

It is interesting first to consider Jahn's experiments upon the addition of small amounts of hydrogen to moist mixtures of carbon monoxide with air or oxygen.[5] Jahn observed in each case that such addition caused an increase in burning velocity. Similar increases have been reported by other workers upon the addition of small amounts of water vapor to dry carbon monoxide flames.[12, 13]

We have calculated equilibrium partial pressures of free radicals for a number of Jahn's mixtures and have found, significantly, that the equilibrium partial pressures of hydroxyl radicals and of hydrogen atoms always increase upon the addition of molecular hydrogen. To take just one example (the figures come from Table I): in a mixture of 60 percent moist carbon monoxide with 39.4 percent oxygen and 0.6 percent nitrogen the equilibrium partial pressure of hydrogen atoms is 2.4×10^{-3} atm.; upon the addition of 1.5 percent of hydrogen to the carbon monoxide this figure rises to 3.8×10^{-3} atm. The corresponding figures for hydroxyl radical concentration are 0.86×10^{-2} and 1.3×10^{-2} atm., respectively. The observed burning velocities are 68 cm/sec. without hydrogen and 93 cm/sec. with hydrogen. It should be noted that the equilibrium partial pressures of oxygen atoms do not undergo important changes upon hydrogen addition.

This series of experiments on the addition of hydrogen is particularly crucial because no variables which can be thought of as directly affecting the burning velocity, other than these free radical concentrations, are appreciably altered by such addition. Thus the flame temperature, when calculated to the nearest 10°, is completely unchanged, and changes in thermal and diffusion properties can be only very slight.

It is clearly desirable to extend these calculations to cover the whole range of moist carbon monoxide flames examined by Jahn. Table I contains a series of such calculations for a variety

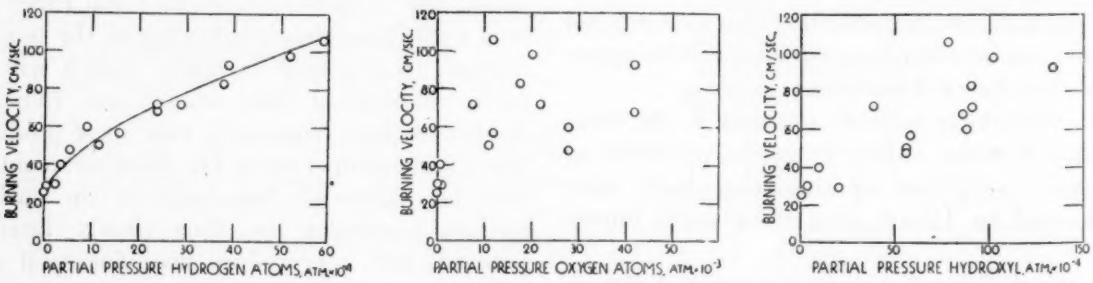
BURNING VELOCITY, CM/SEC.
PARTIAL PRESSURE HYDROGEN ATOMS, ATM.×10⁴
PARTIAL PRESSURE OXYGEN ATOMS, ATM.×10⁻³
PARTIAL PRESSURE HYDROXYL, ATM.×10⁻⁴

FIG. 1. Correlation between burning velocity and free radical concentrations.

[9] B. Lewis and G. von Elbe, *Combustion, Flames and Explosions of Gases* (Cambridge University Press, England, 1938), p. 380.
[10] R. J. Dwyer and O. Oldenberg, J. Chem. Phys. **12**, 351 (1944).
[11] D. D. Wagman, J. E. Kilpatrick, W. J. Taylor, K. S. Pitzer, and F. D. Rossini, J. Research Nat. Bur. Stand. **34**, 143 (1945).
[12] L. Ubbelohde and O. Dommer, J. Gasbel. **57**, 757, 781 (1914).
[13] E. F. Fiock and C. H. Roeder, N.A.C.A. Reports 532 (1935), 553 (1936).

of mixtures, varying from rich mixtures with only one-half the stoichiometric amount of oxygen to lean mixtures with three times the stoichiometric oxygen content. Moreover, the ratio of oxygen to nitrogen varies from 1:4 to 65:1, and mixtures with and without added hydrogen are included. The last column of Table I contains Jahn's experimental burning velocities, and in Fig. 1 these have been plotted against values of the partial pressures of hydroxyl radicals and of hydrogen and oxygen atoms. It is apparent that no correlation exists between burning velocity and oxygen atom concentration, and a slight one at best between burning velocity and hydroxyl radical concentration. On the other hand, a striking correlation is seen to exist between burning velocity and hydrogen atom concentration.

That such a correlation should exist for hydrogen atom concentration, but not for oxygen atom or hydroxyl radical concentration, is not unexpected. For, if the extent to which free radicals in the flame can be utilized in the combustion process depends upon diffusion—and it is logical to make such a supposition—the effect of hydrogen atoms, because of their very high rates of diffusion, will overshadow that of any of the other radicals. It would further appear that if such a correlation exists in carbon monoxide flames, it should also hold true for pure hydrogen flames. Preliminary calculations show that this is indeed true, and further work on such flames is planned.

Another paper will be presented in the very near future which will suggest a theoretical basis for the results outlined above.

THE JOURNAL OF CHEMICAL PHYSICS VOLUME 15, NUMBER 7 JULY, 1947

Theory of Burning Velocity. I. Temperature and Free Radical Concentrations Near the Flame Front, Relative Importance of Heat Conduction and Diffusion[1]

CHARLES TANFORD[2]
Department of Chemistry, Princeton University, Princeton, New Jersey
(Received April 21, 1947)

A previous paper having suggested that hydrogen atoms play an important part in combustion, an investigation is made of the relative importance of heat conduction and diffusion in establishing concentrations of hydrogen atoms near the flame front. To do this, differential equations are set up for heat transfer and for material transport. These equations are solved for two typical mixtures, one containing moist carbon monoxide, the other containing hydrogen. It is shown that the temperature falls rapidly as the distance from the flame front increases, and that the local thermal equilibrium concentration of hydrogen atoms, being a negative exponential of that temperature, falls more rapidly still. On the other hand, the local non-equilibrium concentration of hydrogen atoms, which is caused by diffusion from the flame front into unburnt gas, falls only slowly with distance. It is thus concluded that diffusion plays a more important role than heat transfer.

INTRODUCTION

IT has already been suggested by Lewis and von Elbe[3] that the diffusion of atoms and free radicals is more important than heat conduction in initiating combustion. This idea received support in a communication from this laboratory[4] in which calculations were made of equilibrium atom and free radical concentrations in moist carbon monoxide flames for points at which combustion has proceeded adiabatically to equilibrium. It was shown that there exists a very close correlation between such calculated hydrogen atom concentrations and experimentally

[1] Abstracted in part from a thesis submitted in partial fulfillment of the requirements for the degree of Doctor of Philosophy at Princeton University.
[2] National Research Council Predoctoral Fellow in Chemistry, 1946–47.
[3] B. Lewis and G. von Elbe, J. Chem. Phys. **2**, 537 (1934).
[4] C. Tanford and R. N. Pease, J. Chem. Phys. **15**, 431 (1947).

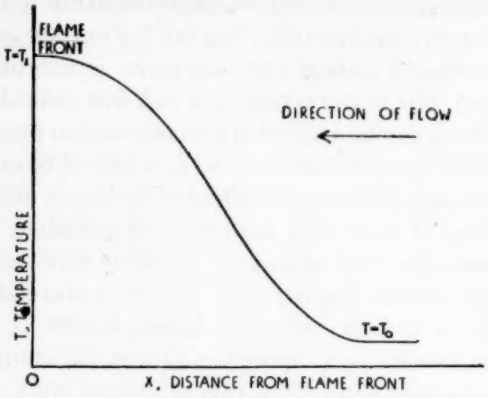

FIG. 1. Flame front and combustion zone.

determined burning velocities. Less correlation was found for hydroxyl radicals, and none at all for oxygen atoms. This observation is a reasonable one if we suppose that the extent to which free radicals in the flame can be utilized for flame propagation depends upon diffusion, for then the effect of hydrogen atoms, because of their very high rate of diffusion, will overshadow that of any other free radicals.

On the other hand, this correlation is not readily explained by theories of burning velocity based upon heat conduction,[5] for, according to such theories, the burning velocity depends upon the rate at which unburnt gas can be ignited by heat conducted from the flame front (which in this paper is defined as the surface of the flame where combustion has gone to equilibrium). From our present knowledge of combustion processes we would interpret the ignition of gas mixtures by heat conduction as caused by the formation by thermal dissociation of a local concentration of atoms or free radicals high enough to initiate and maintain a chain process leading to combustion.

Thus two alternative pictures of combustion processes present themselves: (1) that the unburnt gas is ignited by free radicals produced locally by thermal dissociation following heat conduction, and (2) that it is ignited by free radicals supplied to the unburnt gas by diffusion from the flame front. It is clearly of advantage to investigate these possibilities more thoroughly.

Accordingly, we have in this paper set up an equation for heat transfer by means of which the static temperature at any point in the combustion zone can be obtained. From a knowledge of this temperature the thermal equilibrium concentration of any free radical at any point can be calculated. Similarly, we have set up an equation for material transport, from which, if we know the equilibrium concentration of any free radical at the flame front, we can calculate the stationary diffusion concentration of such a radical at any other point in the combustion zone.

It will be shown that in two typical and common cases such stationary non-equilibrium concentrations of hydrogen atoms are much higher than thermal concentrations. Hence in these cases heat conduction cannot play a major role in the determination of burning velocities, which are more probably determined entirely by diffusion of hydrogen atoms from the flame front.

THE TEMPERATURE DISTRIBUTION

In order to obtain the temperature distribution in the vicinity of the flame front we consider the simple model illustrated in Fig. 1. Let the reaction zone be stationary with respect to the coordinate system $x-T$. Then the unburnt gas, initially at the temperature T_0, moves in the direction of the arrow towards the flame front, which is taken as the point where $x=0$ and where the temperature is the equilibrium flame temperature, T_1. The flow is taken normal to the flame front, so that in the cold unburnt gas ($T=T_0$) the flow velocity must be the burning velocity as defined in the usual manner.[6] It is here designated by the symbol u_0.

We now set up the differential equation for heat transfer, considering at each point (1) the motion of the gas stream, which tends to replace gas of temperature $T(x)$ by cooler gas, and the opposing processes (2) of heat conduction from left to right along the negative temperature gradient, and (3) of heat release by chemical reaction. To obtain the equation for the steady temperature we must find expressions for the rate of change of temperature at any point by each of these three processes, and equate the sum of these changes to zero.

[5] E. Mallard and H. L. Le Chatelier, Ann. Mines **4**, 274 (1883), and subsequent modifications.

[6] W. Jost, *Explosions- und Verbrennungsvorgänge in Gasen* (Verlagsbuchandlung Julius Springer, Berlin, 1939), p. 63.

Taking first the rate of change of temperature due to gas motion, we consider a volume element $dS \cdot dx$, parallel to an element dS of the flame front. The gas streaming towards the flame front will replace gas in this element, of temperature T, by that in an adjoining element, of temperature $T+(\partial T/\partial x)dx$, in a time $dt=dx/u$. Hence, per second,

$$\left(\frac{\partial T}{\partial t}\right)_1 = \frac{\partial T}{\partial x}dx \Big/ \frac{dx}{u} = u\frac{\partial T}{\partial x}. \tag{1}$$

The rate of change of temperature due to heat conduction is given by Fourier's equation. Where c, the specific heat, and k, the thermal conductivity, are regarded as constant over the whole combustion zone, we obtain, where ρ is the density at any point,

$$(\partial T/\partial t)_2 = (k/c\rho)(\partial^2 T/\partial x^2). \tag{2}$$

Finally, the rate of change of temperature due to the release of chemical energy can be expressed in terms of a variable λ, which defines the progress of the chemical reaction (as measured by the heat release) as a function of x. The variable λ is equal to zero at all points outside the combustion zone (i.e., where x is sufficiently large) and is equal to unity where $x=0$. If Q is defined as the total amount of heat released in the combustion of one gram of unburnt gas, then, if we consider again a volume element $dS \cdot dx$, the amount of heat released per second in this element must be the mass of gas passing through the element per second ($\rho u dS$), multiplied by the factor $-Q(\partial\lambda/\partial x)dx$. This amount of heat released per second must be equal to the rate of change of temperature in the element multiplied by the mass of gas in the element ($\rho dSdx$) multiplied by the specific heat, i.e.,

$$(\partial T/\partial t)_3 c\rho dSdx = -Q(\partial\lambda/\partial x)\rho u dSdx,$$

or

$$(\partial T/\partial t)_3 = -(Qu/c)(\partial\lambda/\partial x). \tag{3}$$

Adding Eqs. 1, 2, and 3, equating to zero, and replacing partial by total derivatives, we obtain

$$\frac{k}{c\rho}\cdot\frac{d^2T}{dx^2} + u\frac{dT}{dx} - \frac{Qu}{c}\frac{d\lambda}{dx} = 0.$$

Multiplying by $c\rho/k$, and introducing the condition of conservation of mass, $\rho u = \text{constant} = \rho_0 u_0$, this reduces to

$$\frac{d^2T}{dx^2} + \frac{c\rho_0 u_0}{k}\frac{dT}{dx} - \frac{Q\rho_0 u_0}{k}\frac{d\lambda}{dx} = 0. \tag{4}$$

To solve this equation it becomes necessary to make an assumption regarding $d\lambda/dx$. Two simple ones suggest themselves: (a) all heat is released at the flame front ($x=0$) and none elsewhere, so that $d\lambda/dx$ vanishes except at $x=0$; (b) the chemical reaction proceeds evenly over the whole of the combustion zone, which shall be taken to be of thickness δ, so that $d\lambda/dx$ becomes equal to a constant, $-1/\delta$. The true state of affairs is certainly intermediate between these two assumptions. Assumption (a) can therefore be expected to yield too steep a temperature gradient, while assumption (b) probably results in too gradual a drop. In practice it will be found that the results obtained by use of these two assumptions do not differ very greatly, so that a fairly close estimate of the true temperature at any point can be obtained.

Under these two assumptions, Eq. 4 reduces, respectively, to

$$(d^2T/dx^2) + A(dT/dx) = 0, \tag{5a}$$

or to

$$(d^2T/dx^2) + A(dT/dx) + AB = 0, \tag{5b}$$

where A and B are used to designate the products $c\rho_0 u_0/k$ and $Q/c\delta$, respectively. It should be noted that Eq. (5b) applies only between the limits $0 \leq x \leq \delta$; where $x > \delta$ no heat is released, and Eq. (5a) must be applied also to the case of assumption (b).

To solve these equations we must introduce the boundary conditions, $T=T_1$ where $x=0$, and $dT/dx=0$ where $T=T_0$. In the case of assumption (b) we must in addition specify that T and dT/dx are continuous at the point $x=\delta$. The two solutions then become: for assumption (a)

$$(T-T_0) = (T_1-T_0)e^{-Ax}, \tag{6a}$$

and for assumption (b)

$$(T-T_0) = \{T_1-T_0-B(1/A+\delta)\}e^{-Ax} - Bx + B(1/A+\delta), \tag{6b}$$

where Eq. (6b) applies for $0 \leq x \leq \delta$. The solution

TABLE I. Data for combustible mixtures.

	Mixture No. 1	Mixture No. 2
Composition	60% CO,[a] 39.4% O_2, 0.6% N_2	40% H_2, 24% O_2, 36% N_2
T_1, °K[b]	2930	2750
T_0, °K	298	298
ρ_0, g/cc[c]	1.22×10^{-3}	7.6×10^{-4}
u_0, cm/sec.[d]	68	362
c, cal./g °C[e]	0.29	0.43
k, cal./sec. cm °C	1.95×10^{-4}	4.0×10^{-4}
Q, cal./g[b]	795	1015
δ, cm	0.01	0.005
$A=c\rho_0u_0/k$	123	296
$B=Q/c\delta$	2.74×10^5	4.72×10^5
p_H, atmos.[b]	2.4×10^{-3}	1.35×10^{-2}
D_0, cm²/sec.[g]	1.95	2.75
B' (see Eq. (16))	1.35	1.13

[a] CO contains 1.35 percent H_2O.
[b] Calculated as shown in reference 4.
[c] Density at 1 atmos. and 298°K.
[d] Jahn, *Der Zündvorgang in Gasgemischen* (Oldenbourg, Berlin, 1934).
[e] Estimate from values given by Wagman, Kilpatrick, Taylor, Pitzer, and Rossini, J. Research Nat. Bur. Stand. **34**, 143 (1945).
[f] Extrapolation and estimate for mixtures from values given by McAdams, *Heat Transmission* (McGraw-Hill Book Company, Inc., New York, 1942).
[g] Calculated from Stefan-Maxwell equation, using molecular radii from Chapman and Cowling, *The Mathematical Theory of Non-Uniform Gases* (Cambridge University Press, England, 1939), p. 248; and the value 0.53A (the Bohr radius) for the hydrogen atom. Values for mixtures obtained by suitable interpolation.

for $x>\delta$ is

$$(T-T_0)=\{T_1-T_0-B(1/A+\delta)+(B/A)e^{A\delta}\}e^{-Ax}. \quad (6c)$$

Equations (6a), (6b), and (6c) have been used to evaluate the temperature distributions of two typical mixtures, one containing moist carbon monoxide, the other containing hydrogen, for both of which experimental values of the burning velocity are available. Estimates of 0.01 and 0.005 cm, respectively, have been made for the thickness of the flame front, these being the distances beyond which the lower limit of the temperature falls below 1000°K.[7] Other data used in the evaluation (as well as those used in the diffusion calculation below) are listed in Table I, together with references to the sources from which they have been obtained.

The resulting temperature distributions are plotted in Figs. 2 and 3. The lower limit of the temperature distribution is probably closer to the truth than the upper limit, for the velocities of any rate-determining chemical reactions must increase exponentially with temperature, with the result that the heat release is probably concentrated much closer to the flame front than has been supposed in assumption (b).

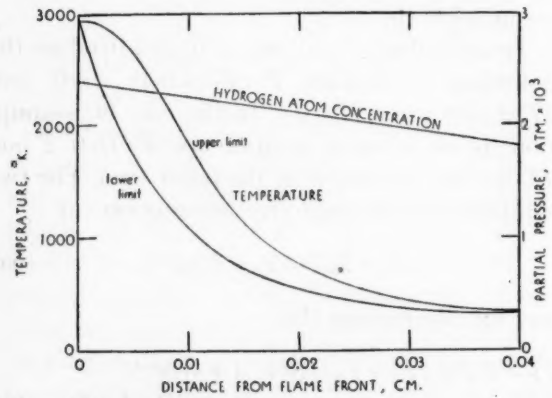

FIG. 2. Temperature and hydrogen atom concentration near flame front in carbon monoxide mixture (mixture No. 1).

RADICAL CONCENTRATION DUE TO DIFFUSION

In order to obtain the concentration of any free radical at any point in the combustion zone and due to diffusion from the flame front, it is necessary first to calculate the equilibrium partial pressure, p, of the radical at the flame front, using the method described in our previous paper.[4] A differential equation for material transport can then be set up, similar to that for heat transfer given above. Unfortunately, if this equation is set up in rigorous form, with the temperature gradient taken into account, it becomes insoluble by ordinary means. Thus it becomes necessary to simplify the problem by assuming that the flame front and the whole combustion zone are all at

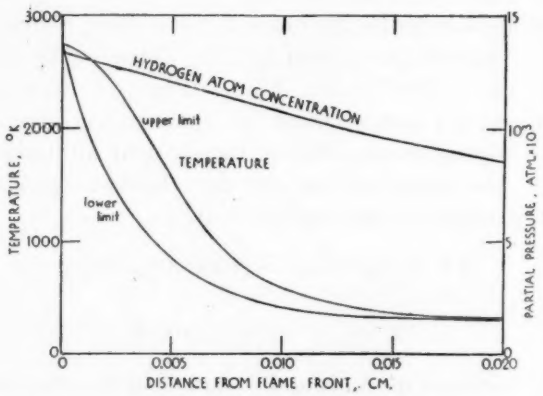

FIG. 3. Temperature and hydrogen atom concentration near flame front in hydrogen mixture (mixture No. 2).

[7] These are extreme estimates. Most observers give smaller values, e.g. Lewis and von Elbe, reference 3, compute a thickness of 10^{-3} to 10^{-4} cm. Use of such a small value would, of course, bring the upper limit of the temperature obtained by us even closer to the lower limit.

one constant mean temperature, T_m, which we shall take, in general, to be some fraction of the flame temperature. The effect of such a simplification is to give to the density and the flow velocity values ρ_m and u_m, which are constant over the entire combustion zone.

As in the case of heat transfer, we now enumerate the changes in radical concentration, c, taking place at any point, and, since we are interested in the steady state, equate the sum of these changes to zero. The changes in radical concentration which we must consider are (1) those due to the motion of the gas stream, which tends to replace gas of radical concentration $c(x)$ by gas with a smaller concentration, (2) those due to chemical processes, and (3) those due to diffusion.

Taking first the rate of change due to gas motion: by reasoning exactly analogous to that used in the case of heat transfer we get

$$(\partial c/\partial t)_1 = u_m(\partial c/\partial x). \tag{7}$$

Next, the chemical processes: these may be of zero, first, or second order with respect to the radical concentration. Since the differential equation which we shall obtain will be non-linear if we include terms in c^2, it will be necessary to estimate the rates of second-order processes relative to the first order processes and to take them into account in the first-order term. Zero-order terms can be taken care of without difficulty where they occur: they are of no importance in the cases which we shall discuss in this paper, and so are omitted for the sake of simplicity. The net effect of chemical reactions is then described by a term

$$(\partial c/\partial t)_2 = A'c, \tag{8}$$

where A' is negative if there is a net loss of radicals because of chemical reaction.

Finally, Fick's equation gives the rate of increase of radical concentration due to diffusion from left to right. Where D_m is used to designate the diffusion coefficient of a given radical into unburnt gas at the temperature T_m, we have

$$(\partial c/\partial t)_3 = D_m(\partial^2 c/\partial x^2). \tag{9}$$

We now add Eqs. (7)–(9) and equate to zero. Since x is our only independent variable, we can replace partial by total derivatives, and so obtain

$$D_m(d^2c/dx^2) + u_m(dc/dx) + A'c = 0. \tag{10}$$

At the point $x=0$ the partial pressure of any free radical, and, hence, the corresponding concentration, c_1, are known. Also, as x becomes large, both c and dc/dt tend to zero. Allowing for these boundary conditions, and giving to A' an average value independent of x, we can solve Eq. (10) and obtain

$$c = c_1 \times \exp\left(-\{\tfrac{1}{2}[1+(1-4A'D_m/u_m^2)^{\frac{1}{2}}]\}\frac{u_m x}{D_m}\right); \tag{11}$$

or

$$c = c_1 \exp(-B'u_m x/D_m), \tag{12}$$

where we have replaced the expression in brackets in Eq. (11) by the symbol B'. We see that where changes in radical concentration due to chemical processes are negligible, i.e., where A' vanishes, B' is equal to unity.

Since hydrogen atoms appear to be the most important free radicals in the combustion of hydrogen and carbon monoxide,[4] we shall evaluate by means of Eq. (12) the concentrations of hydrogen atoms in the two mixtures already discussed above. To do so we must first find appropriate expressions for B'.

Of the possible reactions involving hydrogen atoms, only two are probably fast enough to have an appreciable effect upon the hydrogen atom concentration. These are

$$H + O_2 + M \rightarrow HO_2 + M \tag{I}$$

and

$$H + H + M \rightarrow H_2 + M, \tag{II}$$

where M represents any third body.[8] From a knowledge of the rates of these reactions it will be possible to evaluate A' (Eq. (11)), and, hence, B'.

The rate of disappearance of hydrogen atoms by reaction (I) is most conveniently expressed by

$$-dc_H/dt = k_1 q_M q_{O_2} c_H, \tag{13}$$

where q_M is the mole fraction (total pressure one atmosphere) of all possible third bodies, which is, of course, equal to unity, while q_{O_2} is a mean value of the oxygen mole fraction over the reac-

[8] V. Kondratev, [Bull. acad. sci. U.R.S.S., Classe sci. chim. 501 (1940)] and others have shown that the reactions $OH + CO \rightarrow CO_2 + H$, and $OH + H_2 \rightarrow H_2O + H$ are slow compared with I. G. von Elbe and B. Lewis (reference 9) arrive at a slow rate for HO_2 formation in the absence of a third body.

tion zone. The rate constant k_1 is then in units of sec.$^{-1}$. Now von Elbe and Lewis[9] give for the three-body reaction $H+O_2+M$ a rate constant of 0.81×10^{13} cm^6 mole^{-2} sec.$^{-1}$ (298°K) where the third body is hydrogen, and about one-third of that where the third body is oxygen or nitrogen. There is apparently no change in the rate constant with temperature. For mixture No. 1, therefore, which consists largely of O_2, N_2, and CO (cf. Table I), the best value of this rate constant is probably about 0.3×10^{13} cm^6 mole^{-2} sec.$^{-1}$. Converting to the units of k_1 by multiplication by $L^2/N^2\theta_m^2$, where N is Avogadro's number, L is the number of molecules per cc at room temperature, and θ_m is T_m/T_0, the ratio of the mean temperature to room temperature, we obtain $k_1=6000/\theta_m^2$. For mixture No. 2 a similar estimate yields $k_1=11{,}000/\theta_m^2$. Hence, by comparison of Eq. (13) with Eq. (8), the contribution of reaction (I) to A' must be, for mixture No. 1,

$$A_1'=-\frac{6000}{\theta_m^2}q_{O_2} \tag{14}$$

while A' for mixture No. 2 is 11/6 of this expression.

The rate of disappearance of hydrogen atoms by the recombination reaction (II) is

$$-dc_H/dt=2k_2'q_Mc_H^2,$$

the number 2 indicating that two hydrogen atoms are lost per successful collision. Since, as has already been mentioned, we must make this expression first order with respect to the hydrogen atom concentration, c_H, we shall introduce in place of one of the terms c_H an average hydrogen atom concentration. Choosing for this one-half the equilibrium concentration at the flame front, and again expressing in the most convenient units, we obtain

$$-dc_H/dt=k_2q_Mp_Hc_H,$$

where q_M is again equal to unity, and p_H is the equilibrium partial pressure of hydrogen atoms at the flame front. Steiner[10] has found the rate constant of reaction (II) to be 1.1×10^{16} cm^6 mole^{-2} sec.$^{-1}$. Again converting to the proper units we obtain $k_2=2.2\times10^7/\theta_m^2$, i.e., the contribution of reaction (II) to A′, for both mixtures 1 and 2, is

$$A_2'=-\frac{2.2\times10^7}{\theta_m^2}p_H. \tag{15}$$

Adding contributions (14) and (15), we obtain for the correction term B', for mixture No. 1,

$$B'=\tfrac{1}{2}\left\{1+\left[1+\frac{24{,}000D_0}{u_0^2\theta_m^2}(q_{O_2}+3700p_H)\right]^{\frac{1}{2}}\right\}, \tag{16a}$$

and for mixture No. 2,

$$B'=\tfrac{1}{2}\left\{1+\left[1+\frac{44{,}000D_0}{u_0^2\theta_m^2}(q_{O_2}+2000p_H)\right]^{\frac{1}{2}}\right\}. \tag{16b}$$

Equation 12, with the proper expressions for B', has been applied to the two mixtures discussed in the last section. For θ_m we have used the value $0.7T_1/T_0$, for D_m we have used the value $D_0\theta_m^2$, where D_0 is the diffusion coefficient for hydrogen atoms into the unburnt gas at room temperature, and for u_m we have used the value $u_0\theta_m$, where u_0 is the normal flow velocity of the unburnt gas, i.e. the burning velocity. A value for q_{O_2} has been estimated from initial and final compositions; all other necessary numerical data are contained in Table I.

The resulting hydrogen atom concentrations are given in the last column of Table II and are plotted in Figs. 2 and 3. It is seen that the hydrogen atom concentration changes with distance more slowly than does the temperature. This is not unexpected, since the conduction of heat, depending on the mean free path of an average molecule, is less efficient than the diffusion of hydrogen atoms, which depends on the relatively large mean free path of hydrogen atoms.

It should be remembered that these radical concentrations have been obtained on the assumption of a constant temperature, T_m, over the whole combustion zone. The effect of this assumption has been to steepen the concentration curve very near the flame front, and to flatten it at greater distances.

RELATIVE IMPORTANCE OF HEAT CONDUCTION AND DIFFUSION

As was mentioned in the introduction, these calculations have been made not only for their

[9] G. von Elbe and B. Lewis, J. Chem. Phys. **7**, 710 (1939).
[10] W. Steiner, Trans. Faraday Soc. **31**, 623 (1935).

own intrinsic interest, but also to decide whether the ignition of unburnt gas approaching the flame front is more likely to be caused by hydrogen atoms or other free radicals produced thermally (heat conduction theory), or by hydrogen atoms supplied by diffusion from the flame front. Hence it is desirable to compare the calculated hydrogen atom concentrations due to diffusion with local equilibrium concentrations to be expected from thermal dissociation.

To estimate the latter, a maximum value of the molecular hydrogen concentration has been assumed for every point. For mixture No. 1, which has no hydrogen present initially, we have taken this concentration to be the equilibrium concentration due to water dissociation at the flame temperature; for mixture No. 2 we have assumed that all of the molecular hydrogen initially present remains unchanged up to a distance of 0.001 cm from the flame front. For both mixtures the equilibrium constants for hydrogen dissociation given by Lewis and von Elbe[11] have then been used to calculate the thermal hydrogen atom concentrations. Since the molecular hydrogen concentrations are maximum values, the atomic concentrations will also be maximum ones.

Figures for such a comparison, for the two mixtures already discussed, are given in Table II, in which are listed, for various distances from the flame front, the temperature half-way between the upper and lower limits (Figs. 2 and 3), the equilibrium thermal hydrogen atom concentration at that temperature, and, finally, the hydrogen atom concentration due to diffusion. It is seen that the thermal equilibrium concentration, being a negative exponential of the temperature, drops with extraordinary rapidity. The diffusion concentration, however, drops only very slowly.

It is clear from Table II that heat conduction is not a factor of importance in establishing hydrogen atom concentrations in unburnt gas approaching a combustion zone, but that such atom concentrations are more probably determined entirely by diffusion from the flame front. It should be mentioned that no consideration has been given here to the possibility of a maximum in the hydrogen atom concentration at a point other than the flame front, due to chain branching. Such a maximum is unlikely to occur for hydrogen atoms, however, because of the high rates of three-body recombination and reaction to form HO_2.

TABLE II. Hydrogen atom concentrations due to thermal dissociation and to diffusion.

		Partial pressure H atoms, atmos.	
x, cm	T, °K	Therm. dissoc. (Maximum value)	Diffusion
		Mixture No. 1	
0	2930	2.4×10^{-3}	—
0.002	2630	8.5×10^{-4}	2.4×10^{-3}
0.004	2330	2.3×10^{-4}	2.3×10^{-3}
0.006	2030	4.0×10^{-5}	2.3×10^{-3}
0.008	1740	4.4×10^{-6}	2.3×10^{-3}
0.010	1460	2.2×10^{-7}	2.2×10^{-3}
0.012	1200	4×10^{-9}	2.2×10^{-3}
0.014	1000	5×10^{-11}	2.2×10^{-3}
0.016	850	5×10^{-13}	2.2×10^{-3}
0.018	720	2×10^{-15}	2.1×10^{-3}
0.020	630	1×10^{-17}	2.1×10^{-3}
		Mixture No. 2	
0	2750	1.35×10^{-2}	—
0.001	2390	9.6×10^{-3}	1.32×10^{-2}
0.002	2060	5.2×10^{-3}	1.29×10^{-2}
0.003	1760	1.8×10^{-4}	1.26×10^{-2}
0.004	1480	9.6×10^{-6}	1.23×10^{-2}
0.005	1200	2×10^{-7}	1.20×10^{-2}
0.006	970	1×10^{-9}	1.17×10^{-2}
0.007	800	2×10^{-12}	1.15×10^{-2}
0.008	680	6×10^{-15}	1.12×10^{-2}
0.009	580	6×10^{-18}	1.09×10^{-2}
0.010	500	6×10^{-21}	1.07×10^{-2}

A quantitative theory for burning velocity based upon the concept that diffusion from the flame front is the determining factor, and utilizing some of the equations derived in this paper, will be presented in the near future.

ACKNOWLEDGMENTS

The author wishes to express his gratitude to Professor Robert N. Pease for his advice and for much helpful discussion in the preparation of this paper, as well as to Professor Walter Kauzmann for reading and pointing out some errors in the manuscript.

[11] B. Lewis and G. von Elbe, *Combustion, Flames and Explosions of Gases* (Cambridge University Press, England, 1938), p. 382.

Separation of the Nitrogen Isotopes by the Exchange Reaction between Ammonia and Solutions of Ammonium Nitrate*

ISIDOR KIRSHENBAUM,[1] JAMES S. SMITH,[2] THOMAS CROWELL, JACOB GRAFF, AND ROBERT MCKEE
Columbia University, New York, New York

(Received April 7, 1947)

The fractionation factor for the exchange reaction between ammonia and ammonium nitrate was determined as a function of the dissolved ammonia content. It was found that for a stock solution containing 59.3–59.6 percent ammonium nitrate

$$\alpha = -0.029M + 1.034,$$

where α is the fractionation factor at 25°C and M the fraction (Moles NH_3)/(Moles NH_3 + Moles NH_4NO_3), in solution. From these data, the equilibrium constant for the exchange reaction

$$N^{14}H_4^+(sol) + N^{15}H_3(gas) \rightleftharpoons N^{15}H_4^+(sol) + N^{14}H_3(gas)$$

was calculated to be 1.034, while that for the reaction

$$N^{14}H_3(sol) + N^{15}H_3(gas) \rightleftharpoons N^{15}H_3(sol) + N^{14}H_3(gas)$$

was found to be 1.005. Vapor pressure and density data were determined for the ammonia-ammonium nitrate solutions as a function of the ammonia concentration.

INTRODUCTION

UREY and co-workers[3–6] have studied the exchange reaction as a means of concentrating the nitrogen isotopes. They have shown that high concentrations of N^{15} can be obtained by the use of this exchange reaction in a cascade of packed columns operating as a counter-current system. The data obtained indicate that the fractionation factor

$$\alpha = \left[\frac{N^{14}}{N^{15}}\right]_{gas} \Big/ \left[\frac{N^{14}}{N^{15}}\right]_{sol}$$

is larger the greater the concentration of NH_4^+ ion in solution. Thus the fractionation factor obtained by using a 60 percent ammonium nitrate solution in water with a total pressure over the solution of 180 mm of Hg was about 1.021 as compared to a value of only 1.012 for a 15 percent ammonium sulfate solution with a pressure of 200 mm of Hg. Additional data taken from the paper by Urey, Huffman, Thode, and Fox[4] are summarized in Table I. It is for this reason, and also because the more concentrated the NH_4^+ solution the smaller the fractionating columns need be for a given throughput of NH_4^+, that it was found advisable to use ammonium nitrate as the ammonium salt. Ammonium nitrate has a solubility of about 60 percent by weight at room temperature.

TABLE I. Effect of NH_4^+ concentration upon the fractionation factor.

Weight % $(NH_4)_2SO_4$ in stock solution	Fractionation factor (α)
0	1.006
5	1.0067
14	1.012
31	1.021
34	1.022

For proper design of a plant for the separation of the nitrogen isotopes by means of the exchange between ammonia and ammonium nitrate, it is necessary to know the fractionation factor as accurately as possible. This is so because the size of the plant, and therefore its cost, and perhaps feasibility, is inversely proportional to $(\alpha - 1)^2$. Three different values have been re-

* This paper is based on the work performed under Contract No. W-7405-eng-50 for the Manhattan Project at Columbia University.

[1] Present Address: Standard Oil Development Company, Research Division, Elizabeth, New Jersey.

[2] Present Address: E. I. DuPont de Nemours and Company, Inc., Towanda, Pennsylvania.

[3] H. C. Urey and A. H. W. Aten, Jr., Phys. Rev. **50**, 575 (1936).

[4] H. C. Urey, J. R. Huffman, H. G. Thode, and M. Fox, J. Chem. Phys. **5**, 856 (1937).

[5] H. G. Thode, J. E. Gorham, and H. C. Urey, J. Chem. Phys. **6**, 296 (1938).

[6] H. G. Thode and H. C. Urey, J. Chem. Phys. **7**, 34 (1939).

ported for the fractionation factor for the exchange between ammonia and ammonium ion. Urey and Aten[3] reported a value of 1.027 using a Rayleigh distillation method with a solution of ammonium chloride. Urey, Huffman, Thode, and Fox[4] obtained a value of 1.021 as calculated from the operational data obtained for a countercurrent system in a glass column using a 60 weight percent ammonium nitrate solution and also using a 31–34 weight percent ammonium sulfate solution. Recently, Thode, Graham, and Ziegler[7] published a value of 1.031 ± 0.003 for α at 25°C for the exchange reaction between ammonia and ammonium nitrate.

It must be realized that in a solution containing both ammonia and ammonium ion in equilibrium with a gas phase containing ammonia, at least two equilibria are involved; namely,

$$N^{14}H_4^+(sol)+N^{15}H_3(gas)\rightleftharpoons N^{15}H_4^+(sol)+N^{14}H_3(gas)$$

and

$$N^{14}H_3(sol)+N^{15}H_3(gas)\rightleftharpoons N^{15}H_3(sol)+N^{14}H_3(gas),$$

where $NH_3(sol)$ refers to all compounds that the dissolved ammonia may form in solution. Thus the observed fractionation factor is probably a function of the equilibrium constants for both reactions. Its dependence upon these constants can be obtained mathematically if one makes several simple assumptions. This is done in the following section.

MATHEMATICAL CONSIDERATIONS

It is assumed that the following isotopic equilibria are involved in the liquid-vapor system H_2O, NH_3, and NH_4NO_3 at 25°C:

$$N^{14}H_4^+(sol)+N^{15}H_3(gas)\rightleftharpoons N^{15}H_4^+(sol)+N^{14}H_3(gas) \quad (1)$$

$$N^{14}H_3(sol)+N^{15}H_3(gas)\rightleftharpoons N^{15}H_3(sol)+N^{14}H_3(gas), \quad (2)$$

where $NH_3(sol)$ refers to all molecular species which the dissolved ammonia may form in solution. Designating the concentrations by the following symbols:

$$A=(N^{14}H_4^+)sol,\quad B=(N^{15}H_3)gas,$$
$$C=(N^{15}H_4^+)sol,\quad D=(N^{14}H_3)gas,$$
$$E=(N^{14}H_3)sol,\quad \text{and}\quad F=(N^{15}H_3)sol,$$

then

$$K_1=CD/AB \quad (3)$$

and

$$K_2=FD/EB. \quad (4)$$

By definition,

$$\alpha=\frac{D}{B}\Big/\frac{A+E}{C+F}, \quad (5)$$

where α is the fractionation factor. It is easily shown from these equations that

$$\alpha=K_1-(K_1-K_2)E/A+E.$$

Defining M as the ratio of moles of ammonia in solution to moles of ammonia plus moles of ammonium ion in solution,

$$M=E+F/E+F+A+C.$$

In the experiments to be described $F\ll E$ and $C\ll A$, since both $E/E+F$ and $C/A+C$ are approximately 0.0038. Consequently, $M=E/E+A$, and

$$\alpha=M(K_2-K_1)+K_1 \quad (6)$$

or

$$\alpha-1=M(K_2-K_1)+(K_1-1). \quad (6')$$

If K_2 and K_1 are constant, then a plot of $\alpha-1$ *vs.* M, or α *vs.* M, should give a straight line. This assumption presupposes that

(a) The presence of ammonium nitrate has no effect on the isotopic equilibrium between $NH_3(sol)$ and $NH_3(gas)$, i.e., K_2 is not a function of the ammonium nitrate concentration of the solution.

(b) The amount of water present as a solvent does not affect either equilibrium constant.

DETERMINATION OF THE FRACTIONATION FACTOR

Aliquots of stock solutions containing approximately 60 weight percent ammonium nitrate were equilibrated with gaseous ammonia at various pressures at 25°C. A sample of the vapor phase was taken under its own pressure by means of a mercury displacement device. A sample of the liquid phase was then taken by means of a syphon. Alkali was added to the

[7] H. G. Thode, R. L. Graham, and J. A. Ziegler, Can. J. Research **23B**, 40 (1945).

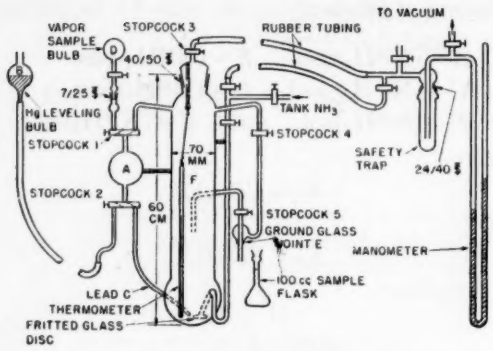

FIG. 1. Apparatus for the determination of the fractionation factor.

liquid sample and the liberated ammonia was completely removed. This ammonia, as well as that obtained as a vapor sample, was oxidized over copper oxide to nitrogen. Since in all cases conversions were complete, the isotopic content of a nitrogen sample was considered to represent that of the ammonia sample from which it was formed. The nitrogen samples were then analyzed on a Nier 60° sector field mass spectrometer for isotopic content. The $N^{14}N^{15}/N^{14}N^{14}$ ratio for the nitrogen from the ammonia of the liquid sample was compared directly to the same ratio for the nitrogen of the ammonia from the vapor sample. Thus the mass spectrometer readings gave α (the fractionation factor) directly.

The apparatus used for the equilibration is shown schematically in Fig. 1. Actually two equilibration flasks (*F* in Fig. 1) were used, one for equilibration with ammonia at relatively low pressures ($\sim$150 mm) and the other for the equilibration experiments with ammonia gas at higher pressures. The two apparatus were similar, differing only in length and in the relative position of the liquid syphon, with a larger vapor phase in the apparatus used for the lower pressures.

An aliquot of stock solution containing approximately 60 weight percent ammonium nitrate was poured into the well-dried equilibration flask. The amount of solution used for an experiment was governed primarily by the pressure of ammonia at which the equilibration was to be done. The volume of the solution was not at all critical except that, since the volume increased as ammonia dissolved in the solution during the equilibration, care had to be taken to assure that an adequate size vapor sample could be obtained. The greater the initial liquid volume and the greater the final pressure of ammonia, the smaller the available vapor phase.

After addition of the solution, the system was connected as shown and evacuated. Care was taken not to boil off too much water from the solution during evacuation. It might be stated at this point that all of the stopcocks and ground glass joints were lubricated with Lubriseal grease. After evacuation, ammonia was passed into the solution *via* the fritted glass disk. In some experiments the ammonia gas was passed into the solution rapidly, whereas in others the rate of addition of ammonia was very slow. When the predetermined total pressure (sum of the partial pressures of both the ammonia and water) was reached, as indicated on the mercury manometer, the system was isolated from the tank of ammonia and then pumped upon for a few moments. This was done in order to assure the absence of all air. Then a little ammonia was added to readjust the pressure to the proper value at 25°C. During the addition of the ammonia, an attempt was made to maintain the temperature of the solution at 25°C. This was not too difficult except during those experiments in which ammonia was added rapidly. But in all experiments, after the proper pressure was attained at 25°C, the equilibration flask was submerged in a thermostat maintained at 25.00$\pm$0.01°C. Periodically the flask was removed from the thermostat and well shaken, care being taken to mix the liquid and vapor phases efficiently. This mixing assured isotopic exchange equilibrium at 25.0°C.

To understand best how a gas sample was taken, reference should be made to Fig. 1. Bulb *A* was well dried and filled completely with mercury by means of the leveling bulb *B*. Stopcock 1 was then turned to connect the mercury-filled bulb *A* to the vapor in the equilibration flask, *F*, proper. Following this, stopcock 2 was turned connecting bulb *A* with lead *C*. As the mercury flowed into the bottom of the equilibration flask it displaced solution which in turn forced an equal volume of vapor into the bulb *A* without any pressure changes occurring. Stopcocks 1 and 2 were then turned so that mercury could flow into *A* from the leveling bulb, and in

TABLE II. Fractionation factors for the exchange.

$N^{14}H_4^+(sol) + N^{15}H_3(gas) \rightleftharpoons N^{15}H_4^+(sol) + N^{14}H_3(gas)$

Solution	Exp. No.	Composition of solution in wt. % NH_3	H_2O	NH_4NO_3	$\frac{\text{Moles } NH_3}{\text{Moles } NH_3 + \text{Moles } NH_4NO_3}$	Fractionation factor Obs.**	Calc.	Diff.
C-1	20	7.3	37.8	54.9	0.385	1.023 ±0.004	1.023	0.000
C-2	22	8.2	37.4	54.4	0.414	1.020 ±0.004	1.022	+0.002
D-1	15	9.0	38.4	52.6	0.446	1.017 ±0.004	1.021	+0.004
B-2	5	11.5	35.8	52.7	0.507	1.026 ±0.003	1.019	−0.007
D-3	12	13.0	36.7	50.3	0.550	1.026 ±0.005	1.018	−0.008
D-4	16	15.3	35.7	48.9	0.596	1.015 ±0.002	1.017	+0.002
B-4	10	16.0	34.0	50.1	0.599	1.018 ±0.005	1.017	−0.001
B-5	6	16.8	33.7	49.6	0.615	1.011 ±0.005	1.016	+0.005
C-3	19	17.8	33.5	48.6	0.633	1.013 ±0.004	1.016	+0.003
D-5	13	17.8	34.7	47.5	0.639	1.020 ±0.002	1.015	−0.005
E-1	3	21.9	32.4	45.7	0.693	1.010 ±0.003	1.014	+0.004
B-6	9	25.0	30.4	44.7	0.725	1.008 ±0.005	1.013	+0.005
D-7	14	25.6	31.4	43.0	0.737	1.011 ±0.003	1.013	+0.002
Thode		*	*	*	0.058	1.031 ±0.003	1.032	+0.001
Urey and Aten		—	—	—	1.000	1.006	1.005	−0.001

* This equilibrium mixture contained 0.195 moles of NH_4NO_3, 0.578 moles of H_2O, and 0.012 moles of NH_3. The NH_3 was introduced by the addition of 0.012 moles of NaOH to the NH_4NO_3 solution in an evacuated 100 cc flask.
** The ±0.004, etc., give the spectrometer precision (or, in some cases, an estimate of the accuracy of the spectrometer analyses).

this manner the vapor was forced into sample bulb *D*. The stopcocks were then turned so that another vapor sample was taken. This sample was also forced into the sample bulb. This procedure was continued until a vapor sample of about 200 cc at one atmosphere pressure was obtained. Air was then admitted into the vapor space *via* stopcock 3, and a liquid sample taken through the syphon by opening stopcocks 4 and 5. The liquid sample was taken directly into a 100 cc volumetric flask, joint *E* being a male ground glass joint fitting all standard 100 cc volumetric flasks. Since the volumetric flasks used had been calibrated, the density of the solution was obtained quite easily. After the density was determined, several aliquots of solution were removed from the volumetric flask and analyzed by titration for free ammonia. Knowing the composition of the stock solution, only this analysis was necessary to permit calculation of the composition of all components in the final solution. In some cases these calculated values were checked by a Kjeldahl analysis for total ammonia and a Karl Fischer analysis for water. Incidentally, the stock solutions were analyzed by means of the Kjeldahl method for the ammonium nitrate content and usually also for the water content by means of the Karl Fischer reagent. The analytical methods are discussed later in this paper.

Another aliquot of the final solution was then taken from the volumetric flask and *all* of the ammonia liberated. This ammonia was converted to nitrogen by circulating over hot copper oxide. The vapor sample was then frozen down with liquid nitrogen and any air present was removed by pumping. Actually very little air was found in these samples. In one case in which a large amount of air was present, the sample was rejected. After pumping, if any was necessary, the vapor sample was admitted into the conversion apparatus and oxidized to nitrogen. Thus, for any one equilibration experiment there were two nitrogen gas samples, one corresponding to the vapor phase and one to the liquid phase. During the conversions, precautions were taken to minimize errors that might arise from either dilution or fractionation.

The nitrogen gas samples were analyzed on a Nier mass spectrometer. The vapor phase sample was compared with the corresponding liquid phase sample. First, the isotopic ratio of one sample was obtained by measuring galvanometer deflections caused by the $(N^{14}N^{14})^+$ and $(N^{14}N^{15})^+$ ion beams. This was then done for the second sample and then again for the first. This procedure was followed two or more times, giving a number of isotopic ratios obtained alternately

TABLE III. Composition of stock solution.

Solution	Weight percent NH_4NO_3	H_2O
B	59.6	40.4
C	59.2	40.8
D	57.8	42.2
E	58.5	41.5

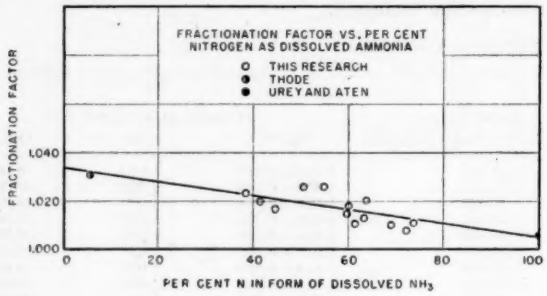

FIG. 2.

for the corresponding vapor and liquid samples. The fractionation factor, α, was obtained directly from these ratios. Thus for experiment No. 20, the following analyses were obtained:

Sample	No. of readings	$R \propto \frac{\text{Mass 28 intensity}}{\text{Mass 29 intensity}}$	$\frac{R_{vapor}}{R_{solution}}=\alpha$
Vapor	12	1.136	
			1.023
Solution	9	1.111	
			1.027
Vapor	10	1.141	
			1.030
Solution	9	1.108	
			1.024
Vapor	11	1.135	
			1.014
Solution	9	1.119	
			1.021
Vapor	9	1.142	
		average	1.023±0.004

It is obvious that the use of different shunts for the 28 and 29 mass peaks did not introduce any error into α. In analyzing samples from experiments 12 to 22 (Table II), the background contributed about 2 percent to the intensities of the 28 and 29 peaks. This introduced a negligible error in α because of the cancellation of errors in taking a ratio of ratios. The background was slightly worse for the analyses of the samples from experiments 3, 5, 6, 9, and 10 (Table II). Samples 3 and 5 were analyzed by comparing the intensity of the mass 14 and 15 peaks as well as the 28 and 29 peaks. The agreement was just within experimental error. In every case the gas samples were analyzed qualitatively for significant quantities of oxygen. None was found.

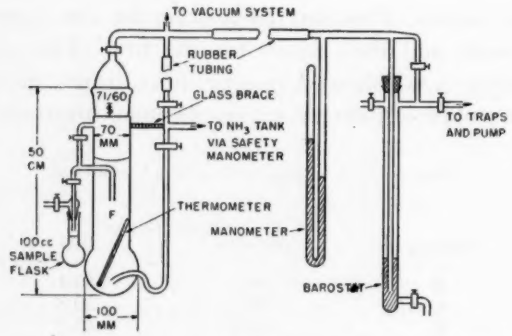

FIG. 3. Apparatus for the determination of the densities and vapor pressures of solutions of ammonia in water.

The experimental results are summarized in Table II.

The first column indicates the stock solution used. The compositions of the stock solutions are given in Table III.

The second column gives the experiment number and the third, fourth, and fifth show the composition of the final solution. The sixth column gives the fraction of the total nitrogen ($NH_3+NH_4^+$) in solution that is present in the form of ammonia. This corresponds to M in Eq. (6). The next column lists the observed fractionation factors. These are plotted as a function of M in Fig. 2. Applying Eq. (6),

$$\alpha = M(K_2-K_1)+K_1,$$

to the data and solving for K_1 and K_2-K_1 by means of the method of least squares, the equation

$$\alpha = -0.029M+1.034 \qquad (7)$$

is obtained as representing the experimental data. Column 8 gives the values for α as calculated from this equation. The differences between the observed and calculated values for α are given in the last column. These differences indicate a random scattering.

The data in Table II and Fig. 2 include the value for α as observed by Thode *et al.*[7,8] for a solution with $M=0.058$. The equilibrium mixture contained 0.195 moles of ammonium nitrate, 0.578 moles of water, and 0.012 moles of ammonia. The latter was introduced by the addition of 0.012 moles of sodium hydroxide to the ammonium nitrate solution in an evacuated 100 cc flask. After 24 hours at 25°C, a sample was obtained by the rapid turning of a stopcock. The table and figure also include the value for the frac-

[8] H. G. Thode (private communication, May 16, 1945).

TABLE IV. Vapor pressures and densities of ammoniacal solutions of ammonium nitrate.

Solution	Exp. No.	Density g/cc	Total pressure of sol'n mm Hg	Composition of solution in Wt. % by analysis NH₃	H₂O	NH₄NO₃	from dilution data using NH₃ analysis NH₃	H₂O	NH₄NO₃
Stock *A*		1.2748	—		40.6	59.1		40.7	59.3
A-1	*A*	1.2107	110	5.5	38.2	56.0	(5.5)	38.4	56.1
A-2	*B*	1.2044	113	6.1	38.4	55.7	(6.1)	38.2	55.6
A-3	*C*	1.1367	260	12.8	35.2	51.2	(12.8)	35.4	51.6
A-4	*D*	1.1151	347	15.2	—	50.5	(15.2)	34.5	50.6
A-5	*E*	1.0692	538	20.3	—	47.4	(20.3)	32.5	47.2
A-6	*F*	1.0434	730	23.6	—	45.5	(23.6)	31.1	45.3
A-7	*G*	1.0335	762	24.1	30.9	45.3	(24.1)	30.9	45.0
Stock *B*		1.2748	—		—	59.6		40.4	(59.6)
B-1	8	1.1794	—	8.6	—	—	(8.6)	36.9	54.5
B-2	5	1.1493	—	11.5	—	—	(11.5)	35.8	52.7
B-3	7	1.1202	—	14.5	—	—	(14.5)	34.5	51.0
B-4	10	1.1070	—	16.0	—	—	(16.0)	33.9	50.1
B-5	6	1.1002	—	16.8	—	—	(16.8)	33.6	49.6
B-6	9	1.0311	—	25.0	—	—	(25.0)	30.3	44.7
Stock *C*		1.2740	15.5		—	59.2		40.8	(59.2)
C-1	20	1.1927	133	7.3	—	—	(7.3)	37.8	54.9
C-2	22	1.1838	147	8.2	—	—	(8.2)	37.5	54.4
C-3	19	1.0897	415	17.8	—	—	(17.8)	33.5	48.6

tionation factor for the exchange reaction

$$N^{14}H_3(sol)+N^{15}H_3(gas)\rightleftharpoons N^{15}H_3(sol)+N^{14}H_3(gas)$$

as observed by Urey and Aten.[3,4] By comparing Eqs. (6) and (7), one obtains the equilibrium constants for the two ammonia exchange reactions

$$N^{14}H_4^+(sol)+N^{15}H_3(gas)\rightleftharpoons N^{15}H_4^+(sol)+N^{14}H_3(gas) \quad K_1=1.034$$

$$N^{14}H_3(sol)+N^{15}H_3(gas)\rightleftharpoons N^{15}H_3(sol)+N^{14}H_3(gas) \quad K_2=1.005.$$

DENSITIES AND VAPOR PRESSURES OF THE AMMONIACAL SOLUTIONS

In addition to fractionation factors, the densities and vapor pressures at 25°C of various solutions containing both ammonium nitrate and ammonia were obtained. The apparatus used for these experiments is shown in Fig. 3. As in the determination of the fractionation factor, an appropriate amount of stock solution was placed into vessel *F* and saturated with ammonia gas. The saturation pressure was fixed by adjustment of the mercury barostat and measured on the mercury manometer. After saturation with ammonia, the liquid level was well above the top of the syphon. As in the case of the fractionation experiments, after saturation was attained, the entire system was evacuated for a few moments and then a little ammonia was added to adjust the pressure to the desired value. This evacuation was necessary because tank ammonia was found to contain some inert gases.

The density of the solution was determined using a calibrated 100 cc volumetric flask. The saturated solutions were also analyzed for their composition. In all cases the free ammonia was determined directly by adding excess standardized hydrochloric acid from a weight-burette to

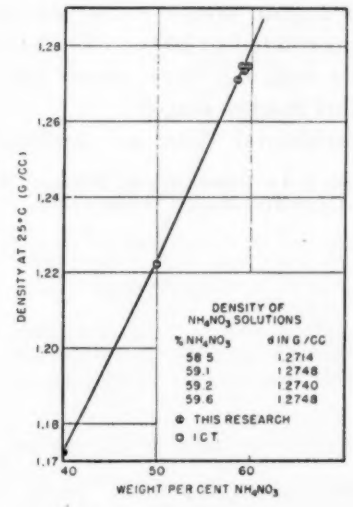

FIG. 4.

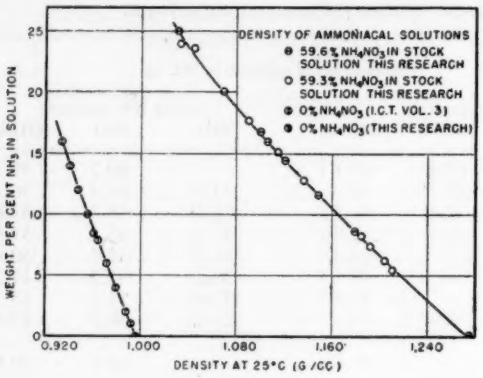

FIG. 5.

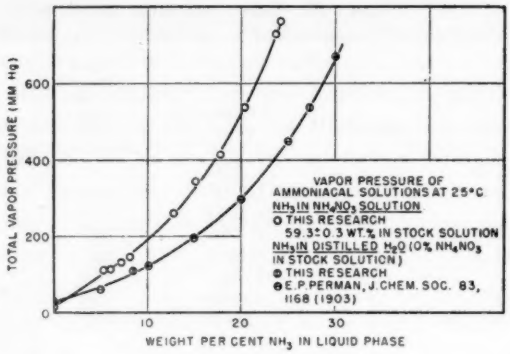
VAPOR PRESSURE OF AMMONIACAL SOLUTIONS AT 25°C
NH_3 IN NH_4NO_3 SOLUTION
○ THIS RESEARCH
59.32-3 WT.% IN STOCK SOLUTION
NH_3 IN DISTILLED H_2O (0% NH_4NO_3 IN STOCK SOLUTION)
● THIS RESEARCH
● E.P.PERMAN, J.CHEM.SOC. 83, 1168 (1903)
TOTAL VAPOR PRESSURE (MM Hg)
WEIGHT PER CENT NH_3 IN LIQUID PHASE

FIG. 6.

a weighed aliquot of the solution and then back-titrating with standard sodium hydroxide solution using methyl red as indicator. Since the composition of the stock solution was known, this one analysis permitted calculation of the composition of the final solution. In a number of experiments, the calculation was checked by a direct determination of the amounts of ammonium nitrate and water in the solution. The agreement was very good.

The ammonium nitrate content was found by determining the total amount of ammonia in solution by means of a modified Kjeldahl analysis similar to that described by Rieman, Neuss, and Naiman.[9] The difference between the total ammonia and free ammonia content of the solution permitted calculation of the weight percent of ammonium nitrate. The water content of the solutions was determined by a Karl Fischer titration. A 2 gram sample of the solution to be analyzed was diluted to 100 cc with dry dioxane. After mixing well, a 2–10 cc aliquot was titrated with the Karl Fischer reagent.

The experimental data are summarized in Table IV and Figs. 4–6. The headings on the various columns of the table are self-explanatory. The accuracy of the method used in this work was checked by two experiments using only ammonia and water. The agreement with the values in the literature may be seen from the data in Figs. 5 and 6 and Table V. This agreement is within the experimental errors involved in this research and in the work in the literature.

TABLE V. Vapor pressures and densities of ammonia and water solutions.

Weight % NH_3	Density g/cc		Total vapor pressure mm Hg at 25°C	
	Observed	I.C.T. Vol. 3	Observed	Perman, J. Chem. Soc. 83, 1168 (1903)
8.46	0.9611	0.962	112	103
27.31	0.8969	—	540	538

ACKNOWLEDGMENT

The authors wish to express their appreciation to Professor Harold C. Urey for his advice and helpful discussion during the course of this work. Thanks are owed to M. G. Inghram and M. Fox for analyzing nitrogen samples 3, 5, 6, 9, and 10 (Table II) on their mass spectrometer.

[9] W. Rieman, J. D. Neuss, and B. Naiman, *Quantitative Analysis* (McGraw-Hill Book Company, Inc., New York, 1942).

The Rate of Adsorption of Phosgene and Chloropicrin on Charcoal

MALCOLM DOLE
Department of Chemistry, Northwestern University, Evanston, Illinois
(Received January 30, 1947)

Making use of a relationship between the adsorption rate constant and the maximum slope of the effluent concentration-time curves derived from the rate equation of Bohart and Adams, it has been possible to estimate an absolute rate of adsorption of phosgene and chloropicrin on charcoal from the experimental data of Dole and Klotz. It is shown that diffusion to the most accessible part of the charcoal surface will occur faster than the observed rate, but more slowly to the least accessible surface areas. Calculated rates of adsorption using the statistical equations of Glasstone, Laidler, and Eyring and of Temkin are also of the correct order of magnitude when plausible assumptions are made concerning the nature of the activated state. It is concluded that both diffusion and surface reaction mechanisms must be postulated to gain a complete understanding of the adsorption rate of the two gases, but with diffusion being less important in the case of phosgene.

INTRODUCTION

RELIABLE data for the rate of adsorption of gases on surfaces of known area have in the past been extremely scanty, but with the development of improved methods of obtaining significant information concerning the surface area of adsorbents and catalysts more rate data should become available. Because of extensive work done under the auspices of the OSRD on activated charcoal it has been possible for us to estimate from our data and the data of others experimental rate values for the adsorption of phosgene and chloropicrin. These estimated rates come from a study of effluent concentration-time curves and are significant to the extent that the theory on which the estimates are based is significant as explained below. Chemical engineers have been active and successful in inventing empirical functions which describe the data, but there has been no attempt, as far as we know, to relate these chemical engineering functions to absolute reaction rate theories.

The rates given in this paper refer to the rate on charcoal which is in equilibrium with air; possibly, the initial displacement of adsorbed air molecules by the adsorbate may complicate the interpretation of the data as was, indeed, pointed out many years ago by Harned.[1] It would be interesting to repeat the measurements of Dole and Klotz using helium as the carrier gas. Emmett and Cines[2] have shown that previous chemisorption of hydrogen does not in general reduce the adsorption area of nitrogen except for possible cases where the chemisorbed gas may block the smallest pores of the adsorbent. Perhaps this latter phenomenon was present in Harned's case as his charcoal had only about $\frac{2}{3}$ of the adsorptive capacity of ours.

DETERMINATION OF RATE CONSTANT

In our experimental work[3] gas at influent concentration c_0 in p.p.m. by volume was passed through a granular charcoal bed of length x cm,

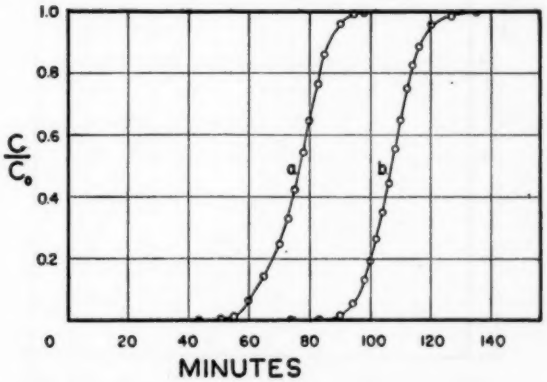

FIG. 1. Effluent to influent concentration-time curves. Curve *a*: chloropicrin at 7900 p.p.m., 62 liters/hour flow rate. Curve *b*: phosgene at 1760 p.p.m., 62 liters/hour flow rate.

[1] H. S. Harned, J. Am. Chem. Soc. **42**, 372 (1920).

[2] P. H. Emmett and M. Cines, J. Am. Chem. Soc. **68**, 2535 (1946).

[3] M. Dole and I. M. Klotz, Ind. Eng. Chem. **38**, 1289 (1946); I. M. Klotz and M. Dole, Ind. Eng. Chem. Anal. Edition **18**, 741 (1946).

of cross-sectional area A squared cm, at a flow rate L cc per sec., at 25°C, and under conditions such that the effluent concentration c could be measured at minute intervals. This effluent concentration which is a function of time, flow rate, initial concentration, length and area of bed, mesh size of charcoal, and temperature is illustrated in the case of two typical experiments on chloropicrin and phosgene in Fig. 1 where c/c_0, the ratio of effluent to influent concentration, is plotted as a function of time. For a tabulation of the more important data used in our calculations, see Appendix.

Bohart and Adams[4] have developed an adsorption rate theory assuming that the rate of adsorption, $\partial n/\partial t$, is proportional to the instantaneous concentration, c, (in this case of the gas in contact with the charcoal) and to the available free surface of the charcoal, n_0-n, or

$$\partial n/\partial t = k\cdot c(n_0-n). \qquad (1a)$$

In our calculations n will be given in units of number of adsorbing sites which are occupied per sq. cm, (when n is used in connection with Eq. (1b) or (2) it should be expressed in units of no. per cc) t in sec., c in molecules per cc, n_0 represents the total number of adsorbing sites per sq. cm, occupied or unoccupied. Related to (1a) is the equation

$$\partial c/\partial x = -(k/u)c(n_0-n), \qquad (1b)$$

which expresses the rate of change of concentration with distance.

On integration the following equation is obtained:[5]

$$\ln[(c_0/c)-1]=\ln[\exp[kn_0(x/u)]-1]-kc_0t, \quad (2)$$

where u, in cm per sec., when given by L/A is the linear velocity of the gas-air stream in the adsorbent tube when empty. For the actual linear velocity between granules, L/A must be divided by the fraction of void space in the charcoal bed. For constant velocity of flow and constant input concentration, the effluent concentration, c, should be the following function of the time:

$$\log[(c_0/c)-1]=\text{con}-(kc_0t/2.303). \qquad (3)$$

Thus a plot of $\log[c_0/c-1]$ against the time should give a straight line if this formulation is correct. In Fig. 2 we have plotted the data of Fig. 1 for both phosgene and chloropicrin according to the relationship expressed by Eq. (3). The phosgene data agree with Eq. (3) somewhat better than do the chloropicrin data.

Differentiating Eq. (2) with respect to time we obtain

$$\partial(c/c_0)/\partial t = k[c-(c^2/c_0)]. \qquad (4)$$

At the moment when $c/c_0=0.5$, the rate of rise of effluent concentration with time is a maximum; thus, at this point there should be an inflection point in the curve with slope given according to the theory by the equation

$$[\partial(c/c_0)/\partial t]_{c/c_0=0.5}=kc_0/4=S_{\max}. \qquad (5)$$

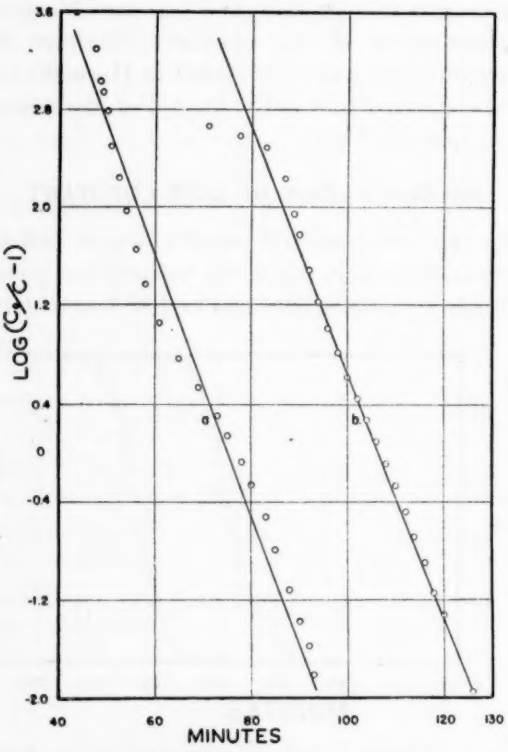

FIG. 2. Test of the Bohart-Adams adsorption rate equation. Curve a: chlorpicrin. Curve b: phosgene.

[4] G. S. Bohart and E. Q. Adams, J. Am. Chem. Soc. **42**, 523 (1920). For a review of adsorption rate theories see the paper by I. M. Klotz, *Chem. Rev.* **39**, 241 (1946), and S. Brunauer, *The Adsorption of Gases and Vapors* (Princeton University Press, Princeton, New Jersey, 1943), Chapter XIII.

[5] A similar treatment has recently been given by Danby, Davoud, Everett, Hinshelwood, and Lodge, J. Chem. Soc. 918 (1946).

In Fig. 3 a number of observed maximum slopes of the c/c_0-t curves, S_{max}, are plotted as a function of the influent concentration. A linear relation, extrapolating to the origin in accordance with the theory, is observed.

However, the situation is complicated by the influence of flow rate on S_{max} in contradiction to Eq. (5), particularly in the case of chloropicrin. Variation in particle size will also probably produce a slight change in S_{max}, although we have no data to test this point. Figure 4 illustrates the variation of S_{max} with flow rate. Unfortunately the OSRD sponsored research did not include a comprehensive study of the variation of S_{max} with particle size and flow rate, but the data of Fig. 4 show that the phosgene S_{max} values are affected only slightly by the change of flow rate, but the chloropicrin S_{max} data somewhat more so. As a first approximation we shall assume that the slopes of the straight lines of Fig. 3 correctly give the value of $k/4$ for the two gases; at any particular concentration, then, k can be calculated from the equation

$$k=4S_{max}/c_0. \tag{6}$$

The rate constant, k, can be estimated also from the slopes of the curves of Fig. 2; when so determined there is fairly good agreement with the value of k given by the method used here in the case of phosgene, whose data follow the integrated Eq. (3) relationship much better than do the chloropicrin data. The rate constant for this latter gas may vary as much as 75 percent depending on which part of the curve of Fig. 2 is used in computing the slope. However, we have not used the slopes of the curves of Fig. 2 for either chloropicrin or phosgene in calculating k because the slopes so determined do not vary as nearly linearly with the concentration, and do not extrapolate as well to zero at zero concentration as do the points of Fig. 3. For this reason we believe that the k values determined from the linear curves of Fig. 3 are somewhat more significant.

For the calculation of the absolute reaction rate from the rate constant of Eq. (6) it is necessary to know the surface area available for adsorption per gram of charcoal. Emmett and coworkers[6] have determined the surface area of the

[6] P. H. Emmett *et. al.*, Private communication.

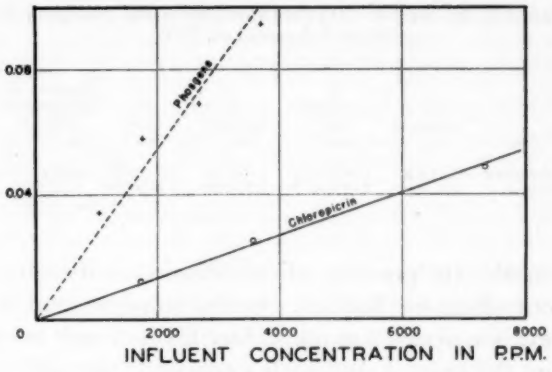

FIG. 3. Test of Eq. (5).

charcoal we used for nitrogen, chloropicrin, and a number of other gases, but not phosgene. For the latter we have chosen a reasonable estimate which is undoubtedly of the correct order of magnitude. Knowing k and n_0, the actual absolute rate, $\partial n/\partial t$ can be calculated from Eq. (1) for any chosen values of c and n_0-n. In Table I the maximum rate of adsorption, which would be a rate at zero time when c equals c_0, and n_0-n equals n_0, is tabulated along with other related data. Such a rate could only be produced experimentally at x equal to zero.

THE ROLE OF DIFFUSION

Before proceeding to consideration of the interpretation of the data on the basis of an absolute reaction rate theory, it is interesting to

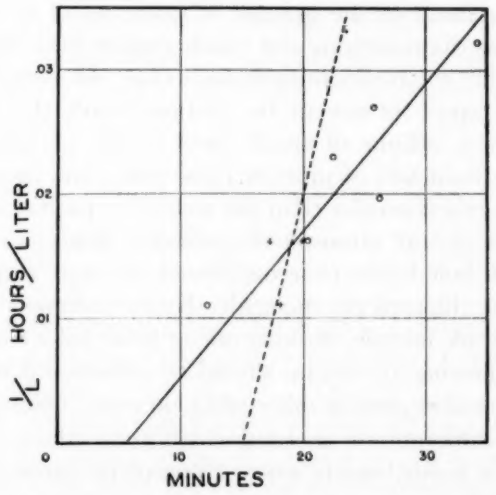

FIG. 4. Variation of adsorption rate constant with flow rate. Circles: chloropicrin. Crosses: phosgene. Abscissa is reciprocal of S_{max}.

TABLE I. Adsorption data for chloropicrin and phosgene on activated charcoal at 25°C.

Gas	Area of adsorbent $cm^2\ g^{-1}$	k cm^3 molecules^{-1} sec.$^{-1}$	c_0 molecules cm^{-3}	n_0 sites cm^{-2}	Maximum rate of adsorption molecules cm^{-2} sec.$^{-1}$
Chloropicrin	1.13×10^{7}	1.89×10^{-20}	1.93×10^{17}	2.9×10^{14}	1.06×10^{12}
Phosgene	1.5×10^{7}	7.62×10^{-20}	4.34×10^{16}	3.42×10^{13}	1.13×10^{11}

consider the possible role of diffusion as the rate-controlling mechanism. For the simplest case of diffusion across a plane surface layer of unit area and thickness δ, and with a concentration difference equal to c_0, the rate is given by the equation

$$v = Dc_0/\delta, \tag{7}$$

where D is the diffusion coefficient of the gas in air.

To apply Eq. (7) which should be valid for the calculation of the maximum rate of adsorption because at the first moment of adsorption the concentration of gas right at the charcoal surface will be effectively zero, we need to know the length of path and the area through which diffusion is taking place. Gamson, Thodos, and Hougen[7] give a table of effective area of mass transfer for particles of different mesh sizes. In our case of 12–14 mesh particles having 45 percent void space (bulk density equal to 0.48), the gross surface area of the particles is 792 sq. ft. per cubic ft. of volume or 54.1 sq. cm per g. The charcoal granule itself contains many pores having a distribution of sizes; roughly 45 percent by volume of the granule is made up of pores whose diameters are not much greater than that of the chloropicrin molecule. (The 45 percent void space is not to be confused with the 45 percent volume of small pores in the granule.) The diameters of most of these pores are, therefore, much smaller than the mean free path of air molecules at atmospheric pressure; hence, each small hole in the charcoal should act as a "trap" for a chloropicrin molecule. Every chloropicrin molecule initially striking one of these holes from the flowing air stream should be adsorbed if the adsorption process takes place on every collision of a chloropicrin molecule with the surface. In other words, nearly every chloropicrin molecule striking one of these holes must collide with the charcoal surface before it diffuses out of the hole.

From the kinetic theory of gases or from the absolute reaction rate theory of Eyring and coworkers, the rate at which molecules strike unit area of surface per sec. is given by the following equation:[8]

$$v = c_0[\mathbf{k}T/2\pi m]^{\frac{1}{2}}. \tag{8}$$

For chloropicrin at $c_0 = 1.93\times10^{17}$ molecules/cm^3

$$v = 9.47\times10^{20}\ \text{molecules/cm}^2\text{/sec.},$$

and for phosgene at $c_0 = 4.34\times10^{16}$ molecules/cm^3

$$v = 2.75\times10^{20}\ \text{molecules/cm}^2\text{/sec.}$$

However, the above calculations refer to the rate at which molecules would be striking unit area; for an area of 45 percent of 54 cm^2 per gram, the rates become

2.30×10^{22} molecules/gram/sec. for chloropicrin, and
6.68×10^{21} molecules/gram/sec. for phosgene.

The observed rates are

1.20×10^{19} molecules/gram/sec. for chloropicrin, and
1.60×10^{18} molecules/gram/sec. for phosgene

which is about 2000 times smaller than was calculated. Apparently there must be many molecules which diffuse out of the holes without being adsorbed.

We shall now consider the rate at which molecules can diffuse into the granule through the pores, but the validity of our calculations will be somewhat in doubt because we do not know the complete details of the pore structure of the charcoal granules or the true diffusion rates in the pores. Apparently the pores can be divided roughly into two groups; macropores with diameter of the order of 10^{-4} cm and micropores whose diameters lie between 10^{-7} and 10^{-6} cm.[9] We shall assume that the diffusion constants for diffusion through the macropores are equal to those for diffusion in air, which as determined in this laboratory for chloropicrin and phosgene are, respectively, 0.088 and 0.099 cm^2/sec. For diffusion in the micropores we make use of the diffusion

[7] B. W. Gamson, G. Thodos, and D. A. Hougen, Trans. Am. Inst. Chem. Eng. **39**, 1 (1943).

[8] See S. Glasstone, K. J. Laidler, and H. Eyring, *The Theory of Rate Processes* (McGraw-Hill Book Company, New York, 1941), p. 351.

[9] See S. Brunauer, *The Adsorption of Gases and Vapors* (Princeton University Press, Princeton, New Jersey, 1943).

constant calculated from the following equation[9] derived for uni-dimensional gaseous diffusion through a cylindrical pore,

$$D_i = \tfrac{2}{3} r(8RT/M)^{\frac{1}{2}},$$

where r is the radius of the pore. Surface diffusion will not be considered because we are dealing with the rate of adsorption at zero time when the charcoal is free of adsorbate. The micropore diffusion constants as calculated for chloropicrin and phosgene are, respectively, 1.17×10^{-3} and 1.52×10^{-3} cm²/sec., for r approximately 10^{-7} cm.

The average radius of the charcoal granules of 12–14 mesh, again taken from Gamson, Thodos, and Hougen, is 0.0635 cm. From Eq. (7) we can calculate that the rate of diffusion through a concentration gradient equal to c_0, through an area of 45 percent of 54 cm² per grams, and along a distance of 0.0635 cm is

$v = 8.7\times10^{16}$ molecules/gram/sec. for chloropicrin, and
$v = 2.57\times10^{16}$ molecules/gram/sec. for phosgene,

about 100 times slower than was observed. For diffusion through the macropores the calculated rate is

$v = 2.02\times10^{18}$ molecules/gram/sec. for chloropicrin, and
$v = 5.11\times10^{17}$ molecules/gram/sec. for phosgene,

which is within an order of magnitude of the observed rates. For distances of diffusion shorter than 0.0635 cm the rate would be faster than that observed.

This calculation suggests that diffusion to the most readily accessible areas of the charcoal where δ is much smaller than 0.0635 cm can proceed faster through the large pores than the observed initial adsorption rate. At later stages of the process where the gas has to diffuse through small pores to reach unused charcoal surface, the diffusion rate would be slower and perhaps rate determining. If this is true, the asymmetric shape of the effluent concentration-time curves and the influence of flow velocity on the rate can be at least partially understood. However, it should be emphasized that these calculations are not sufficiently exact for the possibility of a diffusion-controlling mechanism to be definitely excluded. Agreement of the data with Eq. (3) also does not definitely exclude the possibility that the magnitude of the constant k is determined by diffusion, but any diffusion theory will have to explain the fourfold greater value of k for phosgene as compared to chloropicrin which it cannot do if only diffusion through air is considered.

The question naturally arises as to whether diffusion from the moving air stream to the gross surface of the charcoal is the limiting factor. Although this diffusion probably determines in large part the "critical bed depth" we do not believe that it is entirely responsible for the adsorption rate as given above for the following reasons: (a) if diffusion from the moving gas stream is determinative, the S_{max} slopes should be independent of initial concentration and greatly dependent on the flow rate[10] whereas the reverse is true; (b) the rate constants, k, for chloropicrin and phosgene should be nearly equal because of their nearly equal diffusion coefficients, but the observed rate constant for phosgene is four times that for chloropicrin.

We shall now investigate the extent to which the absolute surface reaction rate theory can explain the observed values.

APPLICATION OF THE ABSOLUTE REACTION RATE THEORY

In order to apply the equation derived by Laidler, Glasstone, and Eyring,[11] and Temkin[12] to the interpretation of the reaction rate constants it is necessary to know the moments of inertia of the chloropicrin and phosgene molecules. In the case of chloropicrin we have made use of the following bond distances and bond angles:

C–N	1.47A
C–Cl	1.77A
N=O	1.21A
Angle Cl–C–Cl	111°
Angle O–N–O	127°

Assuming free rotation about the C–N bond, the equations for the separate moments of inertia

[10] This follows from the diffusion theory of C. C. Furnas, Trans. Am. Inst. Chem. Eng. 24, 1942 (1930).
[11] K. J. Laidler, S. Glasstone, and H. Eyring, J. Chem. Phys. 8, 659 (1940); *The Theory of Rate Processes* (McGraw-Hill Book Company, New York, 1941), Chapt. VII.
[12] M. Temkin, Acta Physicochim. U.R.S.S. 8, 141 1938).

have been set up as follows:

$$I_x = 2m_O\left(r_{N-O}\sin\frac{127°}{2}\right)^2 + 3m_{Cl}\left(r_{C-Cl}\frac{\sin(111°/2)}{\sin 60°}\right)^2 = 5.64\times10^{-38}\text{ g cm}^2,$$

$$I_y = I_z = 3m_{Cl}\times\left[r_x + r_{C-Cl}\left(1-\left(\frac{\sin(111°/2)}{\sin 60°}\right)^2\right)^{\frac{1}{2}}\right]^2 \quad (9)$$
$$+\tfrac{3}{2}m_{Cl}\left[r_{C-Cl}\frac{\sin(111°/2)}{\sin 60°}\right]^2 + m_C r_x^2 + m_N[r_{C-N}-r_x]^2 + 2m_O[r_{C-N}-r_x+r_{N-O}\cos(127°/2)]^2 + m_O[r_{N-O}\sin(127°/2)]^2,$$

where

$$r_x = \Big[m_N\cdot r_{C-N} + 2m_O(r_{C-N}+r_{NO}\cos(127/2)) - 3m_{Cl}\cdot r_{C-Cl}\times\left(1-\left(\frac{\sin(111°/2)}{\sin 60°}\right)^2\right)^{\frac{1}{2}}\Big] \Big/ m_{CCl_3NO_2} = 0.16\text{A}. \quad (10)$$

Hence, $I_y = I_z = 5.92\times10^{-38}$ g cm^2. (If free rotation is not assumed, $I_y \neq I_z$, but the product I_yI_z remains unchanged, which is all that concerns us here). The simpler calculations of the moments of inertia of phosgene yielded the results

$$I_x = A = 1.81\times10^{-38}\text{ g cm}^2,$$
$$I_y = B = 1.72\times10^{-38},$$
$$I_z = A+B = C = 3.53\times10^{-38}.$$

As we shall assume that the vibrational partition function ratio in the free and adsorbed states is unity, we do not need to consider vibration frequencies.

The general equation for the rate of adsorption is, in the symbolism of Glasstone, Laidler, and Eyring

$$v = c_g\cdot c_s\frac{\mathbf{k}T}{h}\cdot\frac{f_\ddagger}{F_g f_s}\exp\left[-\frac{\epsilon}{\mathbf{k}T}\right], \quad (11)$$

where c_g is the gas concentration in molecules per cc, c_s the number of adsorbing points per sq. cm., $f_\ddagger$ the partition function of the activated complex (with the contribution of the degree of translational freedom normal to the adsorbing surface factored out), F_g the partition function per unit volume of the gas undergoing adsorption, f_s the partition function of the adsorbing centers (taken as unity) and ϵ is the activation energy for adsorption per molecule at the absolute zero. The maximum rate of adsorption given by Eq. (1) when the concentration is equal to the influent concentration and the surface is bare can be expressed by the equation

$$v = k\cdot c_g\cdot c_s. \quad (12)$$

Combining Eqs. (11) and (12)

$$k = \frac{\mathbf{k}T}{h}\frac{f_\ddagger}{F_g}e^{-\epsilon/\mathbf{k}T}. \quad (13)$$

Remembering that k can be calculated from Eq. (6) without a knowledge of n_0, it is seen that the absolute theory of reaction rates can be tested without knowing either the surface area of the adsorbent or the number of adsorbing centers per sq. cm. Only the validity of Eq. (6) is required.

In applying Eq. (13) three cases have been tested; first, the case in which the adsorbate loses its translational degrees of freedom in the activated complex (except in the direction required for adsorption); second, the adsorbate loses its translational and two of its rotational degrees of freedom; and third, the adsorbate becomes completely immobile losing all translational and rotational degrees of freedom. Equations for k based on these assumptions are as follows:[13]

Case 1.

$$k = [h^2/(2\pi m)^{\frac{1}{2}}(\mathbf{k}T)^{\frac{1}{2}}]\exp[-(\epsilon/\mathbf{k}T)]. \quad (14)$$

Case 2.

$$k = (\sigma/\sigma_\ddagger)\times[h^4/8\pi^2(BC)^{\frac{1}{2}}(2\pi m\mathbf{k}T)^{\frac{1}{2}}]\exp[-\epsilon/\mathbf{k}T]. \quad (15)$$

[13] The equation given for the rate of a heterogeneous unimolecular first-order reaction involving a nonlinear polyatomic molecule by Glasstone, Laidler, and Eyring, reference 11, should be divided by a factor $(\mathbf{k}T)^{\frac{1}{2}}$.

Case 3.

$$k=(\sigma/\sigma_{\ddagger})[h^5/(2\pi m)^{\frac{1}{2}}8\pi^2(8\pi^3ABC)^{\frac{1}{2}}(kT)^2]$$
$$\times\exp[-\epsilon/\mathbf{k}T]. \quad (16)$$

In Table II valuesof k calculated from (14)–(16), assuming zero activation energy, are given along with ratios of k for the two gases and other pertinent data.

Before coming to any conclusions as to the validity of the theory, it is important to consider the effect of activation energy and change of temperature on the rate constants. By inspection of Eqs. (14)–(16) it can be seen that if the activation energy is really zero, the rate constants should decrease with rise of temperature; if there is no temperature dependence of the rate constant, it may be because the increase of the factor $\exp[-\epsilon/\mathbf{k}T]$ with increase of the temperature has balanced the decrease of the terms $(\mathbf{k}T)^{-\frac{1}{2}}$, $(\mathbf{k}T)^{-\frac{3}{2}}$, or $(\mathbf{k}T)^{-2}$ over the temperature interval from 0 to 25°C.

Unfortunately only one rate experiment was carried out at 0°C from which the activation energy could be calculated; hence, the exact value of the rate constant at 0°C given in Table II is uncertain. We believe that the change in k over the 25°C temperature interval would be no greater than that indicated in Table II.

If allowance is made for the variation in k because of the $\mathbf{k}T$ factors of Eqs. (14), (15), and (16), the values of E necessary to explain the observed change in k with temperature, given in the last column of Table II, are obtained; recalculating the rate constants by Eqs. (14), (15), and (16) by use of these values of the activation energy, the values given in the next to the last column result.

Whether an activation energy exists or not, it is obvious that the absolute reaction rate theory can reproduce the observed data depending on the assumptions as to the status of the adsorbed chloropicrin and phosgene molecules in the activated state.

TABLE II. Comparison of experimental and theoretical adsorption rate constants.

	Chloropicrin (k in cm³ sec⁻¹ at 25°C)	Phosgene	Ratio	k, chloropicrin temp. corrected	E cal./mole
k, obs. 25°	1.89×10^{-20}	7.62×10^{-20}	4.03		
k, obs. 0°	1.17×10^{-20}				
k, Eq. (14)	3.06×10^{-15}	6.52×10^{-15}	2.13	7.83×10^{-18}	3500
k, Eq. (15)	6.99×10^{-19}	3.57×10^{-18}	5.10	6.89×10^{-22}	4100
k, Eq. (16)	6.09×10^{-21}	5.51×10^{-20}	9.05	3.79×10^{-24}	4400

CONCLUSIONS

In conclusion we believe that our calculations demonstrate that both the diffusion and surface reaction mechanisms of adsorption are involved in the actual adsorption process. As explained in the previous paper of Dole and Klotz the diffusion theory alone is inadequate because (1) the critical bed depths do not extrapolate to zero for zero particle diameter, (2) the maximum slope of the effluent concentration-time curve is so strongly dependent upon the concentration, and (3) the rate constant for phosgene is four times as great as that for chloropicrin, although the diffusion constant of phosgene is only slightly greater than that of chloropicrin. It should be noted that we have not postulated any condensed surface film of gas through which diffusion at a slower rate must take place; however, the influence of flow velocity on the rate is to be considered as an increase of net rate of transfer of gas to the charcoal surface with increased flow velocity.

The difficulty of expressing the rate of adsorption by a single equation undoubtedly stems from the mixture of mechanisms entering into the adsorption process.

Danby, Davoud, Everett, Hinshelwood, and Lodge[5] have recently carried out an experimental and theoretical analysis of adsorption rates similar to that of Dole and Klotz. They believe that the adsorption of chloropicrin is diffusion controlled because their adsorption rate constants are proportional to the square root of the flow rate, and inversely proportional to the square root of the molecular weight (the latter because of an assumed proportionality between the diffusion constant and the square root of the molecular weight). These relationships are not verified in our work and, in fact, the diffusion coefficients of gases in air do not follow the square root of molecular-weight law. Unfortunately we did not study effluent concentration-time curves as a function of particle size, hence we cannot comment on their suggestion that n_0 is a decreasing linear function of the particle diameter.

APPENDIX

MALCOLM DOLE AND I. M. KLOTZ

Experimental Data from Which Figs. 1, 2, and 3 Were Constructed[14]

Chloropicrin. (Bed depth 5.3 cm, diameter 1.4 cm, and temperature 25°C except where otherwise specified.)

Exp. 15, c_0, 7900 p.p.m. Flow rate 62 liters/hour. Bed depth 6.3 cm

Time min.	c/c_0	Time min.	c/c_0
43.5	0.0003	71	.273
47.5	.0005	72	.303
48.5	.0009	73	.332
49	.0011	74	.366
50	.0020	75	.423
51	.0032	76	.463
52.5	.0057	78	.544
53	.0068	79	.600
54	.0104	80	.646
55	.0158	81	.686
56	.0216	82	.731
57	.0295	83	.768
58	.0399	84	.819
59	.0512	85	.861
60	.0647	86	.886
61	.0800	87	.910
62	.0952	88	.930
63	.112	89	.950
64	.129	90	.960
65	.145	91	.970
66	.163	92	.975
67	.182	93	.985
68	.202	94	.990
69	.227	98	1.000
70	.248		

Exp. 17, c_0, 7350 p.p.m. Flow rate 62 liters/hour

Time min.	c/c_0	Time min.	c/c_0
36	0.0003	59	.235
38	.0004	60	.267
39	.0015	61	.299
40	.0025	62	.338
41	.0037	63	.374
42	.0054	64	.418
43	.0079	65	.476
44	.0113	67	.553
45	.0159	68	.607
46	.0219	69	.653
47	.0290	70	.717
48	.0376	71	.769
49	.0474	72	.817
50	.0543	73	.857
51	.0709	74	.897
52	.0845	75	.917
53	.1000	76	.953
54	.113	77	.969
55	.136	78	.979
56	.157	79	.984
57	.179	80	.995
58	.204	84	1.000

Exp. 25, c_0, 3600 p.p.m. Flow rate 62 liters/hour

Time min.	c/c_0
82.5	0.0006
84	.0014
85	.0014
86	.0020
88	.0022
90	.0039
91	.0045
94	.0070
96	.0093
99	.0163
103	.0334
104	.0379
106	.0497
109	.0756
114	.152
115	.169
116	.190
118	.234
120	.280
121	.302
123	.351
125	.399
127	.447
129	.499
136	.689
141	.809
145	.885
150	.981
156	1.000

Exp. 30, c_0, 1740 p.p.m. Flow rate 62 liters/hour

Time min.	c/c_0
156	0.0006
171	.0069
175	.0103
179	.0161
185	.0264
193	.0467
196	.0555
200	.0700
204	.0918
208	.106
212	.129
216	.155
220	.188
223	.216
227	.253
230	.287
234	.338
241	.432
246	.498
256	.609
266	.720
280	.870
300	.98
315	1.00

[14] Dole and Klotz, Ind. Eng. Chem. **38**, 1289 (1946).

Phosgene. (Bed depth, 5.0 cm, bed diameter 1.4 cm, and temp. 25°C except when otherwise stated.)

Exp. 1, c_0, 1790 p.p.m. Flow rate, 62 liters/hour

Time min.	c/c_0
36	0.0020
38	.0026
40	.0045
42	.0073
43	.0094
44	.0126
46	.0208
48	.0384
50	.0601
52	.0975
54	.1530
56	.2282
58	.3187
60.5	.4520
62	.5380
64	.6570
66	.7630
68	.8400
70	.8965
72.5	.9350
75	.9630
77	.9750
80	.9850
83	.9960
85	1.0000

Exp. 4, c_0, 1800 p.p.m. Flow rate, 62 liters/hour. Bed depth, 10.0 cm

Time min.	c/c_0
71	0.0021
77.5	.0026
83	.0032
87	.0058
89	.0110
90	.0162
92	.0316
94	.0552
96	.0884
98	.1328
100	.1920
102	.2650
104	.3500
106	.4450
108	.5540
110	.6500
112	.7500
114	.8270
116	.8890
118	.9340
120	.9550
127	.9890
135	1.0000

Exp. 40, c_0, 3700 p.p.m. Flow rate 62 liters/hour

Time min.	c/c_0
27.5	0.0010
29.5	.0468
31	.1268
32.5	.1749
33	.2210
34.5	.3135
35	.3700
36	.4400
37	.5090
38	.5970
39.5	.7460
40.5	.7760
42	.8560
44.5	.9390
46.5	.9660
50.5	1.0000

Exp. 42, c_0, 2700 p.p.m. Flow rate 62 liters/hour

Time min.	c/c_0
28.5	0.0006
30.5	.0023
32.5	.0069
34	.0174
35	.0287
36	.0452
37	.0634
38	.0915
39.5	.1272
40.5	.1740
42	.3120
45	.4140
46	.5200
47.5	.5950
49	.6990
50.5	.8050
52	.8400
53.5	.8810
55	.9230
57	.9530
58	.9600
64	.9790
72	.9410
83	.9910
95	.9950
113	1.0000

Exp. 43, c_0, 1060 p.p.m. Flow rate, 62 liters/hour

Time min.	c/c_0
42.5	0.0014
45	.0025
46.5	.0065
50	.0127
53.5	.0196
57	.0330
63	.0723
69	.1240
73.5	.1520
79	.2900
88.5	.5620
98.5	.7980
114	.9030
192	1.0000

THE JOURNAL OF CHEMICAL PHYSICS VOLUME 15, NUMBER 7 JULY, 1947

The Study of Reaction Intermediates by Means of a Mass Spectrometer

Part I. Apparatus and Method

G. C. ELTENTON
Shell Development Company, Emeryville, California

(Received April 7, 1947)

A method for coupling a reaction chamber to a Dempster-type mass spectrometer in such a manner that short lived intermediates can reach the electron beam is described. The presence of radicals is denoted by an increase in the ion current of the corresponding mass. The sensitivity of the method depends on the difference between the appearance potential of the given ion produced by electron bombardment of either reactants or end products and the ionization potential of the free radical. It is shown experimentally that excited molecules are not present in sufficient quantity to invalidate the assumption that free radicals are responsible for the changes in ion current. The method has already extended more than tenfold the pressure range in which radicals are detectable, thus bridging the gap between mirror and spectroscopic methods so that low pressure combustion phenomena may be studied.

INTRODUCTION

THE investigation reported in this communication was undertaken before the war primarily to study the possibilities of a new approach to the experimental study of reaction kinetics.

The Paneth mirror method of detecting transient intermediates has yielded valuable data but is unfortunately restricted to low pressures and essentially oxygen-free reactions. Spectroscopic methods have been developed for such radicals as OH, CH, and SO, but they cannot be a complete solution so long as the spectral complexities of such simple radicals as CH_3 remain unsolved. Moreover, because of the absorption by oxygen in the Schumann region, the application to combustion studies is again limited.

It was not anticipated that a mass spectrometric method would be free from difficulties of its own. Nevertheless, it was thought that the uniqueness with which, in some cases, a measure of mass is a guide to radical identity and adaptability to higher pressures and oxygen-containing atmospheres, warranted a careful survey. One additional advantage which might compensate for the complexity of the method lies in the fact that direct continuous measurements can be made of changing concentrations, thus avoiding the necessity and uncertainties of renewing mirrors or photographic plates for each parameter change. No attempt has been made in this investigation to study any one particular reaction exhaustively, since it was realized that the apparatus as originally constructed would serve to explore only semiquantitatively a limited range of applications, and that as a result of accumulating experience a more accurate and universal apparatus might be designed.

PRINCIPLE OF THE METHOD

If a molecule, XY, is bombarded by electrons of energy, E, it will ionize and dissociate with a certain probability when $E \geq A(X^+)$ where $A(X^+)$ is the appearance potential for the ion X^+ formed by electron bombardment of the parent molecule XY. If, however, atoms or radicals X are already present as a consequence of thermal or chemical dissociation of the parent molecule, then an energy $E \geq I(X^+)$ will be effective in producing ions X^+, where $I(X^+)$ is the ionization potential of the free radical or atom X. Since $I(X^+) < A(X^+)$ by an amount which depends on the dissociation energy of the parent molecule and the kinetic energies of the separating fragments, it should be possible to select for each radical a value of the electron bombarding energy which is sufficient to ionize the radical but insufficient to ionize and dissociate the parent molecule. In this way a positive-ion current of a given mass in a mass spectrometer becomes a measure of the concentration of a given free radical.

In order to ensure that radicals produced by

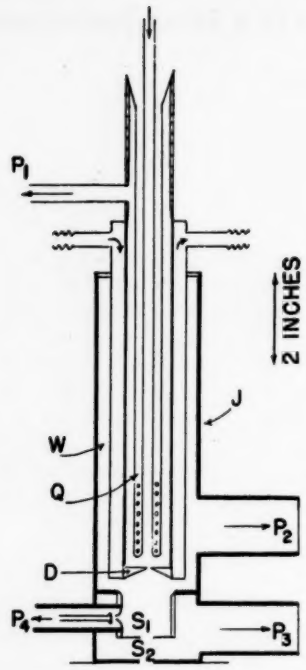

FIG. 1. Low pressure quartz reactor $R.1$ attached to ionization chamber of mass spectrometer. Ground joint J, water-cooled jacket W, quartz double-walled tube Q, diaphragm D, ion-collimating slits S_1 and S_2, pumping leads P_1, P_2, P_3, and P_4.

chemical reaction in a reactor adjacent to the ionization chamber shall reach the latter, it is necessary to provide a practically collision-free path. The ordinary means of sample extraction by capillary are clearly useless, and resort has to be made to thin diaphragms separating the reactor from the ionization chamber. With a pumping speed of about 7 l/sec. at the diaphragm, it has been found possible to maintain a pressure of *ca.* 100 mm in the reactor and a vacuum of *ca.* 10^{-3} mm in the ionization chamber.

APPARATUS

Mass Spectrometer

In the exploratory work described here, a simple Dempster 180° type mass spectrometer was used. The radius of curvature of the ions was 3.5 cm, and the magnetic field was stabilized by batteries and ballast tubes. Entrance slits of 0.2 and 0.3 mm by 6 mm were used at various times, and these were mounted in soft iron eccentrics for vertical and lateral adjustment. The whole ionization chamber was enclosed in a soft iron shield to minimize the effect of stray field on the low velocity electron beam. It is essential that the source of electrons be separated from the ionization chamber in order to avoid competition between radicals produced in the furnace and those produced at the hot emitter. A number of different types of electron gun were tried, but in spite of the apparent advantages of the acceleration-retardation type employing two or more anodes, a simple platinum cone directed towards the emitter was found to be more satisfactory. For the lower paraffins an indirectly heated oxide emitter possesses the advantages of low temperature, low velocity spread, and high emission. However, such emitters rapidly become poisoned by organo-metallic compounds and higher hydrocarbons. In such cases it was necessary to use bare tungsten filaments coiled into a flat spiral and backed by a platinum cup attached to the negative end of the filament.

The ionization and collimating chambers were evacuated by two four-stage oil diffusion pumps of 25 l/sec. capacity, while the filament and analyzing chambers were evacuated by two single-stage air-cooled oil diffusion pumps (1.5 l/sec.) backed by a low vacuum diffusion pump of similar design. Octoil was used throughout, and a single Megavac exhausted the fore-vacuum manifold for all five diffusion pumps.

A Western Electric D-96475 tube in a stabilized DuBridge circuit with a Leeds and Northrup galvanometer of 10^{-10} amp./mm sensitivity was used to record the ion currents. The galvanometer deflections were registered by a photo-pen recorder[1] to which were geared potentiometers for varying either the electron or ion accelerating potentials. These potentiometers were additional to the usual manual controls and were of value in checking sensitivity and resolving power automatically. When using the instrument for studying changes of radical concentration with temperature, all electrical parameters were maintained constant and the abscissa of the photo-pen recorder then represented a time base.

The over-all sensitivity was controlled from the main panel by solenoid switches inside an evacuated and shielded housing surrounding the

[1] D. J. Pompeo and C. J. Penther, Rev. Sci. Inst. 13, 218 (1942).

D-96475 tube. These solenoid switches were designed with two positions of mechanical stability so that only a momentary application of current in one direction or the other was required in order to cut in or out a range of grid leak resistors from 10^8 to 10^{12} ohms.

One of the main experimental difficulties encountered throughout was occasioned by changes in sensitivity resulting from polarizing layers in the ionization chamber. Since the all-metal construction did not lend itself to thermal outgassing, an additional filament was used in the earlier stages as a source of intense electron bombardment. It was later found that coating the inside of the ionization chamber with Aquadag gave greater reproducibility and higher sensitivity.

The Reactor

Three main types of reactor have been used. Fow low reaction pressures (up to *ca.* 4 mm) it is not essential, although quite desirable, that the temperature at the place of exit of the gas sample be the same as that of the furnace. At higher pressures this condition must be met in order to approximate to the ideal of infinitely rapid expansion and freezing of the sample between the place of origin (reactor) and the place of analysis (ionization chamber).

The low pressure reactor, *R*.1, attached to the mass spectrometer at a ground joint, *J*, is illustrated in Fig. 1. The reactor consists of a water-cooled jacket, *W*, the inner wall of which is a stainless steel tube threaded at the lower end to receive the diaphragm holder.

The furnace consists of a double-walled quartz tube, *Q*, down the center of which the reactants enter. A platinum heating spiral with quartz dust insulation and a thermocouple (not shown) occupy the space between the quartz walls at the lower end. The main bulk of the reactants and products, after passing through the hot zone, are deflected upwards along the inner walls of the cooler to the exit where they are pumped away by mercury diffusion and Megavac pumps. Flow speed, pressure, and residence time are controlled by suitable valves and measuring devices. The size of the diaphragm, *D*, is selected so that a pressure of *ca.* 0.001 mm can be maintained in the ionization chamber for the required reactor pressure.

In certain investigations the quartz-tube furnace was replaced by a grid of five carbon filaments (Fig. 2) which could be lowered into a position just above the diaphragm. This type of reactor will be referred to as *R*.2. Temperatures were estimated by means of an optical pyrometer focused on the grid through a plane window situated on top of the reactor.

At higher pressures, such as are required for the study of unstable or reactive intermediates formed during combustion, neither *R*.1 nor *R*.2 are suitable. With an effective pumping speed of *ca.* 7 l/sec. at the diaphragm, it has been possible to work at reaction pressures up to 140 mm using the reactor, *R*.3, illustrated in Fig. 3. As before, this reactor is attached to the mass spectrometer at a joint, *J*, and consists of a water cooler, *W*, which is essentially a thick copper cylinder with vertical interconnecting channels milled in the outer surface, over which a tightly fitting thin brass sleeve is fitted. The water thus follows a number of up and down

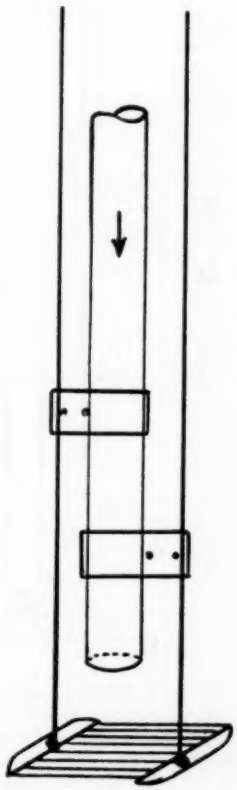

FIG. 2. Carbon filament reactor *R*.2. This replaces the quartz tube *Q* of Fig. 1. The short carbon filaments then lie immediately above the diaphragm *D*.

zig-zags around the copper surface, and provides efficient cooling for the waste gas as well as for the vacuum joints. In order to minimize pumping resistance and to leave reasonable space inside the reactor for the development of chains, the reactor is itself the heating element *H*. The furnace was made from a solid bar of 18:8 stainless steel, accurately bored internally to $\frac{5}{8}''$ diameter. The outer surface, except at the two ends, was then turned on a lathe until the wall thickness was approximately 20 mil and, after shaping the lower end to preserve a uniform mass of metal over any annular section of constant radial width, the furnace was heated by passing a heavy current through it. The temperature profile along the length was measured with a thermocouple, and metal was removed from those parts which were at a low temperature. With this design and method of manufacture a furnace was obtained which not only preserved a uniform temperature distribution over a considerable distance up from the bottom in which the thin diaphragm was fitted, but also exposed a minimum of heated surface to the ionization chamber. At high reaction pressures the diaphragm hole is of necessity small (<1 mil), and the danger of leaks between the reactor and the ionization chamber correspondingly great. The lower end of the reactor was screwed into the water cooler and sealed with a lead wire gasket under high mechanical compression. The diaphragm, usually an 0.8-mil gold disk, was compressed between gold washers against a recessed shoulder in the bottom of the furnace. By using Bethlon A (Bethlehem Steel) for the threaded compression plug retaining the diaphragm, the tendency of the metals to seize at high temperatures (up to 1000°C) was minimized, and little trouble was encountered in changing diaphragms. The upper end of the furnace was screwed into a thick copper tube, *C*, which served as one lead for the transformer current, the other lead being the water cooler. Waste gas passed through eight tubular ports in the cylinderical walls near the flat bottom and passed to exhaust *via* the spherical ground joint and sylphon *M*. In order to avoid distortion of the thin-walled reactor, the upper end of the copper tube, *C*, was brought out through the sylphon, *S*, which was held in neutral equilibrium by spiral springs which counteracted the differential pressures between the outside and inside of the reactor. The furnace was therefore free to expand, and the relative motion between the ends of the sylphon, *S*, amplified by a dial gauge, was in fact a convenient indicator of the wall temperature.

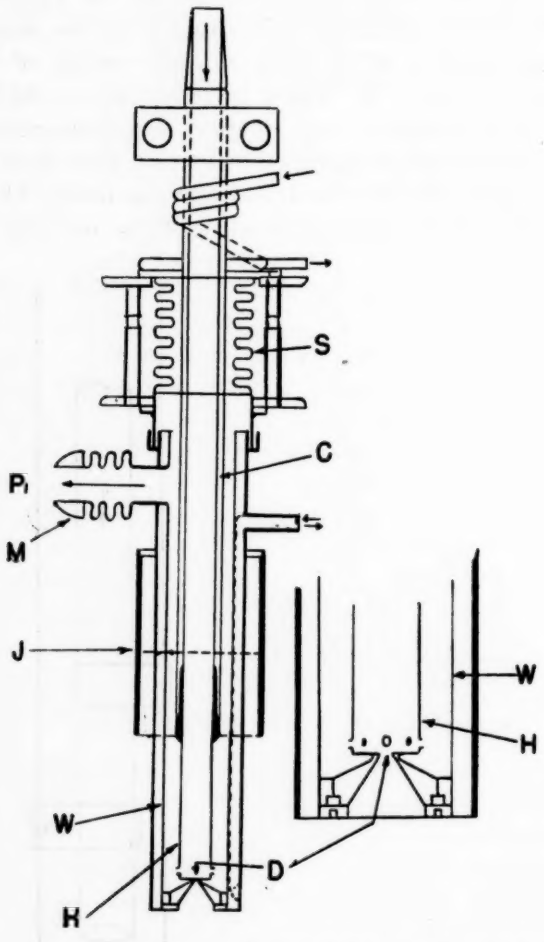

FIG. 3. High pressure reactor *R*.3. Stainless steel furnace *H*, water-cooled jacket *W*, joints for attachment to mass spectrometer *J*, and to exhaust *M*, copper conductor *C*, expansion joint *S*, diaphragm recess *D*. Enlarged view of furnace bottom in insert on right.

One of the chief difficulties with the steel furnace was the tendency of the diaphragm to become plugged. This was especially the case during a study of carbon monoxide combustion, and some evidence was obtained that this was caused by carbonyl formation and subsequent decomposition on the gold diaphragm. This difficulty was overcome by fabricating an exact thin gold replica of the inside surface of the reactor. The replica was obtained as a 0.7-mil electro-

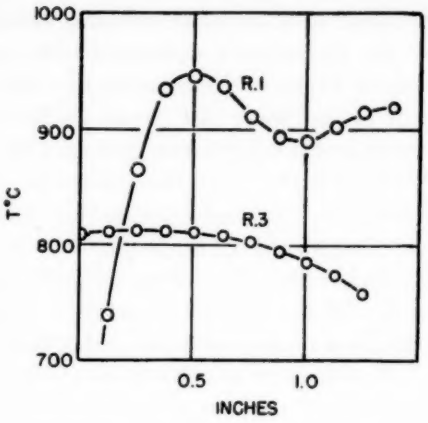

FIG. 4. Temperature profiles of quartz reactor *R*.1 and steel reactor *R*.3 in the vicinity of the diaphragm.

deposit on a polished copper form. After burnishing the gold, the copper was dissolved in acid and the thin shell inserted, with clearances of <1 mil, into the steel furnace. Gold was chosen for its low catalytic activity in hydrocarbon decompositions.

PERFORMANCE AND OPERATION

By means of a movable Chromel-Alumel thermocouple, the temperature gradient in the vicinity of the diaphragm was taken under operating conditions. Typical curves for *R*.1 and *R*.3 are shown in Fig. 4, with the distance in inches above the diaphragm plotted as abscissa. It is clear that the particular design of *R*.3 has provided a sensibly zero gradient in the immediate vicinity of the point of extraction, and equilibrium will therefore be maintained. In some models of the furnace, *R*.3, an additional heater was placed between the upper surface of the cone and the lower surface of the bottom. In this case either negative or positive temperature gradients could be maintained, but in general this refinement was considered unnecessary.

The procedure adopted in detecting reaction products was briefly the following. After suitable outgassing, the flow of reactants was adjusted until the pressure below the diaphragm remained constant at some pressure between 10^{-3} and 10^{-4} mm. Input and output flow values were adjusted to give a residence time in the hot zone of 10^{-1} to 10^{-3} sec. If the particular required product was also a product of the electron bombardment of one of the reactants, the electron voltage was increased until the ion appeared in sufficient strength to be focused on the final slit by adjustment of the ion accelerating field. The ion peak was then extinguished by lowering the electron voltage to the appearance potential, and the current through the furnace was increased slowly by means of a Variac in series with a low voltage transformer. The temperature was followed on a potentiometer and marked off along the time base of the photo-pen recorder. The photo-pen recorded any increase in the ion current occasioned by the formation in the reactor of the radical under investigation.

Rigid tests of the effect on the electrons and ions of the alternating magnetic field accompanying the heavy heating currents (up to 500 amp. in the case of *R*.3) failed to reveal any measurable influence. The complete axial symmetry of the furnace unit is instrumental in achieving this result.

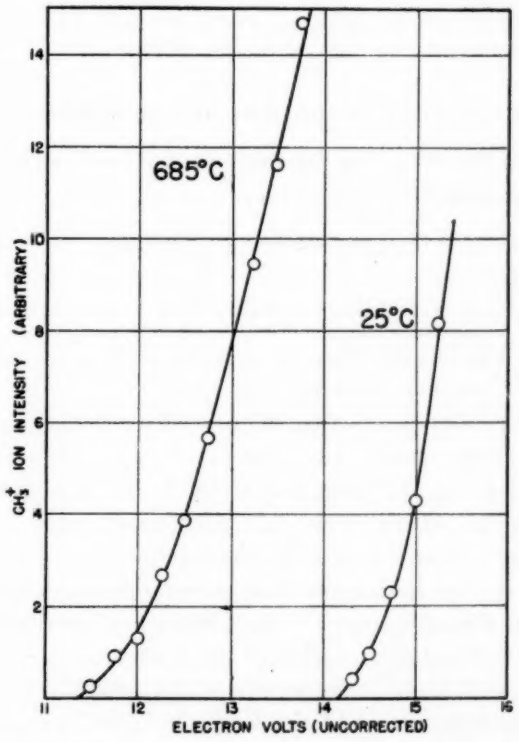

FIG. 5. Ionization functions of CH_3^+ with *R*.1 hot and cold, showing that in an ethane stream containing 0.6 percent $Pb(CH_3)_4$ sufficient radicals are produced to lower the normal appearance potential approximately 3 volts. Reaction pressure *ca*. 0.2 mm.

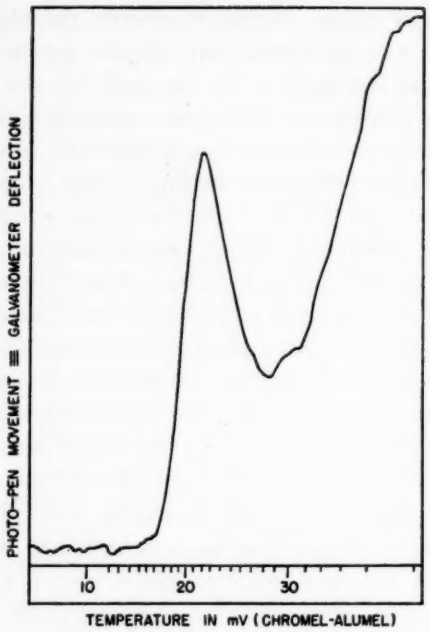

FIG. 6. Tracing taken from a photo-pen recording of the change of methyl radical concentration with time as the temperature of the furnace was increased. Markings along the abscissa indicate positions when the thermocouple registered integral values on a potentiometer. Time of complete record, approximately 10 min. Mixture, C_2H_6 +0.6 percent $Pb(CH_3)_4$ at 0.15 mm pressure.

THE VALIDITY OF UNDERLYING ASSUMPTIONS

In Fig. 5 the low potential ionization functions corresponding to the two processes

$$C_2H_6+\tilde{e}\rightarrow CH_3^++CH_3+2e \qquad (1)$$

and

$$CH_3+\tilde{e}\rightarrow CH_3^++2e \qquad (2)$$

are reproduced. These were obtained in a mixture C_2H_6+0.006 $Pb(CH_3)_4$ in reactor *R*.1 at a reaction pressure of *ca.* 0.2 mm. With the furnace at room temperature, process (1) is the only source of CH_3^+ ions, but at 685°C, the temperature at which curve (2) was taken, there is clearly a source of CH_3^+ ions requiring a lower energy for ionization. It is reasonable to assume that this new source is the CH_3 radical produced by thermal dissociation of the lead tetramethyl. At still higher temperatures (*ca.* 800°C) it is unnecessary to add the lead alkyl, and a curve similar to (2) is obtained by thermal dissociation of the pure ethane.

The curves of Fig. 5 were taken considerably prior to the publication by J. A. Hipple and D. P. Stevenson[2] of a paper in which a study was made of the ionization potential of CH_3 radicals produced by thermal dissociation of lead tetramethyl at low pressure (10^{-5} mm) in the ionization chamber of a mass spectrometer. Our value of 11.3 volts for the ionization potential of CH_3 taken from curve (2) agrees with that found by R. G. T. Fraser and T. N. Jewitt[3] but is about one volt higher than that found by Hipple and Stevenson. Since we were primarily interested in the maximum electron potential which could be applied without dissociating the parent molecule electronically, the causes for the discrepancy have not been sought. The low concentration of radicals compared with the carrier gas is undoubtedly a factor in our experiments which would decrease the apparent difference between $A(CH_3^+)$ and $I(CH_3^+)$.

Figure 6 is a photo-reproduction of an actual record taken of the thermal decomposition of the same mixture as used for Fig. 5, but with the electron acceleration, *E*, held constant just below the appearance potential, and the temperature increased manually. The temperatures marked off along the horizontal time base are those of the uncorrected furnace thermocouple. The details of this and similar curves obtained with different carrier gases will be discussed in Part II. Here it is sufficient to note that the concentration of CH_3 radicals apparently passes through a maximum and a minimum. The steep rise (when replotted on a linear temperature scale) after the minimum corresponds to a similar increase obtained in the absence of lead tetramethyl and is, therefore, attributable to a chemical change occurring in ethane.

The question arises as to whether the second increase in CH_3^+ ions can be unequivocally attributed to an increasing concentration of methyl radicals or to some other mechanism. There are three other alternatives. Some secondary decomposition product of ethane might have a lower $A(CH_3^+)$. One of the products, e.g., C_2H_4, might dissociate under electron impact to give the methylene ion in sufficient abundance so that the $C^{13}H_2$ isotope would account for the increase

[2] J. A. Hipple and D. P. Stevenson, Phys. Rev. **63**, 121 (1943).
[3] R. G. T. Fraser and T. N. Jewitt, Phys. Rev. **50**, 1091 (1936); Proc. Roy. Soc. **A160**, 563 (1937).

in mass 15. And finally there might be a sufficient concentration of vibrationally excited ethane molecules entering the ionization chamber so that the appearance potential of CH_3^+ is shifted below the fixed value of E chosen for the experiment.

The first possibility can be ruled out on the grounds that the value of $A(CH_3^+)$ is lower for ethane than for any C_nH_m hydrocarbon. The published values for methane, ethane, propane, *n*- and *i*-butane are 14.4, 14.2, 17.0, 22.5, and 20.7 volts, respectively. Actually the values for hydrocarbons higher than ethane mean very little since the "tail" of the ionization curve extends a considerable distance towards lower voltages. Nevertheless, the absolute intensity at voltages below 14.2 is quite negligible as was confirmed repeatedly in the present work.

The electronic production of CH_2^+ ions from ethylene can also be ruled out at 14.2 volts, since at least 19 volts would be required and the intensity of the isotope would be only 1.1 percent even at this high potential. No CH_2^+ ions were detectable in our apparatus, even at potentials where CH_3^+ was giving off-scale deflections.

The third possibility, namely, that the appearance of CH_3^+ ions on heating the gas is attributable to excited molecules rather than free radicals, is more difficult to disprove. From energy considerations it is natural to suppose that the rate of production of excited molecules will be greater than that of free radicals. However, it is probable that this increased rate will not be wholly represented in an increased equilibrium concentration because of the greater ease with which the vibrational energy can be dissipated. In the case of the decomposition of methane, it was possible to show that at high temperatures CH_3^+ ions could be detected at electron energies below the ionization potential of methane itself. To explain such a result on the basis of vibrational energy would require the hypothesis that excited molecules when struck by a low voltage electron can *only* dissociate to give a CH_3^+ ion. Yet any reasonable assignment of Morse curves coupled with the requirements of the Frank-Condon principle would lead one to expect that vibrational energy would lower *both* the ionization potential of the parent molecules (in this case methane), and the appearance potential of the CH_3^+ ion. We should, therefore, expect that since under normal conditions $CH_4^+ > CH_3^+$, no such violent change in this ratio as was actually found could take place on increasing the temperature, unless new particles such as free radicals are being formed thermally.

In the case of ethane it is not so easy to obtain such unequivocal experimental proof on account of the lower ionization potential of ethane and the large difference in mass. Nevertheless, other contributory evidence points to the same conclusion and is briefly reviewed below.

In one series of experiments, in order to study the effect of surface on radical concentration, a small, flat, movable spiral of tungsten was mounted inside the quartz tube of *R*.1. Keeping a constant temperature in the furnace windings, the spiral was gradually lowered towards the diaphragm. This resulted in a decrease in CH_3^+ concentration as indicated by the galvanometer deflection. With the spiral in its lowest position it was then heated by an electric current, whereupon the residual deflection disappeared almost completely. Thus the addition of energy had decreased the concentration of excited molecules or free radicals between the furnace and the diaphragm. Such a result is much more plausible on the hypothesis of a recombination of methyl radicals requiring an energy of activation than on the supposition of deactivation of excited molecules. With the spiral heated to still higher temperatures, the galvanometer deflection began to increase, indicating that the spiral was itself becoming a source of free radicals. This behavior parallels very closely the phenomena of recombination of atoms on heated surfaces studied by Roginsky and Schechter.[4]

Other evidence tending to confirm the radical rather than the molecular origin of the increase of CH_3^+ with temperature was obtained when the temperature coefficient was found to be independent of the electron accelerating potential. If excited molecules were responsible, we might anticipate that as the electron energy was increased the thermal activation energy would decrease as lower vibrational levels became effective. This was not the case. Such a result,

[4] S. Roginsky and A. B. Schechter, Acta Phys. Chim. U.S.S.R. 6, 401 (1937).

however, is quite consistent with the requirement that a free radical is involved in the change of methyl ion concentration with temperature.

Finally it was found that the ratio of the height of the minimum to that of the maximum, in curves similar to that depicted in Fig. 6, was independent of the electron potential (provided of course the latter did not exceed $A(CH_3^+)$ from unexcited ethane). This result also is consistent with the view that the same species of particle is responsible for both the low and high temperature increase of CH_3^+, and since there can be little doubt as to the radical origin of the decomposition product of lead tetramethyl, it follows with considerable certainty that the high temperature decomposition of ethane into free radicals can be studied by following the low voltage production of CH_3^+ ions.

There remains one other feature which might invalidate results obtained at higher pressures using *R*.3. As the reaction pressure is increased, it is necessary to reduce the size of the aperture in the diaphragm separating the reactor from the ionization chamber. The diaphragm, however, is at the same temperature as the reactor, and its underside is exposed to the gas in the ionization chamber. Since all investigators are apparently agreed that the detection of free radicals by the mirror method becomes increasingly difficult as the reaction pressure rises above a few mm Hg, it might at first sight seem surprising that the mass-spectrometric method has already extended the pressure range tenfold without approaching any insuperable difficulties. Using reactor *R*.1, in which the diaphragm is essentially at room temperature, the upper useful limit of pressure was *ca.* 15 mm, whereas with reactor *R*.3 radicals have been detected at 120 mm.

In order to examine the implication of this result more closely, let us take the two primary reaction mechanisms which have been proposed for the formation of methyl radicals from ethane:

$$2C_2H_6 = 2CH_3 + C_2H_6 \qquad (3)$$

and

$$C_2H_6 = 2CH_3. \qquad (4)$$

The main mechanism for the removal of methyl radicals will be

$$CH_3 + C_2H_6 \rightarrow C_2H_5 + CH_4, \qquad (5)$$

so that the equilibrium concentration of methyl radicals in the reactor will be,

$$[CH_3]_1 = k_1/k_3 \cdot C_2H_6$$

in the first case and

$$[CH_3]_2 = k_2/k_3 \text{ in the second,}$$

where k_1, k_2, and k_3 are the rate constants for reactions (3), (4), and (5), respectively. If now we have a series of diaphragms, $d_1, d_2, \cdots d_n$, such that reaction pressures $p_1, p_2, \cdots p_n$ above the diaphragm will give a constant pressure p' (*ca.* 10^{-3} mm) in the ionization chamber below, and if the primary production of methyl radicals proceeds according to a bimolecular mechanism, the partial pressure of the radicals in the ionization chamber will be

$$p_R = \frac{k_1}{k_3} \cdot [C_2H_6] \cdot \frac{p'}{p_n} = \frac{k_1}{k_3} \cdot p',$$

i.e., independent of the reaction pressure. If, however, the primary production is unimolecular the partial pressure of the radicals will be

$$p_R = \frac{k_2}{k_3} \cdot \frac{p'}{p_n}$$

and will decrease as the reaction pressure is increased to accommodate smaller diaphragms.

Hence it only will be possible to detect free radicals over a wide range of pressures if the order of the producing mechanism is the same as or greater than that of the radical removing mechanism.

Since, however, the radical partial pressure in the ionization chamber depends on the ratio k_1/k_3, which in turn depends exponentially on the difference between the activation energies E_1 and E_3 of the two reactions (where $E_1 \gg E_3$), it is clear that the radical concentration will decrease rapidly with increasing pressure if the radicals have to pass through a long length of cooler gas as in the mirror technique.

Thus our finding that methyl radicals could be readily detected at high pressures would indicate a bimolecular mechanism for their production and an absence of an appreciable cool zone in reactor *R*.3, provided we eliminate any possible additional source of radicals such as the hot

surface of the diaphragm exposed to the ionization chamber.

This source of uncertainty in the interpretation was removed by comparing the concentration of methyl ions under identical conditions, except that in the one case a pressure of 10^{-3} mm was maintained in the usual way by ethane at a high pressure effusing into the ionization chamber through the reactor diaphragm, whereas in the second case a pressure of 10^{-3} mm was maintained in both the reactor and the ionization chamber by means of an auxiliary leak to the latter. Even when the pressure was increased to 3.10^{-3} mm there was no deflection attributable to CH_3 radicals in the second case. Thus there can be no doubt that the radicals observed in the first case were actually coming from inside of the furnace and not from the heated underside of the diaphragm.

LIMITATIONS OF THE METHOD

As a result of the control experiments summarized above, the validity and usefulness of the method were considered well established. Before proceeding to a more detailed discussion of the application of the method to specific examples, certain limitations will be briefly discussed.

Sensitivity

It is not possible to give any one figure which will represent the lower limit of concentration which can be detected. Apart from the usual reciprocal relationship between resolving power and slit-width, there is the important factor that the upper limit of allowable electron energy is the appearance potential of the particular radical ion formed by electron bombardment of either the parent molecule or one of the reaction products—whichever is the lower. For example, a study of Table I, in which data have been collected on the products of electron dissociation of ethane, ethylene, and methane from the measurements of Hipple,[5] Kusch, Hustrulid, Tate,[6] L. G. Smith,[7] and others, reveals considerable differences between the probable detectability of different products. Of the end products of the thermal decomposition of ethane, both hydrogen and methane are detectable in quantities far smaller than ordinarily required in chemical analysis. Ethylene, because of its great abundance in the electron spectrum of ethane, and the relatively small difference (1.3 ±0.6 volts) between the appearance and ionization potentials, is less detectable—though relatively easily detectable compared with the low concentration radicals. Preliminary calculations indicated that methyl and methylene radicals with potential differences of 4.2±0.3 and 4.3±1.0 volts, respectively, should be detectable in concentrations down to *ca.* 0.001 percent or even lower with an improved design of mass spectrometer.

The ethyl radical deserves mention on account of its predicted abundance in the decomposition of ethane and because it serves to illustrate the caution required in this type of analysis. The difference between the appearance and ionization potentials being 4.2±0.2 volts, its detectability might be expected to be moderately high. However, much larger amounts of ethylene will accompany the formation of ethyl at moderate pressures and contact times, so that we have to reckon with the ethylene isotope of mass 29 which will also be present to the extent of 2.2 percent of the ethylene formed. Since the ionization potential of ethylene is 10.8±0.5, this potential, and not the appearance potential 12.9±0.2, must be used when searching for the ethyl radical. This naturally decreases very materially the sensitivity in this particular case.

TABLE I.

Ion	Ionization potential	Appearance potential from C_2H_6	Appearance potential from C_2H_4
$C_2H_6^+$	11.6±0.1	11.6±0.1	—
$C_2H_5^+$	8.7±0.2	12.9±0.2	—
$C_2H_4^+$	10.8±0.5	12.1±0.1	10.8±0.5
$C_2H_3^+$	9.9	15.2±0.3	14.1±0.1
$C_2H_2^+$	11.2±0.1	15.0±0.3	13.4±0.2
C_2H^+	11.3	27.0±1.0	19.2±1.0
C_2^+		31.5±1.0	26.4±1.0
CH_4^+	13.1±0.4	—	—
CH_3^+	10.0	14.2±0.3	—
CH_2^+	11.9	16.2±1.0	19.2±0.3
CH^+	11.1	24.5±1.0	22.9±0.5
C^+	(11.3)	30.4±1.5	24.6±0.5
H_2^+	15.4	28.0±1.5	22.4±1.5
H^+	13.5	20.8±1.0	26.2±1.5

[5] J. A. Hipple, Jr., Phys. Rev. **53**, 530 (1938); J. A. Hipple, Jr. and D. P. Stevenson, Phys. Rev. **63**, 121 (1943); D. P. Stevenson, J. Am. Chem. Soc. **65**, 209 (1943).

[6] P. Kusch, A. Hustrulid, and J. T. Tate, Phys. Rev. **52**, 843 (1937).

[7] L. G. Smith, Phys. Rev. **51**, 263 (1937).

Calibration

Theoretically, if we know the potential at which the measurements are made and the probability of ionization, it would be possible to estimate the absolute concentration of the radicals. Ionization probabilities at low potentials are mostly unknown, however, and are naturally sensitive to such factors as electron energy spread and space charge in the ionization chamber. Calibration for the permanent end products of a reaction is carried out in the conventional manner by comparing ion deflections of a given product, when the latter is produced thermally, and by addition of a known amount to the gas stream.

In order to calibrate for a transient radical there is no such golden rule, in fact no rule at all in most cases. In the case of methyl radicals, by working at low pressures and with neutral carrier gases containing small known amounts of lead tetramethyl, curves similar to Fig. 5 (except that the deflection reaches a plateau instead of passing through a maximum and minimum) may be used to indicate the maximum deflection corresponding to total decomposition of the lead tetramethyl. Similar techniques, in which are used diazomethane for CH_2, lead tetraethyl for C_2H_5, and Bonhoeffer and Reichardt's[8] steam equilibria data for OH, might be applicable but have not been tried in the present work. For the allyl and vinyl radicals there is at present no such known approach.

DISCUSSION

During the course of the experiments reported above and in the two communications which follow, it became increasingly clear that considerable improvements in performance could be expected by making use of the Nier-type mass spectrometer employing a 90° magnetic path. In this way the ion source is sufficiently far from the pole pieces to allow a more effective location of the pump with respect to the diaphragm through which the radicals are issuing.

This feature, which is of relatively little importance at low reaction pressures where the aperture in the diaphragm is comparatively large, may be decisive in the detection of certain radicals at higher pressures.

For a pumping speed of S liters per sec. in the ionization chamber, the diameter of the aperture, D, required to maintain a differential pressure ratio $p:10^{-3}$ mm, where p is the reaction and 10^{-3} the ionization pressure, will be given approximately by

$$D=\left(\frac{4S}{\pi}\cdot\frac{10^{-3}}{12p}\right)^{\frac{1}{3}}\text{ cm.} \tag{6}$$

Substituting $S=7$ l/sec. and $p=100$ mm, we get $D=2.7\cdot10^{-3}$ cm or 27μ.

Now the average number of collisions (n) made by each molecule on the walls of a short channel of length L and diameter D can be shown to be approximately $4L/D$ during the time of transfusion. Hence radicals or atoms which are sensitive to a single wall collision at high temperature will be removed almost completely from the sample when $4L/D>1$.

If we adopt as a criterion of "free" passage through the aperture the condition that

$$n\gtrsim0.8,$$

which will allow at least 20 percent of the radicals to transpire without suffering a wall collision, then with $L=10\mu$, which probably represents a practicable lower limit of diaphragm thickness, the diameter, D, must be at least 50μ, and the pumping speed (from Eq. 4) must be approximately 25 l/sec. for a reaction pressure of 100 mm.

This seeming diversion into the realm of future development of the method was deemed necessary to illustrate the care with which a negative result must be treated. There is evidence that the lower hydrocarbon radicals are fairly stable towards surface collision at moderate temperatures. Atoms such as H, O, and the radical OH are probably less stable (W. V. Smith[9]), and although theoretically it might be possible to select specific materials such as Ta for H atoms or W for O atoms to minimize recombination, the more general approach of high pumping speed would appear preferable.

In concluding this section it is a privilege to record my deep appreciation of those who at

[8] K. F. Bonhoeffer and H. Reichardt, Zeits. f. physik. Chemie **A139**, 75 (1928).

[9] W. V. Smith, J. Chem. Phys. **11**, 110 (1943).

various times have contributed to the development of the method—Professors N. N. Semenov and V. N. Kondratjew in whose laboratories the groundwork was laid, E. Luttrop, N. S. Heikes, and the Fanger Research Laboratories for constructional ideas and skill, and Dr. O. Beeck for his steady interest during all phases of the work.

Part II. The Thermal Decomposition of Some Lower Hydrocarbons

The method described in Part I has been applied in a preliminary survey of certain intermediates occurring during the decomposition of methane, ethane, propane, propylene, butanes, butylenes, oxygen, and nitric oxide with and without admixtures of lead tetramethyl, and in dimethyl ether and diazomethane. Methylene appeared in the last named case but not in the low pressure decomposition of methane. Methyl radicals both at high and low pressures were detectable and reasons are given for the belief that the primary decomposition of ethane is bimolecular. The interaction of methyl with ethane and propylene has been followed up to 1000°C, and, in the case of propylene, the allyl radical was detectable but not vinyl. The interaction between methyl and various carrier gases falls qualitatively in the following series of descending order, C_3H_6, NO, C_2H_6, C_2H_4, H_2, O_2, and He. CH_3O from methyl ether is apparently more reactive or unstable than methyl. The rate constant of decomposing $Pb(CH_3)_4$ is found to be $k=1.5\cdot10^{10}\exp(-28{,}000/RT)$. Hydrogen atoms and ethyl radicals have been found in certain instances, but further refinements in technique will be required before these and heavier radicals can be studied systematically.

The results which form the subject of this communication were obtained during an investigation of the range of application of the method described in Part I. The original objective had been to extend if possible the range of pressures at which radicals can be detected so that combustion phenomena could be studied more directly. The choice of hydrocarbon decompositions was dictated by their comparative simplicity and the desirability of having a basis of comparison between the mirror and mass spectrometric methods. Although results obtained with several hydrocarbons are reported, this should not be taken as meaning that such hydrocarbons have as yet been studied exhaustively by the new method. It was considered expedient at this stage of development to survey a broad field semiquantitatively.

The following abbreviations will be used:

R.1—quartz furnace with cool diaphragm,
R.2—carbon filaments above the cool diaphragm,
R.3—steel furnace with uniform temperature distribution in the neighborhood of the diaphragm,
E—electron accelerating potential.

METHANE

Using a freshly blown and outgassed quartz furnace no CH_3 radicals could be detected in pure methane in the pressure range 0.01 to 0.3 mm, up to temperatures of 1100°C. After heating the tube to *ca.* 950°C in a stream of ethane or natural gas at *ca.* 1-mm pressure for one hour, it was found that methyl radicals could readily be detected in pure methane and that the surface activity then persisted even after such treatments as outgassing, heating in air, or washing in nitric acid.

The growth of CH_3^+ with temperature at a reaction pressure of 0.014 mm is illustrated in Fig. 1. In spite of the non-uniform temperature profile of *R*.1 (see Part I, Fig. 4) a reasonable estimate of the temperature coefficient at this pressure can be made from the $\log CH_3 \sim 1/T$ replot given in Fig. 2. From the slope of the line

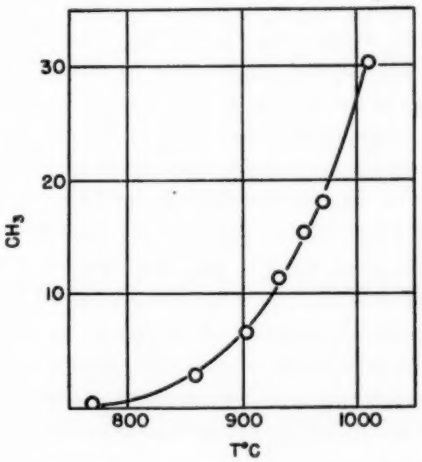

FIG. 1. Growth of CH_3^+ with temperature in methane. Reaction pressure, 0.014 mm. Concentration of CH_3 in arbitrary units.

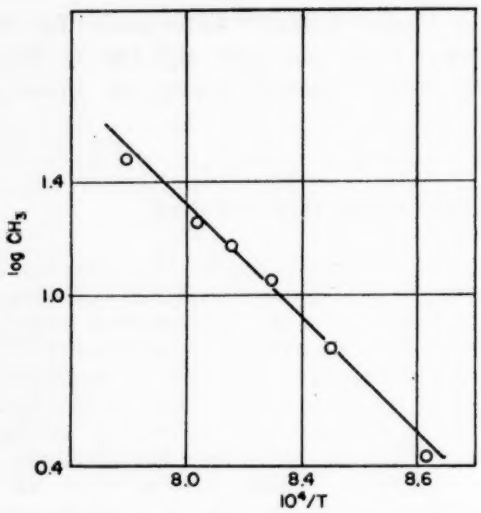

FIG. 2. Temperature coefficient of methyl concentration in methane. Reaction pressure, 0.014 mm.

we get a value of *ca.* 46 kcal. for the activation energy. At 0.014-mm pressure, the mean free path is of the same order as the diameter of the reactor (3 mm) and very much greater than the diameter of the pores of the surface structure, created presumably during activation. In such cases, as Zeldowich[1] has shown, a lowering of the activation energy by a factor of two may be expected at high temperatures.

Repeated efforts to detect CH_2 radicals and H atoms with the quartz reactor failed. In both cases the mass-spectrometric conditions are quite favorable. Thus Smith[2] gives for the appearance and ionization potentials of CH_2, 15.7 ± 0.5 and ≤ 12.0 volts, respectively, and in the case of hydrogen atoms we have the corresponding values of 18.0 and 13.5 volts. In the latter case the value of the appearance potential in hydrogen is taken rather than the value in methane (22.7 ± 0.5 volts), since molecular hydrogen was detectable in the decomposition products.

In practice, the sensitivity for methylene detection is even greater than for methyl radicals on account of the much lower yield of CH_2^+ from electron bombardment of methane. In order to check the possibility of detecting free methylene, experiments were conducted in which helium, purified by passage over active charcoal in liquid nitrogen, was passed over a 3 percent solution of diazomethane in diethyl ether contained in a low temperature trap. The helium pressure in *R*.1 was varied from 0.1 to 0.01 mm. With the trap at -110°C there was no evidence of CH_2, but on increasing the temperature to -90°C, deflections as high as 50 cm could be obtained at *ca.* 500°C. The deflection was still increasing at 900°C, indicating that at these low pressures, and residence times of the order 10^{-3} second, decomposition was not complete. On decreasing the pumping speed the deflections increased rapidly, indicating that reaction products were not appreciably diminishing the methylene concentration.

These qualitative results proved conclusively that the absence of methylene radicals in the low pressure decomposition of methane could not be attributed to a failure of the method of detection.

Belchetz and Rideal[3] have published evidence that the methylene radical can be detected in methane by interaction with a cooled iodine mirror, provided the place of origin of the radicals is within the mean free path of the detecting surface. The yields were very small and only after some four hours had sufficient methylene iodide accumulated for analysis. Methyl radicals made their appearance when the distance between the hot carbon filament and the iodine was increased from 3 mm to 1 cm, which at 0.1-mm pressure is greater than the mean free path. F. O. Rice[4] has repeated part of this work using tellurium mirrors and found no evidence of CH_2. Methyl radicals were detectable at separations greater than the mean free path as in Belchetz and Rideal's experiments. Pearson, Purcell, and Saigh[5] conclude from the behavior of CH_2, produced thermally from diazomethane and photo-chemically from ketene in various carrier gases, that the results of Belchetz and Rideal are more plausible.

Since the only direct evidence of CH_2 radicals from methane has been obtained when using platinum or carbon filaments as the source of heat, a similar source was constructed using

[1] Ya. B. Zeldowich, J. Phys. Chem. U.S.S.R. **13**, 163 (1939).
[2] L. G. Smith, Phys. Rev. **51**, 263 (1937).
[3] L. Belchetz and E. K. Rideal, J. Am. Chem. Soc. **57**, 1168 (1935).
[4] F. O. Rice, J. Am. Chem. Soc. **61**, 213 (1939).
[5] T. G. Pearson, R. H. Purcell, and G. S. Saigh, J. Chem. Soc. 409 (1938).

several short parallel carbon filaments embedded in Aquadag between nickel foil, and this grid-like heater was placed at a distance of 3 mm above the diaphragm of the water cooler. The aperture in the diaphragm was 1.5 mm so as to give ample opportunity for any CH_2 radicals to escape unhindered into the ionization chamber below. With temperatures up to 1200°C and pressures down to 10^{-3} mm no CH_2 radicals could be detected although CH_3 radicals were abundant. At these low pressures it would appear probable that the methyl radicals are primary and not caused by reaction of methylene and methane. It is difficult to reconcile our results with those of Belchetz and Rideal unless different surface conditions prevailed on the carbon filaments. The fact that Belchetz and Rideal had to renew the iodine surface at frequent intervals in order to obtain measurable quantities of product is possibly of significance since in our experiments, especially with metal filaments, transient phenomena on reheating the filaments were a common feature. Thus, allowing the cool filament to rest for a few minutes in the stream of gas always produced an anomalous distribution of products when the filament was reheated. No attempt was made in this preliminary survey to study these changes systematically, but enough evidence was accumulated to indicate that, with suitable modifications, the mass spectrometric method might be adapted to provide a sensitive means of investigating certain phases of surface reactions, in particular those occurring on single crystals of preferred orientation where the amount of material is usually too small for chemical methods.

At high pressures, up to 100 mm, methyl radicals were readily detectable in methane using *R*.3, but for reasons given later the yield was not studied quantitatively.

ETHANE AND PROPYLENE

In an attempt to obtain a more quantitative estimate of the number of methyl radicals entering the ionization chamber, small concentrations of tetramethyl lead (TML) were carried in a stream of pure helium into *R*.1. A typical decomposition curve showing the growth of CH_3 radicals as a function of temperature is shown in Fig. 3. Provided the reactor was clean, the helium pure, and the pressure low, the curve flattened off at a temperature of *ca.* 700°C depending on the contact time. The general rule in carrying out these calibrations was to keep the TML concentration below 1 percent of the carrier gas so that other decomposition products (CH_4, C_2H_4, and C_2H_6 were identified) would not interfere appreciably with the transport of the methyl radicals to the ionization chamber. In practice it was found convenient to saturate the carrier gas at low pressures and temperatures (*ca.* −70°C) so that the gas line could be rapidly pumped out without evaporating large quantities of TML. Since the vapor pressure of TML at −70°C was not accurately known, a master calibration with a saturator at 0°C and helium at atmospheric pressure was also made. Since a number of approximations have to be made in applying the results of such calibrations in the present apparatus, we can rely only on obtaining the right order of concentration, and in the following it will be assumed that where a concentration x of TML has been totally decomposed, the galvanometer deflection is that produced by a corresponding concentration of methyl radicals.

From curves of the type shown in Fig. 3 we can obtain a value for the heat of activation and the unimolecular frequency factor for the decomposition of TML. Thus the concentration of

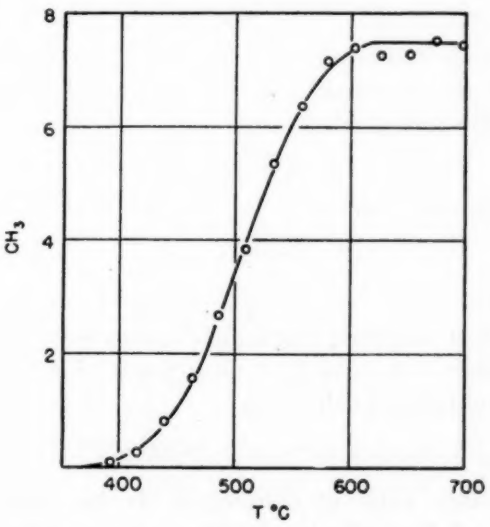

FIG. 3. Growth of methyl concentration with temperature in He+0.006 $Pb(CH_3)_4$ mixture. Reaction pressure, 0.4 mm. Quartz reactor *R*.1.

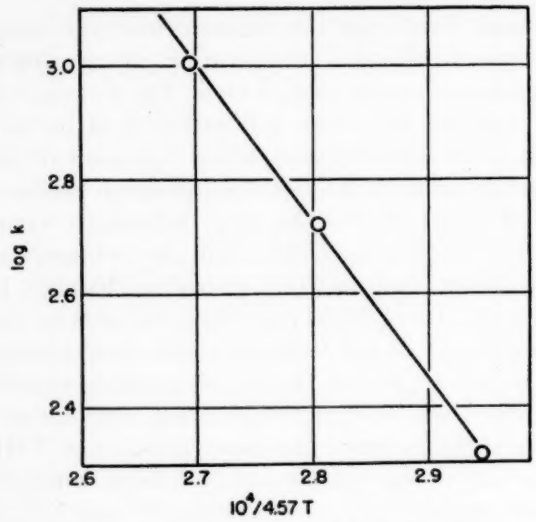

FIG. 4. Temperature coefficient of methyl concentration in a decomposing stream of He+0.006 $Pb(CH_3)_4$. Reaction pressure 0.4 mm. Quartz reactor *R*.1.

radicals in an unreacting atmosphere will be z where

$$z=\alpha(x_0-x). \tag{1}$$

Here x and x_0 are the instantaneous and zero-time concentrations of TML, and α is a constant of the order of unity. We also have

$$-dx/dt=k_1x, \tag{2}$$

where k_1 is the velocity constant for TML decomposition. Thus after integration and substitution we have

$$z=\alpha x_0(1-\exp(-k_1t_0)), \tag{3}$$

where t_0 is the reaction time. Since, by assumption, the maximum value of the radical concentration z_m is given by

$$z_m=\alpha x_0,$$

we obtain finally

$$\ln(z_m-z)/z_m=-k_1t_0. \tag{4}$$

In Fig. 4 the plot of $\log k_1$ against $10^4/4.57T$ is given. From this, and similar curves for slightly different values of t_0, a mean expression for k_1 was obtained in the form

$$k_1=1.5\cdot10^{10}\exp(-28200/RT).$$

The only value of E found in the literature is that of Romm[6] who, in the course of induced polymerization experiments, obtained a value of 23.5 kcal. Leermakers[7] obtained 36.9 kcal. for the decomposition of tetraethyl lead.

The behavior of the radical concentration as a function of temperature was quite different from that illustrated in Fig. 3 when a reactive gas was used as the carrier. A preliminary note[8] on this has already been published in which curves obtained at *ca.* 0.1-mm pressure were reproduced. More reliable data have been obtained for the carrier gases ethane and propylene at higher pressures. The curves, each point on which is the mean of three experimental readings, are reproduced in Fig. 5.

The marked maxima and minima may be explained in the following manner. As the temperature is increased the TML commences to decompose. Simultaneously, some of the radicals are removed by the reaction

$$CH_3+RH\rightarrow CH_4+R.$$

Since the activation energy of this reaction is less than that for TML decomposition, there can be no maximum unless and until appreciable quantities of the TML are decomposed in the first sections of the furnace. These sections being further removed from the diaphragm afford greater time for the removal reaction to "filter out" the radicals. Thus at certain pressures, temperatures, and contact times the removal mechanism will overtake production, and this will continue until a new source of radicals, namely, the carrier gas itself, causes production to overtake removal.

We can set up the equation for such a mechanism in the following way. Assuming unimolecular decomposition and bimolecular removal, the instantaneous rate of production of radicals z will be

$$dz/dt=k_1x+k_2y-k_3zy, \tag{5}$$

where x and y are the instantaneous concentrations of TML and the carrier, respectively. Provided x_0, the initial concentration of TML, is small compared with y, we may regard the latter as constant. Then, since

$$x=x_0\exp(-k_1t), \tag{6}$$

[6] R. S. Romm, J. Gen. Chem. U.S.S.R. 10, 1784 (1940).

[7] J. A. Leermakers, J. Am. Chem. Soc. 55, 4508 (1933).

[8] G. C. Eltenton, J. Chem. Phys. 10, 403 (1942).

we get by substitution and integration

$$z=\frac{k_1x_0}{(k_3y-k_1)}[\exp(-k_1t_0)-\exp(-k_3yt_0)] + \frac{k_2}{k_3}[1-\exp(-k_3yt_0)]. \quad (7)$$

In this equation x_0, t_0, and y are experimentally determinable, while k_1 has already been found for a neutral carrier gas. Thus it is simple, though somewhat laborious, to substitute probable values of k_3 in the first term on the right-hand side of Eq. (7) until the low temperature rise and the maximum are fitted to the experimental curve. A similar procedure with the second term establishes the minimum and the high temperature rise. Unfortunately for this section of the discussion the experimental results were not taken with sufficient refinement to justify placing much weight on numerical values obtained by this procedure. Uncertainties in the temperature distribution and contact time were not eliminated at this stage of development as interest lay in the endeavor to devise techniques for much higher pressures where the removal of CH_3 by the carrier is so rapid that the maximum-minimum character of the curve is obliterated. Such curve-fitting as was attempted with the present inadequate data showed clearly the great sensitivity of the positions of the maxima and minima to the frequency factors. For example, using 9.0 kcal. for E_3 in the case of TML in C_2H_6, a frequency factor as low as 5.10^7 had to be used and the results with propylene suggest that its greater efficiency as a remover of CH_3 may be attributable *in this temperature range* to a higher frequency factor rather than the lower activation energy of 3.1 kcal. as found by Smith and Taylor.[9] It should be noted in passing that Eq. (7) does not take into account the removal of CH_3 by lead liberated in the reaction and deposited in the cooler sections of the reactor, and evidence was subsequently obtained that a more accurate picture might have been obtained had oxygen been used instead of helium in deriving the constants of TML decomposition.

Before leaving the subject of the maximum-minimum type curves depicted in Fig. 5 we may briefly summarize the results obtained with other carrier gases. In argon the behavior, as was to be expected, was similar to that in He. In ethylene and hydrogen there was considerably less removal of CH_3 and less production of CH_4 than in C_2H_6. In oxygen there was, contrary to expectation, less removal than in C_2H_6. An O_2-TML curve plotted on the same scale as that used for C_2H_6 and C_3H_6 is included in Fig. 5. Methyl radicals are, therefore, rather stable towards oxygen, a conclusion which is supported by measurements of methyl radicals in methane-oxygen flames (see following communication). That some reaction is taking place is made evident not only by the appearance of a maximum but also by the appearance of significant amounts of mass 30. This was ascribed to formaldehyde rather than to ethane since only insignificant amounts were formed when nitrogen was substituted for oxygen.

In nitrogen there was significantly less de-

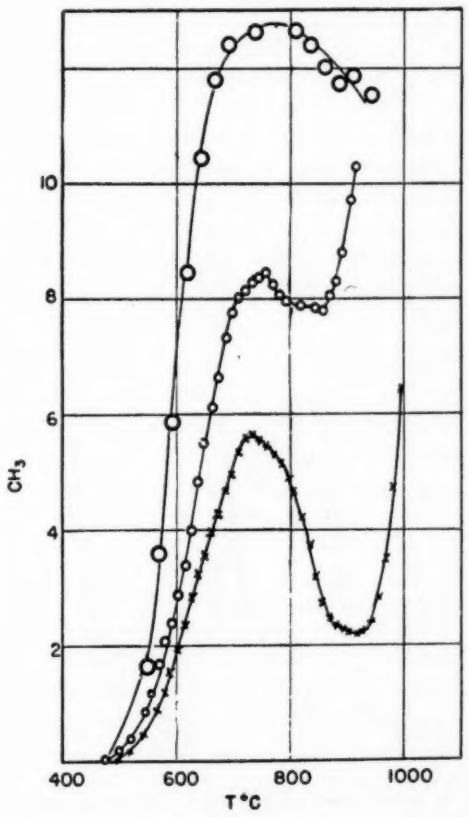

FIG. 5. Production of methyl in mixtures of 0.6 percent $Pb(CH_3)_4$ in oxygen ○, ethane ○, and propylene ×. Quartz reactor *R*.1. Pressure *ca.* 1.1 mm.

[9] H. S. Taylor and J. O. Smith, Jr., J. Chem. Phys. **8**, 543 (1940).

velopment of methyl than in oxygen. This, at first sight, anomalous result is probably an indication of the influence of atomic and deposited lead in reducing radical yields. With oxygen as a carrier it seems plausible to assume that the lead is poisoned and its radical removal efficiency decreased.

When nitric oxide was mixed with ethane in the proportions 1:2 and used as a carrier, there was a scarcely noticeable increase in the rate of removal, indicating that, although a chain breaker, its affinity for methyl does not greatly exceed that of ethane. When using pure nitric oxide as a carrier, the radical concentration was drastically reduced but there was evidence that this was partly a surface effect since, on returning to an ethane stream, several runs had to be made before the normal ethane curve was obtained.

On account of polarizing layers built up on the electrode surfaces when the three butylenes were decomposed, a strict comparison could not be made with these carrier gases. There were indications that iso-butylene removed methyl more effectively than β-butylene and that the activation energy for methyl production in iso- was less than in β-butylene. It is probable that with the improved geometry which could be achieved with a 90° magnetic path less trouble would be encountered, since the molecular beam can be directed parallel with, rather than perpendicular to the plane of the first ion-collecting slit.

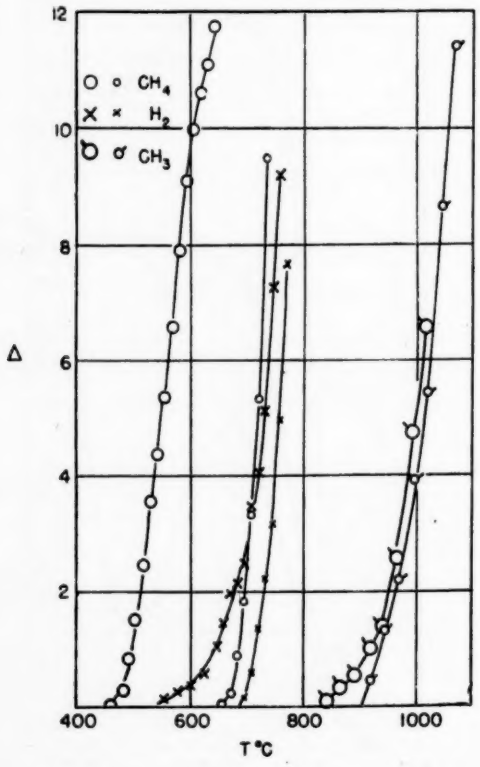

FIG. 6. Production of methane, hydrogen, and methyl in decomposing ethane with and without addition of $Pb(CH_3)_4$. Large symbols—with approximately 0.1 percent TML added. Small symbols—pure ethane. Quartz reactor *R*.1. Pressure 19 mm.

THE EFFECT OF PRESSURE ON THE MAXIMUM-MINIMUM CURVES

The effect of pressure on the shape of the methyl curve can best be explained in terms of what for want of a better expression we shall call the appearance temperature. This is the temperature at which a positive deflection due to ionization of a product appears. Provided the sensitivity of detection remains constant, the appearance temperature is an indication of the partial pressure of the product in the ionization chamber and above the exit from the reactor. By increasing the pressure in the reactor we automatically increase the pressure in the ionization chamber, and we should, therefore, expect the appearance temperature to decrease for both unimolecular and bimolecular processes. However, if as is more desirable though also more laborious, the pressure in the ionization chamber is maintained constant by adjusting the size of the diaphragm, then the appearance temperature will depend on the relative partial pressures of reactant and product, the latter being small. Hence the appearance temperature will increase for a unimolecular production mechanism and should remain sensibly constant for a bimolecular mechanism.

Although we were not primarily interested in this aspect it became clear that over the pressure interval 0.1 to *ca.* 4 mm a bimolecular process in the decomposition of ethane was becoming increasingly dominant over the surface reaction previously mentioned. Above 7 mm the appearance temperature when using *R*.1 increased rapidly, but this can be accounted for by the efficiency of the cool zone between the furnace and the diaphragm in removing radicals much faster than they are produced. In Fig. 6, curves

obtained in C_2H_6 with and without addition of approximately 0.1 percent TML are reproduced for the products CH_4, CH_3, and H_2. It is clear that the CH_3 radicals produced from the TML have been almost completely filtered out and have been replaced by methane. The addition of the TML has also increased the production of hydrogen. The curves for CH_4 and H_2 obtained without TML can be replotted for estimating the activation energies; these replots are shown in Fig. 7. From the slopes we obtain: $E(CH_4)=91$ kcal. and $E(H_2)=77$ kcal.—values which appear slightly high although the latter agrees with that found by Kuchler and Theile[10] and used by Rice and Herzfeld.[11] In a static system we should expect $E(CH_4)$ to equal the activation energy for the primary rupture of ethane into two methyl radicals provided the stationary state, represented by

$$dCH_3/dt=dz/dt=k_2y-k_3zy=0,$$

has been reached. Actually, however, at low pressures and contact times of the order 0.001 second, the stationary state is not reached and we have

$$z=k_2/k_3\cdot(1-\exp(-k_3yt)),$$

whence

$$dCH_4/dt=du/dt=k_2y(1-\alpha),$$

where $\alpha=\exp(-k_3yt)$ and the "activation energy" obtained from the temperature coefficient will be

$$d\ \ln u/d(1/T)=-E_2/R+\beta E_3/R,$$

where

$$\beta=[\alpha(1+k_3yt)-1]/[k_3yt+\alpha-1].$$

β is negative and approaches $-1/k_3yt$ as yt becomes large. Since in general $E_2\gg E_3$, the errors become negligible at pressures above 10 mm, but they may be as high as 6 kcal. at 1 mm.

Convincing evidence that the rise in the appearance temperature with increasing pressure is ascribable to the filtering action of the cool zone rather than to a unimolecular primary rupture was obtained when using *R*.3 where the cool zone is eliminated. Although this reactor was primarily designed for combustion studies and does not have the proper dimensions for establishing temperature equality throughout a given cross section at the streaming velocities required, nevertheless the sample, being drawn from the center, will, if anything, be at a lower temperature than that registered by a thermocouple situated off-axis. Hence any errors will tend to increase the appearance temperature. Actually the appearance temperature at 30 mm is considerably lower than that obtained at 18 mm in *R*.1, and is not sensibly different from values obtained at still higher pressures—up to 110 mm. Although it might be premature at this stage of development to place complete confidence in these semiquantitative results, the evidence is considerable that the primary rupture of ethane is bimolecular, as proposed by Kuchler and Theile, when the pressure is sufficiently high to escape contributions from the unimolecular surface reaction.

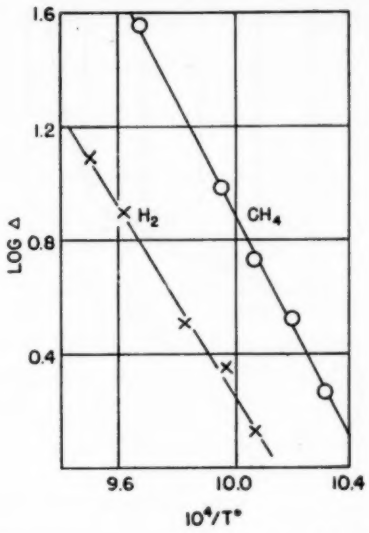

FIG. 7. Temperature coefficient replot of hydrogen and methane production in pure ethane. Quartz reactor *R*.1. Pressure 19 mm.

OTHER RADICALS

C_2H_5—Reference to Table I of Part I in this series shows that although the difference between the ionization potential of C_2H_5 and the appearance potential from C_2H_6 is approximately $8.7-12.9=-4.2$ volts, which should afford sufficient freedom in selecting a potential such that $\Delta_0C_2H_5^+\ll\Delta C_2H_5^+$, where Δ_0 and Δ are the electronically and thermally produced contributions, respectively, nevertheless the ethyl radical

[10] L. Kuchler and H. Theile, Zeits. f. physik. Chemie **B42**, 359 (1939).

[11] F. O. Rice and K. F. Herzfeld, J. Chem. Phys. **7**, 671 (1939).

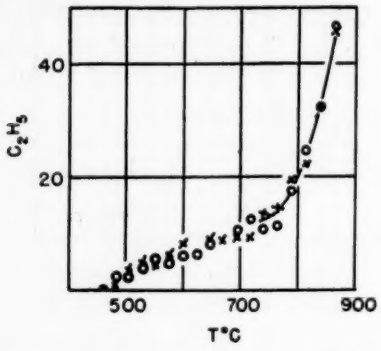

FIG. 8. Growth of the ethyl radical in a decomposing stream of C_2H_6+0.006 percent $Pb(CH_3)_4$. Pressure 0.03 mm. Approximately one-third of the height of the curve is attributable to the $C^{13}C^{12}H_4$ isotope.

has proved to be one of the most difficult to detect with certainty. The difficulty is occasioned by the fact that the ionization potential of C_2H_4 is only about two volts higher than that of C_2H_5 so that in reactions where C_2H_4 appears as an end product its isotope of mass 29 also appears in quantities comparable with, and usually greater than the anticipated concentration of free ethyl. With the present apparatus, limited as it is in resolving power and homogeneity of the electron beam, all the ΔC_2H_5 observed at high pressures can be accounted for as $\Delta C^{12}C^{13}H_4$. At pressures below *ca.* 1 mm we found that the $\Delta 29$ was some threefold greater than could be expected from the isotope of ethylene, and hence the major contribution was ascribed to free ethyl. A curve of ΔC_2H_5 in a C_2H_6+TML mixture is reproduced in Fig. 8.

C_3H_5—This radical may be anticipated as a result of the capture of H by methyl radicals in propylene. Figure 9 shows that it can be detected at temperatures where the removal mechanism is well underway.

C_2H_3—Since propylene has been shown to yield CH_3 at high temperatures, we might expect the simultaneous appearance of the residual vinyl radical. In spite of favorable conditions for its detection none was found. We must conclude that the vinyl radical is particularly reactive and its life time much shorter than that of methyl. Testimony as to its reactivity is afforded by the growth of the C_2H_4 curve (Fig. 9) which is clearly associated with the temperature range where methyl production is considerable. It is possible that the vinyl radical is surface reactive and that redesign of the apparatus to reduce the residence time in the detecting system would reveal measurable concentrations.

CH_2—Although the potential relations for this radical render its detection relatively easy, it was only detected in the decomposition of diazomethane. Its concentration in the detector was estimated for other gases to be at least 100-fold less than that of the methyl radicals.

CH—Hopes were entertained that this might be detectable when decomposing acetylene. Although positive results were obtained, there was considerable discordance, indicating that the condition of the surface of the carbon filaments used for decomposing the acetylene might be a determining factor.

H—Atomic hydrogen was remarkable by its absence at both high and low pressures. Since its concentration in ethane according to the Rice mechanism should be independent of the ethane pressure, its absence at high pressures may be a natural consequence of the diminishing ratio of atomic hydrogen to ethane in the effluent. At low pressures it is probable that its rapid recombination on surfaces operates against detection in the present apparatus. By the use of tungsten or carbon filaments at *ca.* 10^{-2} mm and 1000°C, atomic hydrogen was detectable in city (natural) gas but not in ethane or methane. Here again, the influence of impurities and surface condition was noted but not investigated. It is to be hoped that using the known noncatalytic properties of tantalum in the design of critical parts the detection of H atoms will be feasible. Calculations of its probable concentration in the ethane decomposition indicated that its measurement is only a matter of refined technique.

OTHER GASES

As a guide to future and more detailed investigation propane and *n*- and iso-butane were run through the apparatus. The detectability of methyl radicals increases with carbon number on account of lower activation energies and increasing appearance potentials, which effectively increases the available sensitivity within limits imposed by secondary methane formation. The reverse, however, is true when we attempt the detection of the heavier radicals. Not only must

we contend with lower stability and smaller concentrations but the usable potential differences are considerably reduced. Higher resolving power, sensitivity, and electron-beam homogeneity will be required if quantitative results in this field are contemplated.

An oxygenated compound, dimethyl ether, gave no trouble. Methyl radicals were abundant but a search for the residuum, CH_3O, yielded negative results. Large quantities of HCHO were found, together with CH_4, CH_3OH, CHO, and H_2. Since it might appear at first sight that the absence of CH_3O is connected with its rapid conversion to CHO and H_2, a test was made to discover whether electron bombardment of the main product HCHO would reproduce the quantities of CHO^+ actually found. A comparison of the ratios of $HCHO^+/CHO^+$ from formaldehyde vapor in a stream of argon with the corresponding ratio from decomposing methyl ether indicated that, within the rather large experimental error, the bulk of the CHO^+ was of electronic rather than thermal origin—a result which illustrates the caution with which the appearance of a given mass from a reaction must be interpreted.

DISCUSSION AND CONCLUSIONS

Since this investigation was primarily directed towards finding the limitations of and possible improvements in a new method of approach to the measurement of short-lived intermediates, a detailed discussion of each gas or radical surveyed would be premature. Certain conclusions, however, seem sufficiently well established to be summarized as follows. The method is more sensitive, rapid, and universal than the mirror or spectroscopic methods. The detection of higher radicals of greater instability awaits further refinement. Under favorable conditions the lower limit of detection is at present *ca.* 0.0005 percent. Methylene does not appear in these concentrations except in the case of the decomposition of diazomethane. The reaction between methyl radicals and oxygen is considerably slower than might be expected on the basis of the value $E \gtrsim 3$ kcal. deduced by Bates and Spence[12]—a value which may be drastically increased if we take Jones'[13] value of 12 kcal. for the reaction between methyl and iodine, which would entail a value of $E \gtrsim 15$ kcal. for the oxygen-methyl reaction. It seems probable, however, that the slowness of the reaction should be attributed to a high steric factor rather than a high activation energy. Bates and Spence concluded that a steric factor of 10^{-4} was required. The concentration of methyl radicals from decomposing ethane both at low and high pressures, is higher than can be accounted for without introducing a considerable steric factor into the rate of removal. At low pressures surface catalysis may be partially responsible, but it was found in our experiments at high pressures, using *R.3*, that the introduction of additional surface near the orifice reduced rather than increased the total yield. Until a modified type *R.3* furnace with lower Reynold's number is used, a discussion of the relative roles of activation energy and steric factor must be postponed.

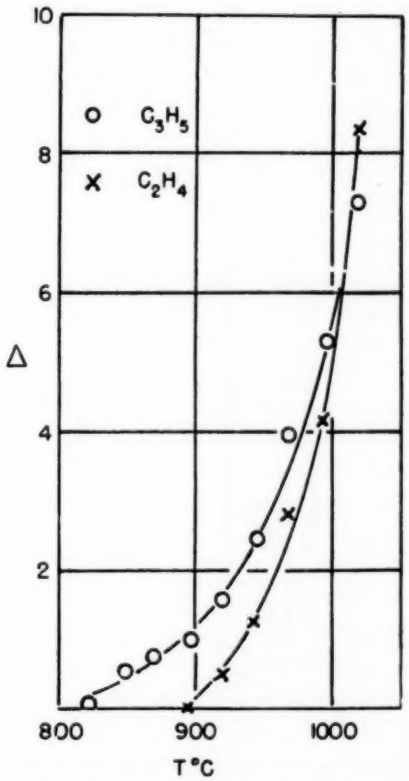

FIG. 9. Appearance of the allyl radical and ethylene during the decomposition of C_3H_6+0.006 percent $Pb(CH_3)_4$ in a quartz reactor at 0.1-mm pressure.

[12] J. R. Bates and R. Spence, Trans. Faraday Soc. **27**, 468 (1931); J. Am. Chem. Soc. **53**, 1689 (1931).

[13] J. L. Jones, J. Am. Chem. Soc. **61**, 3284 (1939).

The main difficulty encountered with the present apparatus at higher pressures lies in the interpretation of a negative result—the absence of a probable radical such as C_2H_3. Absence may be attributable to high volume reactivity or to rapid removal on the walls of the extractor diaphragm. As pointed out in Part I, this difficulty may be largely eliminated by the use of higher pumping speeds and wider diaphragms in future models.

Part III. Low Pressure Flames

The method described in Part I has been applied in a preliminary survey of intermediates formed during the combustion of methane, propane, and carbon monoxide at pressures ranging from 30 mm to 140 mm. The object of the investigation was to obtain data for the improvement of the method rather than to study exhaustively any particular reaction. By following the intensity changes of intermediates formed in mechanically-oscillating and pulsating-flow flames, the intermediates may be assigned to zones or phases of the oscillating or pulsating cycle. Pending more detailed study the following intermediates apparently exist in detectable quantities, HO_2, CH_3O, CH_2O, CHO, C_2H_2, and CH_3. Only doubtful traces of OH were detected, and the low concentration is attributed to the rapidity of surface removal. The temperature coefficients of CH_2O and CHO are strongly negative, of HO_2 slightly negative, and of CH_3 strongly positive. The CH_3 radical is definitely a chemical intermediate and not attributable to thermal decomposition of methane. The production of an intermediate of mass 16 in a propane-oxygen flame is discussed, but as yet it has not been possible to distinguish between CH_4 and atomic oxygen as the source of this mass.

INTRODUCTION

IT is probably not an exaggeration to say that there is no chemical field in which the necessity of introducing the concept of material chains is more apparent, and the experimental detection of the carriers less certain, than in the field of combustion. Since one of the original objectives of our research had been to develop a method of studying intermediates at moderately high pressures, even the limited successes achieved with the present instrument in the field of hydrocarbon decomposition encouraged us to attempt a preliminary survey of the more complex phenomena anticipated in flames. It must be emphasized that the results are suggestive rather than conclusive, since we were primarily interested in discovering the defects and range of application rather than in solving any particular problem. For reasons outlined in Part I of this series, it was recognized that several improvements could be effected by a complete rebuilding of the apparatus. The results reported below have lent precision to our knowledge of the means whereby such improvements can be made effective.

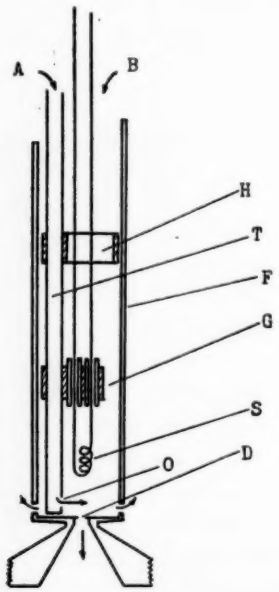

FIG. 1. Internal modifications of steel reactor *R*.3 for flame studies. Gas components *A* and *B* enter as shown, and the flame extends from the side hole *O*, across the diaphragm *D*. The distance *OD* can be varied by oscillating the tube *T* in a vertical direction, lateral movement being prevented by the spring guide *H*. A retractable Pt-Ir coil *S*, moving in guides *G*, serves to ignite the mixture.

APPARATUS

The apparatus was essentially the same as that described in Part I. Copper tubes for preventing flash-back, and traps for removing condensible combustion products were incorporated. In order to prevent condensation in the water cooler, the latter was maintained at *ca.* 35°C by a circulatory system. Reactor *R*.3 was used throughout. In Fig. 1 the internal modifications are illustrated. Since premixing of the com-

bustibles was found to be undesirable, the gases were introduced separately so that with flames burning at pressures between 80 mm and 150 mm one component, (*A*), entered down the narrow stainless steel or quartz tube, *T*, and met the other component, (*B*), at a small side hole, *O*, and the flame was directed across the gold diaphragm, *D*. A movable platinum-iridium heating spiral, *S*, could be lowered towards *O* for ignition, after which it was retracted from the flame zone. In one series of experiments the tube *T* was moved up and down by an external lever mechanism actuated by a synchronous motor which, by gearing, provided one complete oscillation of the flame in 2.5 minutes. The springy steel guide, *H*, maintained the tube *T* in position relative to the axis of the furnace. As before, the furnace walls, *F*, and the diaphragm could be heated by passage of heavy a.c. currents.

In view of the large change of initial pressure accompanying combustion, a device for automatically restoring the pressure during combustion to its pre-combustion value was installed. This has already been described[1] and consists essentially of a pneumatic Wheatstone bridge. The variable resistances in the two gas lines are motor driven Fowler-type valves. The reversible Telechron motors are in circuit with relays operated from two double contacts, one pair in a mercury-filled U-tube, which plays the role of the galvanometer in the electrical analog, and the other pair in a manometer which registers and controls the pressure in the reactor. It was possible in this way to restore the pressure automatically, by increasing the flows of the two components, while maintaining a constant component ratio at any predetermined value. It was also possible to maintain a regular pulsating regime by proper choice of the pneumatic analogs of capacity, resistance, and inductance.

METHOD

Theoretically, every positive ion of low mass occurring in the flame spectrum should be regarded as an electron dissociation fragment of some heavier chemical product unless by calibration with the higher mass it can be proved that the electron velocity is too low to produce the observed yield of lower mass ions. This is a possible but laborious and, at the present stage, unjustifiable procedure. Moreover, it can be avoided in certain instances by using either a pulsating or an oscillating flame.

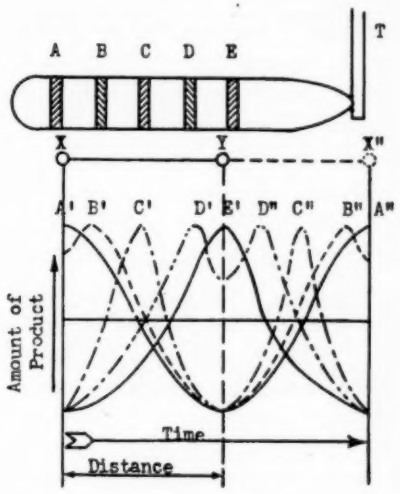

FIG. 2. Schematic representation of reaction zones in a horizontal flame pulsating across the sampling diaphragm. If the latter moves from *x* to *y*, corresponding to an elongation of the flame, the intensities of the zonal products *ABCDE* entering the ionization chamber will pass through maxima *A'*, *B'*, *C'*, *D'*, and *E'*. As the flame contracts the pattern will be repeated, and the maxima on an unfolding time scale will appear at *D''*, *C''*, *B''*, and *A''*.

To simplify the discussion let us suppose that the flame issuing from the side hole in the tube, *T*, is composed of reaction zones and that in the various zones there will be a different distribution of products. Thus the concentration of any given product will vary with distance from the tube *T*. Actually these zones will be conical or spherical, but for simplicity they may be represented schematically as in Fig. 2, where *A*, *B*, *C*, *D*, and *E* are zones in which the concentrations of the products *A*, *B*, *C*, *D*, and *E* are a maximum. It is then obvious that if the diaphragm of the reactor under the flame were to be moved from position *X* to position *Y*, the intensity of the products effusing through the diaphragm would pass through maxima corresponding to *A'*, *B'*, *C'*, *D'*, and *E'* and that as the diaphragm returned from *Y* to *X* to complete the cycle, the maxima would be reproduced a second time so that on a continuously unfolding time scale these second maxima would appear in the positions *D''*, *C''*, *B''*, and *A''*. It is clear that simple maxima will occur only when the zones lie out-

[1] N. Heikes, Ind. Eng. Chem. 15, 133 (1943).

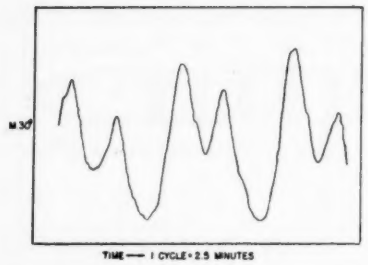

FIG. 3. Variation of formaldehyde ion as flame pulsates across the diaphragm. The three cycles shown indicate by the twin maxima an intermediate zone. Time of one cycle = 2.5 minutes. Mixture, two parts O_2 burning in one part CH_4. Traced from original photo-pen record. Pressure 67 mm.

side the limits of the movement of X. In all other cases, such as B, C, and D, the maxima will be double and the relative depths of the two minima will be a function of the symmetry of the zone with respect to the positions X and Y. The phases of the various products are directly related to their position in the flame, and it follows that if the intensities of B and C, for example, are not coincident in phase then the ion B^+ cannot be either the isotope or the electron-dissociation fragment of the product C. Thus by using a pulsating or oscillating flame with a fixed diaphragm, which is approximately equivalent to using a moving diaphragm with a stationary flame, we not only avoid certain difficulties in interpreting the true origin of a given ion but are also able to say something concerning the chemical sequence occurring in the flame itself.

Restricted as the present instrument is by the geometry of the 180° magnetic field, it was not feasible to move the flame horizontally across the diaphragm. Mechanical oscillations were only possible in a vertical direction. In an auxiliary apparatus it was found visually that with suitable flow speeds and flame size the plane of the diaphragm would in effect penetrate from the outer to the inner mantle of the flame. Both the amplitude and mean position could be altered. In most cases an amplitude of 3 mm was suitable.

With the pulsating flame the pulsations, induced by changes in flow speed instead of mechanical motion, are mainly in a horizontal direction, but the simplicity of the interpretation on the basis of Fig. 2 is to a certain extent obscured by the fact that some change in regime occurs simultaneously as a result of greater combustion, higher temperature, etc. The fact that the flow pulsations were less than 5 percent of the total flow inclines us, however, to the belief that the large changes in ion currents actually observed and the significant phase differences are mainly attributable to the physical motion of concentration zones across the diaphragm rather than to concentration changes in stationary zones.

RESULTS

In order to study the performance of the present instrument and project improvements, methane, propane, and moist carbon monoxide flames were briefly investigated. A preliminary run using the quartz reactor $R.1$ (see Part I of this series) showed that a mixture of methane and oxygen would not burn in the narrow (3-mm) tube but that the production of CH_3 radicals at the cracking temperature was certainly not reduced but, if anything, enhanced by the presence of oxygen. This confirmed the result already obtained when using oxygen-TML mixtures (Part II, Fig. 5).

A tracing taken from part of an actual record of the variation of formaldehyde ions in a pulsating oxygen-in-methane flame is shown in Fig. 3. We note that the intensity passes through two maxima per cycle, indicating that the concentration is a maximum in a zone situated between the inner and outer cones, as illustrated schematically in Fig. 2 at B', B'' or at D', D''. In order to illustrate the marked phase differences among the masses 28 to 32, Fig. 4 has been constructed in which the intensities are arbitrarily equalized, and the pressure and flow variations occurring in the cycle are related to the trace made by a solenoid-operated pen. The solenoid of the latter was coupled to the automatic flow regulator mentioned previously. It will be noted that pressure and flow velocity are not in perfect phase, which may account for certain minor discrepancies in the position of the main minimum. It was found that the phase separation of the maxima was a function of the average flow. This is to be expected since an increase in average flow will tend to shift zone D towards zone C (Fig. 2) and thus increase the separation of the maxima.

In this way it was found that greater differences between the patterns of two nearly identical curves (for example CHO and CO in Fig. 4) could be induced.

From the particular set of patterns illustrated in Fig. 4, it is clear that CH_3O, CH_2O, and CHO are formed in different parts of the flame or under different chemical conditions. If we accept as a working hypothesis the moving-zone postulate, it can be deduced from Fig. 4 that since oxygen is richest in the inner parts of the flame the chemical sequence from the jet to the tip of the flame will be O_2-CH_3O-CH_2O-CHO-CO. Certain reservations have to be made, however, and further study is required. The reservations may be stated briefly as follows.

Firstly, it is possible that methyl alcohol is one of the first products. Detection is rendered difficult by the identity of its mass with that of O_2, the comparatively small electron energy difference between the two ionization potentials (*ca.* $12.2-10.8=1.4$ volts) and the large ratio of oxygen to methyl alcohol concentration. With greater electron-beam homogeneity it might be possible to obtain indications of CH_3OH and thence to determine whether any of its electron-dissociation fragments are contributing to the patterns of the other observed ions such as CH_3O^+. A more definite approach would be to use deuteromethane for this particular control, so as to obtain a mass separation of four units between deuteromethyl alcohol and oxygen.

Secondly, it is possible that CHO is the $C^{13}O$ isotope of CO since the latter is present in great abundance. This possibility was ruled out by measuring the ratio of M^+_{28}/M^+_{29}. It was then found that the isotope would only account for approximately one-sixth of the observed M^+_{29}. Moreover, it was possible to obtain a greater phase differentiation between CO and CHO by increasing the average flow. The phase pattern of CHO then approached that of CH_2O but was sufficiently different from the latter to rule out the possibility that the observed CHO^+ was entirely an electron dissociation product of CH_2O or a combination of this with the $C^{13}O$ isotope. We, therefore, feel reasonably confident that CHO has been detected and could in future work be an object of special study.

The remaining results will be summarized under the heading of the product or intermediate concerned.

O_3 and CO_3—These were not detected in appreciable quantities in any of the three flames (methane, propane, and carbon monoxide). The instrument was not suitable in its present form for masses above 45.

CO_2—The only interesting feature of CO_2 production is the erratic trace which this product gives as compared with CO. All possible instrumental causes of this unsteadiness were eliminated without effect on the erratic behavior. It was concluded that small particles of carbon were oxidized *in toto*, giving rise to bursts of CO_2. If this explanation is correct, it may be deduced that solid carbon under the prevailing conditions is oxidized to CO_2 in one step since the carbon monoxide curves were quite smooth.

H_2O_2—Very few observations were made on this product. In an oxygen-methane oscillating flame the *M*.34 peak was in phase with the oxygen *M*.32 and its magnitude equal to that which would be expected for the $O^{16}O^{18}$ isotope. Under these conditions, therefore, H_2O_2 does

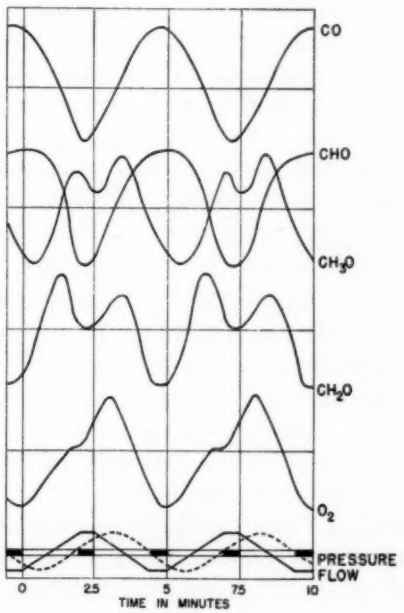

FIG. 4. Summarized phase curves for intermediates measured with a pulsating oxygen-in-methane flame. The amplitudes have been equalized to facilitate recognition of the phase relationships. The solid block marks at the base represent signals transmitted from the flow controller to a solenoid-operated pen giving phase reference points. The flow and pressure lines represent the variation of these parameters during the cycle.

not appear as a major intermediate and cannot be responsible for the oscillations of *M*.33 (*q.v.* under HO_2).

HO_2—In view of the considerable importance of this radical in some theories of oxidation, it was of interest to attempt detection with the present apparatus. Detection is rendered difficult on account of the proximity of the very much larger mass 32 of oxygen and by the contribution of the $O^{17}O^{16}$ isotope of mass 33 identical with that of HO_2. However, both these interferences must decrease when the mixture is ignited owing to the consumption of oxygen, and, hence, if any increase is found it must be attributed to a new product. By setting the electron voltage just below the ionization potential of oxygen a quite definite increase in the positive ion current of mass 33 was observed after ignition of a propane in oxygen flame. The phase was nearly but not quite identical with that of the oxygen, and apparently differed from that of the CH_3O previously mentioned. Since methyl alcohol may contribute to the formation of masses 33 and 31, it is possible that the deflection, or a part of it, observed for mass 33 may have to be attributed to the isotope of methyl alcohol. At present the evidence from the phase differences appears to exclude the possibility that methyl alcohol can be responsible for both CH_3O and HO_2.

In an oxygen-in-methane oscillating flame a much larger phase difference was obtained between *M*.32 and *M*.33.

It was noticeable that with both the propane-oxygen and oxygen-methane flames the application of additional heat to the reactor surrounding the self-sustaining flames (pressure *ca.* 70 mm) decreased slightly the intensity of the *M*.33 peak. This negative temperature coefficient is of some interest and will be referred to in discussing the production of methyl radicals.

***M*.32-*M*.28**—The probable reality of intermediates in this mass range has already been discussed above. Formaldehyde exhibited a very marked negative temperature coefficient.

C_2H_2—In an oscillating propane-oxygen flame *M*.26 was readily identified as a product formed when the flame was closest to the diaphragm. The intensity dropped to zero as the flame moved upward from which we may conclude that either the C_2H_2 formed in the inner mantle is totally consumed in passing through the flame front and into the oxygen-rich outer mantle, or that the production of C_2H_2 takes place only when the inner mantle plays over the metal surface.

C_2H and C_2—Since these masses were in phase with the production of C_2H_2, and the magnitude of the deflections were not inconsistent with an electron-dissociation origin, we are not as yet in a position to identify these products with a chemical process.

OH—In view of the considerable success of the spectrographic method in measuring the concentration of OH radicals in flames, several attempts were made to use this radical as a basis of comparison between the spectrographic and mass-spectrographic methods. It would appear from our preliminary results that whereas the hydroxyl radical is particularly suitable for spectrographic investigation it is particularly difficult to identify in the mass spectrometer. The reasons for this conclusion are not without interest for the future development of the mass-spectrometric method, and, therefore, a more detailed discussion of the problem seems justified. The primary condition, namely, a large energy difference between the appearance potential of OH^+ from H_2O and the ionization potential of free OH is satisfactorily fulfilled since $A(OH^+) = 18.9$ v and $I(OH) = 13.8$ v. However, very large quantities of H_2O are formed during the combustion and the ionization potential of H_2O is $I(H_2O^+) = 12.7$. Thus if we select an electron energy slightly less than 18.9 v the H_2O^+ peak will be strongly developed when the mixture is burning, and unless the resolving power is high there will be sufficient spreading of the *M*.18 peak into the *M*.17 to mask the very small increase anticipated in the latter. In addition it has been found (see next section) that some product of mass 16 is formed under certain conditions and the isotope of this mass may be another factor contributing to the growth of *M*.17. Hence, although large increases in *M*.17 have been recorded, we have not yet had at our disposal sufficient resolving power to overcome the difficulty of interpreting uniquely the origin of these increases, accompanied as they are by enormously greater increases in a neighboring mass. Unfortunately, the additional degree of

freedom provided by the pulsating or oscillating flame did not in this case assist in defining the origin of the *M*.17 increase. Both *M*.17 and *M*.18 were in phase, and it was noticed that the amplitude of the variation was small compared with the mean deflection. This was tentatively interpreted as indicating that the concentration of water vapor in the ionization chamber was buffered by absorption and desorption on the Aquadagged walls.

In an effort to overcome the effect of the large increase in *M*.18 when a hydrocarbon mixture is burnt, a moist mixture of carbon monoxide and oxygen was run through the apparatus and ignited. Kondratjew[2] has shown that at pressures of *ca.* 35 mm approximately one percent of the water vapor is converted by chemical rather than thermal action into OH radicals. Since in this case there is no increase in *M*.18 as a result of combustion, there should be no difficulty in measuring and interpreting the appearance of this comparatively large increase in *M*.17.

At low pressures (35–50 mm) the flame of a stoichiometric mixture of CO and O_2 is not self-sustaining, and the reaction vessel has to be raised above 600°C. The flame is then so diffuse that it resembles a luminous glow, filling a major portion of the reactor, and the technique of oscillating or pulsating the "flame" has no meaning. It was, therefore, necessary to compare the deflections of OH^+ and H_2O^+ with the reactor hot and cold. This introduces the possibility that water driven off the reactor surfaces may contribute to the deflection, but this can be almost entirely eliminated by outgassing, using the behavior of H_2O^+ as a control on the efficiency of the latter process.

By use of the stainless steel reactor with a gold diaphragm, some indication of OH radicals was obtained. However, the results were highly irreproducible owing to the very rapid plugging up of the orifice in the gold diaphragm. Since carbonyl formation on the steel and decomposition on the gold was suspected as a cause of the blocking of the orifice, the entire inner surface of the reactor was lined with a snugly fitting thin gold shell. This eliminated the blocking of the diaphragm, but also eliminated all but a doubtful trace of the hydroxyl radicals entering the ionization chamber. Although data on combustion in gold vessels is not available in the literature, it is known that silver has a particularly strong depressing action. In an auxiliary vessel in which a quartz reactor was partially lined with gold foil, it was noticed that the mixture burnt in the unlined section even when the latter was cooler than the section lined with gold. It was, therefore, concluded that the gold liner was acting as an efficient differential pump for the removal of certain chain carriers, and that although a flame was undoubtedly burning in the gold-lined steel reactor, the concentration of OH radicals at the walls might be much less than in the center.

Finally a thin quartz liner was fabricated by grinding and etching. This was inserted inside the gold liner and the mixture introduced through a quartz tube. Thus the only exposed metal surface was that of the small gold diaphragm and the $\frac{1}{32}$-inch deep walls of the well in which it was held. Even under these conditions the concentration of OH radicals entering the ionization chamber was less than one-tenth of that observed by Kondratjew.

Our essentially negative results with the hydroxyl radical do not constitute a refutation of the positive results obtained by the spectrographic method. In the latter, the light beam passes through a considerable length of gas where the reaction is homogeneous and where the influence of surface is at a minimum. In the mass spectrographic method, on the contrary, the sample is extracted through an orifice which, in the present apparatus, is too narrow to allow collision-free passage for an appreciable fraction of the radicals. As indicated in Part I, this limitation can be reduced in future models, and it should be possible, by varying the ratio of the length and diameter of the orifice, to throw light on the relative sensitivities of various radicals to surface destruction. At present we may conclude that the hydroxyl radical is highly destructable at a gold surface, and in this capacity resembles atomic hydrogen. Recently Smith[3] has shown, by an independent method, that the efficiency of the recombination of hydroxyl radicals on a Pyrex surface at 900°K is of the order 10^{-1}.

[2] V. N. Kondratjew, J. Phys. Chem. U.S.S.R. **14**, 1 (1940).

[3] W. V. Smith, J. Chem. Phys. **11**, 110 (1943).

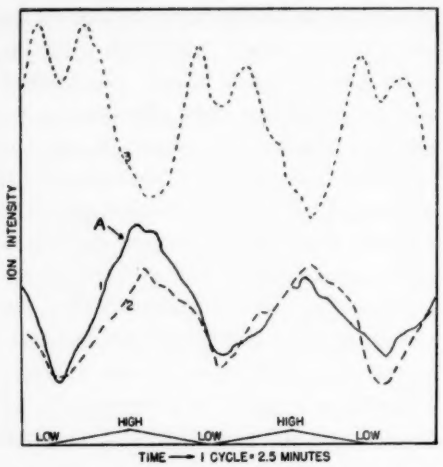

FIG. 5. The production of methyl radicals in an oxygen-in-methane oscillating flame. Curve 1. CH_4^+ at 9.25 ev (uncorrected). At *A*, heat was applied to the furnace and the greater combustion reduces the second maximum without shifting phase. Curve 2. CH_3^+ at 10.0 ev. Furnace unheated. Curve 3. CH_3^+ at 7.75 ev. Furnace heated. The triangular reference line at the base represents the varying height of the flame above the gold diaphragm.

***M*.16**—It was found that in a propane-oxygen flame considerable amounts of *M*.16 could be detected at electron energies below the appearance potential of O^+ from the electron dissociation of either O_2(20.5 v), CO(24 v), CO_2(19.6 v), or H_2O(18.5 v). The only chemical products which could give rise to this mass are atomic oxygen and methane. Since, however, the ionization potentials of these products are 13.6 and 13.1 ± 0.4 volts, respectively, it is clear that the difference is too small to serve as basis for identification. An attempt was therefore made to utilize the electron affinity of oxygen atoms. Pure electron attachment is notoriously inefficient on account of the energy which must be dissipated. At the pressure ruling in the ionization chamber, triple collisions are so rare that we can only rely on radiation to carry off the excess energy (2.2 v) during the time of passage of the electron through the sphere of attraction of the oxygen atom. Thus the probability of attachment will increase as the velocity of the colliding electron decreases. At higher electron energies, negative atomic oxygen ions will make their appearance as a result of dissociation of an oxygen-containing molecule, the remainder of the molecule carrying off the excess energy either kinetically or, at still higher voltages, by formation of a positive ion. These two processes are more probable than that of pure radiative attachment and may be used as a guide in setting the focusing fields and checking the sensitivity.

A number of attempts were made to detect the presence of atomic oxygen, but the results were negative. It was evident from the negative ion curves obtained at electron energies from 5 v to 35 v, with and without ignition of the mixture, that a much more efficient electron gun than was available in the present apparatus would be required. We are, therefore, as yet unable to distinguish between methane and atomic oxygen as the source of the very definite appearance of *M*.16 in the combustion products of a propane-oxygen flame.

CH_3—In view of the relative stability of methyl radicals towards surface collision and oxygen, it was hoped that this radical would be detectable in the oxygen-methane flame. With flame pressures varying from 75 mm to 140 mm the amounts of CH_3^+ recorded were those to be anticipated from electron dissociation of the incompletely burnt methane. Moreover, both CH_4^+ and CH_3^+ were in phase. However, when additional heat was applied to the reactor a very striking change occurred. Not only were methyl ions detectable at electron energies below even the ionization potential of methane, but the phase of these ions in an oscillating flame indicated that their place of origin lay between the oxygen-rich and methane-rich zones. Thus the possibility that the increased methyl ion current was due to thermal decomposition of the methane was convincingly eliminated. In Fig. 5 tracings of short sections taken from much longer experimental curves have been superimposed to illustrate the phase change. Curve 1 is for methane ions with an unheated flame. At the instant marked *A* the furnace temperature was raised, and, since the heat capacity is small, practically the full effect of the increased temperature is developed in the next cycle which shows a decreased intensity. Evidently combustion is more complete in the heated furnace. Curve 2 shows the trace for the *M*.15 ion with a cold furnace. Both the magnitude and phase of this trace indicate that the major component is attributable to electron dissociation of the methane rather than to ionization of free methyl. At

the end of this trace the temperature was again raised, whereupon the *M*.15 ion gave off-scale deflections. The electron energy was therefore reduced by 2.25 volts and curve 3 obtained. A check of the *M*.16 ion at the reduced voltage gave no measurable deflection; hence we may be certain that no electron-dissociation fragment was contributing to curve 3. It is clear from the phase relationships of curves 1 and 3 that the methyl radical is most abundant in a zone between the oxygen-rich and methane-rich zones.

With the propane-oxygen flame there was no evidence of CH_3 production.

In a formal sense both these results might be attributed to direct interaction of the hydrocarbon and oxygen which would yield:

$$CH_4+O_2\rightarrow CH_3+HO_2$$

and

$$C_3H_8+O_2\rightarrow C_3H_7+HO_2.$$

The temperature coefficient of HO_2 formation, however, was slightly negative as compared with the high positive value qualitatively observed in the case of CH_3 formation, and although this might be attributed to greater instability of HO_2 at the higher temperatures, there would seem to be no valid reason at present for abandoning the Lewis and von Elbe scheme whereby methyl radicals are formed as a result of:

$$OH+CH_4\rightarrow CH_3+H_2O$$

followed by

$$CH_3+O_2\rightarrow HCHO+OH.$$

Here also we have to invoke a considerable thermal instability of formaldehyde, since this intermediate was found, as indicated above, to possess a large negative temperature coefficient. Since, however, formaldehyde is assumed to react according to the equation.

$$HCHO+O_2\rightarrow HCOO+OH,$$

a more rapid production of OH would result, and some of these would contribute to the methyl formation.

CONCLUSIONS

It is evident to the author that the results summarized above should not be used as a basis for speculation regarding chemical processes occurring in combustion. However it is to be anticipated that by the utilization of recent advances in mass-spectrometric technique, the employment of wider diaphragms, deutero compounds, and negative ions in certain instances, and more systematic calibrations, a considerable body of otherwise unobtainable material may be accumulated. How far this will confirm or modify our present ideas on combustion is a question for the future. Some of the apparent disadvantages in the present apparatus, such as the destruction of surface-sensitive radicals in the diaphragm, may eventually turn out to be assets and assist in elucidating the important though still obscure role of surface reaction. Undoubtedly the spectroscopic method, in the few instances where it is applicable, is as yet simpler and more reliable than the mass-spectrometric method. The latter, however, is capable of considerable development and should provide a useful means of studying the behavior of intermediates which offer little opportunity for study by any other method.

Low Temperature Transport Properties of Gases. I. Helium

I. AMDUR
Department of Chemistry, Massachusetts Institute of Technology, Cambridge, Massachusetts
(Received April 17, 1947)

Values have been computed for the viscosity, thermal conductivity, and coefficient of self-diffusion of gaseous helium for temperatures below 200°K by application of classical scattering theory within angular regions where diffraction effects are absent. Values of classical total collision cross sections are obtained which are used to evaluate classical cross sections for viscosity, thermal conductivity, and self-diffusion appropriate to a Maxwellian gas. Numerical values of the transport properties are obtained by substitution of the appropriate classical cross sections into the exact transport property formulas of Chapman and Enskog.

In the region 200°−14°K, the average absolute deviations between calculated and experimental values are 1.9 percent for viscosity and 4.6 percent for thermal conductivity. Extrapolation of calculated viscosity values to 1.64°K appears to be justified on the basis of agreement with experimental values. It cannot be stated that similar extrapolation in the case of thermal conductivity is valid because of possible uncertainties in the experimental values between 3.95° and 1.62°K. Values of the self-diffusion coefficient have been calculated between 200° and 5°K, but experimental values are not available for comparison.

VISCOSITY AND THERMAL CONDUCTIVITY

IN recent years the viscosity and thermal conductivity of helium gas at low temperatures have been calculated by applying the quantum theory of scattering to the computation of the appropriate transport cross sections. Massey and Mohr[1] were able to reproduce observed viscosities between 15° and 300°K with a maximum deviation of 7 percent, by treating the helium atom as a hard sphere with a diameter of 2.10A. In a later paper,[2] they eliminated the undesirable feature of assuming an arbitrary hard sphere diameter by using an approximation to the Slater-Kirkwood interaction potential between two helium atoms.[3] The calculated viscosities in this case exceed the measured values by 6 percent at 300°K and by 22 percent at 15°K. Massey and Buckingham[4] assumed that the interaction potential was 1.30 times that computed by Slater and Kirkwood and computed viscosities in the range 0–26°K on the basis of Bose-Einstein and Fermi-Dirac statistics. Their values agree within 3 percent above 15°K, but are in error by 16 percent at 4.23°K and by 36 percent at 1.64°K. On the basis of a Lennard-Jones type potential deduced from equation of state measurements, Uehling and Hellund[5] were able to predict viscosities at 4.23°K and at 273°K within 0.6 percent and 2.6 percent, respectively. A previous calculation by Uehling[6] of viscosities in the range 15°–300°K, using a hard sphere model, gave results in agreement with those obtained by Massey and Mohr.[1] He also calculated thermal conductivities in the range 20°–320°K with the same model, but was unable to obtain agreement closer than 33 percent at the lowest temperature. Much better agreement, about 3 percent, was obtained by deBoer[7] who calculated thermal conductivities in the narrow temperature region, 1.6°–2.8°K, using a Lennard-Jones form of potential, although his value for the viscosity at 1.64°K is in error by 25 percent.

It is the purpose of the present paper to show that a proper application of classical methods can be used to calculate viscosities and thermal conductivities for helium in the range 14°–200°K with good accuracy, and possibly to obtain values down to 1.62°K by extrapolation. The method involves the calculation of classical transport cross sections, taking into account the range of interaction distance in which classical theory does not apply. These cross sections are then inserted into classical expressions developed

[1] H. S. W. Massey and C. B. O. Mohr, Proc. Roy. Soc. **A141**, 434 (1933).
[2] H. S. W. Massey and C. B. O. Mohr, Proc. Roy. Soc. **A144**, 188 (1934).
[3] J. C. Slater and J. G. Kirkwood, Phys. Rev. **37**, 682 (1931).
[4] H. S. W. Massey and R. A. Buckingham, Proc. Roy. Soc. **A168**, 378 (1938); **A169**, 205 (1938).
[5] E. A. Uehling and E. J. Hellund, Phys. Rev. **54**, 479 (1938).
[6] E. A. Uehling, Phys. Rev. **46**, 917 (1934).
[7] J. deBoer, Physica **10**, 348 (1943).

by Chapman[8] and by Enskog[9] to obtain numerical values of the transport properties as functions of temperature.

Classical values for the cross sections effective in viscosity and thermal conductivity can be obtained from classical values of the total collision cross section whose significance can be illustrated as follows: if a stream of N atoms per unit area per second impinges upon a single atom, the number of atoms from the stream deflected per second between angles Θ and $\Theta+d\Theta$ is equal to $2\pi NG(\Theta)d\Theta$, where $G(\Theta)$ is the solid angle scattering coefficient, and Θ, the angle through which the direction of the relative initial velocity, v, of the colliding particles, is turned by collision. The use of the relative coordinates, Θ and v, is equivalent to considering the single scatterer held fixed at all times, instead of free to move before and after collision. The classical total collision cross section, S, may be defined[1,10] as

$$S=2\pi\int_{\Theta_c}^{\pi}G(\Theta)\sin\Theta d\Theta = 2\pi\int_{b\text{ at }\Theta_c}^{b\text{ at }\pi}bdb=\pi[b(\Theta_c)]^2, \quad (1)$$

where Θ_c is the critical relative angle below which classical theory does not apply. This angle may be set equal to $\lambda/(2r_0)$ where λ is the de Broglie wave-length of the colliding system and r_0 the distance of closest approach of the center of a particle in the stream to the center of the scatterer. The wave-length, λ, is equal to $h/(\mu v)$ where h is Planck's constant and μ the reduced mass of the colliding system. For like particles of mass m, μ is $m/2$. The defining equation for $b(\Theta_c)$, the impact parameter, is

$$\left[1-\frac{V(r_0)}{\frac{1}{2}\mu v^2}\right]r_0^2=[b(\Theta_c)]^2. \quad (2)$$

In the present application, the mutual potential energy at the distance of closest approach, $V(r_0)$ will be small compared with the relative kinetic energy, $\frac{1}{2}\mu v^2$, so that r_0 will be nearly equal to $b(\Theta_c)$.

Since the critical angle, Θ_c, is small, it is permissible to use the small angle formula given by Kennard,[10] namely

$$\Theta_c=2r_0/(\mu v^2)\int_{r_0}^{\infty}\frac{[V(r_0)-V(r)]rdr}{(r^2-r_0^2)^{\frac{1}{2}}}. \quad (3)$$

Substituting $\Theta_c=h/(2\mu v r_0)$ into Eq. (3), we obtain

$$v=4r_0^2/h\int_{r_0}^{\infty}\frac{[V(r_0)-V(r)]rdr}{(r^2-r_0^2)^{\frac{1}{2}}}. \quad (4)$$

In order to calculate the classical total collision cross section, S, as a function of the relative velocity, v, it is necessary to express the potential energy $V(r)$ as a suitable function of the separation distance, r. Margenau[11] has computed such functions for helium by extending the calculations of Slater and Kirkwood to include second-order exchange forces as well as dipole-quadrupole and quadrupole-quadrupole interactions. The potential which will be used for the present calculations is that given by Margenau in his 1939 paper, with an additional small quadrupole-quadrupole term computed by him in the earlier paper. It has the form

$$V(r)=\left[7.70e^{-4.60r}-5.60e^{-5.33r}-\frac{0.0139}{r^6}-\frac{0.030}{r^8}-\frac{0.035}{r^{10}}\right]\times10^{-10}\text{ erg}, \quad (5)$$

where r is in angstrom units. This function should be quite accurate for separation distances near the minimum, about 2.9A, and should yield accurate cross sections corresponding to distances not too far removed from this value. It is this fact which limits the present calculations to an upper temperature limit of 200°K corresponding to a separation distance of 2.34A. Since the function in Eq. (5) was evaluated largely from theoretical considerations without recourse to experimental results on the equation of state or transport properties of helium, it seems preferable to limit the present calculations to temperatures

[8] S. Chapman, Phil. Trans. Roy. Soc. **A211**, 433 (1912); **A216**, 279 (1915); **A217**, 115 (1917).
[9] D. Enskog, Inaug. Diss. Upsala, 1917.
[10] E. H. Kennard, *Kinetic Theory of Gases* (McGraw-Hill Book Company, Inc., New York, 1938), Chapter III.
[11] H. Margenau, Phys. Rev. **38**, 747 (1931); **56**, 1000 (1939).

TABLE I. Classical total collision cross section of helium.

r_0, A	v, 10^5 cm/sec.	$b(\Theta_c)$, A	S, A^2
2.30	3.18	2.28	16.33
2.33	2.66	2.31	16.78
2.35	2.32	2.33	17.09
2.38	1.87	2.37	17.60
2.40	1.60	2.39	17.97
2.43	1.23	2.45	18.87
2.45	1.02	2.49	19.43
2.48	0.729	2.61	21.37
2.50	0.559	2.75	23.83

below 200°K rather than to extend the range by empirical variation of the potential energy function. Agreement between calculated and experimental values of viscosity and thermal conductivity will then tend to serve as independent confirmation of the accuracy of Margenau's calculations.

The potential given by Eq. (5) is of the general form

$$V(r)=Ae^{-ar}-Be^{-br}-\frac{C}{r^x}-\frac{D}{r^y}-\frac{E}{r^z}. \tag{6}$$

Methods for evaluating the integral in Eq. (4) for a potential of this form have been worked out by Amdur and Pearlman[12] and by Kennard[10] and lead to the result

$$v=\frac{Aa^{\frac{1}{2}}(2r_0)^{\frac{1}{2}}e^{-ar_0}}{h}\sum_{n=0}^{n=\infty}(-1)^n\binom{-\frac{1}{2}}{n}\times\frac{1}{(2ar_0)^n}\Gamma(n+\tfrac{1}{2})-\frac{Bb^{\frac{1}{2}}(2r_0)^{\frac{1}{2}}e^{-br_0}}{h}\times\sum_{n=0}^{n=\infty}(-1)^n\binom{-\frac{1}{2}}{n}\frac{1}{(2br_0)^n}\Gamma(n+\tfrac{1}{2})-\frac{4xK_xC}{h(r_0)^{x-1}}-\frac{4yK_yD}{h(r_0)^{y-1}}-\frac{4zK_zE}{h(r_0)^{z-1}}, \tag{7}$$

where K_x, K_y, and K_z may be computed from the general relation

$$K_i=\frac{2\cdot4\cdots(i-1+\delta_i^1)}{1\cdot3\cdots i}\text{ for odd } i$$

($\delta_i^1=1$ if $i=1$ but otherwise $=0$),

$$=\frac{1\cdot3\cdots(i-1)}{2\cdot4\cdots i}\frac{\pi}{2}\text{ for even } i. \tag{8}$$

[12] I. Amdur and H. Pearlman, J. Chem. Phys. **9**, 503 (1941).

The summations in Eq. (7) do not converge, but the first part of each series is an asymptotic expression for the contribution of the corresponding portions of the interaction potential to the relative velocity. By taking only the first few terms of each series, therefore, this portion of the relative velocity may be computed quite accurately for values of ar_0 or br_0 greater than about 3. For example, in the present case, only two terms of each series are required for an accuracy better than 0.15 percent, since the values of ar_0 and br_0 which are of interest lie between 7 and 14.

Under these conditions, Eq. (7) reduces to

$$v=\left(\frac{\pi r_0}{8a}\right)^{\frac{1}{2}}\frac{A}{h}(8ar_0-1)e^{-ar_0}-\left(\frac{\pi r_0}{8b}\right)^{\frac{1}{2}}\frac{B}{h}(8br_0-1)e^{-br_0}-\frac{4xK_xC}{h(r_0)^{x-1}}-\frac{4yK_yD}{h(r_0)^{y-1}}-\frac{4zK_zE}{h(r_0)^{z-1}}. \tag{9}$$

The calculation procedure may be outlined as follows:

(A) Values of v are computed from Eq. (9) for given values of r_0 by substituting the numerical values of the constants as given in Eq. (5).

(B) Since Eq. (9) is valid only for $\Theta=\Theta_c$, the values of r_0 chosen in (A) are substituted into Eq. (2) to obtain values of $b(\Theta_c)$.

(C) The above values of $b(\Theta_c)$, as functions of v, are inserted into Eq. (1) to yield values of S as functions of v.

A summary of such calculations for helium is given in Table I.

In order to compute values of the viscosity, η, and the thermal conductivity, K, it is necessary to obtain values for the classical cross section for viscosity and thermal conductivity, $S_{\eta,K}$, as a function of the relative velocity, v. For *hard spheres*[1,10] the classical total collision cross section is given by

$$S=2\pi\int_0^\pi G(\Theta)\sin\Theta d\Theta=2\pi\int_0^\pi(\tfrac{1}{4}r_0^2)\sin\Theta d\Theta=\pi r_0^2 \tag{10}$$

and the classical cross section for viscosity and

thermal conductivity by

$$S_{\eta,K}=2\pi\int_0^{\pi} G(\Theta)\sin^3\Theta d\Theta$$
$$=2\pi\int_0^{\pi}(\tfrac{1}{4}r_0^2)\sin^3\Theta d\Theta=\tfrac{2}{3}\pi r_0^2. \quad (11)$$

It will be assumed that, for any given value of v, the above ratio of $S_{\eta,K}/S=\frac{2}{3}$ holds for particles which do not possess a hard sphere interaction potential. Actually, this assumption is implied in the concept of *equivalent hard sphere* diameters which depend upon the relative velocity. Since it is possible to represent the results of Table I with an average absolute deviation of 0.8 percent and a maximum deviation of 1.6 percent by the relation

$$S=14.70+\frac{5.06\times10^5}{v}\ \text{A}^2\ (v\text{ in cm/sec.}), \quad (12)$$

the dependence of $S_{\eta,K}$ upon v will be given by

$$S_{\eta,K}=9.80+\frac{3.37\times10^5}{v}\ \text{A}^2. \quad (13)$$

For a single gas, the classical expression for the viscosity is[8,9]

$$\eta=\frac{5}{16}\frac{(1+\epsilon)(\pi MRT)^{\frac{1}{2}}}{NQ_{\eta,K}}, \quad (14)$$

where M is the molecular weight, R, the gas constant per mole, N, Avagadro's number, and $Q_{\eta,K}$, the classical cross section for viscosity and thermal conductivity for a Maxwellian gas at temperature, T, defined by

$$Q_{\eta,K}=\frac{M^4}{512R^4T^4}\int_0^{\infty} v^7 S_{\eta,K}\,e^{-Mv^2/(4RT)}dv. \quad (15)$$

The quantity ϵ is 0 for a gas whose molecules possess an inverse fourth power repulsive potential (inverse fifth power repulsive force) and 0.016 for a gas of hard spheres. The latter value will be used as the more suitable approximation for helium. If the expression for $S_{\eta,K}$ given in Eq. (13) is substituted into Eq. (15) with appropriate numerical values for the constants, evaluation of the integral gives the dependence of $Q_{\eta,K}$ in the form

$$Q_{\eta,K}=14.70+\frac{30.80}{T^{\frac{1}{2}}}\ \text{A}^2. \quad (16)$$

The final equation for η is obtained by combining Eqs. (14) and (16) to give

$$\eta=\frac{1.16\times10^{-5}T}{2.10+T^{\frac{1}{2}}}\ \frac{\text{g}}{\text{sec. cm}}. \quad (17)$$

For a monatomic gas, the thermal conductivity,

TABLE II. Comparison of calculated and observed values of viscosity and thermal conductivity.

T (°K)	$Q_{\eta,K}$ (A²)	$\eta_{exp}\times10^5$ $(\frac{g}{sec.\ cm})$	$\eta_{cal}\times10^5$ $(\frac{g}{sec.\ cm})$	$100\lvert\frac{\Delta\eta}{\eta_{exp}}\rvert$ (%)	$K_{exp}\times10^5$ $(\frac{cal}{sec.\ cm\ deg.})$	$K_{cal}\times10^5$ $(\frac{cal}{sec.\ cm\ deg.})$	$100\lvert\frac{\Delta K}{K_{exp}}\rvert$ (%)
200	16.87	14.960	14.29	4.5			
194.6	16.91				26.09	26.6	2.0
190	16.93	14.460	13.88	4.0			
180	17.00	13.950	13.45	3.6			
170	17.06	13.430	13.02	3.0			
160	17.13	12.900	12.58	2.5			
150	17.21	12.365	12.12	2.1			
140	17.30	11.815	11.66	1.4			
130	17.40	11.255	11.17	0.8			
120	17.51	10.680	10.67	0.1			
110	17.64	10.095	10.14	0.4			
100	17.78	9.470	9.59	1.3			
90	17.95	8.845	9.01	1.9			
89.4	17.96				16.5	16.9	2.4
80	18.14	8.205	8.41	2.5			
76.3	18.23				14.6	15.2	4.1
20.9	21.44				6.35	6.83	7.6
20.38	21.52	3.523	3.51	0.4			
20.1	21.57				6.24	6.66	6.7
18.0	21.96				5.85	6.19	5.8
16.8	22.21				5.61	5.91	5.3
16.55	22.27	3.147	3.11	1.2			
14.7	22.73				5.26	5.40	2.7
14.21	22.87	2.846	2.81	1.3			
4.23	(29.68)	1.277	(1.18)				
3.94	(30.22)				1.95	(2.10)	
3.25	(31.78)				1.58	(1.82)	
2.78	(33.17)				1.33	(1.61)	
2.00	(36.48)				0.92	(1.24)	
1.64	(38.75)	0.549	(0.56)				
1.62	(38.90)				0.79	(1.05)	

K, may be written

$$K=(1+\delta)\frac{5}{2}\eta c_v^{8,9}, \tag{18}$$

where c_v is the specific heat at constant volume which will be set equal to $3R/2M$. The value of δ lies between zero, for a gas with an inverse fourth power repulsive potential, and 0.01, for a gas of hard spheres. The hard sphere value will be used, as in the case of viscosity, so that, upon inserting values for R and M,

$$K=1.88\eta \ \frac{\text{cal}}{\text{sec. cm deg.}} \tag{19}$$

where η is in $\frac{\text{g}}{\text{sec. cm}}$.

In Table II values of η and K, calculated from Eqs. (17) and (19) are compared with experimental viscosity values of van Itterbeek and Keesom[13] (1.64°–20.38°K) and of Johnston and Grilly[14] (80°–200°K), and with experimental thermal conductivity values of Ubbink and de Haas[15] (1.62°–89.4°K) and of Eucken[16] (194.6°K). In the range 1.62°–4.23°K, calculated values appear in parentheses since they represent extrapolations beyond the region of demonstrable validity of Eq. (3), the small angle formula which is the basis of the present calculations.

Above the extrapolated region, the average absolute deviation of the calculated η values is 1.9 percent and that of the calculated K values, 4.6 percent. It is interesting that the agreement of the extrapolated thermal conductivities is considerably poorer than that of the extrapolated viscosities. This may be due to several causes, such as low experimental K values, appreciable departure of c_v from the ideal gas value of $(3/2)(R/M)$, or failure of the relation in Eq. (18). In the opinion of the author, it is quite likely that the experimental values are low since the helium pressures (1–4 mm) in the thermal conductivity apparatus may well have been insufficient to yield pressure independent values of K. In fact, Ubbink and de Haas state that, in the liquid helium temperature region, they were unable to test their measured values properly for pressure independence. Although extrapolation seems justified for viscosity, additional experimental results on the thermal conductivity below 4°K appear necessary to determine the validity of extrapolation in the case of thermal conductivity.

[13] A. van Itterbeek and W. H. Keesom, Physica **5**, 257 (1938).
[14] H. L. Johnston and E. R. Grilly, J. Phys. Chem. **46**, 948 (1942).
[15] J. B. Ubbink and W. J. de Haas, Physica **10**, 465 (1943).
[16] A. Eucken, Physik. Zeits. **12**, 1101 (1911).

COEFFICIENT OF SELF-DIFFUSION

Although experimental values of the coefficient of self-diffusion of helium are not available, it seems desirable, for the sake of completeness, to obtain calculated values by procedures similar to those used for viscosity and thermal conductivity.

The classical expression for the coefficient of self-diffusion, $D(1, 1)$, is[8,9]

$$D(1,1)=\frac{3}{8}\frac{(1+\epsilon)(\pi MRT)^{\frac{1}{2}}}{N\rho Q_{D(1,1)}}, \tag{20}$$

where ϵ is the small correction term previously encountered in the expression for η, ρ, the gas density in grams per unit volume, and $Q_{D(1,1)}$, the classical cross section for self-diffusion for a Maxwellian gas at temperature T defined by

$$Q_{D(1,1)}=\frac{M^3}{32R^3T^3}\int_0^\infty v^5 S_{D(1,1)} e^{-Mv^2/(4RT)}dv. \tag{21}$$

The classical cross section for self-diffusion, $S_{D1,1}$, which appears in Eq. (21) is given, for hard spheres, by[1,10]

$$S_{D(1,1)}=2\pi\int_0^\pi G(\Theta)\sin^2\frac{\Theta}{2}\sin\Theta d\Theta$$

$$=2\pi\int_0^\pi (\tfrac{1}{4}r_0^2)\sin^2\frac{\Theta}{2}\sin\Theta d\Theta=\tfrac{1}{2}\pi r_0^2, \tag{22}$$

and since it will be assumed that the hard sphere ratio, $S_{D(1,1)}/S=\frac{1}{2}$, is valid for helium, the dependence of $S_{D(1,1)}$ upon v is obtained simply from Eq. (12) in the form

$$S_{D(1,1)}=7.35+\frac{2.53\times10^5}{v}\ \text{A}^2, \tag{23}$$

TABLE III. Calculated values of the self-diffusion coefficient at 1 atmos.

T, °K	$Q_{D(1,1)}$ A²	$D(1, 1)$, cm²/sec.
200	17.30	0.687
180	17.45	0.582
160	17.61	0.483
140	17.81	0.391
120	18.07	0.306
100	18.39	0.229
80	18.82	0.160
60	19.46	0.100
40	20.53	0.0518
20	22.95	0.0164
15	24.22	0.0101
10	(26.37)	(0.00504)
5	(31.20)	(0.00151)

where v is in cm/sec. Upon combining Eqs. (23) and (21), inserting values for R and M, and integrating, the following relation is obtained for $Q_{D(1,1)}$:

$$Q_{D(1,1)} = 14.70 + \frac{36.89}{\sqrt{T}} \text{ A}^2. \tag{24}$$

If Eq. (24) is combined with Eq. (20), with ϵ set equal to 0.016, the final relation for $D_{1,1}$ becomes

$$D(1, 1) = \frac{1.39\times10^{-5}T}{\rho[2.51+(T)^{\frac{1}{2}}]} \frac{\text{cm}^2}{\text{sec.}} \tag{25}$$

where ρ is in g/cc, or

$$D(1, 1) = \frac{2.89\times10^{2}T^{2}}{P[2.51+(T)^{\frac{1}{2}}]} \frac{\text{cm}^2}{\text{sec.}} \tag{26}$$

where P is in dynes/cm², since $\rho = PM/RT$.

Values of $Q_{D(1,1)}$ computed from Eq. (24) and of $D(1, 1)$ computed from Eq. (26) for $P = 1.01\times10^{6}$ dynes/cm² (1 atmos.) are listed in Table III.

"Structure" in Liquids and the Relation between the Parameters of the Arrhenius Equation for Reactions in the Condensed Phase[1]

CHAS. E. WARING[2] AND PAUL BECHER[3]
Research Laboratory of Physical Chemistry, Polytechnic Institute of Brooklyn, Brooklyn, New York
(Received August 19, 1946)

On the basis of the liquid state being quasi-crystalline, a modification of the transition state theory leads to a simple equation for the temperature dependence of the fluidity, which involves a characteristic frequency of molecular vibration. The parameters of the fluidity equation are shown to have a linear correlation for certain liquids. The quasi-crystalline picture is then extended to a simple collision theory of uni- and bimolecular reactions in solution, and it is shown that the known correlation of the parameters of the Arrhenius equation arises from the fluidity correlation.

I. INTRODUCTION

IN recent years, increasing emphasis has been placed on the concept of "structure" in the liquid state. This train of thought was initiated by the discovery of the x-ray diffraction of liquids by Debye and Scherrer and in the hands of Debye,[4] Zernike, Prins[5] and others, this concept has received its mathematical formulation. Eyring and his co-workers[6] and Lennard-Jones and Devonshire[7] have extended it to predict and explain many properties of the liquid state.

It is the purpose of the present paper to utilize such a model of the liquid state to explain certain phenomena connected with the kinetics of simple non-ionic reactions* in solution. To do this it is necessary first to discuss the effect of the structural concept in relation to the viscosity (or better, "fluidity") of liquids.

[1] Presented in a preliminary form before the Division of Physical and Inorganic Chemistry of the American Chemical Society, 103rd Meeting, Memphis, Tennessee, April 20–24, 1942. Publication delayed by military service.

[2] Present address: Department of Chemistry, University of Connecticut, Storrs, Connecticut.

[3] This paper is from the thesis submitted by Mr. Paul Becher to the Graduate Faculty of the Polytechnic Institute of Brooklyn in partial fulfillment of the requirements for the degree of Master of Science in Chemistry, June, 1942.

[4] P. Debye, Physik. Zeits. **31**, 348 (1930).

[5] F. Zernike and J. A. Prins, Zeits. f. Physik. **41**, 184 (1927); J. A. Prins, *ibid.* **56**, 617 (1929); Naturwiss. **19**, 435 (1931).

[6] H. Eyring, J. Chem. Phys. **4**, 283 (1936); J. F. Kincaid and H. Eyring, *ibid.* **6**, 620 (1938); R. H. Ewell and H. Eyring, *ibid.* **5**, 726 (1937). Also, S. Glasstone, K. J. Laidler, and H. Eyring, *Theory of Rate Processes* (McGraw-Hill Book Company, Inc., New York, 1941).

[7] J. E. Lennard-Jones and A. F. Devonshire, Proc. Roy. Soc. **A163**, 53 (1937); **165**, 1 (1938).

* By a "simple non-ionic reaction" is meant one in which (all things being equal) the rate of reaction is independent of the dielectric properties of the solvent.

II. THE FLUIDITY OF LIQUIDS

Imagine that there exists in the liquid a quasi-crystalline lattice, exhibiting short range order. The lattice is, to be sure, imperfect, but it is these very imperfections which can be considered to be characteristic of the liquid state. Further imagine that, in this quasi-crystalline lattice, the molecules are vibrating with characteristic frequencies, which, for the sake of simplicity, will be assumed to be harmonic and all the same for a given liquid.

Now, because of the imperfections of the lattice, next to any given molecule there may exist a vacant lattice-site. While the molecule is vibrating with a small amplitude, a translation to this neighboring site is not possible, but if the amplitude of vibration should increase (increased energy), then, at a certain critical amplitude the vibration goes over into a translation, and the molecule occupies the next lattice site. The energy required for this jump is (harmonic vibration),

$$\epsilon = 2\pi^2 m \nu^2 q_c^2, \tag{1}$$

where m is the mass of the molecule, ν is the characteristic frequency, and q_c is the critical amplitude.

In the absence of any external shear, there will, of course, be an equal likelihood that this shift in lattice position will take place in all possible directions of the quasi-lattice. However, when a shearing force is applied, there will be an excess of jumps in the direction of shear, and flow occurs. Since, for Newtonian liquids at least, the shearing force will not affect the energy require-

ments for such a lattice jump, the energy of Eq. (1) is evidently the activation energy for flow, and may now be designated ϵ_ϕ, or per mole, E_ϕ.

The foregoing considerations can now be given a more precise mathematical form. In terms of the transition state theory, Eyring[6] has indicated that the fluidity of a Newtonian liquid may be given by

$$\phi = (V/hN)\cdot(F^\ddagger/F)\exp(-E_\phi/RT), \quad (2)$$

where ϕ is the fluidity, V the molar volume, $F^\ddagger$ and F, the partition functions of the activated and unactivated molecules, respectively, and E_ϕ, the activation energy of flow, which may be considered to have the form of (1). N, h, R, and T have the usual meanings.

Now, Eyring has considered that $F^\ddagger$ and F differ only in the *translational* portions of the partition function, and is thus led to an expression for the fluidity which involves a free volume per molecule, which then has to be calculated—a not too simple problem. However, from the considerations indicated above it would appear more likely that they differ in the *vibrational* partition functions. If this is taken to be the case, Eq. (2) will take the form

$$\phi = V\nu/NkT\exp(-E_\phi/RT) = V\nu/RT\exp(-E_\phi/RT), \quad (3)$$

where, of course, E_ϕ is defined in terms of Eq. (1).**

As yet nothing has been said about the nature of the vibrational frequency alluded to in Eqs. (1) and (3), except to describe it as the frequency with which the molecule executes harmonic vibrations about its equilibrium position in the quasi-crystalline lattice. It is desired to give an absolute value to this frequency. It may, in fact, be readily calculated by an extension of our picture of the liquid state.

Debye's[8] modification of the Einstein[9] specific heat theory of crystalline substances supposes that the $3N$ vibrations of the N particles which make up the lattice are the first $3N$ overtones of a continuous solid with the same elastic constants as the crystal. Hence, the $3N$th frequency is given by

$$\nu_D = C(3N/4\pi V)^{\frac{1}{3}}, \quad (4)$$

where C is of the nature of an average velocity of sound in the medium (average because of the possibility of transverse as well as longitudinal waves), and V is the volume. For our purposes, we may assume that all the particles have the same frequency, given by Eq. (4). This is not unjustified; the most probable frequency of a real crystal has nearly that value.

Thus ν_D, as defined by Eq. (4), is identified with the vibrational frequency of the molecules in the quasi-crystalline lattice. One simplification results in the application to the liquid state; since a liquid will not support transverse vibrations, C is no longer an average velocity of sound in the medium, but is equal to the experimentally measured value of the velocity of sound in the liquid. This enables one to calculate the frequency of vibration of the molecule if the velocity of propagation of sound in the liquid, and the molar volume are known.

We now have the value of every parameter in Eq. (3) except q_c, the critical amplitude. In principle, it should be possible to estimate this parameter from a knowledge of the molecular volume and from a knowledge of the x-ray diffraction pattern of the liquid. In practice, however, because of the asymmetry of the molecules, the problem is a fairly complex one. Since the assumption of harmonic motion has introduced an element of uncertainty in any case, it is perhaps futile to attempt this calculation, which would, at best, still be an estimate.

The equation, however, may be tested quite critically in another way. Since we can determine experimentally values for E_ϕ, the activation energy of flow, we may assume a reasonable value for q_c and calculate the frequency from Eq. (1), that is

$$\nu_E = (E_\phi/2\pi^2 m q_c^2 N)^{\frac{1}{2}} \quad (5)$$

(where we have written the frequency with the subscript E to indicate the manner of calculation). If our choice of q_c has been correct, then ν_E should equal ν_D. Now, it is very reasonable to assume that q_c will be about the same for most substances, hence if the same choice of q_c gives

** It is perhaps significant to point out that Eyring does not totally disregard the possibility that the different partition function is the vibrational one; this possibility is mentioned in the first paper listed in reference (6).

[8] P. P. Debye, Ann. d. Physik **39**, 789 (1912).

[9] A. Einstein, Ann. d. Physik (4), **22**, 180 (1907).

good agreement between ν_E and ν_D for a number of substances, we may feel that the theory has been rather critically tested.

In Tables I and II the results of such a calculation are set forth. For alcohols, a value of 0.75A has been used; this could be approximately a hydrogen bond radius. For other types of liquids a value of 0.50A appears to be of the correct order of magnitude. The agreement between ν_E and ν_D is seen to be quite good, certainly better than the usual "order of magnitude." Thus, it should be readily possible to calculate the energy of activation of flow for most liquids to within less than 15 percent, using a value of about 0.50A for the critical amplitude of vibration and the experimentally determined velocity of sound in the liquid.

It is of interest to note that Simha,[10] proceeding on a somewhat different concept of the flow process, has derived a similar expression for the temperature dependence of the fluidity, differing only in the inclusion of a packing factor.

III. RELATION OF THE PARAMETERS FOR FLUIDITY

The form of Eq. (3) may be experimentally verified in a rather interesting manner. A discussion of the significance of this result will be deferred, however, until later in the paper.

Equation (3) may be written

$$\phi = B \exp(-E_\phi/RT),$$

in which form it is the familiar semi-empirical equation suggested by Arrhenius[11] and de Guzman.[12]

Comparison of the above equation with Eq. (1) shows that

$$B = f(\nu)$$

and

$$E_\phi = F(\nu^2),$$

from whence it would appear that, for a series of liquids, a relationship should exist between B and E_ϕ. A plot of $\log B$ *vs.* E_ϕ does, indeed, yield a straight line for various groups of liquids—a functional relationship which has not previously been demonstrated. It should be noted, however, that the actual *form* of the relationship is not an immediate consequence of the equations given, even assuming the relative constancy of q_c. While to this extent the relation is somewhat accidental, this is unimportant; it is that the relation does in fact exist that *is* significant.

In Fig. 1 this relation is demonstrated for a number of alcohols, while in Fig. 2 it is shown to exist for aliphatic acids. From its partially accidental nature, this relationship does not necessarily have to be restricted to members of a homologous series, as is shown in Figs. 3 and 4, the latter showing *two* such correlations. It should be noted that iodobenzene and nitrobenzene do not fit these correlations.***

It has been demonstrated that the temperature dependence of fluidity of a mixture of simple liquids can be accurately represented by Eq. (3). Consequently, we felt it reasonable to assume that in the case of a binary mixture, the effective frequency reflected in the energy of fluidity through Eq. (3) would be of the nature of an "average" frequency. Thus, it would vary slightly with concentration, and we should expect to find a similar correlation existing between various concentrations of binary mixtures. This is shown in Figs. 5–7 for the systems benzene-ethanol, water-acetone, and water-ethanol, respectively. The existence of this correlation has also been verified for many more mixtures over a large range of $\log B$ and E_ϕ values, but space considerations forbid their representation here.

By extension, this correlation should also hold for ternary systems, and that this is indeed the case is shown in Fig. 8 for the system water-acetone-ethanol.

IV. REACTIONS IN A QUASI-CRYSTALLINE SOLVENT

A. Unimolecular Reactions

Let us now consider the rates of unimolecular reactions in solution from the point of view of the solvent as quasi-crystalline.

Consider a dilute solution of a molecules of reactant A in b molecules of an inert solvent B, $b \gg a$. Since the solution is dilute, each mole-

[10] R. Simha, J. Chem. Phys. **7**, 302 (1939).
[11] S. Arrhenius, Meddel. Vetenskapsakad. Nobelinst. **3**, 20 (1916).
[12] J. de Guzman, Anal. Soc. Espan. Fis. Quim. **11**, 353 (1913).

*** The reasons for the choice of these particular liquids will appear presently.

cule of A is effectively isolated and will be surrounded by a crystal coordination sphere of n solvent molecules $B(6 \leq n \leq 12)$. Assume that the position of each molecule A relative to the equilibrium positions of the solvent molecules is fixed; then any collisions which take place will occur as a result of the lattice vibrations of B. Further, one may assume that collisions may only take place when the vibrational energy of the B molecules is such that the amplitude of vibration is *very nearly* that which would cause the molecule to tear itself from its lattice point (Eq. (1)). These molecules will then possess an energy which is a definite fraction of the activation energy of flow, i.e., $E_\phi' = \sigma E_\phi$, $0 < \sigma \leq 1$. In general, one may take $\sigma \approx 1 (E_\phi' \approx E_\phi)$.

Now of the n molecules surrounding each molecule A, only $n \exp(-E_\phi'/RT)$ will, therefore, have sufficient energy to collide with the reactant molecule at the extreme of its vibration, and since the molecule is vibrating with a frequency ν, there will be $n\nu \exp(-E_\phi'/RT)$ such collisions per second for each A molecule. Thus the total number of collisions taking place between solvent and reactant molecules per second will be

$$Z_{AB} = an\nu \exp(-E_\phi'/RT), \tag{6}$$

where Z_{AB} is clearly the collision number for the solution.

From the theory of unimolecular reactions[13] it is immediately clear that only those collisions in which more than a certain critical energy (the activation energy) is distributed among a specified number of internal degrees of freedom contribute to the reaction. Thus, the number of collisions *leading to reaction* per second is

$$\begin{aligned} Z_{AB} \frac{1}{(S-1)!} \left(\frac{E_a}{RT}\right)^{S-1} \exp\left(-\frac{E_a}{RT}\right) &= \frac{an\nu}{(S-1)!} \exp\left(-\frac{E_\phi'}{RT}\right) \exp\left(-\frac{E_a}{RT}\right) \\ &= \frac{an\nu}{(S-1)!} \exp(-E_{obs}/RT) \end{aligned} \tag{7}$$

[13] R. H. Fowler and E. A. Guggenheim, *Statistical Thermodynamics* (Cambridge University Press, England, 1939), Chapter XII, especially pp. 519–530.

TABLE I. Calculated vibrational frequencies in alcohols. $q_e = 0.75$A

Compound	ν_D (Velocity of sound) $\times 10^{-13}$	ν_E (Fluidity) $\times 10^{-13}$
Methanol	0.173	0.172
Ethanol	0.164	0.168
Propanol	0.155	0.166
Butanol	0.152	0.152
Pentanol	0.149	0.151

where $E_{obs} = E_\phi' + E_a$ is the observed activation energy, and where E_a is the activation energy which the reaction would require if it were carried out in the gas phase, with all solvent effects removed. The observed change in activation energy for the same reaction from solvent to solvent is thus explained as the effect of the contribution from E_ϕ'.

Equation (7) therefore represents the number of A molecules which react per second.

Now, by definition, for a unimolecular reaction of the first order

$$-d(A)/dt = k_1(A), \tag{8}$$

where (A) is the concentration of A in moles per liter. Now, it may readily be shown that

$$(A) = 10^3 a/bV_B, \tag{9}$$

where V_B is the molar volume of the solvent.

Substituting Eq. (9) in (8), we obtain

$$-da/dt = k_1 a. \tag{10}$$

It is evident that the left-hand side of Eq. (10) represents the number of molecules reacting per

TABLE II. Calculated vibrational frequencies in various liquids. $q_e = 0.50$A

Compound	ν_D (Velocity of sound) $\times 10^{-13}$	ν_E (Fluidity) $\times 10^{-13}$
Chloroform	0.106	0.111
Ether	0.113	0.133
Chlorobenzene	0.148	0.125
Nitrobenzene	0.169	0.142
Benzene	0.155	0.165
Aniline	0.196	0.218
Toluene	0.117	0.137
Ethylbenzene	0.143	0.130
Acetone	0.150	0.104
Carbon tetrachloride	0.105	0.113
n-Hexane	0.115	0.128
n-Heptane	0.115	0.126

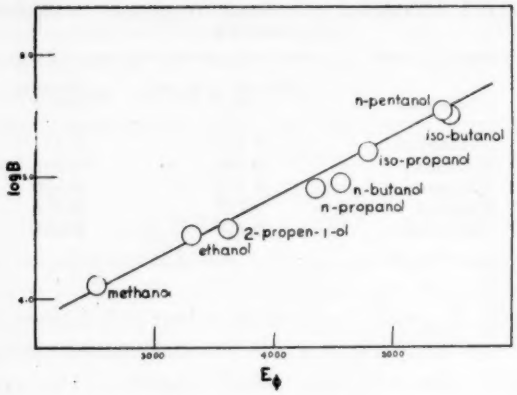

FIG. 1. Fluidity correlation for alcohols.

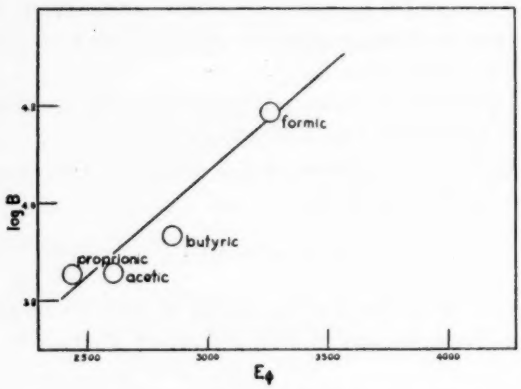

FIG. 2. Fluidity correlation for aliphatic acids.

second, hence the number of collisions leading to reaction per second. It is thus equal to the expression in Eq. (7). Substituting, one obtains

$$k_1=\frac{n\nu}{(S-1)!}\left(\frac{E_a}{RT}\right)^{S-1}\exp(-E_{\text{obs}}/RT), \quad (11)$$

a surprisingly simple result for the rate constant of unimolecular reactions in solution.

B. Bimolecular Reactions

Bimolecular reactions in a quasi-crystalline solvent may be treated in a similar fashion. Assume that there are a molecules A and b molecules B of reactant dissolved in c molecules of an inert solvent $C(c\gg a\approx b)$.

Consider now an A molecule surrounded by n other molecules. The chance that one of these is a B molecule (condition for reaction) is (approximately) bn/c.† For the a molecules A,

$$a(bn/c),$$

such pairs exist.

Now one may assume (if the masses of all the molecules are very nearly equal) that the vibrational frequency of the solvent is "impressed" on the reactant, or, alternatively, that an "average" frequency will predominate. This frequency may in any case be designated ν_C. There are then $(ab/c)n\nu_C$ vibrations per second between A and B molecules of which

$$Z_{AB(C)}=(ab/c)n\nu_C\exp(-E_\phi'/RT) \quad (12)$$

will lead to collision, and where E_ϕ', as before, is a definite fraction of the activation energy of flow for the solvent, and where $Z_{AB(C)}$ is the collision number of A and B molecules in solvent C.

It will be observed that the above equation for

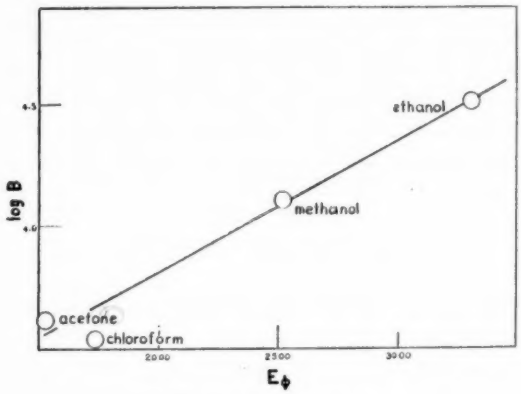

FIG. 3. Fluidity correlation.

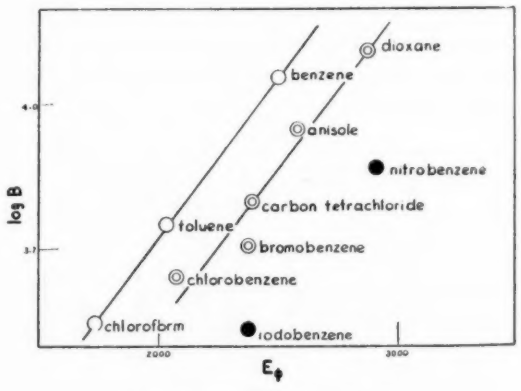

FIG. 4. Fluidity correlation.

† Exactly, of course, the probability would be $(b/a+b+c)n$; but we have assumed that c is much larger than a or b. In fact, for a 0.01M solution, c would be about 10^2a (or b).

the collision number is completely symmetrical, and that, had one started from a consideration of the probability of finding an A molecule in the coordination sphere of a B molecule, exactly the same expression would have been obtained.

From the considerations of the previous section it is clear that the number of collisions leading to reaction per second is then given by

$$(ab/c)n\nu_C \exp(-E_\phi'/RT) \exp(-E_a/RT) = (ab/c)n\nu_C \exp(-E_{obs}/RT). \quad (13)$$

From Eq. (9) and the definition of a bimolecular reaction of second order one has

$$-da/dt = -db/dt = k_2(10^3/cV_C)ab. \quad (14)$$

Combining Eqs. (13) and (14)

$$k_2 = (nV_C\nu_C/10^3) \exp(-E_{obs}/RT). \quad (15)$$

This leads to the somewhat surprising result that *all* bimolecular reactions measured in a given solvent should have approximately the same value of the non-exponential term of the Arrhenius equation, although the relative magnitude of the forces between the various types of molecular species would be a complicating factor. Unfortunately, the experimental data recorded in the literature is somewhat too meager to justify a decision, although it would appear that this is approximately the case.

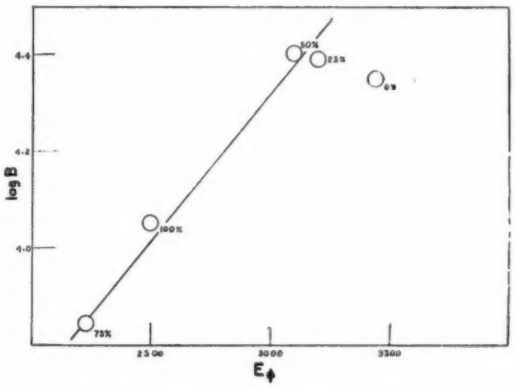

FIG. 5. Fluidity correlation ethanol+wt. % benzene.

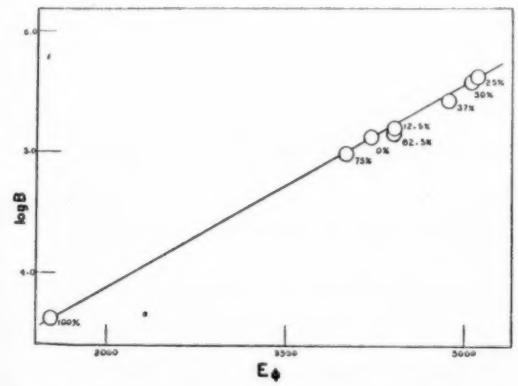

FIG. 6. Fluidity correlation water+vol. % acetone.

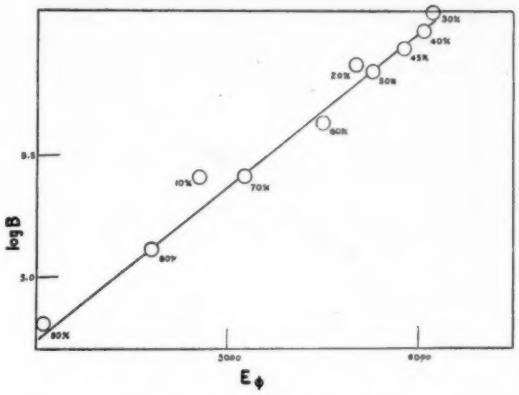

FIG. 7. Fluidity correlation water+wt. % ethanol.

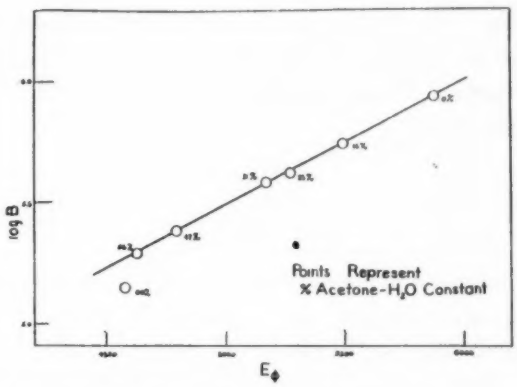

FIG. 8. Fluidity correlation system: water-acetone-ethanol. Composition of solution: 400 grams of water made up to one liter by adding acetone and ethanol. Points indicate weight percent of acetone in mixture.

It should be mentioned that Rabinowitch,[14] by considering the conditions imposed by the necessity of an A molecule *diffusing* into proximity to a B molecule, has arrived at a somewhat similar formulation: the assumption that $\nu \approx \nu_D$ is made in the estimation of an order of magnitude.

V. RELATION OF THE PARAMETERS OF THE ARRHENIUS EQUATION

Both Eqs. (11) and (15) may be written in the form

$$k = A \exp(-E_{obs}/RT),$$

[14] E. Rabinowitch, Trans. Faraday Soc. **33**, 1225 (1937).

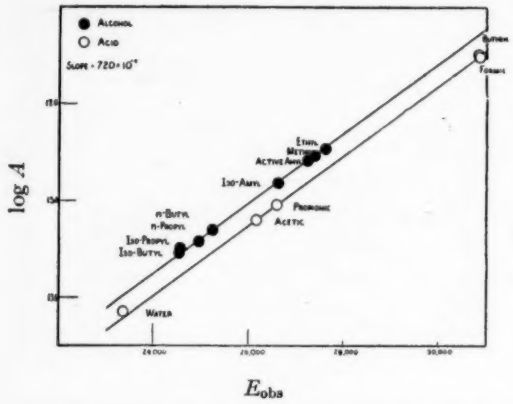

FIG. 9. Decomposition of benzene diazonium chloride.

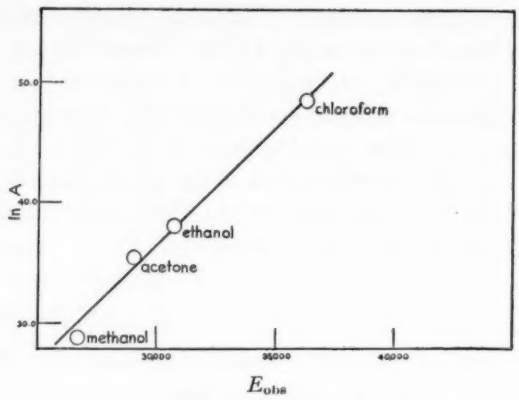

FIG. 11. Decomposition of benzylhydroxy triazolecarboxylic acid ester.

which is the Arrhenius equation for the temperature dependence of the rate constant. Now, examination of both equations yields the interesting result that

$$A = f(\nu_C)$$

and

$$E_{obs} = F(\nu_C^2).$$

Therefore, the changes in E_{obs} and A for a given reaction measured in a series of solvents is entirely due to the change of solvent; further, it is to these very changes that we have ascribed the correlation of parameters of the fluidity equation (Eq. (3)). It may therefore be expected that *if a correlation exists between the parameters of the fluidity equation for a group of solvents, a similar correlation will exist between the parameters of the Arrhenius equation for a given reaction studied in these solvents.*

That this is actually the case may readily be shown. Figure 9 shows the correlation between log$A$ and E_{obs} for the decomposition of benzene diazonium chloride in a series of alcohols and acids[15] (cf. Figs. 1 and 2). In Fig. 10 is shown the correlation for the decomposition of acetone-dicarboxylic acid[16] in a series of alcohols (cf. Fig. 1). Figure 11 indicates the correlation for the decomposition of benzylhydroxytriazole carboxylic acid ester[17] in a number of solvents (cf. Fig. 3). All of the above are unimolecular reactions.

We now turn to the case of bimolecular reactions, where the same effect is to be expected. This is shown in Fig. 12 which gives the correlation for the reaction between pyridine and methyl iodide[18] for a large number of solvents.

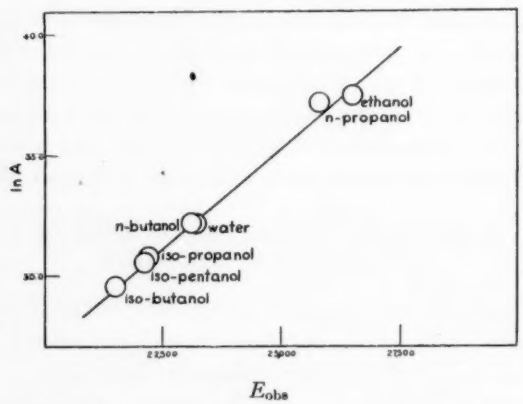

FIG. 10. Decomposition of acetone dicarboxylic acid.

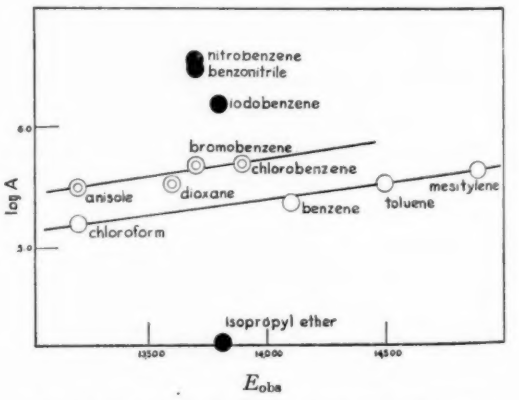

FIG. 12. Reaction of pyridine and methyl iodide.

[15] Chas. E. Waring and J. Abrams. J. Am. Chem. Soc. **63**, 2757 (1941).
[16] E. O. Wiig, J. Phys. Chem. **32**, 961 (1928); *ibid.* **34**, 596 (1930).
[17] O. Dimroth, Annalen **373**, 367 (1910).
[18] N. J. Pickles and C. N. Hinshelwood, J. Chem. Soc. **1936**, 1353.

Comparison of this plot with Fig. 4 provides a striking verification of our predictions. For example, attention was called to the fact that iodobenzene and nitrobenzene failed to correlate with the other liquids presented in Fig. 4. It is significant, therefore, that the reaction between pyridine and methyl iodide in these two solvents does not exhibit the same functional relationship as it does in those liquids in which the fluidities correlated. Unfortunately, no data for the variation of fluidity with temperature was available for benzonitrile and isopropyl ether.

Next is shown in Fig. 13 the correlation for the same reaction in a set of binary solvents[19] (cf. Fig. 5). Figures 14 and 15 represent the correlation of log$A$ and E_{obs} for the hydrolysis of benzoic and m-nitrobenzoic esters[20] in water-acetone

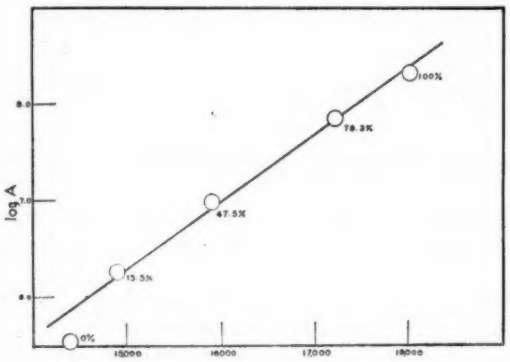

E_{obs}

FIG. 13. Reaction of pyridine and methyl iodide in benzene +wt. % ethanol.

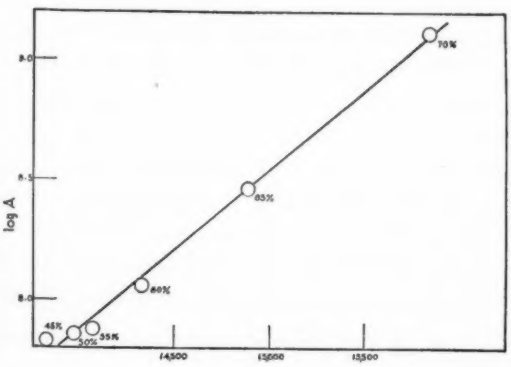

E_{obs}

FIG. 14. Hydrolysis of benzoic ester in water +vol. % acetone.

[19] R. A. Fairclough and C. N. Hinshelwood, J. Chem. Soc. **1937**, 1573.

[20] R. A. Harman, Trans. Faraday Soc. **35**, 1336 (1939).

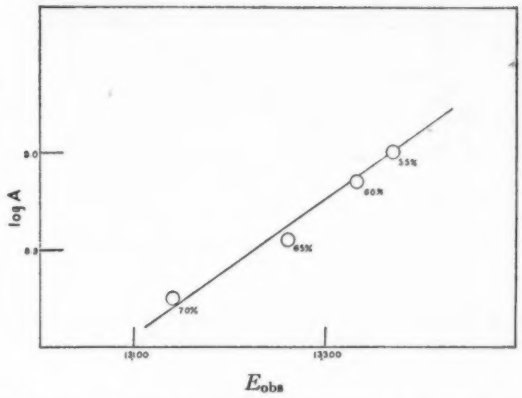

E_{obs}

FIG. 15. Hydrolysis of m-nitrobenzoic ester in water +wt. % acetone.

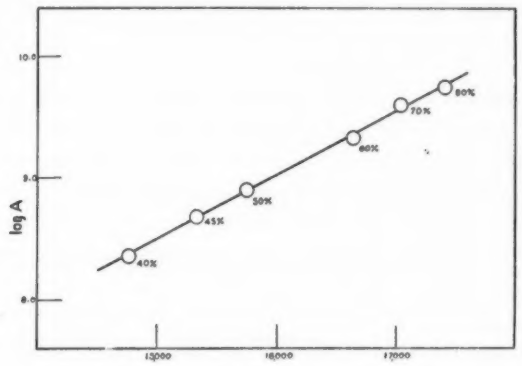

E_{obs}

FIG. 16. Hydrolysis of benzoic ester in water +vol. % ethanol.

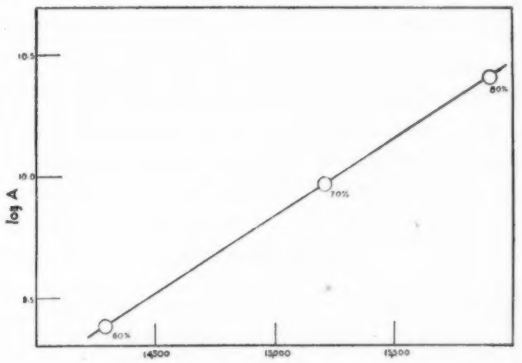

E_{obs}

FIG. 17. Hydrolysis of m-nitrobenzoic ester in water +vol. % ethanol.

mixtures (cf. Fig. 6); while Figs. 16 and 17 show the same reaction in water-ethanol mixtures (cf. Fig. 7).

Figure 18 shows the correlations for the alkaline hydrolysis of benzoic ester in a set of

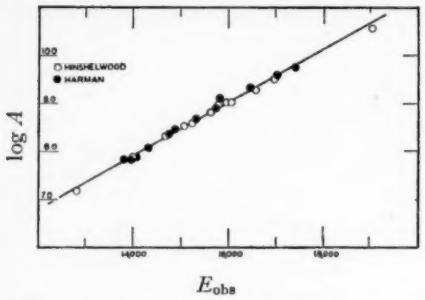

FIG. 18. Saponification of ethyl benzoate in water-acetone-ethyl alcohol mixtures.

ternary mixtures of acetone-ethanol-water[20,21] (cf. Fig. 8).

[21] R. A. Fairclough and C. N. Hinshelwood, J. Chem. Soc. **1937**, 538.

The existence of the correlation for the Arrhenius equation has, of course, been empirically known for some time (see, for example, references (19) and (21)), and it has been suspected that it was a solvent effect. It is quite satisfying to be able to derive it so simply from the concept of the quasi-crystalline liquid.

ACKNOWLEDGMENT

The authors wish to express their appreciation to Dr. R. Simha for his encouragement and many valuable suggestions during the course of this work. We also wish to thank Dr. H. Eyring for valuable suggestions as to the presentation of this material.

THE JOURNAL OF CHEMICAL PHYSICS VOLUME 15, NUMBER 7 JULY, 1947

Solubilization by Solutions of Long-Chain Colloidal Electrolytes*

RICHARD S. STEARNS, HANS OPPENHEIMER, ERIC SIMON, AND WILLIAM D. HARKINS
George Herbert Jones Chemical Laboratory, University of Chicago, Chicago, Illinois

Increase in the concentration of a soap or other detergent does not increase the solubility of an oil above that in water until the critical concentration for the formation of micelles (*cmc*) is attained. Above this the solubility, designated as solubilization, increases and, in general, more rapidly as the soap concentration increases; i.e., per mole of soap the solubilization is greater in a 25 percent than in a 5 percent soap solution. For a homologous series the volume of oil solubilized at a constant temperature is to a first approximation inversely proportional to the molar volume. The polarity and shape of the molecules solubilized also play a role. Salts increase the extent of the solubilization; at low concentrations to an extent which may be accounted for by the increase in micellar area resulting from the depression of the *cmc* by the salt. At higher soap concentrations the increase in solubilization is greater than can be accounted for in this way.

I. INTRODUCTION

ONE of the most outstanding properties of solutions of long chain colloidal electrolytes, inclusive of soaps and many other detergents, is their ability to solubilize various organic substances. This property, utilized commercially since 1874, is of fundamental importance both in their use as detergents and in emulsion polymerization.[1] Engler and Dieckhoff[1e] made very early, by the use of visual observations, a distinction between true solution and solubility in a detergent. Pickering,[2] in 1917, found that oils dissolve in concentrated soap solutions. Smith,[3]

* This investigation was carried out under the sponsorship of the Reconstruction Finance Corporation, Office of Rubber Reserve, in connection with the Government's synthetic rubber program.

[1a] G. Link in Friedlander's *Fortschritte der Teerfarbenfabrikation* (1877–88), Vol. I, p. 11.
[b] F. Von Heyden, D.R.P. 57842 (1890).
[c] C. Engler and E. Dieckhoff, Arch. Pharm. **230**, 561 (1892).
[d] G. A. Rappenstrauch, *Ibid.* **229**, 201 (1891).
[e] R. Otto, Ber. **27**, 2131 (1894).
[f] F. Nottbrack, Chem. Ztg. **32**, 100 (1908).
[2] S. U. Pickering, J. Chem. Soc. **111**, 86 (1917).
[3] E. L. Smith, J. Phys. Chem. **36**, 1401, 1672, 2455 (1932).

McBain,[4] and others have determined the solubility of oils, dyes, etc., in soap solution as well as the effect of salts on solubilization. However, their work is concerned largely with the solubilization of water insoluble dyes, and apparently there exist no published data which give the solubility of an oil at various concentrations of the same soap solution. A general theory of the loci of emulsion polymerization had been developed by Harkins in 1942, and he requested the Rubber Director's Office to arrange that Professor W. B. Reynolds of the University of Cincinnati cooperate in obtaining evidence bearing on the theory. On account of the importance in this theory of the thin monomer layers in micelles, work on solubilization was begun by Stearns and Jura at Chicago on February 1, 1943, and similar work was begun at Cincinnati at about the same time.[5] The topics of the investigation as it proceeded were outlined in numerous conferences between Reynolds and Harkins, and it was decided that the former should study particularly the effect of salts in increasing the solubility of oils in soap solutions and polymerization in solutions of short-chain soaps such as the caprylate and caprate in the presence of electrolytes. The importance of salts in connection with solubilization was suggested by an experiment of Hartley[6] who discovered that sodium chloride increases the solubility of trans-azobenzene in solutions of pyridinium salts. The very extensive data on the solubilization of various oils in both the absence and the presence of salts as obtained by Reynolds and collaborators[7] will be published elsewhere.

At Cincinnati and in the initial work at Chicago, the procedure used for the determination of the solubility was the very old method of observing visually the appearance of turbidity as more and more oil is added. However, none of the results obtained by this method are included here, since the higher accuracy given by the use of a photometer is needed for a more careful consideration of the relations involved.

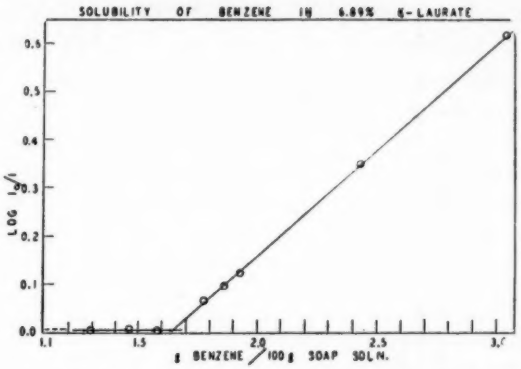

FIG. 1. Exhibits essential constancy in the optical density of a 6.89 percent potassium laurate solution with increasing amounts of dissolved benzene. The rapid increase of I_0/I begins where emulsion droplets first appear. The intersection of the two straight lines is considered to give the solubility of benzene in the soap solution.

The present paper deals with the solubilization of various hydrocarbons in solutions of potassium laurate and potassium myristate and the effect of salts and of mixtures of soaps on solubilization. This effect has long been a matter of discussion, and in spite of the extensive work done on these subjects the problem is still far from its solution. However, it has been found in this laboratory that soap solutions contain aggregates each of which, designated as a micelle, contains soap molecules, varying in number but of the general order of 100. It also seems to be established that soap solutions exhibit a critical concentration below which no micelles exist.

In a recent paper[8] Harkins, Mattoon, and Corrin have discussed the structure of soap micelles as indicated by x-rays and the theory of molecular orientation. The x-ray work discussed in this paper, taken together with more recent work, indicates that each micelle consists of a double layer of soap molecules with their hydrocarbon chains oriented towards each other and with their polar ends toward the water. The effect

[4] J. W. McBain and M. E. Laing McBain, J. Am. Chem. Soc. **58**, 2610 (1936); J. W. McBain and J. J. O'Connor, *ibid.* **62**, 2855 (1940); J. W. McBain and R. C. Merrill, Ind. Eng. Chem. **34**, 915 (1942); J. W. McBain and K. E. Johnson, J. Am. Chem. Soc. **66**, 9 (1944); J. W. McBain and P. H. Richards, Ind. Eng. Chem. **38**, 642 (1946); J. W. McBain and Sister Agnes Ann Green, J. Am. Chem. Soc. **68**, 1731 (1946).

[5] The earliest work of Reynolds on styrene and of Jura on butadiene was reported in a private communication from the University of Chicago, March 19, 1943; and that of McBain from Stanford University on both materials on March 23, 1943.

[6] G. S. Hartley, J. Chem. Soc., London **1938**, 1970.

[7] W. B. Reynolds, P. J. Canterino, E. W. Cotten, R. E. Holland, and J. E. Wicklatz. Many private communications (University of Cincinnati, Cincinnati, Ohio, 1943–4).

[8] W. D. Harkins, R. W. Mattoon, and M. L. Corrin, J. Am. Chem. Soc. **68**, 220 (1946).

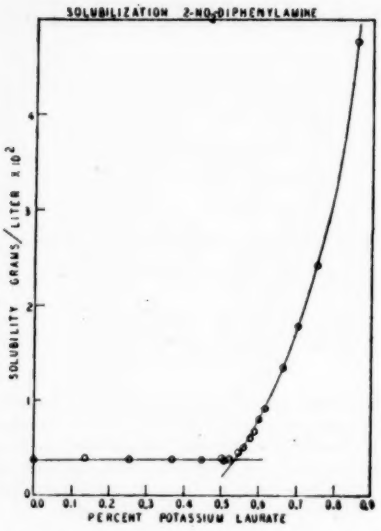

FIG. 2. Solubility of 2-nitrodiphenylamine in dilute potassium laurate solutions. The solubility remains constant until the critical concentration is passed after which there is a sharp increase due to solubilization in soap micelles.

of solubilized oil on the x-ray diffraction bands[9] seems to indicate that the oil is solubilized in the hydrocarbon interior of the micelle, presumably between the hydrocarbon ends of the soap micelles. The critical concentrations of the soaps considered here have been determined accurately by Corrin[10] as 0.393 for potassium caprylate, 0.100 for potassium caprate, 0.023 for potassium laurate, and 0.0059 for potassium myristate, as expressed in moles per liter.

II. METHOD OF DETERMINING SOLUBILIZATION

The extent of solubilization of the hydrocarbons was found by use of a turbidimetric method, in which a photometer was used to determine the turbidity. It was assumed as a criterion of solubility that as the saturation point is exceeded, the excess oil is emulsified and the solutions therefore become turbid.

To determine the solubility of a hydrocarbon in a soap solution at one given concentration the following procedure was adopted. The soap solution was weighed into a glass ampule, a weighed amount of oil was added, and the ampule was sealed. At a constant soap concentration a series of ampules was prepared, each successive ampule containing an increasing amount of oil. The samples were shaken vigorously for at least forty-eight hours in order to attain equilibrium. At the end of this time the turbidity of the solutions was measured by the use of a photometer. For those samples in which the amount of added oil was below the saturation value the turbidity was equal to that of the original soap solution. As soon as an excess of oil was present, the solutions exhibited a rapid increase of turbidity, caused by the appearance of emulsion droplets, with increase in the amount of oil. A plot was made of the turbidity against the amount of oil added, and the sharp break in the curve was considered as the saturation point. Figure 1 shows the type of curve obtained upon addition of benzene to a 6.89 percent solution of potassium laurate.

The turbidimetric method as described here works well if there is a large difference between the refractive index of the oil and that of the soap solution. It becomes less and less sensitive as the refractive index of the oil approaches that of the

TABLE I. Solubilization in potassium laurate.

$\left(\frac{\text{Grams soap}}{\text{100 g solution}}\times 100\right)$ Percent K-laurate	Moles K-laurate / 1000 g solution	Grams oil / 100 g soap solution
	Benzene	
H_2O	—	0.185
0.545	0.0228	0.187
0.769	0.0322	0.217
2.02	0.0846	0.472
3.34	0.1400	0.760
5.08	0.213	1.170
6.89	0.289	1.64
9.65	0.405	2.50
11.93	0.501	3.27
15.00	0.629	4.38
16.64	0.697	5.01
19.95	0.836	6.41
	Ethylbenzene	
2.11	0.088	0.212
5.16	0.216	0.710
9.70	0.406	1.67
14.85	0.624	2.97
20.65	0.869	4.68
	n-Heptane	
2.11	0.088	0.068
5.02	0.211	0.255
9.55	0.400	0.67
15.00	0.630	1.30
19.25	0.810	1.88
24.25	1.020	2.57

[9] W. D. Harkins, R. W. Mattoon, M. L. Corrin, J. Colloid Sci. **1**, 105 (1946); R. W. Mattoon, R. S. Stearns, W. D. Harkins, J. Chem. Physics, **15**, 209 (1947).

[10] M. L. Corrin, W. D. Harkins, and S. H. Herzfeld (private communication).

soap solution. When the refractive index of the oil equals that of the soap solution, the solution no longer appears cloudy when excess oil is present, since there is no light scattering by the emulsion drops present. For some of the higher hydrocarbons the emulsions formed are not at all stable, and in these cases also this method is of little value, since the turbidity changes during the period in which the measurements are being made.

For the solubilization measurements made with solid colored compounds the procedure was to shake the soap solution with an excess of the solid until equilibrium was reached, and then to measure the amount of solubilization by measuring the depth of color of the solution by standard spectrophotometric methods. The solubilization measurements were made at room temperature, 25±3°C. This variation of temperature introduced no appreciable error into the solubilization determinations.

TABLE II. Solubilization in potassium myristate.

Percent K-myristate ($\frac{\text{Grams soap}}{\text{100 g solution}} \times 100$)	Moles K-myristate / 1000 g solution	Grams oil / 100 g soap solution
	n-Heptane	
H_2O	—	0.007
0.506	0.019	0.039
1.043	0.0392	0.058
2.03	0.0763	0.192
3.025	0.114	0.29
5.04	0.189	0.53
7.47	0.280	0.886
8.69	0.326	1.05
10.00	0.376	1.275
14.9	0.560	2.10
20.15	0.757	2.95
	Benzene	
H_2O	—	0.186
0.50	0.0189	0.275
1.01	0.0379	0.42
2.01	0.0755	0.70
3.05	0.115	1.05
4.02	0.151	1.36
5.03	0.189	1.75
7.27	0.273	2.7
10.05	0.378	4.04
15.03	0.566	6.70
	Ethylbenzene	
2.6	0.097	0.57
5.0	0.188	1.32
7.5	0.282	2.15
10.0	0.376	3.06
12.5	0.470	4.10
15.0	0.563	5.10
	n-Propylbenzene	
H_2O	—	0.012
1.01	0.038	0.15
5.00	0.188	1.06
10.15	0.381	2.75
15.08	0.567	4.30
	Iso-propylbenzene	
H_2O	—	0.017
1.025	0.0385	0.20
3.01	0.113	0.75
4.98	0.187	1.40
7.46	0.280	2.37
9.95	0.373	3.30
14.98	0.563	5.10
	n-Decanol	
H_2O	—	0.005
0.985	0.037	0.195
2.00	0.075	0.438
3.485	0.131	0.85
5.25	0.197	1.35
9.85	0.370	2.75
14.85	0.556	4.30

III. SOLUBILITY BELOW THE CRITICAL CONCENTRATION

It has been assumed that below the critical concentration micelles do not exist. If solu-

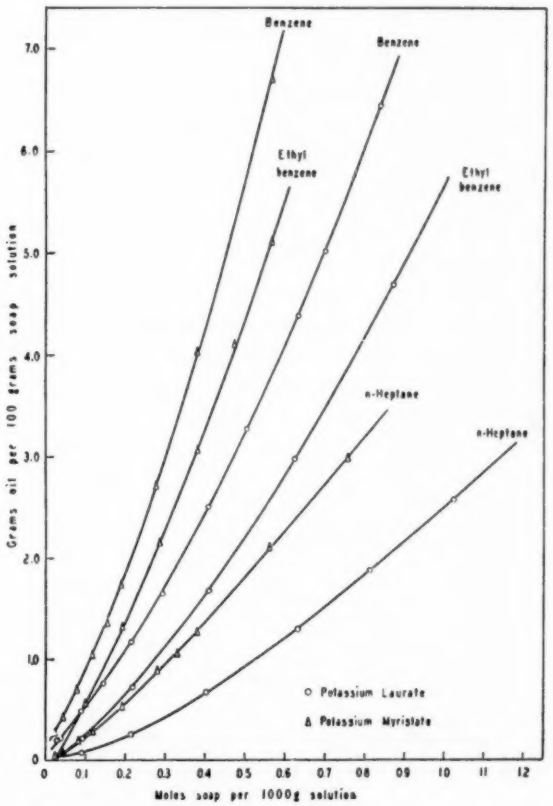

FIG. 3. Solubilization of *n*-heptane, benzene, and ethylbenzene in aqueous solutions of potassium laurate and potassium myristate. The magnitude of the solubilization is much greater in the 14 carbon atom than in the 12 carbon atom soap.

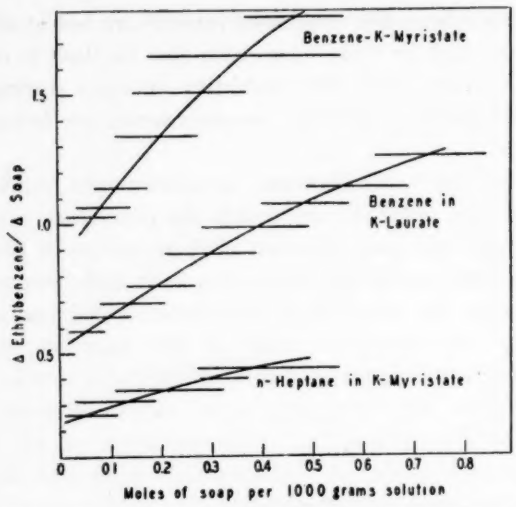

FIG. 4. Chord plots from the data of Fig. 3 illustrate the increment in the number of moles of solubilized oil per unit increment in the number of moles of soap as a function of soap concentration.

bilization is the result of incorporation in or adsorption on the micelle, then in the absence of micelles there should be no solubilization.

The solubility of 2-nitrodiphenylamine, a yellow solid compound, was determined in dilute solutions of potassium laurate. It was found that within the limits of accuracy of our measurements the solubility remained constant until the concentration of soap reached 2.26×10^{-2} mole per liter, after which there was a sharp increase in the solubility (Fig. 2). It may be noted that the dye method of Corrin and Harkins gave 2.3×10^{-2}, and from this excellent agreement it seems that there is no solubilization, above the solubility in water, below the critical concentration for those soaps which exhibit a sharp break at this point.

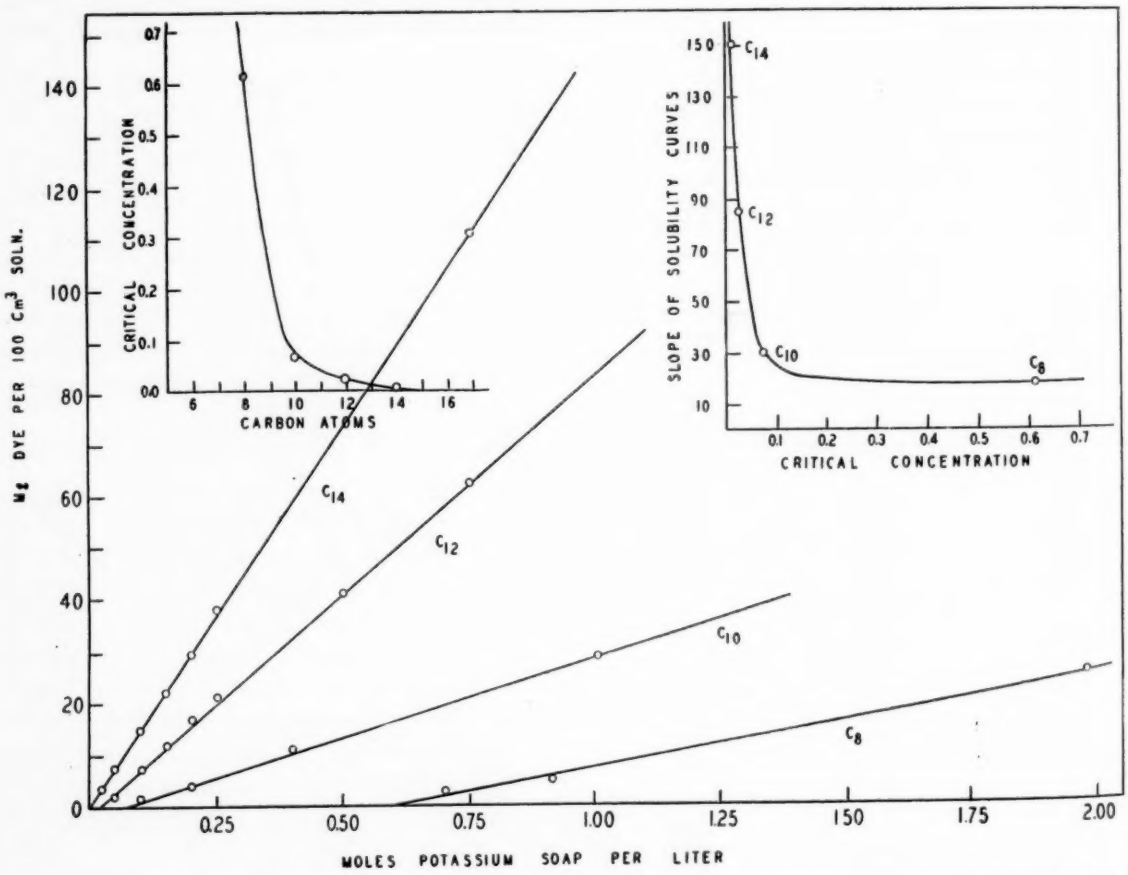

FIG. 5. Weight of dye (1-*o*-tolylazo-β-naphthol) solubilized as a function of soap concentration and chain length from the data of McBain and Johnson [J. Am. Chem. Soc. **66**, 9 (1944)]. The intercepts of the straight lines with the *x* axis should give the critical micelle concentrations of the soaps which are the potassium salts of the normal long chain acids. The critical concentration given for potassium octoate is 0.6, whereas the correct value is 0.4 molar. The other critical concentrations are more accurate. McBain and Johnson plotted moles of dye per mole of soap as a function of soap concentration, which obscured the linear relation, the value of the critical concentration, and the other relations shown here.

IV. SOLUBILIZATION IN SOLUTIONS OF POTASSIUM LAURATE AND POTASSIUM MYRISTATE AS A FUNCTION OF THE SOAP CONCENTRATION

The extent of solubilization of benzene, ethylbenzene, and *n*-heptane was determined in solutions of potassium laurate (Table I), and that of benzene, ethylbenzene, *n*-heptane, *n*-propylbenzene, isopropylbenzene, and *n*-decanol in solutions of potassium myristate (Table II). In Fig. 3 the extent of solubilization at equilibrium, expressed as grams of oil per 100 grams of solution, for benzene, ethylbenzene, and *n*-heptane in solutions of potassium laurate and potassium myristate is plotted as a function of the soap concentration expressed as moles of soap per 1000 grams of solution. The curves of Fig. 3 show that the solubility is not a linear function of soap concentration and that the solubility of a given oil is greater in the myristate than in the laurate. These data are of the greatest value when employed to find the variation in the number of moles of oil solubilized per mole of soap.

However, a false impression may be obtained from the ratio of the total number of moles of oil to soap present. In order to find correctly the variation in the moles of oil solubilized per moles of soap, i.e., the solubilizing power of the soap, the derivative of the curves in Fig. 3 should be found. This may be done by the chord-area method as illustrated in Fig. 4 for benzene in potassium laurate, and heptane and benzene in potassium myristate. This method of plotting the data shows clearly that the solubilizing power of the soap solution per unit amount of soap increases as the soap concentration increases.

An exception appears in the results of Kolthoff[11] and in the earlier much more extensive results of McBain and collaborators.[5] These show (Fig. 5) that "insoluble" dyes exhibit, in the range investigated by them, a linear increase in the amount solubilized with increase of soap concentration. That this is true was not shown by McBain and collaborators, since their method of plotting obscured this relation. They plotted molar ratios, and this has a deceptive effect, as considered in the paragraphs which follow. In order to determine whether the linear relation is valid for "insoluble" substances, the writers investigated the solubilization of 2,4-dinitrodiphenylamine in solutions of potassium laurate (Fig. 6). The linear relation exhibited here and in the work of McBain seems to be in disagreement with that of Fig. 2 for 2-nitro-diphenylamine, which is highly non-linear just above the critical concentration (2.34×10^{-2} molar) of the soap.

However, there is no real disagreement, since the amine exhibits a solubility of 1.72×10^{-5} molar in water, whereas the dye used by McBain is very much less soluble. When plotted in the simple way chosen by us, McBain's data show

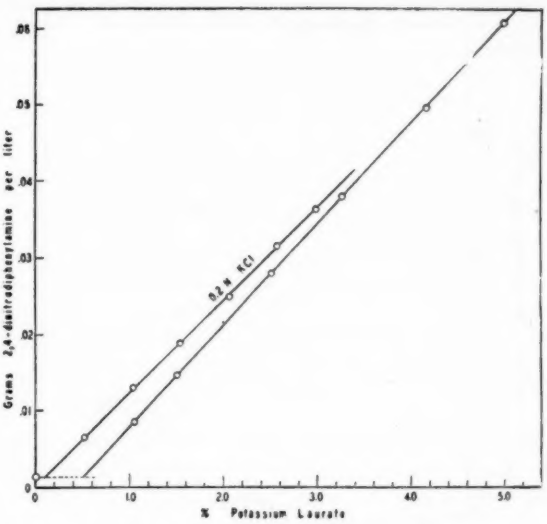

FIG. 6. Solubilization of 2,4-dinitrodiphenylamine in aqueous solutions of potassium laurate. The upper line shows the increase due to 0.2 normal salt.

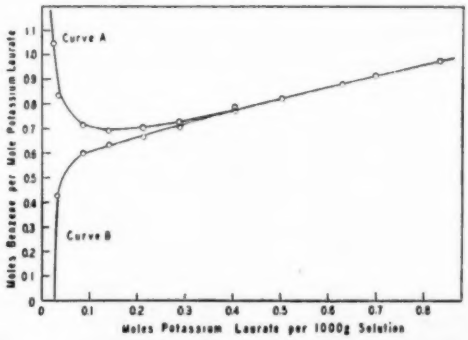

FIG. 7. In curve *A* the solubility data for benzene solubilized in potassium laurate are plotted as the moles of oil per mole of soap. This curve illustrates the incorrect way of plotting solubility data used by some authors and leading to incorrect conclusions. In curve *B* the solubility of benzene in water has been subtracted from the total solubility.

[11] I. M. Kolthoff and W. F. Johnson, J. Phys. Chem. **50**, 440 (1946).

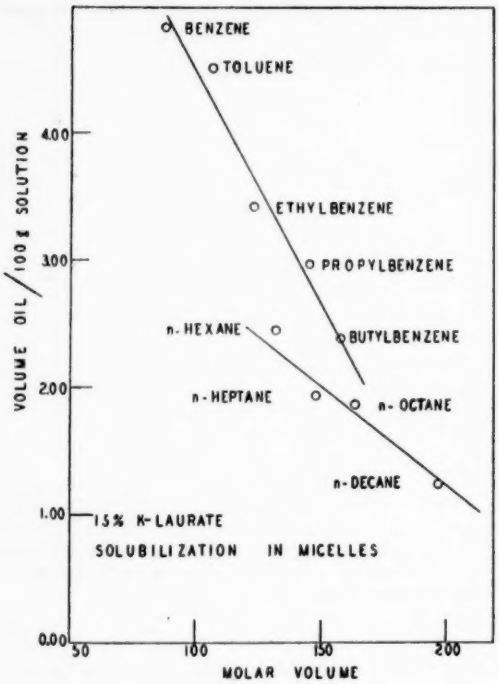

FIG. 8. Effect of molar volume on the solubilization of hydrocarbons in a 15.0 percent solution of potassium laurate at 25°C. Obviously the relations would be different if vapors of the liquids were solubilized at constant pressure.

that the constant rate of increase of solubiiization with soap concentration:

1. Decreases rapidly with decrease in the number of carbon atoms in the soap molecule;
2. Decreases rapidly with increase of critical concentration, extremely rapidly as the number of carbon atoms decreases from 14 to 12 to 10, and very much more slowly in the further decrease to 8.

The general relations found by the writers are the same, with the exception that the straight lines are changed to curves when organic substances much more soluble in water are used.

In Fig. 7, Curve *A*,[12] the solubility data for benzene in potassium laurate are plotted as moles of oil solubilized per mole of soap against the soap concentration. It will be noted that this curve exhibits a minimum. This minimum is a mathematical necessity, since the curve must go to infinity at zero soap concentration, and its position and depth depend upon the solubility of the oil in water. The solubility of benzene in water is rather large (0.186 grams per 100 g water). If it is assumed that the solubility of the benzene in water is not affected by the amount of soap present and if this is subtracted from the total, the "solubilization in the micelles" thus obtained exhibits no minimum. If the ratio of this value to the total number of moles of soap is plotted, Curve *B*, Fig. 7, is obtained. Both curves (*A* and *B*) coincide at higher soap concentrations when the total solubility is so large that the solubility in water is no longer an important part of the whole.

There is one more deceptive feature in plotting solubilization as the ratio of total moles of oil to total moles of soap. It has been shown that below the critical concentration there is no solubilization, and the amount of soap present in the form of micelles, supposedly responsible for solubilization above the critical concentration, is presumably zero. The chord-area method of finding the solubilizing power eliminates the ambiguity resulting from the mole ratio method of describing solubility data.

A theory of the increase in the solubilizing power of the soap solutions with concentration and the increase in solubilization at constant concentration with increase in the chain length of the soap will be discussed in a later paper.

TABLE III. The effect of molar volume on solubilization.

Oil	Molar volume	Grams oil / 100 g soap solution	Solubility, oil in water	Volume of oil in micelles per 100 g soap solution
		15% K-Laurate (0.630M)		
n-Hexane	131.5	1.60	0.014	2.44
n-Heptane	147.8	1.31	0.005	1.93
n-Octane	163.1	1.30	0.002	1.85
n-Decane	196.1	0.89	—	1.22
Benzene	88.5	4.38	0.186	4.82
Toluene	107.0	3.93	0.050	4.50
Ethylbenzene	123.0	2.95	0.015	3.40
n-Propylbenzene	140.5	2.54	0.010	2.95
n-Butylbenzene	157.0	2.03	0.005	2.37
		15% K-Myristate (0.564M)		
Benzene	88.5	6.70	0.186	7.46
Toluene	107.0	6.00	0.050	6.90
Ethylbenzene	123.0	5.10	0.015	5.90
n-Propylbenzene	140.5	4.30	0.010	5.00
(Iso-propylbenzene)	(140.4)	(5.10)	(0.017)	(5.92)

[12] W. Heller and H. B. Klevens in a letter on solubilization, J. Chem. Phys. **14**, 567 (1946), state that the minimum in this type of curve gives the critical concentration of the soap, "providing thereby a new method for determining c_{cr} from solubilization measurements." However the minimum for Curve *A* is at 0.14 molar potassium laurate, whereas the value of the critical concentration of this soap as given by Corrin and Harkins and cited by them is 0.023 molar. Thus the minimum does not give the critical concentration. However, it approaches the critical concentration as the solubility of the solubilized substance decreases. However, a direct plot of solubility gives the critical concentration in a much better way.

V. EFFECT OF MOLAR VOLUME AND POLARITY OF AN OIL ON ITS SOLUBILIZATION

The solubilization was determined for compounds in the series benzene, toluene, ethylbenzene, *n*-propylbenzene, and butylbenzene; also for *n*-hexane, *n*-heptane, *n*-octane, and *n*-decane in 15.00 percent potassium laurate solutions and, in addition, for benzene, toluene, ethylbenzene, *n*-propylbenzene, and iso-propylbenzene in 15.00 percent potassium myristate solutions. In Table III the solubilization data and the molar volumes are tabulated. A plot of these data (Fig. 8) shows that the solubility in the micelles is to a first approximation an inverse function of the molar volume for a homologous series. Undoubtedly, the polarity and shape of the molecule, as well as its volume, determine the extent of solubilization in the micelles. The effect of polarity is well illustrated by comparing the solubility of *n*-decanol and *n*-decane. The former is soluble to the extent of 3.31 cc per 100 grams of 10 percent potassium myristate solution, and the latter only to 1.05 cc. That the solubility is to a first approximation inversely proportional to the molar volume is what is to be expected if solubilization is the incorporation of the oil in the micelles. The effect of a double bond on solubilization is illustrated by comparing the solubility of ethylbenzene and styrene (Fig. 9).

VI. DENSITY OF POTASSIUM LAURATE SOLUTIONS CONTAINING SOLUBILIZED ETHYLBENZENE

In an endeavor to obtain knowledge which may be of use in determining the mechanism of solubilization of hydrocarbons by soap solutions, the density of a series of soap solutions with increasing amounts of solubilized ethylbenzene was determined.[12b]

The solutions of 15.0 percent potassium laurate which contained solubilized ethylbenzene were made up on a weight basis. The samples were shaken for forty-eight hours at room temperature to insure complete solubilization. The densities of the original soap solution and the soap solutions plus solubilized ethylbenzene were determined at a temperature of 25±0.005°C in a pycnometer of about 25 cm³ capacity having a capillary neck 2 mm in diameter. The height of the liquid in the capillary was read to ±0.01 mm by means of a cathetometer.

[12b] The density relations and apparent specific volumes of *n*-heptane and triptane are given by W. D. Harkins, R. W. Mattoon, and M. L. Corrin, J. Colloid Sci. **1**, 110 (1946).

TABLE IV. Density of 15.000% potassium laurate solutions containing solubilized ethylbenzene.

Grams ethylbenzene / 100 g soap solution	Density 25±.01°C
0.0000	1.01062
0.6755	1.00949
1.0448	1.00885
1.5119	1.00802
2.3269	1.00676
2.8615	1.00578

The pycnometer was calibrated with boiled redistilled water. All weighings were made to ±0.005 mg with calibrated weights and the corrected weights reduced to *vacuo*. The variation in the volume of the pycnometer was about 0.007 cm³ per 1 mm on the neck of the capillary. A precision of one part in 10^5 was obtained in the density measurements. The concentrations of ethylbenzene and the densities of the solutions are given in Table IV, and the data are plotted in Fig. 10. The experimental points are best represented by a straight line, the "least square"

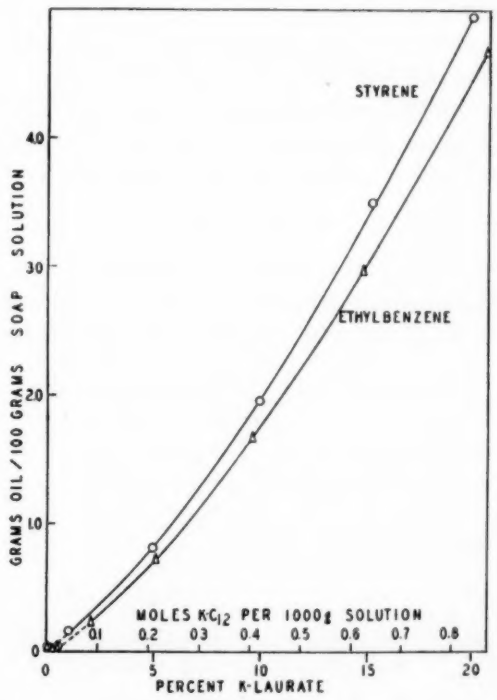

FIG. 9. Increase in solubilization of an oil by a double bond.

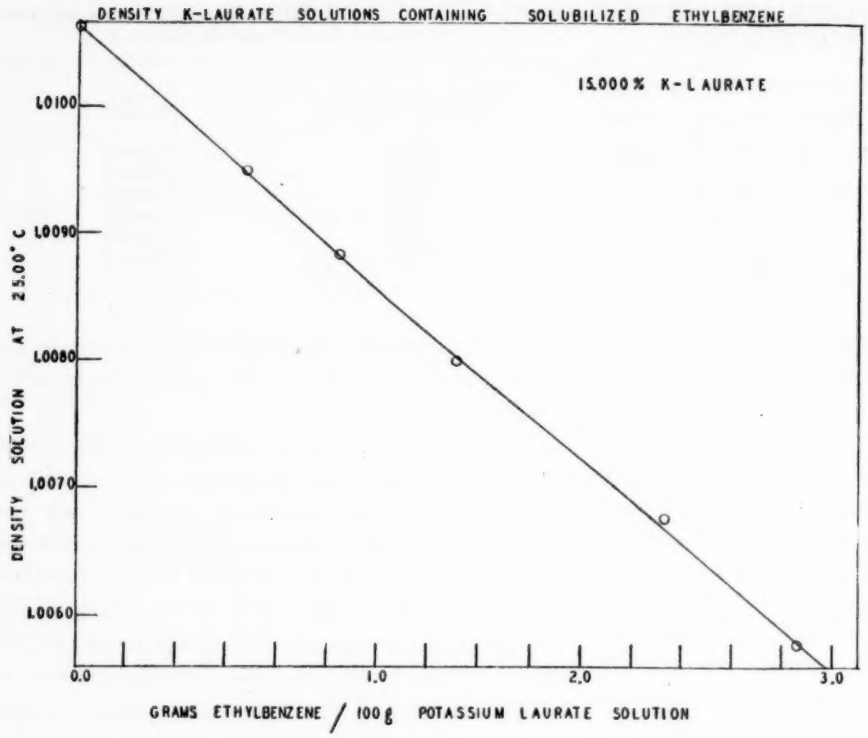

FIG. 10. Density of a 15.000 percent potassium laurate solution as a function of the amount of solubilized ethylbenzene.

equation for which is:

$$\rho = 1.0106128 - 1.68124495 \times 10^{-3} C,$$

where ρ is the density of the solution and C is the concentration of ethylbenzene expressed as grams per 100 grams soap solution.

From the above equation the apparent volumes and apparent densities of the solubilized ethylbenzene have been calculated from the formula:

$$\varphi = (V_T - v_S/C)$$

where φ is the apparent specific volume of solubilized ethylbenzene, $V_T = 1/\rho$ is the specific volume of the soap solution plus the solubilized benzene, v_S is the specific volume of the soap solution, and C is the concentration of ethylbenzene expressed as grams per 100 grams soap solution. The data are tabulated in Table V and plotted in Fig. 11.

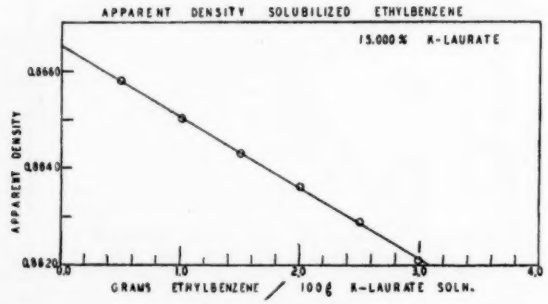

FIG. 11. Apparent density of ethylbenzene solubilized in a 15.000 percent potassium laurate solution.

The solubility of ethylbenzene in 15.000 percent potassium laurate solution is 3.00 grams oil/100 grams soap solution as determined by turbidity measurements. The bulk density of ethylbenzene was determined by us to be 0.86205 g/cm³ at 25.00°C. From Fig. 11 it will be noted that at saturation the apparent density of the solubilized ethylbenzene equals the bulk density within experimental error.

The significance of the decrease in the apparent density of the solubilized ethylbenzene as satura-

TABLE V. Apparent volumes and densities of ethylbenzene solubilized in 15.000% potassium laurate solutions.

Grams ethylbenzene / 100 g soap solution	Apparent volume	Apparent density
0.500	1.15507 cm³/g	0.8657 g/cm³
1.000	1.15603	0.8650
1.500	1.15700	0.8643
2.000	1.15796	0.8636
2.500	1.15893	0.8629
3.000	1.15990	0.8621

tion is approached is difficult to interpret, even when the assumptions inherent in all calculations of apparent values of the density are taken into account.

TABLE VI. Solubilization of ethylbenzene in soap+salt solutions.

Moles salt / 1000 g water	Grams ethylbenzene / 100 g soap solution
A. 10% K-laurate+KCl (0.42 m KC_{12})	
0.00	1.70
0.025	1.81
0.050	1.89
0.075	1.96
0.100	2.02
0.150	2.14
0.200	2.24
0.300	2.43
0.500	2.83
B. 2.6% K-myristate+KCl (0.1 m KC_{14})	
0.00	0.570
0.0187	0.656
0.0396	0.723
0.0810	0.840
0.1465	0.930
0.2445	1.08
0.347	1.18
0.638	1.42
1.503	1.79
2.00	1.87
C. 2.6% K-myristate+NaCl (0.1 m KC_{14})	
0.000	0.570
0.00557	0.610
0.0204	0.706
0.0319	0.776
0.0479	0.812
0.0705	0.909
0.0989	1.005
D. 2.6% K-myristate+K_2SO_4 (0.1 m KC_{14})	
0.0000	0.57
0.0577	0.81
0.1622	0.96
0.3645	1.19
0.5735	1.35
E. 2.6% K-myristate+$K_4Fe(CN)_6 \cdot 3H_2O$ (0.1 m KC_{14})	
0.0000	0.57
0.02875	0.70
0.1030	0.94
0.2028	1.08
0.2868	1.10
0.4988	1.10
F. 2.6% K-myristate+K_3PO_4 (0.1 m KC_{14})	
0.4783	1.12
G. 2.6% K-myristate+1.383 molal salt (0.1 m KC_{14})	
No salt	0.57
KF $2H_2O$	1.43
KCl	1.76
KBr	1.37
KI	1.31
KSCN	1.52

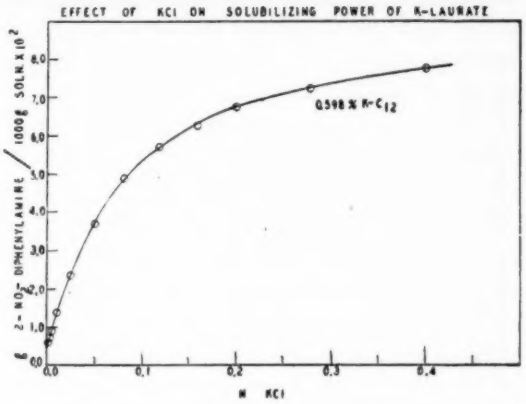

FIG. 12. Effect of added salt on the solubilization of 2-nitrodiphenylamine in a 0.598 percent solution of potassium laurate.

VII. THE EFFECT OF SALTS ON SOLUBILIZATION

The addition of salts, such as potassium chloride, to soap solutions greatly increases their solubilizing power. The effect of potassium chloride on the solubilizing power of a dilute potassium laurate solution was investigated by the use of 2-nitro-diphenylamine. At a constant soap concentration of 0.59 percent potassium

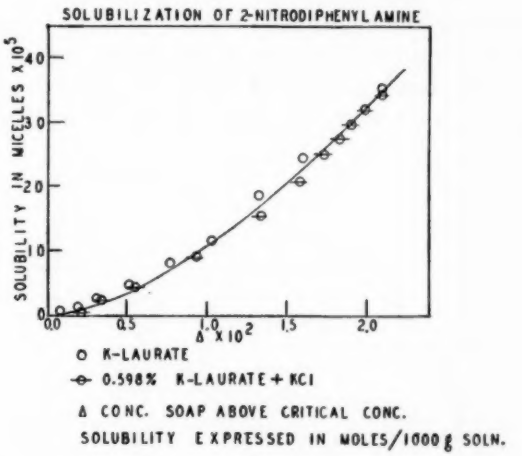
SOLUBILIZATION OF 2-NITRODIPHENYL AMINE
SOLUBILITY IN MICELLES X10^5
Δ X10^2
O K-LAURATE
0.598% K-LAURATE + KCl
Δ CONC. SOAP ABOVE CRITICAL CONC.
SOLUBILITY EXPRESSED IN MOLES/1000 g SOLN.

FIG. 13. In this figure Δ is the increase between the critical concentration and the total soap concentration. At a constant soap concentration when increasing amounts of salts are added, the value of Δ is increased, since the critical concentration is lowered. The solubility of 2-nitrodiphenylamine is expressed in moles solubilized in the micelles per 1000 g solution. The open circles (○) represent the solubilization in potassium laurate with increasing soap concentration. The circles with lines (⊖) represent the solubilization in a 0.598 percent potassium laurate solution containing increasing amounts of salts.

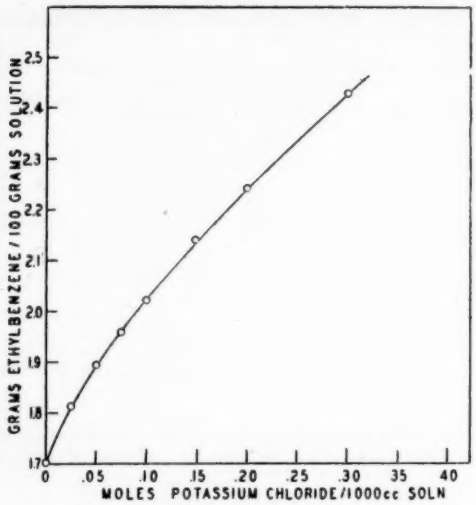

FIG. 14. Increase in the solubilization of ethylbenzene in a 10 percent solution of potassium laurate when KCl is added.

laurate, a concentration very slightly above the critical concentration, the solubility of 2-nitrodiphenylamine was determined as a function of the amount of potassium chloride present. The very large increase of solubility caused by the added salt, particularly at such a low soap concentration as that used here, is well illustrated by Fig. 12 as well as in Fig. 6.

The lowering of the critical concentration of potassium laurate in the presence of added salts was determined.[13] It is very interesting to combine the data on the lowering of the critical concentration with the data on the increase in solubilizing power of potassium laurate in the presence of potassium chloride. The assumptions are made that no "solubilization" takes place below the critical concentration, that above the critical concentration there is always an amount of "free" molecular soap present, the concentration of which is given by the critical concentration, and that the amount of solubilization in the micelles is the total amount of material solubilized minus the solubility in water. At constant soap concentration the addition of increasing amounts of salt lowers the critical concentration, thus increasing the amount of micellar soap. This difference between the total soap concentration and the critical concentration is designated as Δ. In Fig. 13 are plotted values of

TABLE VII. Solubilization of ethylbenzene in 0.1 molal solutions.

Mole fraction K-myristate	Grams oil / 100 g soap solution
A. Of K-laurate and K-myristate	
0.000	0.23
0.260	0.31
0.500	0.38
0.733	0.48
1.00	0.57
B. Of K-caprylate and K-myristate	
0.000	0.025
0.101	0.10
0.246	0.22
0.500	0.39
0.740	0.48
1.000	0.57

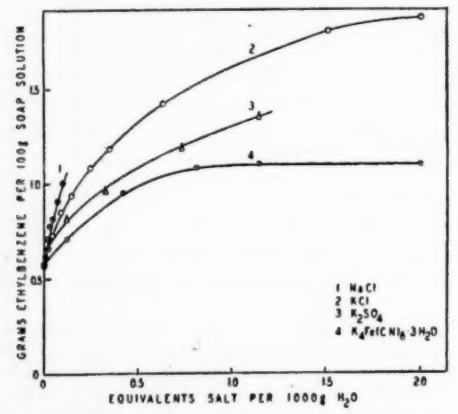

FIG. 15. Effect of various salts on the solubilization of ethylbenzene in a 2.6 percent (0.1 m) potassium myristate solution.

[13] M. L. Corrin and W. D. Harkins, J. Am. Chem. Soc. 69, 683 (1947).

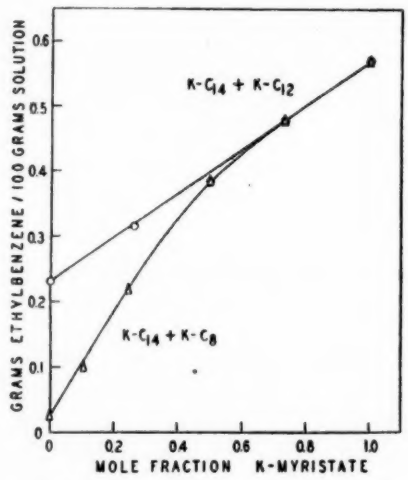

FIG. 16. Effect of mixtures of soaps on the solubilization of ethylbenzene.

the solubility of 2-nitrodiphenylamine in the micelles as a function of Δ, both for solutions of increasing concentrations of potassium laurate and for solutions of a constant soap concentration but increasing salt concentrations. Within the accuracy of the experiments it is seen that the solubilization is determined by the amount of micellar soap at the low soap concentration employed. Since there is a pronounced curvature in the plot presented in Fig. 13 the amount of solubilization must be a function of the state of aggregation of the micelles as well as the amount of material in the micellar form.

At higher soap concentrations the effect of added salts on solubilization is not as large as that observed near the critical point. The effect of potassium chloride on the solubilization of ethylbenzene in 10.00 percent potassium laurate solutions and the effect of a number of salts on the solubilization of ethylbenzene in 2.60 percent solution of potassium myristate were investigated. The solubilization data are presented in Table VI and plotted in Figs. 14 and 15. At these higher soap concentrations the increase in solubility in the presence of added salts cannot be accounted for by the decrease in critical concentration with the resulting increase in micellar soap. The addition of sodium chloride to a potassium soap changes the nature of the soap, and therefore it is difficult to correlate the effect of this salt with that of potassium salts.

While the change in the critical concentration has been shown to be dependent only on the total equivalents of the cation in the case of anionic soaps,[13] the data given here show that the change of solubility on addition of salts is dependent on both the nature of the cation and anion. Thus, KCl is more effective in increasing solubilization than is K_2SO_4, which in turn is more effective than $K_4Fe(CN)_6 \cdot 3H_2O$. That this effect is in some way connected with the size of the anion is shown by the fact that in the series of salts, KCl, KBr, and KI, the KCl has the greatest effect and KI the least effect in increasing solubilization. Unfortunately, KF and KSCN do not fall in the proper order as seen from the data in Table VI. These results are similar to those reported by McBain.[4]

VIII. SOLUBILIZATION IN MIXTURES OF SOAPS

Data for solubilization of ethylbenzene in mixtures of potassium laurate and potassium myristate and in mixtures of potassium caprylate and potassium myristate are given in Table VII and represented by Fig. 16. It is interesting to note that in mixtures of potassium laurate and myristate the solubility is a linear function of the mole fraction of soap present. For mixtures of potassium caprylate and myristate this linear relation no longer holds, which is presumably because of the fact that the critical point of the potassium caprylate is high, and this results in its action as a salt in its effect on the potassium myristate.

The Magnetic Susceptibilities of the Vapors of Benzene and Carbon Tetrachloride

R. K. REBER* AND G. F. BOEKER
*The College of the City of New York,** New York, New York*

(Received October 30, 1946)

An apparatus has been constructed for measuring at elevated temperatures and at independently controlled pressures the magnetic susceptibility of vapors of substances which are normally in the liquid or solid state. Besides greatly increasing the range of substances for which such measurements can be made, the measurement at elevated temperatures is believed to permit considerably greater accuracy than has been attained previously in the susceptibility measurements on vapors. Determinations of the susceptibilities of the vapors of benzene and carbon tetrachloride have been carried out at 110°C. The extreme limits of uncertainty in the results are estimated to be 3 percent. The values found for the mass susceptibilities of the vapors are in very close agreement with values which have been obtained for the liquids.

INTRODUCTION

INVESTIGATIONS of the magnetic susceptibility of vapors and gases have been concerned mainly with substances which are gases at ordinary temperatures. The first and most extensive measurements of magnetic susceptibilities of substances which are liquids at ordinary temperature were made by Vaidyanathan.[1,2] Using a Curie balance-type of apparatus, Vaidyanathan investigated the vapors of twelve organic compounds whose boiling points range from 30° to 100°C. Nine of these substances were reinvestigated by the Faraday test-body method. The values obtained by the two methods differed by an average of about 9 percent. For most of the substances investigated the measured values of the susceptibilities of the vapors differed from the best values for the liquids by no more than the estimated experimental error. For benzene and carbon disulfide, however, the differences were about 35 percent and were considered to be too large to be accounted for by experimental error.

Sivaramakrishman[3] measured the susceptibility of benzene vapor by the Faraday method and obtained a value intermediate between the two values of Vaidyanathan. Rao and Varadachari[4] pointed out that both Vaidyanathan and Sivaramakrishman had assumed the validity of Boyle's law for the vapors. Using corrected vapor densities they found much better agreement between vapor and liquid benzene, but stated that for carbon disulphide the susceptibility of the vapor was still 30 percent greater than for the liquid.

Yanus and Shur[5,6] investigated the vapors of benzene and carbon disulfide by a method that does not involve the use of a test body. They concluded that the susceptibilities of the vapors of both substances are practically the same as those of the liquids. A like result was obtained for bromine vapor.[7]

Except for Yanus and Shur's investigation of bromine vapor, which was carried out at 60°C, all the measurements of the magnetic susceptibilities of vapors of substances which are normally liquids have been carried out at room temperature. Because of the low vapor densities at room temperature and of the difficulty of accurately determining the density, and because of the difficulty of avoiding errors caused by surface adsorption on the test body, it is doubtful that the accuracy and reliability of these measurements are comparable with those of the most accurate measurements on gases.

The apparatus used in this investigation was designed to make measurements of the susceptibility of substances expected to be paramagnetic in the vapor state, and of substances which are

* Now with the Navy Bureau of Ships, Washington, D. C.

** This investigation was carried out in the laboratories of Columbia University.

[1] V. I. Vaidyanathan, Phys. Rev. **30**, 512 (1927).

[2] V. I. Vaidyanathan, Ind. J. Phys. **2**, 1935 (1928).

[3] G. Sivaramakrishman, J. Annamalai Univ. **3**, 48 (1934).

[4] S. R. Rao and P. S. Varadachari, Nature **134**, 812 (1934).

[5] R. I. Yanus and J. Shur, Nature **134**, 101 (1934).

[6] J. Shur, Physik. Zeits. Sowjetunion **11**, 194 (1937).

[7] J. Shur and R. I. Yanus, Physik. Zeits. Sowjetunion **7**, 501 (1935).

known to be highly associated in the liquid state. Most of these substances have a relatively high boiling point. Both to increase the range of substances which could be tested and to obtain the highest accuracy, it was considered essential to have an apparatus with which measurements could be carried out over a considerable range of temperatures and at independently controlled pressures.

Because of the war it was necessary to discontinue the experiments after making measurements on benzene and carbon tetrachloride. These substances were chosen for the initial measurements because they were considered most suitable for the thorough testing of the apparatus. Because the results are believed to be more accurate than any previously reported for vapors, it was felt that they should be published.

APPARATUS AND EXPERIMENTAL PROCEDURE

The magnetic measurements were made by the Faraday test-body method. This consists of the comparison of the torques produced by a non-homogeneous magnetic field on a test body when suspended in the gas or vapor to be measured, and when suspended in a gas of known susceptibility. In the present investigation the method of obtaining the homogeneous field and the design of the test body were patterned largely on those of Rao and Sivaramakrishman.[8] Figure 1 shows the apparatus used.

The non-homogeneous field is produced by the arrangement shown in Fig. 1(b). The pole pieces tapered from a height of 10 cm and a width of 6 cm, to a height of 8 cm and a width of 4 cm. The air gap was 5 cm in width. Vertical cylindrical iron bars having a diameter of 2 cm were placed symmetrically at the sides to increase the inhomogeneity of the field. This arrangement produced a field which was symmetrical about two vertical planes, one parallel and the other perpendicular to the direction of the field at the center of the gap. When the magnet was energized the field strength at the center of the gap was approximately 3000 oersteds.

The test body consisted of four thin glass tubes

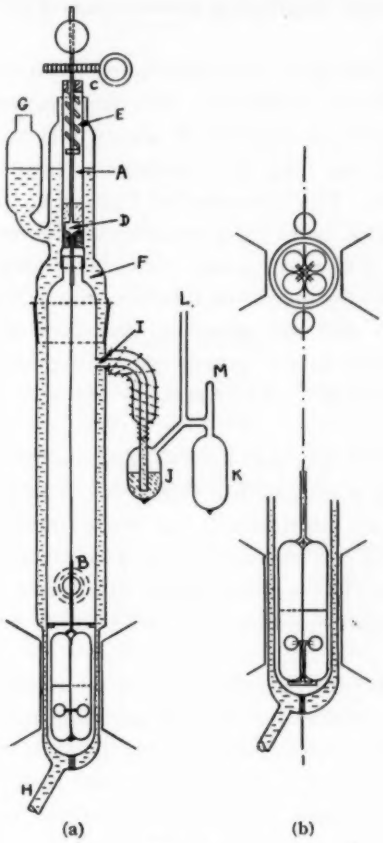

FIG. 1.

12 mm in diameter, sealed together at the top as shown in Fig. 1(b). Two of the tubes were 8 cm long and were located on opposite sides of the central axis. They were closed and evacuated. Each of the other pair of tubes was of half-length and was open at the bottom. This design, which differs essentially from that of Rao and Sivaramakrishman only in that the latter used full-length open tubes, was intended to minimize errors resulting from surface adsorption. For, when oriented in the field as shown in the figure, the surface area exposed to the vapor at a given field strength and at corresponding distances from the symmetric planes was approximately the same for the open as for the closed tubes, the former having a double surface. The weight of the test body was approximately 8 grams.

In order to obtain an approximate magnetic balance when the test body was suspended in a vacuum, a small glass ball was placed below each of the open tubes. They were held in

[8] S. R. Rao and G. Sivaramakrishman, Proc. Phys. Soc. London **46**, 318 (1934).

position by small glass rods attached to a central stem.

The test body was suspended from rod (*A*) of Fig. 1(a) by means of a 50 cm phosphor bronze wire having a diameter of about 0.03 mm. A null method was used for comparing torques on the test body. This consisted of balancing the torque on the test body by a rotation of the rod (*A*) by means of a worm screw. Angular positions were observed by means of mirrors, one at the top of rod (*A*) and the other on the stem of the test body. The latter mirror was observed through two windows (*B*) separated by an evacuated space.

The rod (*A*) was held in position by a bearing (*C*) and a ground joint (*D*). A continuous pressure was maintained on the ground seat by means of a spring acting on a collar attached to the rod. The ground joint was made gas tight by a small amount of Wood's metal above the joint.

A constant temperature was maintained by the circulation of a liquid from a thermostatically controlled temperature bath through the chamber (*F*) which surrounds the tube containing the vapor. There was no mechanical connection between the apparatus and the outer circulating system. The liquid entered at (*G*) from an overflow of the bath and flowed out at (*H*) into a pump which returned the liquid to the bath. Except for the part between the pole pieces, the apparatus was well insulated.

The highest temperature at which the apparatus could be operated was limited by the available circulating fluids. All the experiments here reported were made at 110°C using ethylene glycol as the circulating fluid. However, in preliminary experiments, measurements were made at temperatures up to 270°C using vegetable oil. At high temperatures some instability was experienced because of vapor convection currents. To minimize these currents a thin diaphragm was inserted across the tube immediately above the test body.

The vapor was introduced through the side tube (*I*) which dipped into the liquid reservoir (*J*). A non-uniformly wound heating coil surrounding the tube produced a temperature gradient along the tube, the highest temperature occurring at the top. Vapor was introduced into the system by slowly admitting gas into an outer glass system connected to the reservoir, thus forcing the liquid up the tube until the desired vapor pressure was attained. The vapor pressure characteristic of the temperature of the top of the liquid column was equal to the outer gas pressure less the hydrostatic pressure of the liquid column. Thus the vapor pressure could be easily controlled and its value could be accurately determined. This method of controlling vapor pressures is essentially that of Zahn.[9]

CO_2 was used as the comparison gas. Its susceptibility is relatively large and is probably as accurately known as that of any other diamagnetic gas. Before admitting the gas into the apparatus it was passed through a tube containing heated copper shavings to remove any traces of oxygen and through a tube containing anhydrone to remove water vapor.

Experiment showed that the torque produced on the test body when in a magnetic field was proportional to the pressure. So, to obtain a calibration measurements were made at only two pressures. A lower pressure of 2 cm of mercury was used, as it was found that at pressures below $\frac{1}{2}$ cm of mercury there was appreciable drift in the neutral position, possibly caused by thermal effects.

A reading was made as follows: With no current in the magnet coil, the rod (*A*) was rotated until the test body had the desired position as indicated by the mirror attached to its stem. The magnetic field was then brought up to a fixed value and the rotation of rod (*A*) necessary to restore the position of the test body was noted. The magnet-coil circuit was then opened and another determination of the zero point was made.

This procedure was followed, first with CO_2 at a pressure of about 2 cm, then for the same gas at a pressure of about 70 cm, and then repeated again at the low pressure of about 2 cm. The difference in the rotations necessary to balance the effect of the field at the two pressures was thus determined. Successive trials gave consistent results. The sensitivity was such that a rotation of rod (*A*) of one degree corresponds to a change of volume susceptibility of approximately 2×10^{-10}.

[9] C. T. Zahn, Rev. Sci. Inst. **1**, 299 (1930).

Before introducing the test liquid the apparatus was evacuated and filled with CO_2 through the tube (L). The tube (M) was then broken off and the CO_2 was permitted to flow slowly from (L) out through (M) during the entire time the latter was open to the atmosphere. The test liquid was introduced into the reservoir (K) through (M) and about a third of the liquid was boiled off. It was then solidified by surrounding the reservoir with a low temperature bath. Tube (M) was again resealed.

With the test substance in a solid state the apparatus was evacuated. The low temperature bath was then transferred from reservoir (K) to reservoir (J) and about one-half the liquid was distilled into (J).

Measurements were then made at low and high vapor pressures using the same procedure as was outlined for CO_2 above. To obtain a low vapor pressure of no more than a few cm of mercury the reservoir was surrounded by a cold-water bath.

The benzene and carbon tetrachloride used were the best obtainable product of Eimer and Amend and were redistilled before using.

RESULTS

The measurements with the apparatus gave a direct comparison of volume susceptibilities of the vapors and of CO_2. The results can be translated into a comparison of the mass susceptibilities only if the densities are known. At the highest pressures used the densities of benzene and carbon tetrachloride vapors are expected to be several percent greater than the perfect gas values. For a better approximation the densities were calculated on the basis of Berthelot's law. The results are given in Tables I and II. Five separate determinations were made for each vapor.

TABLE I. Mass susceptibility of benzene vapor at 110°C.

Cm Hg		$-\chi\times10^6$	
Lower pressure	Higher pressure	Boyle's law	Berthelot's law
8.5	33.3	0.700	0.690
8.5	67.5	0.706	0.688
5.0	65.0	0.724	0.697
5.0	65.1	0.722	0.695
4.0	65.8	0.730	0.713
mean		0.716	0.697

TABLE II. Mass susceptibility of carbon tetrachloride vapor at 110°C.

Cm Hg		$-\chi\times10^6$	
Lower pressure	Higher pressure	Boyle's law	Berthelot's law
3.0	59.7	0.441	0.431
4.0	57.4	0.447	0.438
1.6	26.07	0.436	0.432
2.5	66.0	0.437	0.427
7.0	57.0	0.440	0.430
mean		0.440	0.432

DISCUSSION

The following unique features of the apparatus and method used in this investigation are believed to be important for the attainment of the highest accuracy and reliability in measurements on vapors:

(a) By carrying out measurements at 110° it was possible to use much larger vapor densities and at the same time to limit the vapor pressures to a smaller fraction of the saturation pressure than in previous experiments. The result has been to increase the effective sensitivity, to limit the amount of adsorbed vapor on the test body and to minimize its relative importance, and to permit a more accurate estimate of the vapor density.

(b) The design of the test body to give equal exposed surface in each of the four quadrants further minimized the effect of adsorbed vapors.

(c) The large air gap and relatively large separation between the test body and pole pieces made for high stability as evidenced by a negligible change in the calibration constant over a period of several months and by its insensitivity to small adjustments in the horizontal position of the suspension support.

(d) Experiment showed that the rather lengthy procedure which was used in this investigation for making magnetic measurements was essential to obtain consistent results. The usual procedure of observing the change in torque produced by a constant field when vapors or gases are introduced or when the density is varied was used in preliminary tests, but did not give as consistent results, probably because of the small shifts in zero position which were frequently observed when the density was increased or decreased. Similar shifts were observed by Vaidyanathan.[2]

Aside from accidental errors of measurement,

possible sources of error were considered to be adsorption of vapor on the test body, uncertainty in the density of the vapors, and uncertainty in the susceptibility of the comparison CO_2. In view of the measures taken to minimize the effects of adsorbed vapors the error caused by this factor is believed to be negligible. This is supported by the fact that the results appear to be independent of the vapor pressures used.

To check the accuracy of Berthelot's law for determining the vapor density, data for benzene are available from the very careful measurements of Ramsay and Steele.[10] On p. 513 of the article by Ramsay and Steele are summarized the results of measurements of PV/mT for two samples of benzene, each at temperatures of 99.7° and 129°C, and at four pressures between 320 and 680 mm Hg. Here P, V, and T are the observed pressure, volume, and temperature, respectively, and m is the mass of the sample. Calculation of PV/mT by Berthelot's equation at each of the indicated temperatures and pressures gives values which differ from the experimental values in no case by more than 0.2 percent and in most cases by no more than 0.1 percent. Corresponding data are not available for carbon tetrachloride, but for the saturated vapor the density obtained using Berthelot's law at 110°C is about 1.5 percent less than the experimental value given by Young,[11] while for benzene the calculated value is approximately 1 percent too small. Since the vapor pressures used in the present experiment were less than 40 percent of the saturation pressure it is considered that the uncertainty in the densities is not more than 0.2–0.3 percent.

The molar susceptibility of CO_2 was taken to be -20.8×10^{-6}. This value was given by Stoner,[12] who estimated the extreme limits of error to be about 2 percent. Subsequently Rao and Sivaramakrishman[8] obtained a value of $-20.88\pm.08\times10^{-6}$ and Sivaramakrishman[3] reported a value of -20.79×10^{-6}.

Considering all sources of error the extreme limits of uncertainty in the susceptibilities as given by the averages of the last columns of Tables I and II are considered to be about 3 percent.

Table III gives the susceptibilities of the vapors of benzene and carbon tetrachloride and the approximate limits of error which have been reported by various observers. For convenience of comparison all reported values have been converted into gram-mass susceptibilities. The last column gives the values of the susceptibilities of benzene obtained by Rao and Vardichari from the results of Vaidyanathan and Sivaramakrishman by correcting for deviations from Boyle's law. Corrections were not given for carbon tetrachloride. It is observed that all previous values of the susceptibility of benzene vapor are larger than the value obtained by the writers, though Sivaramakrishman's corrected value is only 5 percent larger and that of Yanus and Shur is only 8 percent larger than the value obtained in this investigation.

TABLE III.

Observer	$-\chi\times10^6$ for CCl_4 Reported values	$-\chi\times10^6$ for C_6H_6 Reported values	Corrected[4] for density
Vaidyanathan[1]	0.514 ± 0.030	$1.06\ \pm0.064$	0.827
Vaidyanathan[2]	0.500 ± 0.038	0.948 ± 0.075	0.760
Yanus and Shur[5]		0.756 ± 0.038	
Sivaramakrishman[3]		0.796	0.732
Reber and Boeker	0.432 ± 0.013	0.697 ± 0.021	

The susceptibilities of benzene and carbon tetrachoride liquids probably have been studied more extensively than those of any other organic compounds. Seely[13] gives for benzene an average value of -0.7038×10^{-6} obtained from the results of ten observers and for carbon tetrachloride an average value of -0.4308×10^{-6} obtained from the results of seven observers. On comparing these values with those of four of the most recent observers[13–16] who studied both liquids it is found that the maximum difference is 0.5 percent for carbon tetrachloride and 0.9 percent for benzene.

The differences between the values of the mass susceptibilities of the vapors obtained in the present investigation and the average values for the liquids given by Seely are less than 1 percent.

Theoretically any appreciable difference be-

[10] W. Ramsay and B. D. Steele, Phil. Mag. **6**, 492 (1903).
[11] S. Young, Proc. Roy. Dublin Soc. **12**, 374 (1910).
[12] E. Stoner, *Magnetism and Matter* (Methuen and Company).
[13] S. Seely, Phys. Rev. **49**, 812 (1936).
[14] S. P. Ranganadham, Ind. J. Phys. **6**, 421 (1931).
[15] S. R. Rao and G. Sivaramakrishman, Ind. J. Phys. **6**, 509 (1932).
[16] G. F. Boeker, Phys. Rev. **43**, 756 (1933).

tween the mass susceptibilities of the vapor and liquid would appear to require inter-molecular forces in the liquid state sufficient to produce a substantial alteration of electronic orbits. Certainly, for liquids composed of symmetrical molecules such as benzene and carbon tetrachloride it would be difficult to account for inter-molecular forces of a type to effect importantly the susceptibility. It is noteworthy that neither Oxley[17] nor Cabrera and Fahlenbrach[18] found any detectible difference in the magnetic susceptibilities of benzene in the crystalline and liquid states, though small differences were found for other organic substances. Cabrera and Fahlenbrach found that in general the change in susceptibility in passing from the crystalline to the liquid state was smaller the smaller the electric dipole moment of the molecules. Further evidence that inter-molecular forces do not have much effect on the susceptibility of non-polar liquids is given by measurements on non-polar liquid mixtures[13–15] which have shown that the additivity principle of susceptibility holds to within 0.5 percent. The results of the present investigation are consistent with the hypotheses that for benzene and carbon tetrachloride there is negligible difference between the mass susceptibilities in the vapor and liquid states.

The authors are deeply indebted to Columbia University for the use of its facilities.

[17] A. E. Oxley, Phil. Trans. **214A**, 109 (1914).
[18] B. Cabrera and H. Fahlenbrach, Zeits. f. Physik **85**, 568 (1933); **89**, 682 (1934).

THE JOURNAL OF CHEMICAL PHYSICS VOLUME 15, NUMBER 7 JULY, 1947

Statistical Mechanics of Binary Mixtures

A. R. MILLER
Cavendish Laboratory, University of Cambridge, Cambridge, England

The possibility of specifying both the enumeration of the complexions of an assembly and the evaluation of its configurational energy in terms of the numbers of closest neighbor pairs of sites of various kinds, without introducing parameters explicitly to specify the occupation of individual sites, is considered. The formula obtained on such a basis by Alfrey and Mark is examined. Their work depends on an assumption which at first sight appears plausible. Furthermore, if this assumption could be justified, it would imply that the quasi-chemical equation, which has been introduced in the theory of regular assemblies as an *ad hoc* assumption, could be derived from the Boltzmann equilibrium law and the elementary formulas of algebraic combinations. If a pair of closest neighbor sites of which one is occupied by a molecule of species i and the other by a molecule of species j is called an $i-j$ pair, then it is shown that the assumption made by Alfrey and Mark is equivalent to neglecting the restrictions on the free allocation (amongst the $\frac{1}{2}zN$ pairs available in all) of pairs of different kinds which are inherent in the interconnections of an assembly of interacting particles. It is concluded, therefore, that the assumption in question is unjustified and leads to an incorrect result, and that consequently the quasi-chemical equation is correctly introduced as an *ad hoc* assumption.

1. INTRODUCTION

THE basic problem in the determination of the equilibrium properties of an assembly of interacting particles is the evaluation of the appropriate combinatory factor which is necessary in order to set up the partition function for the assembly. Much work has been devoted to this question. A detailed discussion of it can be dispensed with here as reviews[1,2] have appeared elsewhere. We consider a simple binary mixture containing N_i molecules of a species i and N_j molecules of a species j on an array of N $(=N_i+N_j)$ sites formed by the points of a regular lattice. It is assumed further that the molecules of each species are of about the same size and roughly spherical in shape, and that the interaction energy of the assembly can be expressed as the sum of closest neighbor contributions. If X_{ii}, X_{ij}, and X_{jj}, respectively, are the numbers of $i-i$, $i-j$, and $j-j$ closest

[1] F. C. Nix and W. Shockley, Rev. Mod. Phys. **10**, 1 (1938).
[2] G. H. Wannier, Rev. Mod. Phys. **17**, 50 (1945).

neighbor pairs, then the interaction energy is given by

$$E=X_{ii}V_{ii}+X_{ij}V_{ij}+X_{jj}V_{jj}$$

where V_{ii}, V_{ij}, and V_{jj}, respectively, are the interaction energies of a pair of particles of the kind denoted by the suffixes. With suitable choice of the energy zero this can be written as

$$E=X_{ij}w_{ij} \tag{1}$$

where w_{ij} is the energy of mixing. The partition function can then be written as

$$Z=\sum_{X_{ij}} g(N_i, N_j, X_{ij}) \exp(-X_{ij}w_{ij}/kT)b_i^{N_i}b_j^{N_j} \tag{2}$$

where b_i, b_j are terms which include factors to take account of the partition functions corresponding to the internal degrees of freedom of the molecules and of their effective free volumes. In this expression $g(N_i, N_j, X_{ij})$ is the number of distinct configurations of the given numbers of molecules of each kind in which there are X_{ij} closest neighbor pairs of the kind $i-j$. Certain simple relations exist between the various parameters N and X; we have, in fact, made use of these relations in obtaining an expression for the energy which depends only on X_{ij}. These relations are

$$2X_{ii}+X_{ij}=zN_i, \tag{3}$$

$$2X_{ij}+X_{ij}=zN_j. \tag{4}$$

These relations also imply that of the five quantities which have been introduced to specify the system, only three of them are independent. It therefore follows that the partition function could be written in terms of X_{ii}, X_{ij}, and X_{jj} equally well as in terms of N_i, N_j, and X_{ij}. It was pointed out by Alfrey and Mark[3] that the difficulty of evaluating the combinatory factor lies in the fact that ordinarily different variables are used for enumerating the complexions of the assembly and for determining its configurational energy. Whereas the distinguishable configurations of the assembly are specified by the occupation of individual lattice sites, the configurational energy arises from closest neighbor (or more distant) interactions and has to be determined by the specification of closest neighbor (or more distant) pairs of sites. It therefore follows that if a means could be found by which both the evaluation of the configurational energy and the enumeration of the complexions of the assembly could be carried out in terms of one and the same kind of variable (that is, by the specification either of pairs of sites or of the occupation of individual sites, but not both) one could hope greatly to simplify this task. It is clear that the configurational energy can be expressed only in terms of the specification of pairs of sites; can, then, the distinguishable complexions of the assembly also be expressed in terms of these variables? This was attempted by Alfrey and Mark[3] with the help of an assumption, which is described in Section 2 below (Eq. (7)), concerning the occurrence of closest neighbor pairs of different kinds. The purpose of the present note is to discuss this assumption and the reasons that the specification of pairs of sites fails to provide an alternative method, far less a simpler one, than those already proposed[4-8] for evaluating the combinatory factors appropriate in the study of cooperative phenomena and of mixtures which contain polymer molecules.

2. STATISTICAL FORMULAS

We first examine the procedure adopted by Alfrey and Mark. They consider a set of $N/2$ numbered pairs of closest neighbor lattice sites which are chosen in such a way that each site of the lattice belongs to one and to only one pair. If among the selected set of $N/2$ closest neighbor pairs there are X $i-j$ pairs, then the number of $i-i$ and $j-j$ pairs are $\frac{1}{2}(N_i-X)$ and $\frac{1}{2}(N_j-X)$, respectively. The number of configurations is then calculated by considering (i) the number of ways of arranging X indistinguishable elements of one kind, $\frac{1}{2}(N_i-X)$ indistinguishable elements of a second type, and $\frac{1}{2}(N_j-X)$ indistinguishable elements of a third type among the $\frac{1}{2}N$ available places, and (ii) by allowing for the fact that each $i-j$ pair can be arranged in two distinct ways within its reference position. On this basis, they give, for the combinatory factor,

[3] T. Alfrey and H. Mark, J. Chem. Phys. **10**, 303 (1942).

[4] T. S. Chang, Proc. Camb. Phil. Soc. **35**, 265 (1939).
[5] A. R. Miller, Proc. Camb. Phil. Soc. **39**, 54 (1943).
[6] P. J. Flory, J. Chem. Phys. **10**, 51 (1942).
[7] M. L. Huggins, J. Phys. Chem. **46**, 151 (1942).
[8] E. A. Guggenheim, Proc. Roy. Soc. **A183**, 203 (1944).

an expression

$$\phi(X)=\frac{(N/2)!2^X}{X!\{\frac{1}{2}(N_i-X)\}!\{\frac{1}{2}(N_j-X)\}!}, \quad (5)$$

and, correspondingly, for the partition function

$$Z=\sum_X \phi(X)\exp(-zXw_{ij}/kT), \quad (6)$$

apart from factors allowing for the internal motions of the molecules.

This treatment involves the assumption that if in the selected group of $\frac{1}{2}N$ closest neighbor pairs there are X pairs of the kind $i-j$, then in the complete assembly the total number of $i-j$ pairs is exactly zX. This also implies that the total numbers of $i-i$ and $j-j$ pairs are $\frac{1}{2}z(N_i-X)$ and $\frac{1}{2}z(N_j-X)$, respectively. In fact, in terms of our notation, it is assumed that

$$\left.\begin{aligned} zX&=X_{ij}\\ \tfrac{1}{2}z(N_i-X)&=X_{ii}=\tfrac{1}{2}(zN_i-X_{ij})\\ \tfrac{1}{2}z(N_j-X)&=X_{jj}=\tfrac{1}{2}(zN_j-X_{ij})\end{aligned}\right\}. \quad (7)$$

This assumption is essential in the treatment given by Alfrey and Mark for two reasons: (i) In order that the interaction energy, which we have seen is equal to $X_{ij}w_{ij}$, can be expressed in terms of the parameter X which they introduce, namely as zXw_{ij}. This is the specific form in which Alfrey and Mark express this assumption in Eq. (7) of their paper. (ii) It is also necessary because their treatment assumes that the particular arrangement of particles on the lattice in which there are X_{ii}, X_{ij}, and X_{jj} pairs of $i-i$, $i-j$, and $j-j$ closest neighbors, respectively, is equivalent to, and can be described precisely by, the allocation of X, $\frac{1}{2}(N_i-X)$, and $\frac{1}{2}(N_j-X)$, respectively, $i-j$, $i-i$, and $j-j$, pairs among the group of $\frac{1}{2}N$ pairs selected in the way specified. This is considered further in the discussion below (Eqs. (9) and (10)).

In fact, from a lattice of N sites in which no closest neighbors of any site are also closest neighbors of one another, a group of $\frac{1}{2}N$ closest neighbor pairs which are such that every lattice point belongs to one and to only one pair can be chosen in $\{(z-1)^{z-1}/z^{z-2}\}^{\frac{1}{2}N}$ different ways.[9] While, at first sight, it appears possible that the assumption made by Alfrey and Mark might be valid (or nearly so) for a sufficient number of these possible selections of the group of pairs to enable the method to give a reasonable estimate of the combinatory factor, they offer no justification of it. Furthermore, it is difficult to see how any formal justification of their assumption could be constructed. When the problem is examined from a somewhat different viewpoint, the nature and implications of the assumption made by Alfrey and Mark become clearer, and it is seen to be far from justified.

3. DISCUSSION

It has been noted above that X_{ii}, X_{ij}, and X_{jj} can be taken as the three independent parameters which are used to specify the assembly. With this specification, the determination of the combinatory factor reduces to the evaluation of the number of ways in which X_{ii} indistinguishable elements of one type, X_{ij} indistinguishable elements of a second type, and X_{jj} indistinguishable elements of a third type can be distributed among $\frac{1}{2}zN$ available pairs, *subject to any restrictions inherent in the interconnections of the assembly*. The closing phrase indicates where the difficulty lies. A little reflection shows that if, from the total number of available pairs, X_{ii} are chosen for the $i-i$ closest neighbors, then not all the remaining $(\frac{1}{2}zN-X_{ii})$ pairs can be utilized to accommodate a $j-j$ pair, for it is inherent in the interconnections of the pairs that a large number of those now remaining can accommodate only an $i-j$ pair. Furthermore, the position is not helped by selecting the pairs for the $i-j$ closest neighbor pairs second, for unless severe restrictions on our freedom of choice of the required number of pairs are accepted, we would be left finally with a large number of pairs which could not accommodate a $j-j$ closest neighbor pair and at the same time an insufficient number of possible pairs to accommodate all the $j-j$ closest neighbors. In passing it should also be noted that the precise specification of these restrictions, if not impossible, is certainly neither simple nor straightforward. It appears likely that it is in this restriction on the free choice of elements to accommodate the closest neighbor pairs of different kinds that the implications of the assumption made by Alfrey and Mark are to be found.

[9] A. R. Miller, Proc. Camb. Phil. Soc. **38**, 108 (1942), Eq. (16).

We now proceed to show that this is, in fact, the case.

Stirling's theorem for the asymptotic behavior of a factorial ensures that for large values of r and s and a constant α then

$$\alpha \log\left[\frac{(r+s)!}{r!s!}\right]=\log\left[\frac{\{\alpha(r+s)\}!}{(\alpha r)!(\alpha s)!}\right]. \quad (8)$$

If the three Eqs. (7) are valid, that is, if the assumption made by Alfrey and Mark can be justified, it then follows that

$$\left[\frac{(N/2)!}{X!\{\frac{1}{2}(N_i-X)\}!\{\frac{1}{2}(N_j-X)\}!}\right]^z = \frac{(zN/2)!}{X_{ij}!\{\frac{1}{2}(zN_i-X_{ij})\}!\{\frac{1}{2}(zN_j-X_{ij})\}!}. \quad (9)$$

The right-hand member of Eq. (9) reduces to

$$\frac{(zN/2)!}{X_{ii}!X_{ij}!X_{jj}!}, \quad (10)$$

which is precisely the number of ways of arranging X_{ii} elements of one kind, X_{ij} elements of a second kind, and X_{jj} elements of a third kind among $\frac{1}{2}zN$ positions *without any restriction whatsoever*. Thus, the assumption made by Alfrey and Mark amounts to neglecting the restrictions on the allocation of the closest neighbor pairs of different kinds which are inherent in the arrangements of two or more species of molecules on a regular lattice. It will thus give a value for the combinatory factor which is far from the correct value, being, in fact, far too large.

In the case of polymer molecules, each of which has to be regarded as occupying several sites on the lattice, the restrictions on the distribution of the pairs are even more severe. For each polymer molecule which consists of r units or submolecules there are x pairs of closest neighbor sites which are occupied by adjacent units of the polymer molecule, where[10]

$$2x=z(r-q)N_i. \quad (11)$$

In this equation q is determined by the fact that zq is the number of closest neighbor pairs of sites which are formed by the sites which are occupied by a given polymer molecule and the remaining sites of the lattice. In this case the various kinds of pairs would have to be arranged among the $\frac{1}{2}zN$ available positions so that the x "internal pairs" corresponding to each polymer molecule would be allotted to adjacent closest neighbor pairs, since they define a polymer molecule. Without further elaboration it is clear that in this case one cannot specify the occupation of a group of sites by a polymer molecule without specifying the occupation of each individual lattice site. It therefore follows that the number of configurations of the assembly cannot be determined by the specification of closest neighbor pairs of sites alone.

A value for $g(N_i, N_j, X_{ij})$ in the case of a binary mixture of simple molecules was given by Chang;[5] his formula is included in the general formula given by Guggenheim.[11] For a binary mixture of simple molecules, their result can be written,

$$g(N_i, N_j, X_{ij}) = \frac{\{N_i!N_j!\}^{(z-1)}}{(N!)^{\frac{1}{2}z-1}\{(N_i-X_{ij})!\}^{\frac{1}{2}z}\{X_{ij}!\}^z\{(N_j-X_{ij})!\}^{\frac{1}{2}z}} \quad (12)$$

where zX_{ij} is defined as the total number of $i-j$ interactions. If this formula is compared with the value given by Alfrey and Mark (Eq. (5)) it indicates that their value is too large by a factor of the order of

$$\frac{\{N_i!N_j!\}^{z-1}}{\{N!\}^{\frac{1}{2}z}}. \quad (13)$$

There is one other point to be noted. The most probable value of X can be obtained by maximizing the general term in the partition function. If Stirling's approximation be used and the expression given by Alfrey and Mark for $\phi(X)$ (Eq. (5)) be differentiated with respect to X and the derivative equated to zero, we get

$$\bar{X}^2=(N_i-\bar{X})(N_j-\bar{X})\exp(-2w_{ij}/kT). \quad (14)$$

This equation has the familiar form of the equation of quasi-chemical equilibrium. It was originally introduced by Guggenheim[12] as providing a more exact approximation than that

[10] A. R. Miller, Proc. Camb. Phil. Soc. (1947) (to be published) Eq. (6).

[11] E. A. Guggenheim, Proc. Roy. Soc. **A183**, 213 (1944), Eqs. (5.5) and (8.1).

[12] E. A. Guggenheim, Proc. Roy. Soc. **A148**, 304 (1935).

which had been used previously in the theory of solutions. It is, however, an *ad hoc* assumption based on analogy with the equation of equilibrium for a chemical reaction. It was the fact that it could be derived from the formula which was given by Alfrey and Mark for $\phi(X)$ which originally led me to look more closely into the nature of the apparently innocent assumption on which their argument is based. For, if it were justified, it would have meant that Eq. (14) followed simply from the Boltzmann equilibrium law and the elementary formulas of algebraic combinations. In view of the way in which this equation of quasi-chemical equilibrium had been introduced in other applications,[13,14] it hardly seemed possible that this could be so. The foregoing analysis confirms the correctness of this scepticism.

[13] E. A. Guggenheim, Proc. Roy. Soc. **A169**, 134 (1938).
[14] R. H. Fowler and E. A. Guggenheim, Proc. Roy. Soc. **A174**, 189 (1940).

4. CONCLUSIONS

It is concluded that the assumption made by Alfrey and Mark amounts to neglecting the restrictions on the free allocation of closest neighbor pairs of different kinds, which are inherent in the interconnections of an assembly of interacting particles of different kinds, and leads to an incorrect value for the combinatory factor. It also appears that the combinatory factors, appropriate both for a cooperative assembly and for a mixture containing polymer molecules, cannot be determined by the specification of pairs of sites alone without specifying the occupation of each individual lattice site. It is also shown that the quasi-chemical equation, which would be implied by Boltzmann's distribution law and the elementary formulae of algebraic combinations, if the assumption made by Alfrey and Mark could be justified, is correctly introduced as an *ad hoc* assumption.

An Equation of State for Gases at Extremely High Pressures and Temperatures from the Hydrodynamic Theory of Detonation

MELVIN A. COOK[1]

*Eastern Laboratory, Explosives Department, E. I. du Pont de Nemours and Company, Inc., Gibbstown, New Jersey**

(Received February 12, 1947)

The hydrodynamic theory of detonation is derived in a convenient form for practical utility by employing the general equation of state $pv=nRT+\alpha(T, v)p$. Two methods of solution of the general equations based on measured detonation velocity are discussed. In method (a) the detailed form of $\alpha(T, v)$ is unspecified. It is therefore, in principle, at least, a general solution. However, in practice one finds that it is impossible due to the experimental error in detonation velocities to evaluate the heat capacity at constant volume and hence the detonation temperature without specifying a particular form of $\alpha(T, v)$. The postulate (used only in the calculation of temperature) is $\alpha=\alpha(v)$. Method (b) employs the approximation $\alpha=\alpha(v)$ throughout. Methods (a) and (b) lead to identical results which one will find in view of the comparative nature of the two methods, is good evidence (but not conclusive proof) for the validity of the above approximation. This is supported also by the discovery that the same α *vs.* v_2 curve applies to all explosives yet considered. As a matter of fact, it has been found that the detonation velocities may themselves be computed within experimental error, evidently for explosives of all types (where sufficient heat data are available) by employing the $\alpha(v)$ function evaluated from a few selected explosives. Several additional arguments supporting the above approximation are discussed. Data on the detonation properties of several explosives are presented and correlated with similar data obtained by other investigators.

INTRODUCTION

THE hydrodynamic theory of detonation developed by Chapman,[2] Jouguet,[3] Becker,[4] Schmidt,[5] and others has recently been carefully scrutinized and extended by various investigators including Landau and Stanyukovich,[6] Ratner,[7] Kistiakowsky and Wilson,[8] von Neumann,[9] Brinkley and Wilson,[10] Eyring and collaborators,[11] and others. In the application of the hydrodynamic theory of detonation to condensed explosives a particular form of the equation of state is generally assumed and the parameters are evaluated experimentally through the hydrodynamic theory, by introducing measured detonation velocities. Consequently, the theory has not yet been demonstrated for condensed explosives as directly as might be desired, although much convincing indirect evidence is available and the general validity of the theory is unquestioned at the present time. The objectives of the present study are (1) to derive the theory for condensed explosives in a useful form, (2) to show how the theory and measured velocities may be used to derive an equation of state applicable in the study of other detonation and high pressure phenomena, and (3) to discuss some interesting features of the derived equation of state.

DERIVATION OF EQUATION

The fundamental equations of the hydrodynamic theory of detonation are

$$D=v_1((p_2-p_1)/(v_1-v_2))^{\frac{1}{2}}, \quad (1)$$

$$W=(v_1-v_2)((p_2-p_1)/(v_1-v_2))^{\frac{1}{2}}, \quad (2)$$

$$E_2-E_1=\tfrac{1}{2}(p_2+p_1)(v_1-v_2), \quad (3)$$

$$(p_2-p_1)/(v_1-v_2)=-(\partial p_2/\partial v_2)_S. \quad (4)$$

Equation 3 is the Rankine[12]-Hugoniot[13] adiabatic (or "dynamic adiabatic") relation. Equation (4)

* Present Address: Department of Metallurgical Engineering, University of Utah, Salt Lake City 1, Utah.

[1] This article is based in part on information developed by the author at Eastern Laboratory and made available by du Pont and Company to various service organizations in March, 1943.

[2] D. Chapman, Phil. Mag. **47**, 90 (1899).

[3] E. Jouguet, J. de math. **1**, 347 (1905); **2**, 1 (1906).

[4] R. Becker, Zeits. tech. Physik **8**, 152, 249 (1917), **8**, 321 (1922).

[5] A. Schmidt, Zeits. f. das gesamte Schiess u. Sprengstoffwesen, **31**, 8 (1936).

[6] L. Landau and K. Stanyukovich, comptes rendus (URSS) **36**, 362 (1945).

[7] S. Ratner, comptes rendus (URSS) **48**, 187 (1945).

[8] G. B. Kistiakowsky and E. B. Wilson, Jr., OSRD Report 69.

[9] J. von Neumann, OSRD Report 549.

[10] S. R. Brinkley, Jr. and E. B. Wilson, Jr., OSRD Report 905.

[11] H. Eyring, R. E. Powell, G. H. Duffey, R. B. Parlin, OSRD Report 3796.

[12] W. J. M. Rankine, Phil. Trans. **160**, 277 (1870).

[13] Hugoniot, J. de math. **3**, 477 (1887); J. de l'école Polytech. **57**, 3 (1887); **58**, 1 (1889).

is equivalent to the Chapman-Jouguet postulate

$$D=W+C. \tag{5}$$

Here D is the detonation velocity; W and C are the particle and sound velocities, respectively, in the medium (products of detonation) immediately behind the wave front; v, p, and T are the state variables; E is the total energy and S the entropy. The subscript 1 refers to the thermodynamic quantities in the undetonated explosive, and the subscript 2 to the corresponding quantities in the medium immediately behind the shock front (where the Chapman-Jouguet condition applies).

For a solution of the above equations, the following general equation of state is adopted

$$pv=nRT+\alpha(T,v)p. \tag{6}$$

To derive an expression for $(\partial p_2/\partial v_2)_S$ the following thermodynamic equation for an adiabatic equilibrium process is used:

$$-C_v\partial T_S=((\partial E/\partial v)_T+p)\partial v_S. \tag{7}$$

Differentiating Eq. (6), solving for ∂T_S, and introducing the result into Eq. (7) gives

$$-(\partial p_2/\partial v_2)_S=p_2\beta/(v_2-\alpha), \tag{8}$$

where

$$\beta=(nR+C_v)/C_v-(\partial\alpha/\partial v_2)_S+(\partial E/\partial v)_T nR/C_v p_2. \tag{9}$$

Here C_v is the heat capacity at constant volume (per kilogram), R is the gas constant, and n the number of molecules of gas per kilogram. The subscript 2 is introduced to show that Eqs. (8) and (9) apply immediately behind the wave front.

By employing Eqs. (4), (6), and (8), Eq. (1) becomes

$$D^2=v_1^2p_2\beta/(v_2-\alpha)=v_1^2(nRT_2\beta)/(v_2-\alpha)^2. \tag{10}$$

Since $p_2\gg p_1$ in condensed explosives, Eqs. (4) and (8) give

$$\beta=(v_2-\alpha)/(v_1-v_2). \tag{11}$$

Combining Eqs. (1) and (6), the equation

$$(v_2-\alpha)(v_1-v_2)=v_1^2(nRT_2)/D^2 \tag{12}$$

is obtained. The equation

$$\alpha=v_1-v_1(\beta+1)(nRT_2)^{\frac{1}{2}}/D\beta^{\frac{1}{2}} \tag{13}$$

may then be derived from Eqs. (10) and (11). Similar substitutions in Eqs. (2) and (3) give

$$W=(nRT_2/\beta)^{\frac{1}{2}}, \tag{14}$$

and

$$E_2-E_1=nRT_2/2\beta. \tag{15}$$

The detonation temperature is then given by

$$T_2=(Q+T_1\bar{C}_v)\beta/(\beta\bar{C}_v-\tfrac{1}{2}nR), \tag{16}$$

where Q is the chemical energy released in detonation (the heat of explosion), and $\bar{C}_v$ is the average heat capacity at constant volume (v_2) between T_2 and T_1.

SOLUTION OF EQUATIONS

Either of two quite different methods of solution of the above equations may be used, both of which will be discussed since they prove to be complementary in providing information on the nature of the equation of state.

(a) The first method is a solution in which the detailed form of β is not taken into account. This solution is made possible by the fortuitous cancellation of p_2 in obtaining Eq. (11). The Eqs. (11), (12), (13) and (16) may be solved by successive approximations employing a measured value of D at any given density (ρ_1). A value of β is selected and T_2 calculated from Eq. (16). (In the calculation of T_2, the low density value of $\bar{C}_v$ has been used as discussed below. This is equivalent to the approximation $\alpha=\alpha(v)$ which was used in method (a) only in the evaluation of T_2. This approximation or an equivalent one is necessary because of the experimental error in measured detonation velocity, making a reliable evaluation of $\bar{C}_v$ impossible.) Equation (13) is used to evaluate α, and v_2 is obtained from (12) for these values of α and β. Equation (11) may then be used to check β. If this value of β does not agree with the selected value, the approximations are repeated until the successive β's converge to a constant value. It is here tacitly assumed that n, Q, and $\bar{C}_v$ are known. Actually they must also be evaluated by thermodynamic methods and, in view of their dependence on v_2, T_2, and α, they must be re-evaluated in each successive approximation unless, as is the case in the final approximations, they do not vary appreciably. As a matter of fact the approximations converge quite rapidly since α obtained

from Eq. (13) is quite insensitive to different values of β and nT_2.

For evaluating the products of detonation a modification of the method developed by Brown[14] was employed together with heat data taken from Bichowski and Rossini,[15] and Schmidt.[16] In this modification the experimental equation of state was used in setting up more exact equilibrium equations and the final approximations employed activity or fugacity rather than partial pressures in the thermodynamic equilibrium constants.

In principle $\bar{C}_v$ may be evaluated from the equation

$$\bar{C}_v=\bar{C}_v^*+\frac{1}{T_2-T_1}\int_\infty^{v_2}(\partial E/\partial v)_T dv$$

$$=\bar{C}_v^*+\frac{1}{T_2-T_1}\int_\infty^{v_2}(p_2^2/nR)(\partial\alpha/\partial T)_v dv, \quad (17)$$

where $\bar{C}_v^*$ is the low density average (constant volume) heat capacity between T_2 and T_1. It will be seen that $(\partial\alpha/\partial T)_v$, if not effectively zero, is exceedingly small relative to p_2. Because of the enormously high pressures occurring in detonation, however, it is quite impossible to evaluate reliably the last term of Eq. (17) directly from the hydrodynamic theory of detonation since the detonation velocity (although known to within about 3 percent) and the necessary heat data are not known accurately enough for this purpose.

In application of method (a) it will be assumed, therefore, that $\bar{C}_v=\bar{C}_v^*$. Several more or less indirect evidences justifying this assumption are discussed in this report. One argument is the following:

Hirschfelder and Roseveare[17] showed that for gases at sufficiently high temperature the internal energy is a linear function of density (ρ). At low density $(\partial E/\partial\rho)_T=-a(T)$, where $a(T)$ is the van der Waals constant (which decreases with increasing temperature). It will be assumed in view of the high detonation temperatures that the linear variation of E with ρ holds over the entire range from low density to v_2. Thus this approximation gives

$$\int_\infty^{v_2}(\partial E/\partial v)_T dv\approx a(T)/v_2<8 \text{ kg cal./kg}$$

for the products of detonation of PETN at a density of 2.0 kg/L. On the other hand,

$$\bar{C}_v(T_2-T_1)=\bar{C}_v^*(T_2-T_1)$$

$$+\int_\infty^{v_2}(\partial E/\partial v)_T dv\approx 1200\text{–}1700 \text{ kg cal./kg}.$$

Hence, according to this method $\bar{C}_v=\bar{C}_v^*$ within 0.5 percent at $v_2=0.5$ L./kg. (Likewise, for use in the alternate method of solution, it may be shown according to this method for evaluating $(\partial E/\partial v)_T$ that the neglect of the last term in Eq. (9) will incur an error of less than 0.1 percent in β.) Hirschfelder and Roseveare showed that the linear variation of E with ρ is valid at least up to 3000 atmos. even at much lower than detonation temperatures. The extension of this linear law to detonation pressures ($\sim$200,000 atmos.) involves, of course, a large extrapolation in p_2. However, further evidence for the approximate validity of the extrapolation will be found in the correlation of the results obtained by method (a) described above, with those obtained from method (b).

(b) This method involves the use of $D(\rho_1)$ data, and the separate evaluation of each term of Eq. (9) for β, the last term in (9) being neglected following the reasoning already given. As a first approximation α may be evaluated from Eq. (13) over a range of densities by taking $\beta=(C_v+nR)/C_v$ or by simply assuming values of β. A plot of α against v_2 is then constructed and the slope taken at various points along the curve giving a series of values of $(\partial\alpha/\partial v_2)_S$. The values of β obtained by including the term from the first approximation are introduced back into Eq. (13) to obtain better values of α, the quantity nT_2 also being corrected according to its dependence on β, v_2, and α. This process is repeated until all parameters converge to constant values. As in method (a) this series of approximations also converges rapidly.

In evaluating β by means of the slope of the

[14] F. W. Brown, "Theoretical Calculations for Explosives," U. S. Bur. of Mines Technical Paper No. 132.

[15] F. R. Bichowski and F. D. Rossini, *Thermochemistry of Chemical Substances* (Reinhold Publishing Company, New York, 1936).

[16] A. Schmidt, Zeits. f. das gesamte Schiess u. Sprengstoffwesen **29**, 259 (1934).

[17] J. O. Hirschfelder and W. E. Roseveare, J. Phys. Chem. **43**, 15 (1939).

α, v curve it was tacitly assumed that the entropy S_2 is constant along the curve. At any density (ρ_1), $dS_2/dv_2=0$ according to the Chapman-Jouguet postulate. In the approximation $\alpha=\alpha(v_2)$, therefore, the change in S_2 along the curve should be zero. There is, of course, a sharp increase in the entropy across the shock front, i.e., $S_2-S_1\gg 0$. Scorah,[18] however, concluded that the increase in entropy (S_2-S_1) is a minimum and that $(S_2-S_1)/A$ is a maximum, where A is the available energy fed into the wave front. The variation of S_2 along the α, v curve may be evaluated at various densities within the accuracy of the equation of state employed by the equation

$$S_2=S_2^0+\bar{C}_v \ln T_2/T_1+nR\int_{v_0}^{v_2} dv/(v-\alpha), \quad (18)$$

where S_2^0 is the entropy of the products of detonation in their standard state T_0, v_0, p_0. Actually Eq. (18) shows that there is a small change in S_2 along the α, v curve amounting to about 0.1 E.U./gram for a change in density (ρ_1) from 0.7 to 1.6 kg/L., the total entropy S_2 being $\sim$1.5 to 2.0 E.U./gram. Since β can be determined only to within about 5 percent (from measured velocities accurate to within 2 to 3 percent) it is evident that the slope of the α, v curve gives $(\partial\alpha/\partial v_2)_S$ with sufficient accuracy in the $\alpha(v)$ approximation.

TABLE I. Constants of Eq. (19) for explosives shown in Fig. 1.

	$D_{1.0}$	$M\left(\frac{\text{m/sec.}}{\text{kg/1.0}}\right)$
PETN	5620	3500
RDX	5900	3570
TNT	4800	3500
Tetryl	5500	3350
Picric acid	5060	3500
Ammonium picrate	4800	3500
Lead azide	5100 ($\rho_1=4.0$)	560
Mercury fulminate	5050 ($\rho_1=4.0$)	890

Figure 1 presents the α, v_2 relations obtained by both methods (a) and (b). The data for the eight explosive compounds calculated by method (a) are best represented by the dotted curve. The solid curve was obtained entirely independently by method (b) for the same and a number of additional explosives, method (b) having preceded method (a) in the development of the theory. The deviations in v_2 and α from either the dotted or solid curve are about the same order of magnitude (≤ 3 percent) as the experimental error involved in the measured detonation

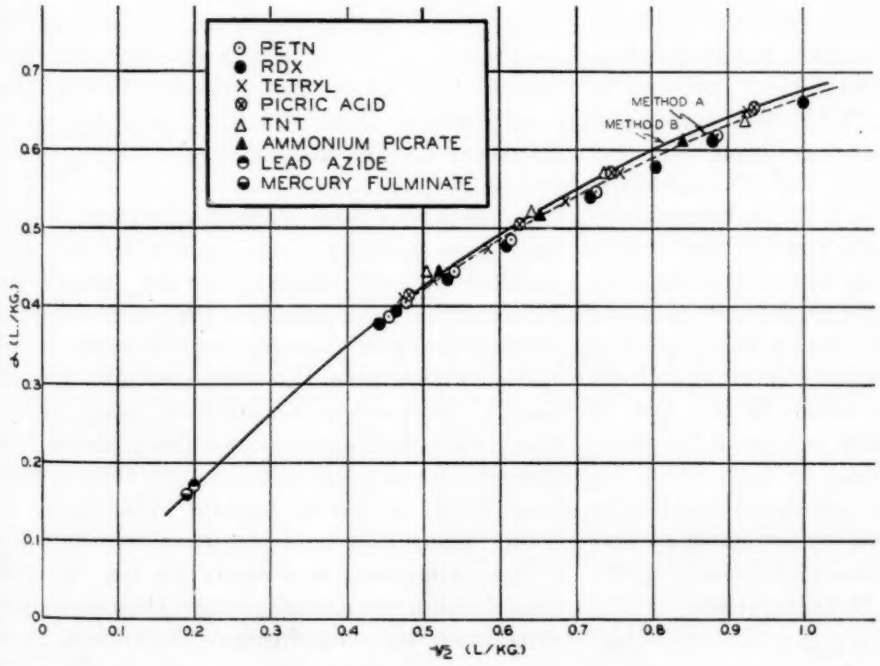

FIG. 1. Variation of α with v_2.

[18] R. L. Scorah, J. Chem. Phys. **3**, 425 (1935).

TABLE II. Equation of state relations from Fig. 1.

ρ_2(kg/1.0)	v_2(1.0/kg)	α(1.0/kg)	$(d\alpha/dv_2)_S$
0.8	1.25	0.75	0.30
1.0	1.0	0.68	0.39
1.2	0.837	0.62	0.47
1.4	0.714	0.56	0.53
1.6	0.625	0.51	0.59
1.8	0.555	0.47	0.65
2.0	0.50	0.43	0.69
2.2	0.455	0.39	0.73

velocities (assuming accurate heat data). The experimental velocity data used in these calculations are given by the following equation, the constants of which are given in Table I.

$$D=D_{1.0}+M(\rho_1-1.0), \tag{19}$$

where $D_{1.0}$ is the velocity (m/sec.) at a density of 1.0 kg/L. and M is the slope of the $D(\rho_1)$ curve in m/sec./kg/L.

CORRELATIONS

Not only do methods (a) and (b) give the same results within the limits of reproducibility of the data, but of even greater significance is the fact that all the explosives follow the same α *vs.* v_2 curve. This appears to be ample evidence that the last term in Eq. (9) is negligible. It is not, however, sufficient evidence that $\bar{C}_v \cong \bar{C}_v^*$ (this approximation was made in both methods), although the validity of this assumption is strongly supported by the generality of the $\alpha(v)$ function. In other words, RDX and PETN have detonation temperatures about 40 percent higher than ammonium picrate, picric acid, and TNT, showing that the dependence of $\alpha(T, v)$ on temperature must be exceedingly small. The fact that values of α for a given v_2 for the latter explosives are consistently slightly higher than those of RDX and PETN at low density cannot be regarded as significant, since more recent velocity data indicate that in these cases values of $D_{1.0}$ and M given in Table I are slightly in error in the direction giving low values of α.

The equation of state employed by Kistiakowsky and Wilson[8] based on Bridgman's equation of state is very convenient for studying the magnitude of $(\partial E/\partial v)_T$. In the equation

$$pv=nRT(1+xe^x). \tag{20}$$

Kistiakowsky and Wilson took $x=K/T^{\frac{1}{4}}v$. For the present purposes, however, the form

$$x=KT^c/v \tag{21}$$

will be employed where K and c are constants, the latter of which will now be investigated. Equations (20) and (21) and the appropriate thermodynamic equation give

$$(\partial E/\partial v)_T=nRTxe^x(1+x)c/v, \tag{22}$$

$$\int_{\infty}^{v_2}(\partial E/\partial v)_T dv=-nRTxe^x c. \tag{23}$$

Comparing Eqs. (6) and (20), it is seen that $xe^x=\alpha/(v-\alpha)$ and from Fig. 1 at $v_2=0.5$ L./kg, $(\partial E/\partial v)_T \approx 2.1p_2c$. Thus the last term in Eq. (9) amounts to about $0.37c$. Since methods (a) and (b) in which the last term in Eq. (9) is neglected give values of β agreeing within 5 percent (the dotted curve actually differs by less than 3 percent from the solid one), $|c|$ cannot exceed 1/15. For $c=-1/15$, Eq. (23) gives an energy amounting to nearly 10 percent of $Q+\Delta E$. It is thus evident that $\bar{C}_v \leq 1.1\bar{C}_v^*$. By comparing results obtained by methods (a) and (b) for a single explosive, e.g., PETN, using the same detonation velocity data, a more accurate comparison may be obtained by eliminating the effect of experimental error in D. Studies of this sort in fact indicate that the difference in β between the two methods is less than 3 percent and that, therefore, $\bar{C}_v \leq 1.06\bar{C}_v^*$ at $v_2=0.5$ L./kg. This result differs from that obtained by using Kistiakowsky and Wilson's value $c=-\frac{1}{3}$, which gives $\bar{C}_v \approx 1.9\bar{C}_v^*$.

In connection with the approximation $\alpha=\alpha(v)$ used in method (b) it is of interest to note that Bullen[19] recently introduced the hypothesis, based on his calculations of the earth's density distribution, that at pressures of the order of one million atmospheres the compressibility may be largely independent of chemical composition. The present investigation provides evidence that this may be at least approximately true even at much lower pressures, perhaps even as low as 25,000 atmos. (for temperatures above 2500°C).

It is interesting to compare the Eq. (6) with the following equation developed from statistical mechanics by Hirschfelder, Stevenson, and

[19] K. Bullen, Nature **157**, 405 (1946).

Eyring[20]

$$(p+a/v^2)v=nRT[1+b/v+0.625(b/v)^2 +0.2869(b/v)^3+0.1928(b/v)^4]. \quad (24)$$

At detonation pressures a/v^2 may be neglected relative to p_2 and Eqs. (6) and (24) then give

$$\alpha=v-v/[1+b/v+0.625(b/v)^2 +0.2869(b/v)^3+0.1928(b/v)^4]. \quad (25)$$

If b is taken to be 0.95 L./kg (a reasonable value), Eq. (25) gives values of $\alpha(v)$ agreeing with those of Fig. 1 within 5 percent at densities (ρ_2) up to 1.8 kg/L. Above 1.8 kg/L. it gives values of α somewhat too large. Under the conditions encountered in detonation, Eq. (24) is equivalent to that proposed by Hirschfelder and Roseveare[17] since the second virial coefficient $B'(T)$ reduces approximately to b at high temperatures.

In reference (20) Happel's equation of state as derived by Rameshchandra Majumdar,[21] namely

$$(p+a/v^2)v=nRT(1+b/v+5/6(b/v)^2 +0.2869(b/v)^3+\cdots), \quad (26)$$

was employed in arriving at Eq. (24). Actually Eq. (26) employing $b=0.95$ L./kg is in much better agreement with the curve of Fig. 1 than Eq. (24). In fact, it gives agreement within 0.03 L./kg in α over the entire range shown. Even in the range of densities where Eq. (24) gives good agreement in α, it does not give good agreement in $(d\alpha/dv)$. Equation (26) on the other hand gives good agreement in both α and $(d\alpha/dv)$ over the whole range of densities of interest in studies of the detonation of condensed explosives.

CALCULATION OF DETONATION VELOCITY

Further rather convincing evidence for the generality of the curve of Fig. 1 is to be found in

TABLE III. Detonation properties of various explosives.

	*	ρ_1 kg/L.	D m/sec.	v_2 L./kg	α L./kg	β	n moles/kg	T_2 °K	W m/sec.	$p_2\times10^{-3}$ atmos.
PETN		1.0		0.725	0.546	0.65	35.2	5350	1540	85
PETN	BW	1.0	(5540)	(0.727)				(4130)	(1510)	(83)
PETN		1.2		0.615	0.488	0.58	35.0	5500	1660	125
PETN	BW	1.2	(6210)	(0.620)				(3960)	(1600)	(117)
PETN	R	1.2								(114)
PETN		1.6		0.478	0.405	0.49	34.9	5700	1820	225
PETN	BW	1.6	(7650)	(0.477)				(3630)	(1800)	(218)
PETN		1.69		0.452	0.387	0.46	34.9	5800	1900	255
PETN	LS	1.69	(8400)	(0.439)					(2000)	(275)
RDX		1.0		0.723	0.545	0.64	40.5	5250	1660	95
RDX	BW	1.0	(5620)	(0.729)				(3980)	(1520)	(84)
		1.6		0.469	0.394	0.48	40.5	5750	2000	255
	BW	1.6	(7520)	(0.478)				(3570)	(1760)	(215)
TNT		1.0		0.740	0.570	0.65	33.1	3700	1250	60
TNT	BW	1.0	(4870)	(0.748)				(3170)	(1250)	(60)
TNT		1.6		0.505	0.447	0.48	24.5	4170	1340	150
TNT	LS	1.6	(7000)	(0.476)					(1680)	(190)
	BW	1.6	(7290)	(0.496)				3170	(1510)	(175)
Tetryl		1.0		0.752	0.573	0.71	37.0	4200	1340	75
	BW	1.0	(5440)	(0.740)				(3620)	(1420)	(75)
		1.6		0.485	0.415	0.50	35.5	4700	1670	200
	BW	1.6	(7720)	(0.486)				3380	1710	209
		1.63		0.473	0.407	0.49	35.5	4750	1720	210
	LS	1.63	(7600)	(0.465)					(1850)	(230)
Picric acid		1.0		0.746	0.572	0.68	36.2	3750	1290	65
	BW	1.0	(5190)	(0.745)				(3180)	(1340)	(69)
		1.6		0.489	0.422	0.49	35.0	4150	1550	180
	BW	1.6	(7680)	(0.492)				(3080)	(1640)	(199)
		1.63		0.478	0.412	0.48	35.0	(4200)	1610	190
	LS	1.62	(7100)	(0.465)					(1730)	(210)

* Data given in ( ) are those computed by the investigators Brinkley and Wilson[10]—BW, Ratner[7]—R, and Landau and Stanyukovich[4]—LS.

[20] J. Hirschfelder, D. Stevenson, and H. Eyring, J. Chem. Phys. **5**, 896 (1937).
[21] H. Happel, Ann. d. Physik **4**, 21, 242 (1906); R. Majumdar, Bull. Calcutta Math. Soc. **21**, 107 (1929).

the fact that the (large diameter) velocities of detonation of explosives of widely different types have been calculated with an accuracy comparable to the experimental methods of velocity measurements by simply using the α *vs.* v_2 data taken from this curve. For example, velocities of various liquid and cast explosives have been calculated agreeing in all cases within 3 percent with measured velocities providing the measured detonation velocities were obtained in large enough diameter so that the maximum or hydrodynamic velocities were obtained. It is of interest to note that many explosives require charge diameters of the order of 5 in. before the maximum (complete reaction) velocity is reached. Whether or not the velocity is a maximum can usually be decided experimentally from velocity *vs.* charge diameter data at constant ρ_1. Table II lists data taken from the solid curve of Fig. 1 which may be used in the calculation of velocity.

PROPERTIES OF EXPLOSIVES

Table III lists some detonation properties of several explosives calculated by method (a) using $\bar{C}_v=\bar{C}_v^*$ and comparisons with results computed by other investigators. It will be observed that in general the agreement in compressibilities (v_1/v_2), W and p_2 is fairly good. The sharp differences in detonation temperature between BW (Brinkley and Wilson) and the present studies are to be expected as discussed previously (since BW used $c=-\frac{1}{4}$ in Eq. (21)). Had BW adjusted the parameters of their equation of state to obtain better agreement between calculated and measured velocities in RDX, TNT, and picric acid the agreement between their studies and the present would have been even better (except for T_2), since $p_2=\rho_1 DW\approx k\rho_1 D^2$. It is possible that the calculations by BW have been improved in later studies. The data of LS for PETN at $\rho_1=1.6$ are questionable, since they are inconsistent with the relation $D/W=v_1/(v_1-v_2)$.

It is quite evident that the detonation temperature is really the only detonation property which may be used to provide experimental information on the accuracy of the various equations of state employed in studies of the hydrodynamic theory of detonation, all other quantities being relatively insensitive to the form of the particular equation of state employed. The detonation temperature, however, is so sensitive to the form of the equation of state that a good method for measuring it should provide a crucial test of the validity of the equation of state. Fox,[22] employing a special spectroscopic technique, measured the temperature from the side of the charge and his results for a number of military explosives correlated well with $T_3-T_1=Q/\bar{C}_v^*$. There is evidence from several types of experimental investigations that the conditions described as "detonation" conditions do not extend to the periphery of the charge, but that an "edge effect" exists. It is thus to be expected that the temperature at the edge of the charge adjacent to the detonation wave would correspond to the "adiabatic" temperature, (T_3), rather than "detonation" temperature, T_2. Cotter and Jacobs[23] measured by similar spectroscopic means the temperature of liquid nitroglycerin both at the side and down the end of the charge and obtained temperatures of 4600°K and >5500°K, respectively. Calculations of the "adiabatic" and "detonation" temperatures by the methods outlined in the present report for nitroglycerin gave 4780°K for T_3 and 5750°K for T_2, in good agreement with the measured values of Cotter and Jacobs. These measurements thus appear to provide evidence for the validity of the approximation $\bar{C}_v\cong\bar{C}_v^*$ and the neglect of $(\partial E/\partial v_2)_T$ relative to p_2 in Eq. (9) for β.[24]

The author wishes to acknowledge the helpful advice, cooperation, and encouragement of his associates within the Explosives Department.

[22] J. G. Fox, Navy Ordnance Report 200–45.

[23] T. P. Cotter and S. J. Jacobs, OSRD Report 5618.

[24] Since this article was prepared an interesting article by P. Caldirola [J. Chem. Phys. **14**, 738 (1946)] has appeared treating by another procedure the subject of this study. Caldirola's method leads to temperatures and pressures which in some cases differ rather sharply from the results reported here. However, his definition of σ (in his Eq. 11) seems to be in error by a factor $\frac{1}{2}$. Moreover it may not in many cases be correct to neglect dA/dv as he has done. The results of the present study do not support the linear relations between ρ and $1/\alpha$ claimed by Caldirola (his Eq. 13) although the discrepancies are not large.

Letters to the Editor

THIS section will accept reports of new work, provided these are terse and contain few figures, and especially few halftone cuts. The Editorial Board will not hold itself responsible for opinions expressed by the correspondents. Contributions to this section should not exceed 600 words in length and must reach the office of the Managing Editor not later than the 15th of the month preceding that of the issue in which the letter is to appear. No proof will be sent to the authors. The usual publication charge ($4.00 per page) will not be made and no reprints will be furnished free.

The Temperature Dependence of Viscosities of Liquids and Activation Energy

M. S. TELANG
Laxminarayan Institute of Technology, Nagpur University, Nagpur, India
June 12, 1947

VARIOUS types of exponential equations for the temperature dependence of viscosities of liquids are to be found in the literature, and some of the well-known equations have been referred to by me in a recent paper.[1] The equation proposed by Eyring *et al.*[2]

$$\eta = Z \exp[E_{vis}/RT], \tag{1}$$

in which η = the viscosity, Z = the "frequency factor," and E_{vis} = the "activation energy" per mole for viscous flow, and the theoretical background of it continues to attract attention. However, the term E_{vis} needs some clarification. Following the theory of Eyring, the energy required to push two molecules apart to provide a suitable site for the jump of a moving molecule from one equilibrium position to the next is synonymous with the energy needed to break a "bond," and this quantity represents the "activation energy." Based on this theory, I obtain the following equation:

$$\eta = Z \exp[\gamma(M/D-d)^{\frac{1}{3}} \cdot N^{\frac{1}{3}}/RT] = Z \exp[f(\cos 30°)^2(\sigma+\delta)\cdot N/NkT], \tag{2}$$

where the symbols correspond to those employed in another paper.[3] According to the same paper,

$$\frac{\gamma(M/D-d)^{\frac{1}{3}}\cdot N}{N^{\frac{1}{3}}} = N \cdot f(\cos 30°)^2(\sigma+\delta)$$

stands for the energy needed to break N "bonds" in a molal volume of $Vc \cdot cs$. Substituting for $\gamma(M/D-d)^{\frac{1}{3}}$ by its equivalent $2kN^{\frac{1}{3}}(T_c-T)$ as given by the Eötvös law, we have

$$\eta = Z \exp[2k \cdot N(T_c-T)/RT] = Z \exp[2(T_c-T)/T]. \tag{3}$$

Taking out logarithms, we have

$$\ln\eta = (\ln Z - 2) + (2T_c/T) \tag{4}$$

or

$$\log_{10}\eta = (\log_{10} Z - 0.87) + 0.87(T_c/T). \tag{5}$$

Adding $\ln V^{\frac{1}{3}}$ to both sides of Eq. (4), we obtain

$$\ln\eta \cdot V^{\frac{1}{3}} = (\ln Z \cdot V^{\frac{1}{3}} - 2) + (2T_c/T). \tag{6}$$

The close resemblance between (6) and an equation proposed and tested by Thomas[4] *viz.*,

$$\ln\eta \cdot V^{\frac{1}{3}} = (c-k') + k'(T_c/T) \tag{7}$$

can now be clearly seen. Comparison of (6) and (7) gives $c = \ln Z \cdot V^{\frac{1}{3}}$ and $k' = 2$. It is of significance to note that the values of k' when expressed in logarithms to the base 10, as given by Thomas in his Table II, lie between 0.6 and 1.1, giving a mean of 0.85, which is in good agreement with the value of 0.87 given by Eq. (5).

Equation (6) leads us to another important conclusion that the usual method of estimating the "activation energy," according to the relation $E_{vis} = R[d \ln\eta/d(1/T)]$ from the linear plot of $\ln\eta$ *vs.* $1/T$, is unreliable. According to Eq. (4) or (6), such a plot gives the slope as $2T_c$, whereas it ought to be

$$\frac{\gamma(M/D-d)^{\frac{1}{3}}\cdot N^{\frac{1}{3}}}{R} = 2(T_c-T)$$

in accordance with Eqs. (2) and (3). It appears that the incorporation of a volume term ($V^{\frac{1}{3}}$) in the non-exponential part of the Eq. (6) or (7) is superfluous, but it need not be stated so definitely at this stage without a thorough investigation. However, whether the incorporation of $V^{\frac{1}{3}}$ in the non-exponential term should be made or not, the exponential term which stands for the "activation energy" remains unaffected. The identity of Eqs. (6) and (7) provides an indirect test of Eq. (2). A detailed examination of Eq. (2) is in progress. It may be tentatively stated that this equation is in harmony with the basic postulates incorporated in my previous paper.[3]

[1] M. S. Telang, J. Phys. Chem. **50**, 384 (1946).
[2] H. Eyring, J. Chem. Phys. **4**, 283 (1936); S. Glasstone, K. J. Laidler, and H. Eyring, *The Theory of Rate Processes* (McGraw-Hill Book Company, Inc., New York, 1941), p. 477.
[3] M. S. Telang, "On the theory and application of the relation between surface tension and orthobaric densities," J. Chem. Phys. (to be published).
[4] L. H. Thomas, J. Chem. Soc. 573 (1946).

On the Possibility of a Chemical Synthesis of Diamond

D. P. MELLOR
Department of Chemistry, The University of Sydney, Sydney, Australia
June 6, 1947

RECENT attempts to synthesize diamond by transforming graphite to diamond under thermodynamically favorable conditions of pressure and temperature having so far failed,[1] it would seem worth while to examine the possibilities of a chemical synthesis by a process of polymerization.

It is of interest that the only synthetic material formed in many experiments carried out over the last seventy years, positively identified as diamond by x-ray diffraction tests,[2,3] is that said to have been produced by J. B. Hannay[2] in 1880. Though the evidence supporting Hannay's claims recently adduced by Bannister and Londsdale[3] is very strong, real proof can be achieved only by a successful repetition of Hannay's work. Hannay's method was to heat a mixture of light paraffin, bone oil (mainly pyridine),

and lithium in a sealed iron container. Only three of eighty cylinders tried withstood the temperature of a red heat. These conditions, inadequate to transform graphite to diamond, might conceivably have produced diamond directly by a process of polymerization.

Parsons,[4] in his Bakerian lecture to the Royal Society of London, states that he tried to repeat Hannay's work, but in the very long list of experiments described at the end of his paper he gives very few details about these particular experiments. With the improved facilities now available it would seem worth while to try to check and possibly to extend Hannay's work. In addition to the light paraffins previously used, other substances possessing more of the diamond structure such as derivatives of methane III,[1-3] cyclopropane,[5] and tricyclo (3.3.1.1)[3,6] decane (adamantane) might repay investigation along these lines.

[1] P. W. Bridgman, J. Chem. Phys. **15**, 92 (1947); P. L. Gunther, P. Geselle, and W. Rebentisch, Zeits. f. anorg. allgem. Chem. **250**, 357 (1943).
[2] J. B. Hannay, Proc. Roy. Soc. (London) **30**, 188 (1880).
[3] F. A. Bannister and K. Londsdale, Mineralog. Mag. **26**, 309 (1943).
[4] C. A. Parsons, Phil. Trans. **A220**, 67 (1919).
[5] M. Beesley and J. Thorpe, J. Chem. Soc. **117**, 602 (1920); see also A. M. Patterson and L. Capell, *The Ring Index* (Reinhold Publishing Corporation, New York, 1940), p. 172, Compound 1191.
[6] W. Nowacki, Helv. Chim. Acta **28**, 1233 (1945); see also A. M. Patterson and L. Capell, *The Ring Index* (Reinhold Publishing Corporation, New York, 1940), p. 275, Compound 2034.

The Nature of the Hydrogen Bond in KHF_2

KENNETH S. PITZER AND EDGAR F. WESTRUM*
Department of Chemistry, University of California, Berkeley, California
June 9, 1947

THE discovery of the residual entropy of ice at low temperatures, and its explanation in terms of a double minimum potential curve for the proton in the O−H−O hydrogen bond,[1] raised the question whether F−H−F system also had a double minimum potential curve. We had undertaken to answer this question by measuring the entropy of KHF_2 by heat capacity measurements from low temperatures and from the reaction $KF(s)+HF(g)=KHF_2(s)$. This work was interrupted in 1943 and is only now being completed. However, the heat capacity curve for KHF_2 was finished. In the interval the excellent measurements of Ketelaar[2] on the infra-red absorption and reflection spectra of KHF_2 have become available to us. These more complete spectra make untenable the earlier postulate of Buswell, Maycock, and Rodebush,[3] which was followed by Glockler and Evans.[4] However, our heat capacities are not consistent with Ketelaar's explanation of his data. We wish to propose the following interpretation of all these data.

Solid KHF_2 shows absorption and reflection peaks at 1450 and 1222 cm^{-1} which are so much stronger than all others as to virtually assure the correctness of their assignment as fundamentals. The HF_2^- ion should have two infra-red active fundamentals, ν_3, where the proton moves along the F−F line, and ν_2, where the proton moves perpendicularly to the F−F line. The latter is degenerate. Also there is the inactive fundamental, ν_1, which is a symmetrical F−F vibration. Ketelaar felt that the two observed peaks were too close together to be the two active fundamentals and that ν_2 would be "much lower than 600 cm^{-1}." Hence he assigned the 1450 and 1222 cm^{-1} peaks to a doubling of ν_3 because of a double minimum potential curve. This is not possible because it would lead to a peak in the heat capacity curve near 20°K which is definitely not present[5] (see Fig. 1). Consequently,

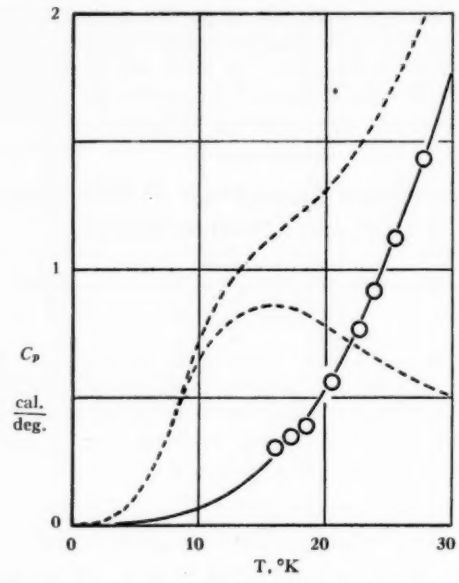

FIG. 1. The molal heat capacity of solid KHF_2: circles, experimental; solid line, T^3 law for lattice vibrations; dotted curves, Ketelaar's model, lower the contribution from the ν_2 doublet above, upper the total including lattice vibrations.

we believe that 1450 and 1222 cm^{-1} peaks represent, respectively, the ν_3 and ν_2 fundamentals. In our opinion the more surprising point is not that ν_2 is so high but that ν_3 is so low. However, this hydrogen bond is considerably shorter than those previously studied so that there is no evidence against the assignment.

The HF_2^- ion has a center of symmetry both internally and with respect to the crystal, hence $2\nu_3$ is forbidden in the infra-red. The peak at 5099 cm^{-1} seems most likely to be $3\nu_3$. If we assume the peak at 4232 cm^{-1} to be $2\nu_3+\nu_2$, then $2\nu_2$ should be approximately 3010 cm^{-1}. These levels show a large negative anharmonicity; indeed they approach somewhat the levels of an oscillator with a fourth power potential as calculated by Bell.[6] There is no indication of any double minimum character with the F−H−F potential. The possibility of a very small potential hill has not been eliminated; however it must not be much higher than the lowest energy level.

* Present address: Department of Chemistry, University of Michigan, Ann Arbor, Michigan.
[1] W. F. Giauque and M. Ashley, Phys. Rev. **43**, 81 (1933); L. Pauling, J. Am. Chem. Soc. **57**, 2680 (1935); W. F. Giauque and J. W. Stout, *ibid.* **58**, 1144 (1936).
[2] J. A. A. Ketelaar, Rec. Trav. Chim. **60**, 523 (1941).
[3] A. M. Buswell, R. L. Maycock, and W. H. Rodebush, J. Chem. Phys. **8**, 362 (1940).
[4] G. Glockler and G. E. Evans, J. Chem. Phys. **10**, 607 (1942).
[5] Other supporting arguments can be given for this conclusion, but they will be postponed until our full paper.
[6] R. P. Bell, Proc. Roy. Soc. London **A183**, 328 (1945).

The Pressure Coefficient of Viscosity

A. BONDI
Shell Development Company, Emeryville, California
May 26, 1947

THE writer showed in a recent paper[1] that the pressure coefficient of viscosity, if expressed in the form proposed by Eyring and co-workers,[2] can be used as a measure of the displacement of a molecule from its equilibrium position during the flow process. The pressure coefficient largely determines, therefore, the magnitude of the energy of activation for hole formation.[1] In order to calculate the latter from first principles, it was found that only $\Delta V_{\ddagger}$[3] remained to be calculable from physical constants not derived from viscosity measurement.

The concept of $\Delta V_{\ddagger}$ as the size of the hole required for a molecule to move into suggests that the amount of available volume in the liquid should influence the numerical value of $\Delta V_{\ddagger}$. One could expect that in a liquid of loose packing the hole-size requirement be smaller than in a closely packed liquid, and *vice versa*. A good measure of the tightness of packing seems to be the expansion at the melting point ΔV_f and the structural type of the lattice system. The latter is today quite generally believed to be carried over from the solid into the liquid state, at least in the neighborhood of the melting point.

A rough indication of the correctness of this picture would be constancy of the volume fraction represented by the sum of $\Delta V_{\ddagger}$ and ΔV_f, e.g.,

$$\Delta V_{\ddagger}+\Delta V_f = V/n, \qquad (1)$$

where n = universal constant, possibly dependent upon the lattice type.

Table I shows that this is indeed the case. For the few liquids, of which viscosity-pressure and melting-point expansion[4] data are available, n appears to have the values 3 and 5, at least for the $\Delta V_{\ddagger}$ determination closest to the melting point. All of the substances for which $n=3$ show rhombic or monoclinic crystal structure in the solid state, whereas cubic or hexagonal arrangement seems to be preferred when $n=5$. This sequence is in accord with the well-known difference in restraint imposed on free rotation of molecules in the respective solid lattices.

TABLE I. Relationship between viscosity-pressure coefficient $\Delta V_{\ddagger}$ and the melting-point expansion ΔV_f.

Substance	$\Delta V_{\ddagger}$ cm³	$(\Delta V_{\ddagger}+\Delta V_f)/V$	t °C	
Benzene	16.6	.32	30	
p-xylene		.32	75	
Aniline	21.3	.32	30	$n\sim3$
Cyclohexane	26.6	.30	75	
Methanol†	7.9	.26/8	30	
Carbon tetrachloride	18.4	.21	30	
Chlorobenzene	13.2	.20	30	
Bromobenzene	13.5	.19	30	
Acetone†	11.7	.20	30	$n\sim5$
Ethyl ether†	10.1	.15	30	
Ethyl bromide†	10.7	.20	30	
Ethyl iodide†	10.5	.17	30	
n-pentane	15.3	.31††	30	
Neopentane	34.4	.32††	30	
n-hexane	17.3	.30††	30	$n\sim3$
Eugenol	34.2	.30††	30	

† These compounds have melting points which are >100°C below the temperature of viscosity measurement. The $\Delta V_{\ddagger}$ data may, therefore, not be comparable with those of the other compounds.
†† ΔV_f values were estimated from rather approximate dTm/dp data.

The temperature and pressure coefficient of ΔV_f does not explain the very complicated temperature and pressure dependence of $\Delta V_{\ddagger}$.

These data indicate quite clearly, however, that $\Delta V_{\ddagger}$ is a function of both the structure of the liquid and the spatial configuration of the individual molecule, as had been pointed out previously.

The writer takes this opportunity to thank Professor F. London for directing his attention to an error made in the numerical calculation of Fig. 1 in reference 1. The lowest point at $\theta=90°$ is at $b=4$ and not at $b=2$. A revised drawing will be presented in a forthcoming paper.

[1] A. Bondi, J. Chem. Phys. **14**, 592 (1946).
[2] A. E. Stearn and H. Eyring, Chem. Rev. **29**, 509 (1941).
[3] $\Delta V_{\ddagger}$ is defined by $(\partial\Delta F_{\ddagger}/\partial p)T=\Delta V_{\ddagger}$, where $\Delta F_{\ddagger}=RT\ln(V\eta/Nh)$ is the free energy of activation for viscous flow.
[4] D. Rozental, Bull. Soc. Chim. Belg. **15**, 585 (1936).

Method for Extending Study of Metal Ion-Cation Exchanger Isotope Fractionation

MAXWELL LEIGH EIDINOFF
Department of Chemistry, Queens College, Flushing, New York
June 2, 1947

FEW experiments dealing with isotope fractionation in cation-cation exchanger equilibria have been reported since the pioneer work of Taylor and Urey.[1] The purpose of this communication is to indicate procedures by which isotope separation data can be obtained for additional elements using equipment available in a relatively large number of laboratories.

Small quantities (about 5 to 50 microcuries, depending on the specific experiment) of radio-isotopes are added to the element in normal abundance and the solutions used in cation-exchange column studies. Detection of small volume "leading samples" is effected by suitably installing one or more Geiger-counter tubes near the exit end of the column. The concentration of the radio-isotope is proportional to the measured sample activity per unit weight of the element when the measurements are made under comparable conditions.

Of special interest from the standpoint of small atomic mass and convenience of measurement are the systems Be^{7}–Be^{9} and Be^{9}–Be^{10}. The systems Na^{22}–Na^{23} and Na^{22}–Na^{24} can be used for sodium studies. The fractionation of K^{39}–K^{41} was explored by Taylor and Urey.[1] Radio-isotope K^{42} can be used in column experiments. It is less convenient to study the fractionation of the naturally radioactive K^{40}, since a relatively large potassium sample is required. In the case of calcium, Ca^{41} and Ca^{45} may be used. The mass difference between the latter and the most abundant natural isotope Ca^{40} is an advantage in this work.

Experiments of this kind should afford a more thorough understanding of the mass effect and the isotope separating properties of the various types of cation exchangers. Several exploratory experiments have been started in our laboratory.

[1] T. I. Taylor and H. C. Urey, J. Chem. Phys. **6**, 429 (1938).